

UNIVERSITY OF YAOUNDE I  
FACULTY OF SCIENCE

\*\*\*\*\*

POST-GRADUATE AND TRAINING  
SCHOOL FOR LIFE SCIENCE,  
HEALTH AND ENVIRONMENT

\*\*\*\*\*

RESEARCH AND DOCTORATE  
TRAINING UNIT IN LIFE SCIENCE



UNIVERSITY OF YAOUNDE I  
FACULTE DES SCIENCES

\*\*\*\*\*

CENTRE DE RECHERCHE ET DE FORMATION  
DOCTORALE EN SCIENCES DE LA VIE, SANTE  
ET ENVIRONNEMENT

\*\*\*\*\*

UNITE DE RECHERCHE ET DE FORMATION  
DOCTORALE EN SCIENCES DE LA VIE

DEPARTMENT OF BIOCHEMISTRY  
DEPARTEMENT DE BIOCHIMIE

LABORATORY FOR PHYTOBIOCHEMISTRY AND MEDICINAL PLANTS STUDIES  
LABORATOIRE DE PHYTOBIOCHIMIE ET D'ETUDE DES PLANTES

ANTIMICROBIAL AND BIOCONTROL AGENTS UNIT  
UNITE DES AGENTS ANTIMICROBIENS ET DE BIOCONTROLE

*Novel antitrypanosomal diaminoquinazoline  
analogues from repurposing the Medicines for  
Malaria Venture Open Access Pathogen Box library*

Thesis submitted in partial fulfilment of the requirements for the award of the Degree of  
**Doctorate-Ph.D. in Biochemistry**

By

DIZE DARLINE  
MSc in Biochemistry  
Registration N° 11R0127

Under the Supervision of

FEKAM BOYOM FABRICE, Professor  
University of Yaoundé I



2023-2024

UNIVERSITE DE YAOUNDE I

\*\*\*\*\*

FACULTE DES SCIENCES

\*\*\*\*\*

CENTRE DE RECHERCHE ET DE FORMATION  
DOCTORALE EN SCIENCES DE LA VIE- SANTE  
ET ENVIRONNEMENT

\*\*\*\*\*



UNIVERSITY OF YAOUNDE I

\*\*\*\*\*

FACULTY OF SCIENCES

\*\*\*\*\*

POST-GRADUATE AND TRAINING  
SCHOOL OF LIFE SCIENCES-HEALTH AND  
ENVIRONMENT

\*\*\*\*\*

DEPARTMENT OF BIOCHEMISTRY

DEPARTEMENT DE BIOCHIMIE

**ATTESTATION OF CORRECTION OF THE DOCTORAL THESIS**

We, the undersigned: Prof. PENLAP Véronique, President; Prof. BIGOGA DAIGA Jude, Prof. NJIOKOU Flaubert, and Prof. NTIE-KANG Fidele, examiners of the thesis, hereby certify that Ms. Darline Dize, Registration Number 11R0127, has made the required corrections in accordance with the Jury's instructions for her Doctoral/PhD thesis in Biochemistry, with a specialization in Biotechnology and Development. The thesis was defended on Wednesday 29<sup>th</sup> May, 2024, at 10:00 am in Room S01/S02 of the Faculty of Sciences at the University of Yaoundé 1, on the title "Novel Antitrypanosomal Diaminoquinazoline Analogues from Repurposing the Medicines for Malaria Venture Open Access Pathogen Box Library".

Yaoundé... 12 SEPT 2024

President of the Jury

PENLAP Véronique, Professor

Handwritten signature of Penlap Véronique in blue ink.

Examiners

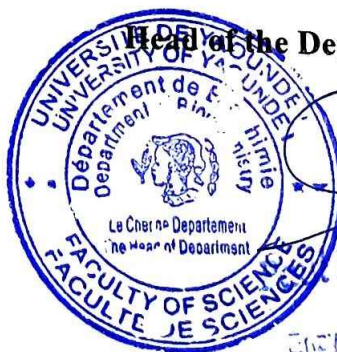
BIGOGA DAIGA Jude, Professor

Handwritten signature of Bigoga Daiga Jude in blue ink.

NJIOKOU Flaubert, Professor

NTIE-KANG Fidele, Associate Professor

Handwritten signature of Ntie-Kang Fidele in blue ink.



Head of the Department of Biochemistry

F. MOUNDIPA  
Professor  
Enzymology & Toxicology

UNIVERSITY OF YAOUNDE I  
FACULTY OF SCIENCE

\*\*\*\*\*

POST-GRADUATE AND TRAINING  
SCHOOL FOR LIFE SCIENCE,  
HEALTH AND ENVIRONMENT

\*\*\*\*\*

RESEARCH AND DOCTORATE  
TRAINING UNIT IN LIFE SCIENCE



UNIVERSITY OF YAOUNDE I  
FACULTE DES SCIENCES

\*\*\*\*\*

CENTRE DE RECHERCHE ET DE FORMATION  
DOCTORALE EN SCIENCES DE LA VIE, SANTE  
ET ENVIRONNEMENT

\*\*\*\*\*

UNITE DE RECHERCHE ET DE FORMATION  
DOCTORALE EN SCIENCES DE LA VIE

DEPARTMENT OF BIOCHEMISTRY  
*DEPARTEMENT DE BIOCHIMIE*

LABORATORY FOR PHYTOBIOCHEMISTRY AND MEDICINAL PLANTS STUDIES  
*LABORATOIRE DE PHYTOBIOCHIMIE ET D'ETUDE DES PLANTES MEDICINALES*

ANTIMICROBIAL AND BIOCONTROL AGENTS UNIT  
*UNITE DES AGENTS ANTIMICROBIENS ET DE BIOCONTROLE*

*Novel antitrypanosomal diaminoquinazoline  
analogues from repurposing the Medicines for  
Malaria Venture Open Access Pathogen Box library*

Thesis submitted in partial fulfilment of the requirements for the award of the Degree of  
Doctorate-Ph.D. in Biochemistry

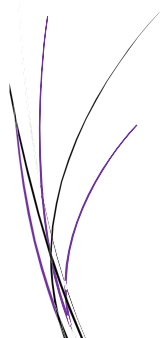
By

DIZE DARLINE  
MSc in Biochemistry  
Registration N° 11R0127

Under the Supervision of

FEKAM BOYOM FABRICE, Professor  
University of Yaoundé I

2023-2024



UNIVERSITE DE YAOUNDE I

\*\*\*\*\*

FACULTE DES SCIENCES

\*\*\*\*\*

CENTRE DE RECHERCHE ET DE FORMATION  
DOCTORALE EN SCIENCES DE LA VIE- SANTE  
ET ENVIRONNEMENT

\*\*\*\*\*

UNITE DE RECHERCHE ET DE FORMATION  
DOCTORALE SCIENCES DE LA VIE



UNIVERSITY OF YAOUNDE I

\*\*\*\*\*

FACULTY OF SCIENCES

\*\*\*\*\*

POST-GRADUATE AND TRAINING  
SCHOOL OF LIFE SCIENCES-HEALTH AND  
ENVIRONMENT

\*\*\*\*\*

POST-GRADUATE AND TRAINING  
UNIT OF LIFE SCIENCES-HEALTH

### DECLARATION OF HONOR

I, **DIZE DARLINE**, hereby declare that the present Doctoral/Ph.D. thesis entitled "Novel antitrypanosomal diaminoquinazoline analogues from repurposing the Medicines for Malaria Venture Open Access Pathogen Box library" is the result of my own research work.

The research for this thesis was conducted within the Antimicrobial Agents and Biocontrol Unit under the supervision of **FEKAM BOYOM Fabrice**, Professor at the University of Yaoundé I (Department of Biochemistry).

This thesis is authentic and has not been previously submitted for the acquisition of any academic or university degrees whatsoever.

Date July 18, 2024

Name and signature of the author

Darline Dize

Date July 19, 2024

Name and signature of the Supervisor

Fabrice F. Boyom



LIST OF PERMANENT TEACHING  
STAFF

LISTE DES ENSEIGNANTS  
PERMANENTS

ACADEMIC YEAR 2023/2024

(By Department and by Grade)

UPDATE: 04 Juin 2024

ADMINISTRATION

**DEAN:** OWONO OWONO Luc-Calvin, Professor

**VICE-DEAN / DPSAA:** ATCHADE Alex de Théodore, Professor

**VICE-DEAN/ DSSE:** NYEGUE Maximilienne Ascension, Professor

**VICE-DEAN / DRC :** NOUNDJEU Pierre, Professor

**Head of Administrative and Financial Division:** NDOYE FOE Marie C. F., Associate professor

**Head of Division of Academic affairs, Research and corporation:** AJEAGAH Gideon AGHAINDUM, *Professor*

1- DEPARTMENT OF BIOCHEMISTRY (BC) (43)			
N°	NAMES AND SURNAMES	GRADE	OBSERVATIONS
1.	BIGOGA DAIGA Jude	Professor	On duty
2.	FEKAM BOYOM Fabrice	Professor	On duty
3.	KANSCI Germain	Professor	On duty
4.	MBACHAM FON Wilfred	Professor	On duty
5.	MOUNDIPA FEWOU Paul	Professor	<b>Head of Department</b>
6.	NGUEFACK Julienne	Professor	On duty
7.	NJAYOU Frédéric Nico	Professor	On duty
8.	OBEN Julius ENYONG	Professor	On duty
9.	ACHU Merci BIH	Associate Professor	On duty
10.	ATOGHO Barbara MMA	Associate Professor	On duty
11.	AZANTSA KINGUE GABIN BORIS	Associate Professor	On duty
12.	BELINGA née NDOYE FOE F. M. C.	Associate Professor	<b>Chief DAF / FS</b>
13.	DJUIDJE NGOUNOUE Marceline	Associate Professor	On duty
14.	DAKOLE DABOY Charles	Associate Professor	On duty
15.	DONGMO LEKAGNE Joseph Blaise	Associate Professor	On duty
16.	DJUJKWO NKONGA Ruth Viviane	Associate Professor	On duty

17.	EFFA ONOMO Pierre	Associate Professor	<b>Vice Dean/FS/Univ Ebolowa</b>
18.	EWANE Cécile Annie	Associate Professor	On duty
19.	KOTUE TAPTUE Charles	Associate Professor	On duty
20.	LUNGA Paul KEILAH	Associate Professor	On duty
21.	MANANGA Marlyse Joséphine	Associate Professor	On duty
22.	MBONG ANGIE M. Mary Anne	Associate Professor	On duty
23.	MOFOR née TEUGWA Clotilde	Associate Professor	<b>Dean FS / UDs</b>
24.	NANA Louise épouse WAKAM	Associate Professor	On duty
25.	NGONDI Judith Laure	Associate Professor	On duty
26.	Palmer MASUMBE NETONGO	Associate Professor	On duty
27.	PECHANGOU NSANGOU Sylvain	Associate Professor	On duty
28.	TCHANA KOUATCHOUA Angèle	Associate Professor	On duty
29.	AKINDEH MBUH NJI	Senior Lecturer	On duty
30.	BEBEE Fadimatou	Senior Lecturer	On duty
31.	BEBOY EDJENGUELE Sara Nathalie	Senior Lecturer	On duty
32.	FONKOUA Martin	Senior Lecturer	On duty
33.	FOUPOUAPOUOGNIGNI Yacouba	Senior Lecturer	On duty
34.	KOUOH ELOMBO Ferdinand	Senior Lecturer	On duty
35.	MBOUCHE FANMOE Marceline Joëlle	Senior Lecturer	On duty
36.	OWONA AYISSI Vincent Brice	Senior Lecturer	On duty
37.	WILFRED ANGIE ABIA	Senior Lecturer	On duty
38.	BAKWO BASSOGOG Christian Bernard	Assistant lecturer	On duty
39.	ELLA Fils Armand	Assistant lecturer	On duty
40.	EYENGA Eliane Flore	Assistant lecturer	On duty
41.	MADIESSE KEMGNE Eugenie Aimée	Assistant lecturer	On duty
42.	MANJIA NJIKAM Jacqueline	Assistant lecturer	On duty
43.	WOGUIA Alice Louise	Assistant lecturer	On duty

## 2- DEPARTMENT OF ANIMAL BIOLOGY AND PHYSIOLOGY (ABP) (49)

1.	AJEAGAH Gideon AGHAINDUM	Professor	<i>DAARS/FS</i>
2.	DIMO Théophile	Professor	On duty
3.	DJIETO LORDON Champlain	Professor	On duty
4.	DZEUFJET DJOMENI Paul Désiré	Professor	On duty
5.	ESSOMBA née NTSAMA MBALA	Professor	<b>DC and Vice dean/FMSB/UIYI</b>
6.	KEKEUNOU Sévilor	Professor	<b>Head of Department</b>
7.	NJAMEN Dieudonné	Professor	On duty
8.	NOLA Moïse	Professor	On duty
9.	TAN Paul VERNYUY	Professor	On duty
10.	TCHUEM TCHUENTE Louis Albert	Professor	<b>Insp. Serv. Coord. Progr. Min Health</b>
11.	ZEBAZE TOGOUET Serge Hubert	Professor	On duty
12.	ALENE Désirée Chantal	Associate Professor	<b>Vice Dean /Univ Ebwa</b>
13.	ATSAMO Albert Donatien	Associate Professor	On duty
14.	BILANDA Danielle Claude	Associate Professor	On duty
15.	DJILOGUE Séfirin	Associate Professor	On duty

16.	GOUNOUE KAMKUMO Raceline épse FOTSING	Associate Professor	On duty
17.	JATSA BOUKENG Hermine épse MEGAPTCHE	Associate Professor	On duty
18.	KANDEDA KAVAYE Antoine	Associate Professor	On duty
19.	LEKEUFACK FOLEFACK Guy B.	Associate Professor	On duty
20.	MAHOB Raymond Joseph	Associate Professor	On duty
21.	MBENOUN MASSE Paul Serge	Associate Professor	On duty
22.	MEGNEKOU Rosette	Associate Professor	On duty
23.	MOUNGANG Luciane Marlyse	Associate Professor	On duty
24.	NOAH EWOTI Olive Vivien	Associate Professor	On duty
25.	MONY Ruth épse NTOINE	Associate Professor	On duty
26.	MVEYO NDANKEU Yves Patrick	Associate Professor	On duty
27.	NGUEGUIM TSOFAK Florence	Associate Professor	On duty
28.	NGUEMBOCK	Associate Professor	On duty
29.	TAMSA ARFAO Antoine	Associate Professor	On duty
30.	TOMBI Jeannette	Associate Professor	On duty
31.	AMBADA NDZENGUE GEORGIA ELNA	Senior Lecturer	On duty
32.	BASSOCK BAYIHA Etienne Didier	Senior Lecturer	On duty
33.	ETEME ENAMA Serge	Senior Lecturer	On duty
34.	FEUGANG YOUMSSI François	Senior Lecturer	On duty
35.	FOKAM Alvine Christelle Epse KENGNE	Senior Lecturer	On duty
36.	GONWOUO NONO Legrand	Senior Lecturer	On duty
37.	KOGA MANG DOBARA	Senior Lecturer	On duty
38.	LEME BANOCK Lucie	Senior Lecturer	On duty
39.	MAPON NSANGOU Indou	Senior Lecturer	On duty
40.	METCHI DONFACK MIREILLE FLAURE EPSE GHOUMO	Senior Lecturer	On duty
41.	NGOULATEU KENFACK Omer Bébé	Senior Lecturer	On duty
42.	NJUA Clarisse YAFI	Senior Lecturer	<b>Head Div. Univ. Bamenda</b>
43.	NWANE Philippe Bienvenu	Senior Lecturer	On duty
44.	TADU Zephyrin	Senior Lecturer	On duty
45.	YEDE	Senior Lecturer	On duty
46.	YOUNOUSSA LAME	Senior Lecturer	On duty
47.	KODJOM WANCHE Jacguy Joyce	Assistant Lecturer	On duty
48.	NDENGUE Jean De Matha	Assistant Lecturer	On duty
49.	ZEMO GAMO Franklin	Assistant Lecturer	On duty

### 3- DEPARTMENT OF PLANT PHYSIOLOGY AND BIOLOGY (PPB) (32)

1.	AMBANG Zachée	Professor	<b>Head of Department</b>
2.	DJOCGOUE Pierre François	Professor	On duty
3.	MBOLO Marie	Professor	On duty
4.	MOSSEBO Dominique Claude	Professor	On duty
5.	NDONGO BEKOLO	Professor	On duty
6.	ZAPFACK Louis	Professor	On duty
7.	ANGONI Hyacinthe	Associate Professor	On duty
8.	BIYE Elvire Hortense	Associate Professor	On duty

9.	MAHBOU SOMO TOUKAM. Gabriel	Associate Professor	On duty
10.	MALA Armand William	Associate Professor	On duty
11.	MBARGA BINDZI Marie Alain	Associate Professor	<b>DAAC/Univ , Douala</b>
12.	NGALLE Hermine BILLE	Associate Professor	On duty
13.	NGONKEU MAGAPTCHE Eddy L.	Associate Professor	<b>CT / MINRESI</b>
14.	TONFACK Libert Brice	Associate Professor	On duty
15.	TSOATA Esaïe	Associate Professor	On duty
16.	ONANA JEAN MICHEL	Associate Professor	On duty
17.	DJEUANI Astride Carole	Senior Lecturer	On duty
18.	GONMADGE CHRISTELLE	Senior Lecturer	On duty
19.	MAFFO MAFFO Nicole Liliane	Senior Lecturer	On duty
20.	MANGA NDJAGA JUDE	Senior Lecturer	On duty
21.	NNANGA MEBENGA Ruth Laure	Senior Lecturer	On duty
22.	NOUKEU KOUAKAM Armelle	Senior Lecturer	On duty
23.	NSOM ZAMBO EPSE PIAL ANNIE CLAUDE	Senior Lecturer	<b>In detachment/ UNESCO MALI</b>
24.	GODSWILL NTSOMBOH NTSEFONG	Senior Lecturer	On duty
25.	KABELONG BANAHOU Louis-Paul-Roger	Senior Lecturer	On duty
26.	KONO Léon Dieudonné	Senior Lecturer	On duty
27.	LIBALAH Moses BAKONCK	Senior Lecturer	On duty
28.	LIKENG-LI-NGUE Benoit C	Senior Lecturer	On duty
29.	TAEDOUNG Evariste Hermann	Senior Lecturer	On duty
30.	TEMEGNE NONO Carine	Senior Lecturer	On duty
31.	DIDA LONTSI Sylvere Landry	Assistant Lecturer	On duty
32.	METSEBING Blondo-Pascal	Assistant Lecturer	On duty

#### 4- DEPARTMENT OF INORGANIC CHEMISTRY (IC) (27)

1.	GHOGOMU Paul MINGO	Professor	<b>Minister in charge of mission. P.R.</b>
2.	NANSEU NJIKI Charles Péguy	Professor	On duty
3.	NDIFON Peter TEKE	Professor	<b>TC MINRESI</b>
4.	NENWA Justin	Professor	On duty
5.	NGOMO Horace MANGA	Professor	<b>Vice Chancellor/ Univ. Buea</b>
6.	NJIOMOU C. épse DJANGANG	Professor	On duty
7.	NJOYA Dayirou	Professor	On duty
8.	ACAYANKA Elie	Associate Professor	On duty
9.	EMADAK Alphonse	Associate Professor	On duty
10.	KAMGANG YOUBI Georges	Associate Professor	On duty
11.	KEMMEGNE MBOUGUEM Jean C.	Associate Professor	On duty
12.	KENNE DEDZO GUSTAVE	Associate Professor	On duty
13.	MBEY Jean Aime	Associate Professor	On duty
14.	NDI NSAMI Julius	Associate Professor	<b>Head of Department</b>
15.	NEBAH Née NDOSIRI Bridget NDOYE	Associate Professor	<b>Senator/SENAT</b>
16.	NYAMEN Linda Dyorisse	Associate Professor	On duty
17.	PABOUDAM GBAMBIE AWAWOU	Associate Professor	On duty

18.	TCHAKOUTE KOUAMO Hervé	Associate Professor	On duty
19.	BELIBI BELIBI Placide Désiré	Associate Professor	<b>Head of Division/ ENS Bertoua</b>
20.	CHEUMANI YONA Arnaud M.	Associate Professor	On duty
21.	KOUOTOU DAOUDA	Associate Professor	On duty
22.	MAKON Thomas Beauregard	Senior Lecturer	On duty
23.	NCHIMI NONO KATIA	Senior Lecturer	On duty
24.	NJANKWA NJABONG N. Eric	Senior Lecturer	On duty
25.	PATOUOSSA ISSOFA	Senior Lecturer	On duty
26.	SIEWE Jean Mermoz	Senior Lecturer	On duty
27.	BOYOM TATCHEMO Franck W.	Assistant Lecturer	On duty

### 5- DEPARTMENT OF ORGANIC CHEMISTRY (OC) (33)

1.	Alex de Théodore ATCHADE	Professor	<b>Vice-Dean/DPSAA</b>
2.	DONGO Etienne	Professor	<b>Vice Dean/CSA/ F.SED/UY1</b>
3.	NGOUELA Silvère Augustin	Professor	<b>Head of Department UDs</b>
4.	PEGNYEMB Dieudonné Emmanuel	Professor	<b>Director MINESUP/ Head of Department</b>
5.	MBAZOA née DJAMA Céline	Professor	On duty
6.	MKOUNGA Pierre	Professor	On duty
7.	AMBASSA Pantaléon	Associate Professor	On duty
8.	EYONG Kenneth OBEN	Associate Professor	On duty
9.	FOTSO WABO Ghislain	Associate Professor	On duty
10.	KAMTO Eutrophe Le Doux	Associate Professor	On duty
11.	KENMOGNE Marguerite	Associate Professor	On duty
12.	KOUAM Jacques	Associate Professor	On duty
13.	MVOT AKAK CARINE	Associate Professor	On duty
14.	NGO MBING Joséphine	Associate Professor	<b>Head of cell MINRESI</b>
15.	NGONO BIKOBO Dominique Serge	Associate Professor	<b>Study charge Ass. n°3/MINESUP</b>
16.	NOTE LOUGBOT Olivier Placide	Associate Professor	<b>DAAC/Univ. Bertoua</b>
17.	NOUNGOUE TCHAMO Diderot	Associate Professor	On duty
18.	OUAHOUE WACHE Blandine M.	Senior Lecturer	On duty
19.	TABOPDA KUATE Turibio	Associate Professor	On duty
20.	TAGATSING FOTSING Maurice	Associate Professor	On duty
21.	ZONDEGOUNBA Ernestine	Associate Professor	On duty
22.	MESSI Angélique Nicolas	Senior Lecturer	On duty
23.	MUNVERA MFIFEN Aristide	Senior Lecturer	On duty
24.	NGNINTEDO Dominique	Senior Lecturer	On duty
25.	NGOMO Orléans	Senior Lecturer	On duty
26.	NONO NONO Éric Carly	Senior Lecturer	On duty
27.	OUETE NANTCHOUANG Judith Laure	Senior Lecturer	On duty
28.	SIELINOU TEDJON Valérie	Senior Lecturer	On duty
29.	TCHAMGOUE Joseph	Senior Lecturer	On duty
30.	TSAFFACK Maurice	Senior Lecturer	On duty
31.	TSAMO TONTSA Armelle	Senior Lecturer	On duty
32.	TSEMEUGNE Joseph	Senior Lecturer	On duty
33.	NDOGO ETEME Olivier	Assistant lecturer	On duty
34.			

**6- DEPARTMENT OF RENEWABLE ENERGIES (RE) (1)**

1.	BODO Bertrand	Professor	<i>Head of Department</i>
----	---------------	-----------	---------------------------

**7- DEPARTMENT OF COMPUTER SCIENCE (CS) (22)**

1	ATSA ETOUNDI Roger	Professor	<b>Chief Div. MINESUP</b>
2	FOUDA NDJODO Marcel Laurent	Professor	<b>Head of department HTTC/Chief IGA. MINESUP</b>
3	NDOUNDAM René	Associate Professor	On duty
4	TSOPZE Norbert	Associate Professor	On duty
5	ABESSOLO ALO'O Gislain	Senior Lecturer	<b>Head of cell MINFOPRA</b>
6	AMINO HALIDOU	Senior Lecturer	<b>Head of Department</b>
7	DJAM Xaviera YOUH - KIMBI	Senior Lecturer	On duty
8	DOMGA KOMGUEM Rodrigue	Senior Lecturer	On duty
9	EBELE Serge Alain	Senior Lecturer	On duty
10	HAMZA Adamou	Senior Lecturer	On duty
11	JIOMEKONG AZANZI Fidel	Senior Lecturer	On duty
12	KOUOKAM KOUOKAM E. A.	Senior Lecturer	On duty
13	MELATAGIA YONTA Paulin	Senior Lecturer	On duty
14	MESSI NGUELE Thomas	Senior Lecturer	On duty
15	MONTHÉ DJIADEU Valéry M.	Senior Lecturer	On duty
16	NZEKON NZEKO'O ARMEL JACQUES	Senior Lecturer	On duty
17	OLLE OLLE Daniel Claude Georges Delort	Senior Lecturer	<b>C/D ENSET Ebolowa</b>
18	TAPAMO Hyppolite	Senior Lecturer	On duty
19	BAYEM Jacques Narcisse	Assistant Lecturer	On duty
20	EKODECK Stéphane Gaël Raymond	Assistant Lecturer	On duty
21	MAKEMBE. S . Oswald	Assistant Lecturer	<b>Director CUTI</b>
22	NKONDOCK. MI. BAHANACK.N.	Assistant Lecturer	On duty

**7- DEPARTMENT OF MATHEMATICS (MA) (33)**

1.	AYISSI Raoult Domingo	Professor	<b>Head of Department</b>
2.	KIANPI Maurice	Associate Professor	On duty
3.	MBANG Joseph	Associate Professor	On duty
4.	MBEHOU Mohamed	Associate Professor	On duty
5.	MBELE BIDIMA Martin Ledoux	Associate Professor	On duty
6.	NOUNDJEU Pierre	Associate Professor	<b>Chief Service of Programs &amp; Diploms/FS/UIYI</b>
7.	TAKAM SOH Patrice	Associate Professor	<b>On duty</b>
8.	TCHAPNDA NJABO Sophonie B.	Associate Professor	<b>Director/AIMS Rwanda</b>
9.	TCHOUNDJA Edgar Landry	Associate Professor	On duty
10.	AGHOUKENG JIOFACK Jean Gérard	Senior Lecturer	<b>Chief Cell MINEPAT</b>
11.	BITYE MVONDO Esther Claudine	Assistant Lecturer	On duty
12.	BOGSO ANTOINE Marie	Senior Lecturer	On duty
13.	CHENDJOU Gilbert	Senior Lecturer	On duty
14.	DJIADEU NGAHA Michel	Senior Lecturer	On duty
15.	DOUANLA YONTA Herman	Senior Lecturer	On duty

16.	KIKI Maxime Armand	Senior Lecturer	On duty
17.	LOUMNGAM KAMGA Victor	Senior Lecturer	On duty
18.	MBAKOP Guy Merlin	Senior Lecturer	On duty
19.	MBATAKOU Salomon Joseph	Senior Lecturer	On duty
20.	MENGUE MENGUE David Joël	Senior Lecturer	<b>Head department / ENS Maroua</b>
21.	MBIAKOP Hilaire George	Senior Lecturer	On duty
22.	NGUEFACK Bernard	Senior Lecturer	On duty
23.	NIMPA PEFOUKEU Romain	Senior Lecturer	On duty
24.	OGADOA AMASSAYOGA	Senior Lecturer	On duty
25.	POLA DOUNDOU Emmanuel	Senior Lecturer	<b>In training course</b>
26.	TCHEUTIA Daniel Duviol	Senior Lecturer	On duty
27.	TETSADJIO TCHILEPECK M. Eric.	Senior Lecturer	On duty
28.	TENKEU JEUFACK Yannick Léa	Senior Lecturer	On duty
29.	FOKAM Jean Marcel	Assistant Lecturer	On duty
30.	GUIDZAVAI KOUCHERE Albert	Assistant Lecturer	On duty
31.	MANN MANYOMBE Martin Luther	Assistant Lecturer	On duty
32.	MEFENZA NOUNTU Thiery	Assistant Lecturer	On duty
33.	NYOUMBI DLEUNA Christelle	Assistant Lecturer	On duty

#### 8- DEPARTMENT OF MICROBIOLOGY (MIB) (24)

1.	ESSIA NGANG Jean Justin	Professor	<b>Head of Department</b>
2.	NYEGUE Maximilienne Ascension	Professor	<b>Vice Dean/DSSE</b>
3.	SADO KAMDEM Sylvain Leroy	Professor	On duty
4.	ASSAM ASSAM Jean Paul	Associate Professor	On duty
5.	BOUGNOM Blaise Pascal	Associate Professor	On duty
6.	BOYOMO ONANA	Associate Professor	On duty
7.	KOUITCHEU MABEKU Epse KOUAM Laure Brigitte	Associate Professor	On duty
8.	RIWOM Sara Honorine	Associate Professor	On duty
9.	NJIKI BIKOÏ Jacky	Associate Professor	On duty
10.	TCHIKOUA Roger	Associate Professor	On duty
11.	ESSONO Damien Marie	Senior Lecturer	On duty
12.	LAMYE Glory MOH	Senior Lecturer	On duty
13.	MEYIN A EBONG Solange	Senior Lecturer	On duty
14.	MONI NDEDI Esther Del Florence	Senior Lecturer	On duty
15.	NKOUDOU ZE Nardis	Senior Lecturer	On duty
16.	NKOUÉ TONG Abraham	Senior Lecturer	On duty
17.	SAKE NGANE Carole Stéphanie	Senior Lecturer	On duty
18.	TAMATCHO KWEYANG Blandine Pulchérie	Senior Lecturer	On duty
19.	TOBOLBAÏ Richard	Senior Lecturer	On duty
20.	EZO'O MENGO Fabrice Télésfor	Assistant Lecturer	On duty
21.	EHETH Jean Samuel	Assistant Lecturer	On duty
22.	MAYI Marie Paule Audrey	Assistant Lecturer	On duty
23.	NGOUEENAM Romial Joël	Assistant Lecturer	On duty
24.	NJAPNDOUNKE Bilkissou	Assistant Lecturer	On duty

**9- DEPARTMENT OF PHYSICS (PY) (43)**

<b>N°</b>	<b>NAMES AND SURNAMES</b>	<b>GRADE</b>	<b>OBSERVATIONS</b>
1.	BEN- BOLIE Germain Hubert	Professor	On duty
2.	BIYA MOTTO Frédéric	Professor	General director /HYDRO Mekin
3.	DJUIDJE KENMOE spouse ALOYEM	Professor	On duty
4.	EKOBENA FOU DA Henri Paul	Professor	Vice-Rector Univ. Ngaoundéré
5.	ESSIMBI ZOBO Bernard	Professor	On duty
6.	EYEBE FOU DA Jean sire	Professor	On duty
7.	HONA Jacques	Professor	On duty
8.	NANA ENGO Serge Guy	Professor	On duty
9.	NANA NBENDJO Blaise	Professor	On duty
10.	NDJAKA Jean Marie Bienvenu	Professor	Head of Department
11.	NJANDJOCK NOUCK Philippe	Professor	On duty
12.	NOUAYOU Robert	Professor	On duty
13.	SAIDOU	Professor	Chief of centre /IRGM/MINRESI
14.	SIMO Elie	Professor	On duty
15.	TABOD Charles TABOD	Professor	Dean FS Univ. Bamenda
16.	TCHAWOUA Clément	Professor	On duty
17.	WOAFO Paul	Professor	On duty
18.	ZEKENG Serge Sylvain	Professor	On duty
19.	ENYEGUE A NYAM épouse BELINGA	Associate Professor	On duty
20.	FEWO Serge Ibraïd	Associate Professor	On duty
21.	FOUEJIO David	Associate Professor	Chief of Cell MINADER
22.	MBINACK Clément	Associate Professor	On duty
23.	MBONO SAMBA Yves Christian U.	Associate Professor	On duty
24.	MEL'I Joelle Larissa	Associate Professor	On duty
25.	MVOGO ALAIN	Associate Professor	On duty
26.	NDOP Joseph	Associate Professor	On duty
27.	SIEWE SIEWE Martin	Associate Professor	On duty
28.	VONDOU Derbetini Appolinaire	Associate Professor	On duty
29.	WAKATA née BEYA Annie Sylvie	Associate Professor	Director/ENS/UIYI
30.	WOULACHE Rosalie Laure	Associate Professor	In training course
31.	ABDOURAHIMI	Senior Lecturer	On duty
32.	AYISSI EYEBE Guy François Valérie	Senior Lecturer	On duty
33.	CHAMANI Roméo	Senior Lecturer	On duty
34.	DJIOTANG TCHOTCHOU Lucie Angennes	Senior Lecturer	On duty
35.	EDONGUE HERVAIS	Senior Lecturer	On duty
36.	KAMENI NEMATCHOUA Modeste	Senior Lecturer	On duty
37.	LAMARA Maurice	Senior Lecturer	On duty
38.	NGA ONGODO Dieudonné	Senior Lecturer	On duty
39.	OTTOU ABE Martin Thierry	Senior Lecturer	Director of reagents production Unit IMPM
40.	TEYOU NGOUPO Ariel	Senior Lecturer	On duty
41.	WANDJI NYAMSI William	Senior Lecturer	On duty
42.	SOUFFO TAGUEU Merimé	Assistant Lecturer	On duty
43.	BEN- BOLIE Germain Hubert	Professor	On duty

<b>10- DEPARTMENT OF EARTH SCIENCES (ES) (42)</b>			
1	BITOM Dieudonné-Lucien	Professor	<b>Dean / FASA /Univ. Dschang</b>
2	EKOMANE Emile	Professor	<b>Head of Division /Univ Ebolowa</b>
3	GANNO Sylvestre	Professor	En poste
4	NDAM NGOUPAYOU Jules-Remy	Professor	On duty
5	NDJIGUI Paul-Désiré	Professor	<b>Head of Department</b>
6	NGOS III Simon	Professor	On duty
7	NKOUMBOU Charles	Professor	On duty
8	NZENTI Jean-Paul	Professor	On duty
9	ONANA Vincent Laurent	Professor	<b>Head of Department/ Univ. Ebolowa</b>
10	YENE ATANGANA Joseph Q.	Professor	<b>Head of Division /MINTP</b>
11	BISSO Dieudonné	Associate Professor	On duty
12	Elisé SABABA	Associate Professor	On duty
13	EYONG John TAKEM	Senior Lecturer	On duty
14	FUH Calistus Gentry	Associate Professor	<b>State secretary /MINMIDT</b>
15	GHOGOMU Richard TANWI	Associate Professor	<b>Head of division /Univ. Bertoua</b>
16	MBIDA YEM	Associate Professor	On duty
17	MBESSE Cécile Olive	Senior Lecturer	On duty
18	METANG Victor	Senior Lecturer	On duty
19	MOUNDI Amidou	Associate Professor	<b>TC /MINIMDT</b>
20	NGO BIDJECK Louise Marie	Associate Professor	On duty
21	NGUEUTCHOUA Gabriel	Associate Professor	<b>CEA/MINRESI</b>
22	NJILAH Isaac KONFOR	Associate Professor	On duty
23	NYECK Bruno	Associate Professor	On duty
24	TCHAKOUNTE Jacqueline épouse NUMBEM	Associate Professor	<b>Chief of Cell /MINRESI</b>
25	TCHOUANKOUE Jean-Pierre	Associate Professor	On duty
26	TEMGA Jean Pierre	Associate Professor	On duty
27	ZO'O ZAME Philémon	Associate Professor	<b>General Director/ART</b>
28	ANABA ONANA Achille Basile	Senior Lecturer	On duty
29	BEKOA Etienne	Senior Lecturer	On duty
30	ESSONO Jean	Senior Lecturer	On duty
31	MAMDEM TAMTO Lionelle Estelle, épouse BITOM	Senior Lecturer	On duty
32	MINYEM Dieudonné	Senior Lecturer	<b>Head of division /Univ. Maroua</b>
33	NGO BELNOUN Rose Noël	Senior Lecturer	On duty
34	NGO'O ZE ARNAUD	Senior Lecturer	On duty
35	NOMO NEGUE Emmanuel	Senior Lecturer	On duty
36	NTSAMA ATANGANA Jacqueline	Senior Lecturer	On duty
37	TCHAPTCHET TCHATO De P.	Senior Lecturer	On duty
38	TEHNA Nathanaël	Senior Lecturer	On duty
39	FEUMBA Roger	Senior Lecturer	On duty
40	MBANGA NYOBE Jules	Senior Lecturer	On duty
41	KOAH NA LEBOGO Serge Parfait	Assistant Lecturer	On duty

42	TENE DJOUKAM Joëlle Flore, spouse KOUANKAP NONO	Assistant Lecturer	On duty
----	--	--------------------	---------

**DISTRIBUTION OF PERMANENT LECTURERS IN THE FACULTY OF  
SCIENCE OF THE UNIVERSITY OF YAOUNDE I ACCORDING TO  
DEPARTMENTS**

<b>NUMBER OF LECTURERS</b>					
<b>Department</b>	<b>Professors</b>	<b>Associate Professors</b>	<b>Senior Lecturers</b>	<b>Assist. Lecturers</b>	<b>Total</b>
BCH	8 (01)	20 (12)	9 (04)	6 (05)	<b>43 (22)</b>
BPA	11 (01)	19 (09)	16 (05)	3 (02)	<b>49 (17)</b>
BPV	6 (01)	10 (02)	14 (08)	2 (00)	<b>32 (11)</b>
CI	7 (01)	14 (04)	5 (01)	1 (00)	<b>27 (06)</b>
CO	7 (01)	15 (05)	11 (05)	1 (00)	<b>33 (11)</b>
RE	1(00)	/	/	/	<b>1(0)</b>
IN	2 (00)	2 (00)	14 (01)	4 (00)	<b>22 (01)</b>
MAT	1 (00)	8 (00)	19 (02)	5 (01)	<b>33 (03)</b>
MIB	3 (01)	7 (03)	9 (05)	5 (02)	<b>24 (11)</b>
PHY	18 (01)	12 (04)	11 (01)	1 (00)	<b>42 (06)</b>
ST	10 (00)	17 (03)	13 (03)	3 (01)	<b>43 (07)</b>
<b>Total</b>	<b>74 (07)</b>	<b>124 (42)</b>	<b>121 (35)</b>	<b>31 (11)</b>	<b>350 (95)</b>

A total of.....**349 (95)**, with :

Professors.....**73 (07)**

Associate Professors.....**124 (42)**

Senior Lecturers.....**121 (35)**

Assistant Lecturers.....**31 (11)**

( ) = Number of women.....**95**

## *DEDICATION*

*This piece of work is dedicated to:*

*MY FAMILY*

## *ACKNOWLEDGEMENTS*

The voices of even a million of angels could not be sufficient to express my great gratitude. All that I am, and ever hope to be, I owe it all to Thee. To God be the glory!!!

This work has been successful due to the endless contributions of many people. I wish to express my profound gratitude to the following persons or group of persons who directly or indirectly contributed to the validation of my dream of presenting this thesis report:

**First and foremost, my supervisor Prof. Fabrice Fekam Boyom:** Professor, just like a father you transmitted to me values, like a mentor you opened the way for me, then like a leader you held my hands to move forward and finally you accompanied me on that way. You have as far as possible spared no effort to help me achieving the objectives related to this work. Also, you believed in me more than anyone, and you judged me capable of bearing this research topic which you qualified as pioneer. I never felt forsaken or neglected at each step and your support has been unwavering from the very beginning. Moreover, the responsibilities and tasks that you entrusted to me enabled me to have additional aptitudes. I am happy for the mileage and the challenges overcome during this journey that enable me to be the one you are proud of today. Find through this masterpiece the testimony of my deep gratitude.

**Prof. Paul Moundipa Fewou:** Head of Department of Biochemistry, Faculty of Science, University of Yaounde I, for the relentless efforts towards the achievement of this study so far and for the facilities placed at my disposal to enable me carry out the studies.

**All the entire staff members of the Department of Biochemistry,** for the knowledge and encouragement during the research.

**Prof Bruno Lenta Ndjakou:** The coordinator of the YaBiNaPA (Yaoundé-Bielefeld Graduate School for Natural Products with Antiparasite and Antibacterial Activity) project through which I could benefit from the materials and important chemicals used in my experiments. Moreover, I would like to congratulate you for the implementation of this project, which provides research facilities to young Ph.D. students in Cameroon.

I am also indebted to my two thesis companions **Dr. Cyrille Armel Njanpa Ngansop,** and **Mr. Mariscal Brice Tchatat Tali** with whom I have worked tirelessly to implement parasite and cell culture as well as antiparasitic drug screening. It has been a pleasure working with such engaging and lovely people. I wish us to remain knit together and build significant contribution toward antiparasitic drug discovery.

A special thank you to **Dr. Rodrigue Keumoe** for his assistance during mode of action assays. I simply could not have done this without you.

**Drs Tsouh Fokou Patrick Valere, Tchokouaha Yamthe Lauve Rachel, Jean Baptiste Hzounda Fokou, Marie Rufin Toghueo Kouipou, Boniface Kamdem Pone, Dongmo Mireille, Jiatsa Mbouna Cedric, Pierre Eke**, your guidance, advice and understanding across the years has been invaluable and deeply appreciated. I am also grateful for help in reviewing this thesis.

My appreciation also goes to **Dr Michelle Inès Mbekou, Mrs Michelle Nguembou, Vanessa Nya Dinango, Aude Dougue**, and **Mr Lavin, Yannick Melogmo** for their unwavering belief in me and words of wisdom during challenging times.

**All the doctors, laboratory seniors, juniors, classmates** of the Antimicrobial and Biocontrol Agent Unit for the warm atmosphere that has always reigned between us, and their various contributions to this work.

I am very lucky to feel the love and support of many school friends, but I extend a special thank you to the closest **Mrs Fustelle Kamka Fotso, Cybelle Fodieu Mezajou, Pamela Tchamfa Kapche, Marie Michele Lonang, Fleurine Lekeulem, Mr. Emmanuel Shalom, Claude Bernard Djomeni, Yvon** for their life-long friendship, their moral support that boosted and encouraged me to complete Ph.D. work.

**All the members of Kamche's, Koliou's families and the Way international** for their prayers, material and financial assistance toward the fulfillment of this research work.

**Mr. Elobo Gervais**, for generously providing a high-performance computer that allowed me to work from data analyses to the drafting of this document.

I am also grateful for the contributions received from the following establishments to achieve this research work :

- ✓ The **MMV** (Medicines for Malaria Venture) for support, design and supply the Pathogen Box and analogues of compound MMV675968.
- ✓ The **Research Unit in Bioinformatics (RUBi)**, Department of Biochemistry and Microbiology, Rhodes University, South Africa for performing computational studies.
- ✓ **The German Academic Exchange Service (DAAD)** through the Yaoundé-Bielefeld Graduate School for Natural Products with Antiparasite and Antibacterial Activities [YaBiNaPA project no. 57316173] for the material and some equipment.
- ✓ **BEI. Resources** (Biodefense and Emerging Infections) for graciously providing us with *Trypanosoma brucei* spp. strains necessary for the *in vitro* antitrypanosomal assays.
- ✓ **The Malaria Research Unit** of the Pasteur Center of Cameroun for kindly providing us with Vero cells for cytotoxicity assessments.

## *FINANCIAL SUPPORT*

This work was supported by the following projects:

- ✓ **The Grand Challenges Africa programme [GCA/DD/rnd3/006 to FFB].**

Grand Challenges Africa is a programme of the African Academy of Sciences (AAS) that was implemented through the Alliance for Accelerating Excellence in Science in Africa (AESA) [an initiative of the AAS, the African Union Development Agency and the New Partnership for Africa's Development (AUDA-NEPAD)]". For this work GC Africa is supported by the African Academy of Sciences (AAS), Bill & Melinda Gates Foundation (BMGF), Medicines for Malaria Venture (MMV), and Drug Discovery and Development Centre of University of Cape Town (H3D).

- ✓ **MMV through the Pathogen Box Challenge grant** number PO 15/01083[03] to Prof. Boyom

# TABLE OF CONTENTS

DEDICATION .....	xiii
ACKNOWLEDGEMENTS .....	xiv
FINANCIAL SUPPORT .....	xvi
TABLE OF CONTENTS .....	xvii
ABBREVIATIONS AND ACRONYMS .....	xxi
LIST OF TABLES .....	xxiii
LIST OF FIGURES .....	xxiv
LIST OF APPENDICES .....	xxvi
ABSTRACT .....	xxvii
RESUME .....	xxix
LITERATURE REVIEW .....	3
<i>I.1. Generalities on African Trypanosomiasis .....</i>	<i>3</i>
<i>I.1.1. Definition .....</i>	<i>3</i>
<i>I.1.2. The pathogen agents .....</i>	<i>3</i>
<i>I.1.2.1. The pathogenic agent .....</i>	<i>3</i>
<i>I.1.2.2. Disease transmission and Vector .....</i>	<i>7</i>
<i>I.1.3. Geographical distribution, epidemiology, and socioeconomic impact of African trypanosomiasis .....</i>	<i>9</i>
<i>I.1.3.1. Geographical distribution .....</i>	<i>9</i>
<i>I.1.3.2. Epidemiology and socioeconomic impact .....</i>	<i>10</i>
<i>I.1.4. Clinical manifestations .....</i>	<i>14</i>
<i>I.1.4.1. HAT symptoms .....</i>	<i>14</i>
<i>I.1.4.2. AAT symptoms .....</i>	<i>17</i>
<i>I.1.5. Diagnosis .....</i>	<i>17</i>
<i>I.1.6 Control measures .....</i>	<i>18</i>
<i>I.1.6.1. Vector control and prospects for vaccine development .....</i>	<i>19</i>
<i>I.1.6.2. Chemotherapy for African Trypanosomiasis .....</i>	<i>19</i>
<i>I.1.7 Dihydrofolate reductase and trypanothione reductase as drug targets in Trypanosoma brucei .....</i>	<i>30</i>
<i>I.2. Drug discovery and development of new candidates for management of trypanosomiasis .....</i>	<i>33</i>
<i>I.2.1. Steps in drug discovery phases .....</i>	<i>33</i>
<i>I.2.1.1. Hit identification and hit to lead phase .....</i>	<i>34</i>
<i>I.2.1.2. Lead optimization phase .....</i>	<i>35</i>
<i>I.2.1.3. Target identification .....</i>	<i>35</i>
<i>I.2.1.4. Target validation .....</i>	<i>35</i>

1.2.1.5. Preclinical and clinical evaluation .....	35
1.2.2. Drug discovery strategies .....	37
1.2.2.1. De novo drug discovery strategy.....	37
1.2.2.2. Target-based approach .....	37
1.2.2.3. Phenotypic drug screening.....	38
1.2.1.4. Drug repositioning approach.....	38
1.3. Molecular docking tools in the drug discovery and development process.....	42
1.3.1. Overview .....	42
1.3.5. Molecular dynamics.....	45
1.4. Pharmacokinetic evaluation in the drug discovery and development process.....	46
1.4.1. Overview .....	46
1.4.2. Key pharmacokinetic parameters .....	47
Aim and objectives.....	50
<b>II. MATERIALS AND METHODS .....</b>	<b>51</b>
<b>II.1. Materials.....</b>	<b>51</b>
II.1.1. MMV Pathogen Box acquisition and storage .....	51
II.1.2. Parasites and mammalian cells .....	51
II.1.2.1. Strains of <i>Trypanosoma brucei</i> .....	51
II.1.2.2. Mammalian cell lines.....	51
II.1.3. Material and reagent sources .....	51
<b>II.2. Methods .....</b>	<b>52</b>
II.2.1. In vitro antitrypanosomal activity of MMV compounds .....	52
II.2.1.1 Antitrypanosomal assay development.....	52
II.2.1.2 Antitrypanosomal screening of the 400 MMV compounds .....	54
II.2.1.3. Cytotoxicity study of selected compounds .....	55
II.2.2. Structure-activity and selectivity relationship study.....	57
II.2.3. In silico and in vitro activities of compounds on their likely molecular target .....	59
II.2.3.1. In silico exploration of the DHFR and TR binding properties of selected analogs.....	59
II.2.3.2. In vitro screening against <i>T.b.b.</i> crude protein extract .....	61
II.2.4. Attempts to elucidate other antitrypanosomal modes of action of the promising analogs and prediction of pharmacokinetic properties.....	64
II.2.4.1. In vitro determination of parasite-killing kinetics of selected derivatives .....	64
II.2.4.2. Assessment of the cidal or static effect of the inhibitors .....	64
II.2.4.3. Effect of compounds on trypanosome plasma membrane integrity .....	64
II.2.4.4. Induction of intracellular reactive oxygen species (ROS) production by trypanosomes upon treatment with inhibitors .....	65

II.2.4.5. Induction of cellular DNA fragmentation upon trypanosome treatment with inhibitors .....	66
II.2.4.6. Determination of the Ferric Ion Reducing Antioxidant Power (FRAP) of inhibitors .....	67
II.2.4.7. Prediction of ADME parameters of selected analogs.....	68
II.3. Statistical analysis .....	68
III. RESULTS AND DISCUSSION .....	69
III.1. Identification of pathogen box compounds as inhibitors of bloodstream forms of <i>Trypanosoma brucei</i> <i>brucei</i> .....	69
III.1.1. Assay development of the antitrypanosomal test .....	69
III.1.1.1. <i>Trypanosoma brucei brucei</i> growth profile .....	69
III.1.1.2. Linearity of resazurin cell viability assays .....	70
III.1.1.3. DMSO tolerance of trypanosomes, median inhibitory concentration ( $IC_{50}$ ) of pentamidine and robustness of the test .....	71
III.1.2. Preliminary screening and median inhibitory concentrations ( $IC_{50}$ ) of selected compounds from the MMV Pathogen Box .....	72
Discussion .....	79
III.2. Rudimentary Structure-Activity-Relationship (SAR) study with 23 analogs of 2,4-diaminoquinazoline (MMV675968) .....	82
III.3. <i>In silico</i> and <i>in vitro</i> activities of compounds on their likely molecular target.....	92
III.3.1. <i>In silico</i> exploration of trypanosomal DHFR and TR inhibition by analogs 7 (MMV1578467) and 10 (MMV1578467) .....	92
III.3.1.1. Accessible protonation states of the compounds and molecular docking .....	92
III.3.1.2. Ligand conformational refinement and binding stability monitoring through molecular dynamics simulations .....	93
III.3.2. Preliminary <i>in vitro</i> validation of DHFR as a target for compounds 7 (MMV1578467) and 10 (MMV1578467) .....	97
III.3.2.1. Protein quantification and confirmation .....	97
III.3.2.2. Enzyme activity and inhibitory effect of 7 (MMV1578467) and 10 (MMV1578467) .....	98
Discussion .....	100
III.4. Tentative elucidation of other modes of action of analogs 7 and 10 against <i>T.b. brucei</i> .....	102
III.4.1. <i>In vitro</i> kinetics of <i>T.b. brucei</i> killing upon treatment with analogs 7 (MMV1578467) and 10 (MMV1578445) .....	102
III.4.2. Effect of analogs 7 (MMV1578467) and 10 (MMV1578445) on plasma membrane integrity .....	105
III.4.3. Induction of oxidative stress in trypanosomes by compounds 7 and 10 .....	105
III.4.4. Analog 10 induces DNA fragmentation in trypanosomes as a marker of cell death .....	106
III.4.5. Ferric ion reducing antioxidant power (FRAP) of Inhibitors .....	107
III.4.6. Predicted pharmacokinetic profile of the compounds of interest .....	108
Discussion .....	111

CONCLUSION ..... 114  
PERSPECTIVES..... 115  
REFERENCES..... 116  
APPENDICES AND PUBLICATION ..... a

## *ABBREVIATIONS AND ACRONYMS*

<b>AAT</b>	African animal trypanosomiasis
<b>ADMET</b>	Absorption, distribution, metabolism, excretion, toxicity
<b>ApoL1</b>	Apolipoprotein-L1
<b>BBB</b>	Blood-brain barrier
<b>Brdu</b>	5'-bromo-2'-deoxyuridine
<b>CATT</b>	Card agglutination test for trypanosomiasis
<b>CC<sub>50</sub></b>	50% cytotoxic concentration
<b>CNS</b>	Central nervous system
<b>CSF</b>	Cerebral spinal fluid
<b>DDT</b>	Dichlorodiphenyltrichloroethane
<b>DHFR</b>	Dihydrofolate reductase
<b>DMEM</b>	Dulbecco's Modified Eagle's Medium
<b>DMQ</b>	Diaminoquinazoline
<b>dUMP</b>	deoxyuridine monophosphate
<b>dTTP</b>	Deoxythymidine triphosphate
<b>EDTA</b>	Ethylenediaminetetraacetic acid
<b>ELISA</b>	Enzyme-Linked ImmunoSorbent Assay
<b>FAO</b>	Food and agriculture organization
<b>FRAP</b>	Ferric ion reducing antioxidant power
<b>GPI</b>	Glycosylphosphatidylinositol
<b>H<sub>2</sub>DCF-DA</b>	2',7'-Dichlorofluorescein diacetate
<b>HAT</b>	Human african trypanosomiasis
<b>HBA</b>	Hydrogen bond acceptor
<b>HBD</b>	Hydrogen bond donor
<b>HIA</b>	Human intestinal absorption
<b>HIFBS</b>	Heat inactivated fetal Bovin Serum
<b>HMI-9</b>	Hirumi's modified Iscove's medium 9
<b>Hp-Hb</b>	Haptoglobin-hemoglobin
<b>HTS</b>	High-throughput screening
<b>IC<sub>50</sub></b>	50% Inhibitory concentration
<b>IMDM</b>	Iscove's modified dulbecco's medium
<b>IND</b>	Investigational new drug
<b>kDa</b>	Kilodalton
<b>MD</b>	Molecular dynamic
<b>MMV</b>	Medecines for malaria venture
<b>MMVPB</b>	Medicine for malaria venture pathogen box
<b>MTX</b>	Methotrexate
<b>MW</b>	Molecular weight

<b>NADPH</b>	Nicotinamide adenine dinucleotide phosphate reduced form
<b>NTD</b>	Neglected tropical disease
<b>Papp</b>	Apparent permeability coefficient
<b>PCR</b>	Polymerase chain reaction
<b>PDB</b>	Protein data bank
<b>PIC<sub>50</sub></b>	Negative log of the IC <sub>50</sub> value when converted in molar
<b>PK</b>	Pharmacokinetic
<b>PKa</b>	Negative base-10 logarithm of a solution's acid dissociation constant
<b>PME</b>	Particle-mesh Ewald
<b>POD</b>	Peroxidase
<b>PPB</b>	Plasma protein binding
<b>P-pg</b>	P-glycoprotein
<b>PPPs</b>	Public private partnerships
<b>PRONETRY</b>	Programme national d' Eradication des trypanosomoses au Cameroun.
<b>RCSB</b>	Research Collaboratory for structural bioinformatics
<b>RMSD</b>	Root mean square deviation
<b>RMSF</b>	Root mean square fluctuation
<b>ROG</b>	Radius of gyration
<b>ROS</b>	Reactive oxygen species
<b>SAR</b>	Structure-activity relationship
<b>SDS-PAGE</b>	Sodium dodecyl sulfate-polyacrylamide gel electrophoresis
<b>SG</b>	Sybr-green
<b>SI</b>	Selectivity index
<b>SIF</b>	Stumpy induction factor
<b>THF</b>	Tetrahydrofolate
<b>TLF-1</b>	Trypanosome lytic factor-1
<b>TS</b>	Thymidylate synthetase
<b>VSG</b>	Variant surface glycoproteins
<b>WHO</b>	World health organization

## LIST OF TABLES

<b>Table I:</b> Drugs approved for the treatment of human and animal African trypanosomiasis.....	25
<b>Table II:</b> Examples of successfully repurposed drugs .....	40
<b>Table III:</b> Role of pharmacokinetics in the development of new drugs.....	47
<b>Table IV:</b> Z'-Factor and IC <sub>50</sub> of the standard drug.....	72
<b>Table V:</b> Antitrypanosomal activity of reference drugs included in the MMV Pathogen Box.....	73
<b>Table VI:</b> <i>In vitro</i> antitrypanosomal and cytotoxic activities of the 25 MMVPB compounds with known anti-kinetoplastid activity .....	75
<b>Table VII:</b> <i>In vitro</i> antitrypanosomal and cytotoxic activities of the 38 MMVPB compounds with known potency against other diseases.....	77
<b>Table VIII:</b> Rudimentary SAR study of 5-chloro-2,4-diaminoquinazoline (MMV675968) analogs for improved antitrypanosomal activity and selectivity. ....	82
<b>Table IX:</b> Residues interacting with compounds 7 and 10 within the binding sites of DHFR and TR .....	96
<b>Table X:</b> Predicted ADME/TOX parameters of compound 1 (MMV675968) and structural analogues 7 (MMV1578467) and 10 (MMV1578445).....	109

## *LIST OF FIGURES*

<b>Figure 1:</b> Cellular structure of an African trypanosome.....	5
<b>Figure 2:</b> A simplified sketch of the life cycle of African trypanosomes .....	7
<b>Figure 3:</b> <i>Glossina fuscipes</i> tsetse fly.....	8
<b>Figure 4:</b> Number of sleeping sickness cases reported by country .....	9
<b>Figure 5:</b> Cameroon HAT notification cases from 2014 to 2019.....	12
<b>Figure 6:</b> The main animal diseases and prevalence .....	14
<b>Figure 7:</b> Clinical manifestations of HAT in the first stage .....	15
<b>Figure 8:</b> Patients with stage 2 HAT .....	16
<b>Figure 9:</b> Cattle trypanosomiasis.....	17
<b>Figure 10:</b> Chemical structure of the drugs used for human and animal African trypanosomiasis treatment.....	29
<b>Figure 11:</b> Folate metabolism and the thymidylate cycle in <i>T. brucei</i> .....	31
<b>Figure 12:</b> Substrates of glutathione reductase (GR) and trypanothion reductase (TR).....	33
<b>Figure 13:</b> Overview of the drug discovery and development process.....	34
<b>Figure 14:</b> Distribution of the disease targeted by the pathogen box compounds and references .	41
<b>Figure 15:</b> Example of a drug candidate (gray–red colors) binding to a target (blue color).....	42
<b>Figure 16:</b> Simplified scheme of the structural modifications performed on the initial compound .....	58
<b>Figure 17:</b> Principle of the cellular DNA fragmentation assay.....	67
<b>Figure 18:</b> Summary of the screening funnel used for the hit optimization process.....	68
<b>Figure 19:</b> Illustration of bloodstream counts of <i>Trypanosoma brucei brucei</i> using a Lumascope LS520 inverted fluorescence .....	69
<b>Figure 20:</b> Linearity between the detected numbers of <i>T. b. brucei</i> parasites and the resazurin reduction signal after 72 h of incubation.....	70

<b>Figure 21:</b> DMSO tolerance and pentamidine isethionate 50% inhibitory concentration estimation from the <i>Trypanosoma brucei brucei</i> resazurin-based viability .....	71
<b>Figure 22:</b> Antitrypanosomal activity cut-off of the 400 MMVPB compounds .....	73
<b>Figure 23:</b> Funnel pipeline of the performed antitrypanosomal drug screening process .....	90
<b>Figure 24:</b> Docking poses and Vina docking scores .....	93
<b>Figure 25:</b> Evolution of ligand RMSD with respect to protein and hydrogen bond numbers during simulation .....	95
<b>Figure 26:</b> Coomassie blue stained SDS–PAGE gel showing the proteins eluted from T. b. b. lysates .....	97
<b>Figure 27:</b> Measurement of the <i>T. b. b.</i> lysate protein activity. ....	98
<b>Figure 28:</b> <i>In vitro</i> concentration-dependent effect of inhibitors on the predicted <i>T. b. b.</i> DHFR enzyme activity .....	100
<b>Figure 29:</b> Growth curves of <i>T.b. brucei</i> in the presence or absence of various concentrations of compounds 7 and 10 and pentamidine. ....	104
<b>Figure 30:</b> Depiction of the effect of inhibitors on membrane integrity .....	105
<b>Figure 31:</b> Production of intracellular reactive oxygen species (ROS).....	106
<b>Figure 32:</b> DNA fragmentation and cytolysis induced by compound 10 in bloodstream forms of <i>Trypanosoma brucei brucei</i> . ....	107

## *LIST OF APPENDICES*

<b>Appendix 1:</b> DHFR substrate structure .....	a
<b>Appendix 2:</b> Preparation of culture media and preservation solutions .....	a
<b>Appendix 3:</b> BSA standard curve generation procedure .....	b
<b>Appendix 4:</b> Supplementary information for the SDS-PAGE procedure .....	c
<b>Appendix 5:</b> IC <sub>99</sub> , IC <sub>90</sub> and IC <sub>10</sub> (μM) of the prioritized compounds.....	d
<b>Appendix 6:</b> Details of the DNA fragmentation procedure .....	d
<b>Appendix 7:</b> Trypanosomes viability percentages following treatment with DMSO and pentamidine at diverse concentrations .....	e
<b>Appendix 8:</b> Chemical structures of the 25 antitrypanosomal MMVPB hit compounds with known anti-kinetoplastid activity.....	g
<b>Appendix 9:</b> Chemical structures of the 38 antitrypanosomal MMVPB hit compounds with known potency against other diseases.....	p

## ABSTRACT

African trypanosomiases are neglected tropical diseases (NTDs) that still exact a considerable toll to humans and animals in endemic countries. Unfortunately, the numerous drawbacks (toxicity, ineffectiveness, treatment duration and resistance) of the currently available therapies represent the main bottleneck for disease management and elimination. Thus, there is an urgent need to develop new alternative, effective and safe treatments to manage this infectious illness. The present work aims to explore the Medicines for Malaria Venture's Open Access Pathogen Box library (MMVPB) for potential antitrypanosomal hits compounds. Within this scope, 400 compounds from the MMVPB library were subjected to preliminary antitrypanosomal screening at a single dose of 10  $\mu\text{M}$  using the resazurin-based cell viability assay. Compounds displaying an inhibitory percentage greater than or equal to 90% were selected for concentration-response studies against *Trypanosoma brucei brucei* Lister 427 VSG 221. The African green monkey kidney cell line Vero was used to determine the selectivity of promising inhibitors. Subsequently, a small library of analogs of one of the identified hits available at MMV as solid materials was screened for antitrypanosomal and cytotoxic activities using the same conditions. Thereafter, in an attempt to determine the metabolic targets of promising hits, *in silico* exploration of the most potent antitrypanosomal analogs was undertaken on trypanosome dihydrofolate reductase (DHFR) and trypanothione reductase (TR). Furthermore, a tentative assessment of the *in vitro* inhibitory activity of these compounds was carried out on DHFR using a crude trypanosome extract. According to previously described protocols, time-kill kinetics, *in vitro* trypanocidal reversibility, plasma membrane integrity tests, measurement of reactive oxygen species, DNA fragmentation analysis and ferric iron reducing potency assays were conducted to uncover other possible antitrypanosomal modes of action of the most promising hits. Overall, from 400 compounds tested against *T.b. brucei*, seventy (63 compounds and 07 reference) showed 90 % inhibition. Most of these compounds showed moderate (42 compounds)-to-high (21 compounds) *in vitro* inhibition against *Trypanosoma brucei brucei* with  $\text{IC}_{50}$  values ranging from 0.0023 to 9.78  $\mu\text{M}$  and high selectivity toward Vero cells (5 - >42,826). The preliminary structure-activity relationship (SAR) study using available analogs of **MMV675968** ( $\text{IC}_{50}$  = 2.8  $\mu\text{M}$ ; SI = 37.87) led to the identification of two hits, **MMV1578445 (10)** ( $\text{IC}_{50}$  = 0.045  $\mu\text{M}$ , SI = 1737) and **MMV1578467 (7)** ( $\text{IC}_{50}$  = 0.06  $\mu\text{M}$ ; SI = 412), that were approximately 40-fold and 60-fold more potent and selective, respectively, than the parent compound (**MMV675968**-,4 diaminoquinazoline). *In silico* deciphering of the effect of analogs **7** and **10** indicated that both compounds are potent binders of the DHFR enzyme, binding in all their accessible protonation states, and engendering interactions with key DHFR ligand recognition residues such as Val32,

Asp54, and Ile160. They also tentatively exhibited significant *in vitro* activity against DHFR in a trypanosome crude protein isolate. The growth pattern of *Trypanosoma brucei brucei* after extended (72 h) and short (4 h) exposure times to drugs revealed fast and irreversible growth arrest (confirmed upon subculture) for analog **MMV1578445 (10)** whereas a slow-acting and reversible profile was recorded when compound **MMV1578467 (7)** was incubated with *T.b. brucei* at their respective IC<sub>99</sub>. Results from the mode of action revealed that analogs **7** and **10** exerted antitrypanosomal effect via reduction of ferric iron and DNA fragmentation or apoptosis, respectively. Noteworthy, compounds **7** and **10** did not affect neither the intracellular level of ROS nor the membrane permeability. Pharmacokinetic studies revealed that the most promising compounds abide to the Lipinski's rules of five that define property boundaries for molecular weight, lipophilicity, polar surface area, hydrogen bonding and charge. The tested compounds were found to possess moderate solubility and high intestinal absorption. The two potent analogues endowed with suitable physicochemical properties are good candidates for further deciphering their potential as starting points for new drug development for HAT.

**Key words:** *Trypanosoma brucei brucei*, MMV Pathogen Box, Antitrypanosomal, 2,4 Diaminoquinazoline, Structure-activity relationship, Mode of action, *In silico*.

## RESUME

La trypanosomiase africaine est une maladie tropicale négligée (MTN) qui affecte à la fois l'Homme et les animaux dans les pays endémiques. Malheureusement, les nombreux inconvénients (toxicité, inefficacité, la longueur du traitement et résistance) associés aux traitements actuels représentent le principal frein pour l'élimination de cette maladie. Cette situation souligne donc l'urgence de développer de nouveaux traitements alternatifs, efficaces et adaptés à la prise en charge de cette maladie infectieuse. Dans cette optique, le présent travail a été conçu pour évaluer l'activité antitrypanosomale d'une collection de composés de la « Medicines for Malaria Venture » (MMV) appelée « Pathogen Box ». Dans ce but, 400 composés de la « Pathogen Box » ont été soumis à un criblage préliminaire de l'activité antitrypanosomale à une concentration fixe de 10  $\mu\text{M}$  en utilisant le test de viabilité cellulaire à la résazurine. Les composés présentant un pourcentage d'inhibition supérieur ou égal à 90 % ont été sélectionnés pour les études concentration-réponse sur la souche *Trypanosoma brucei brucei* Lister 427 VSG 221. D'autre part, la lignée cellulaire du rein de singe vert d'Afrique Vero a été utilisée pour déterminer la cytotoxicité des inhibiteurs prometteurs. Par la suite, une petite collection d'analogues d'un des composés identifiés a été testée pour les activités antitrypanosomales et cytotoxiques dans les mêmes conditions. Subséquemment, dans l'objectif d'identifier les cibles métaboliques des inhibiteurs, les analogues les plus actifs ont été testés *in silico* sur les enzymes dihydrofolate réductase (DHFR) et trypanothione réductase (TR). Par la suite, l'activité observée a été confirmée *in vitro* en utilisant un extrait protéique de *T.b.brucei*. Par ailleurs, d'autres modes d'action tels que la cinétique d'inhibition, la réversibilité de l'effet trypanocide, l'effet sur l'intégrité de la membrane plasmique, l'induction de la production des espèces oxygénées réactives, la fragmentation de l'ADN et le pouvoir réducteur du fer ferrique ont été évalués. Au total, soixante-dix (7 médicaments de référence et 63 composés) composés ont inhibé la croissance de *T.b. brucei* avec un pourcentage d'inhibition supérieur ou égal à 90 %. De l'étude concentration-réponse, il ressort que ces composés ont pour la plupart présenté une inhibition modérée (42) à élevée (21) avec des valeurs de  $\text{CI}_{50}$  variant de 9.78 à 0.0023  $\mu\text{M}$  et une sélectivité élevée sur les cellules Vero (5 - >42,826). L'étude préliminaire de la relation structure-activité du composé **MMV675968** ( $\text{CI}_{50}$  = 2,8  $\mu\text{M}$  ; SI = 37,87) a conduit à l'identification de deux analogues, **MMV1578445** (**10**) ( $\text{CI}_{50}$  = 0,045  $\mu\text{M}$  ; SI=1737) et **MMV1578467** (**7**) ( $\text{CI}_{50}$  = 0,06  $\mu\text{M}$  ; SI = 412), qui étaient environ 40 et 60 fois plus actifs et sélectifs, respectivement, que le composé parent (**MMV675968**). L'étude *in silico* des analogues **7** et **10** sur deux enzymes du trypanosome [dihydrofolate réductase (DHFR) et la trypanothione reductase (TR)] a montré leur effet inhibiteur sur la DHFR uniquement. En effet, des interactions entre le DHFR et les analogues **7** et **10** (sur tous leurs états de protonation) ont été identifiées, avec une présence effective des résidus d'acide

aminés, tels que Val32, Asp54 et Ile160 dans le site d'action. Ils ont également présenté une activité *in vitro* significative sur l'extrait brut de protéine contenant l'enzyme DHFR. Le profil de croissance de *Trypanosoma brucei brucei* après des temps d'exposition prolongés (72 h) et courts (4 h) avec les composés **7** et **10** a révélé un arrêt de croissance rapide et irréversible (confirmé après subculture) pour l'analogue **MMV1578445** (**10**) mais un profil d'action lent et réversible pour l'analogue **MMV1578467** (**7**) à leur IC<sub>99</sub> respective. L'étude du mode d'action a indiqué que les composés **7** et **10** induiraient une réduction du fer ferrique, et une fragmentation de l'ADN du parasite, respectivement. Toutefois, les composés **7** et **10** n'ont pas agi sur la perméabilité membranaire et le taux d'espèces réactives de l'oxygène intracellulaire. L'analyse prédictive des propriétés pharmacocinétiques a révélé que les dérivés sélectionnés possèdent les caractéristiques physico-chimiques d'un potentiel médicament (*Lipinski's rules of five*). De plus, ils ont présenté une solubilité aqueuse modérée et une forte absorption intestinale. En résumé, les composés **7** et **10** ont montré une activité antitrypanosomale *in vitro* et une activité enzymatique (*in silico* et *in vitro*) et pourraient constituer un point de départ pour le développement de nouveaux médicaments contre la trypanosomiase Africaine

**Mots clés :** *Trypanosoma brucei brucei*, MMV Pathogen Box, Activité antitrypanosomal, 2,4 Diaminoquinazoline, Relation structure-activité, Mode d'action, *In silico*.

# Introduction



## INTRODUCTION

Trypanosomiasis, classified as a neglected tropical disease is a huge threat to both humans (Human African trypanosomiasis, HAT) and animals (Animal African trypanosomiasis, AAT) with enormous social and economic impacts in endemic regions. HAT, also called sleeping sickness, is caused by two subspecies of *Trypanosoma brucei* sp.: *Trypanosoma brucei gambiense* (found western and central Africa), and *Trypanosoma brucei rhodesiense* (found in eastern and southern Africa), which are responsible of the chronic and acute forms of the disease, respectively (Steverding, 2008). *Trypanosoma brucei gambiense* and *Trypanosoma brucei rhodesiense* accounts for approximately 92% and 8% of the total number of reported trypanosomiasis cases respectively. Human African trypanosomiasis is distributed across 36 countries in sub-Saharan Africa, with an estimated at risk population of approximately 55 million between 2016 and 2020 (WHO, 2022b). Although the disease is not completely eradicated, multiple control strategies put in place have led to an important decline in the number of cases from almost 40 000 in 1998 to 992 and 663 new cases reported in 2019 and 2020, respectively (WHO, 2022b). However, in 2019, an unusual recrudescence of the disease was observed in the foci of some endemic countries, such as Cameroon (WHO, 2022a; WHO, 2019), supporting the idea of pursuing effort for the global view of eradication rather than slackening disease surveillance. Animal African trypanosomiasis also called nagana disease remains the most important cattle disease in sub-Saharan Africa with severe economic consequences (Giordani et al., 2016). This disease cause approximately 3 million deaths and huge economic loss in cattle production (range of US\$ 1.0-1.2 billion) annually (FAO, 2022). The management of African trypanosomiasis mostly relies on early diagnosis to improve the prospect of an adequate treatment using available chemotherapeutic agents such as pentamidine, suramin, melarsoprol, eflornithine, nifurtimox, fexinidazole etc. (WHO, 2022b). However, these therapies are unsatisfactory due to poor efficacy at the chronic phase, toxicity, undesirable route of administration, and more importantly drug resistance (Fairlamb, 2003; Giordani et al., 2016). Thus, the search for novel and adequate treatments is an urgent priority to achieve the WHO's initiative toward disease elimination by 2030 (WHO, 2022b).

Among the many drug discovery strategies used to date, drug repositioning represents a strategy which aimed at developing novel therapies from approved or investigational drugs that are outside the scope of the original medical indication. This approach has also been used to discover new hit compounds against neglected tropical diseases (Ferreira & Andricopulo, 2016). In this line, organizations such as the Medicines for Malaria Venture (MMV), through

Open Source Drug Discovery programs have made available repositionable compound libraries to facilitate and accelerate the search for new lead compounds against various diseases, including African trypanosomiasis (MMV, 2022a). Among the available compounds' libraries, the Pathogen Box (MMVPB) library consists of 400 diverse drug-like molecules with known activity against tuberculosis, malaria, kinetoplastids, helminths, cryptosporidiosis, toxoplasmosis, and dengue (MMV, 2022b). Since the public launch of MMVPB, it has been intensively investigated worldwide, leading to the discovery of active compounds against various pathogens, including *Giardia lamblia* and *Cryptosporidium parvum* (Hennessey et al., 2018), helminths and Barber's pole worm (Preston et al., 2016), *Toxoplasma gondii* (Spalenka et al., 2018), *Trypanosoma brucei brucei*, *Trypanosoma cruzi*, *Leishmania donovani* (Duffy et al., 2017) and *Echinococcus multilocularis* (Rufener et al., 2018). Hence, to contribute to the elimination of sleeping sickness by 2030 as set by the WHO's initiative the present study was designed to identify potential antitrypanosomal hit compounds from repurposing the MMV Pathogen Box.

Specifically, the work consisted of the following:

1. Identify inhibitors of *Trypanosoma brucei brucei* from the *in vitro* screening of MMV Pathogen Box and structure-activity and selectivity relationship studies of the selected hit;
2. Evaluate the inhibitory activity of the promising analogs on dihydrofolate reductase by *in silico* and *in vitro* means;
3. Elucidate other possible modes of action (time-kill kinetics, reversibility of trypanocidal effect, plasma membrane integrity assessment, measurement of reactive oxygen species, DNA fragmentation analysis and ferric iron reducing potency) and predict the pharmacokinetic properties of the most promising analogs.

# *Chapter-I*

## *Literature Review*



## LITERATURE REVIEW

### *1.1. Generalities on African Trypanosomiasis*

#### *1.1.1. Definition*

Trypanosomiasis is a neglected disease caused by *Trypanosoma* parasites and transmitted through the bite of infected tsetse flies (*Glossina* spp.) (Steverding, 2008). African trypanosomiasis can be classified into two main types of diseases including human African trypanosomiasis (HAT) or sleeping sickness and African animal trypanosomiasis (AAT) or Nagana disease (Barrett et al., 2003).

#### *1.1.2. The pathogen agents*

##### *1.1.2.1. The pathogenic agent*

###### *i. Taxonomy and classification*

African trypanosomiasis is caused by flagellated parasites belonging to the Kingdom Protista, subkingdom protozoa, phylum Sarcomastigophora, class Mastigophora and order Kinetoplastida due to the presence of a DNA-containing granule in their single mitochondrion known as the kinetoplast (Hoare, 1972). Trypanosomes are then classified into the Trypanosomatidae family and the genus *Trypanosoma*, which has two groups, Stercoraria and Salivaria (Hoare, 1972).

The Stercoraria group contains genera in which the trypanosome completes its development in the hindgut or posterior chamber of the insect and is transmitted through contamination of bite wounds with the insect's feces. The species in Stercoraria include *Trypanosoma cruzi*, which causes Chagas disease in South America (Hoare, 1972). By contrast, the Salivarian group matures in the salivary medium of the "anterior station" and are transmitted by inoculation into susceptible vertebrate hosts (Hoare, 1972) from the salivary glands (e.g., *Trypanosoma brucei* spp) or from the proboscis (*Trypanosoma congolense* and *Trypanosoma vivax*) (Hoare, 1972). This Salivaria group consists of four subgenera (Hoare, 1972):

- Duttonella with *Trypanosoma uniforme* and *Trypanosoma vivax* with the latter known to infect cattle in sub-Saharan Africa and South America (Jones & Davila, 2001);

- Nannomonas, which includes the species *Trypanosoma simiae* and *Trypanosoma congolense*, one of the main causative agents of disease in cattle, goats, pigs, and dogs (Uilenberg, 1998; Auty et al., 2015),
- Pycnomonas that include the specie *Trypanosoma suis*
- Trypanozoon includes *Trypanosoma evansi* is considered as the pathogen in camels and equidae in North Africa or cattle and water buffalo in South America and East Asia (Reid, 2002; Mekata et al., 2009; Desquesnes et al., 2013), whereas *Trypanosoma equinum* and *Trypanosoma equiperdum*, are venereally transmitted to horses and other equids during mating (Claes et al., 2005; Lai et al., 2008).

Moreover, Trypanozoon subgenera contains *T. brucei* species such as *Trypanosoma brucei brucei*, *Trypanosoma brucei rhodesiense*, and *Trypanosoma brucei gambiense* (Hoare, 1972). Among these, only two subspecies are responsible for sleeping sickness in humans:

- *Trypanosoma brucei gambiense* (*T. b. gambiense*): found in west and central Africa and accounts for 92% of reported cases of sleeping sickness and causes a chronic infection (WHO, 2022b)
- *Trypanosoma brucei rhodesiense* (*T. b. rhodesiense*): found in eastern and southern Africa, and responsible for approximately 8% of the reported cases and causes an acute infection (WHO, 2022b).

In contrast to *T. b. gambiense* and *T. b. rhodesiense*, *Trypanosoma brucei brucei* (*T. b. brucei*), is one of the causative agent of animal African trypanosomiasis in various domestic ungulates (cattle, buffalo, giraffe, pigs, etc.), but it is also virulent in dogs, camels, horses; and is fatal to these animals if left untreated (Auty et al., 2015; Giordani et al., 2016). The sensitivity of this parasite to the human serum hinders its survival, and render it noninfectious to humans. Because of its similarity (99%) to the two African subspecies responsible for HAT (Jackson et al., 2010), its lack of pathogenicity to humans, and ease of *in vitro* cultivation, *T. b. brucei* is the main model for studying *T. brucei* in the laboratory (Ammar, 2013).

## ii. Morphological features of trypanosomes

Trypanosomes are unicellular flagellated eukaryotic protozoa (Figure 1) of 8-40 µm in length depending on the species. They possess an undulating membrane and flagellum that emerges from an invagination of the cell membrane known as the flagellar pocket at the anterior end (Wilkowsky, 2018). Organelles such as mitochondria, nucleus, endoplasmic reticulum, Golgi apparatus and ribosomes are enclosed by the plasma membrane (Figure 1). In addition,

there is a kinetoplast at the base of the flagellum, located toward the posterior end of the trypomastigote forms of the parasite (Uilenberg, 1998; Wilkowsky, 2018). The kinetoplast is an enlarged region of the mitochondrion that contains condensed mitochondrial DNA forming a network of interlocked circular molecules of about 1 kb and 22 kb for minicircles and maxicircles, respectively (Wilkowsky, 2018). Different morphological forms appear in the life cycle of trypanosomes, distinguished mainly by the position, length, and cell body attachment of the flagellum. Trypanosomes present two main morphologically distinguishable forms: epimastigote, in which the kinetoplast is anterior to the nucleus and trypomastigote which includes the slender bloodstream and non-proliferative stumpy forms along with the procyclic and nonproliferative metacyclic forms ( Wheeler et al., 2013; Kaufer et al., 2017). Trypanosomes bloodstream forms possess protective cell coat of antigens called variant surface glycoproteins (VSGs), which are the major antigens of the parasite. The antigenicity of the VSGs is in continuous changes to evade the host immune system (Baral, 2010; Wilkowsky, 2018).

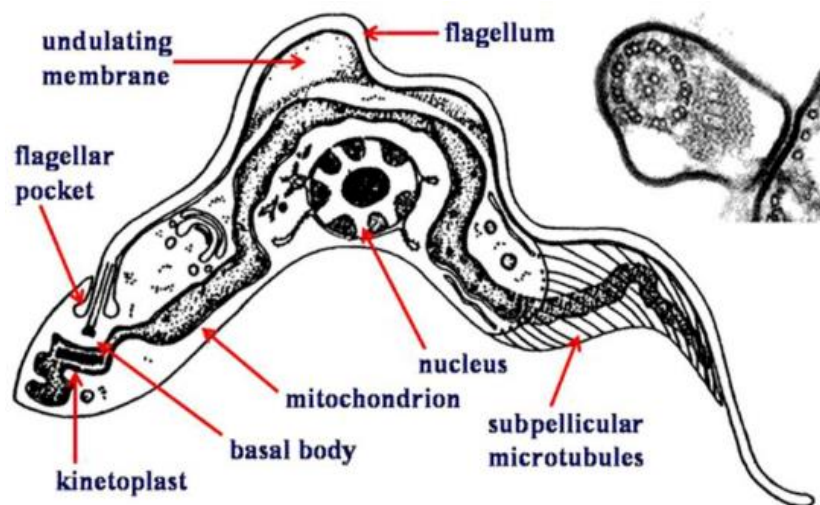


**Figure 1:** Cellular structure of Trypanosoma (Wiser, 1999).

### *iii. Life cycle*

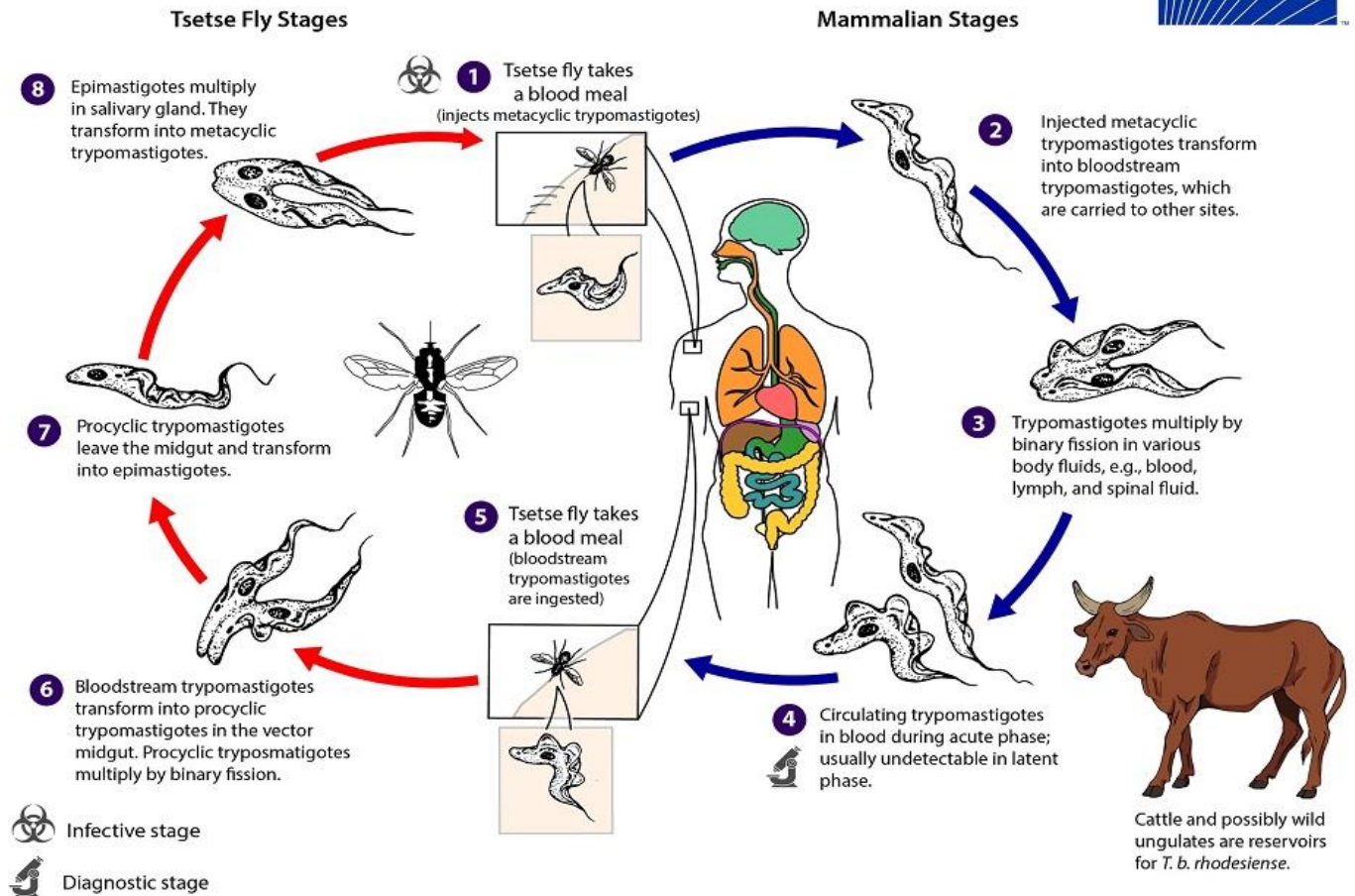
In mammalian hosts, the infection is initiated when metacyclic trypomastigotes are injected by an infected tsetse fly during a blood meal (1) (Figure 2).

After several days of multiplication by binary fission, the metacyclic trypomastigote transforms into a long slender bloodstream trypomastigote form (2) ( Kristensson et al., 2013; Hameed, 2019). Next, the parasites will then spread via the lymphatic system and pass through

the bloodstream to reach other body fluids (lymph, spinal fluid) or peripheral organs and tissues, and continue their replication by binary fission (3) (CDC, 2020). Since their Krebs cycle is silenced, the bloodstream forms rely exclusively on glucose (glycolysis in glycosomes), which is freely and abundantly available in the host (Vickerman, 1985). As the parasite population increases, a strong antibody response is then generated against the predominant and highly immunogenic VSG. These antibodies facilitate parasite decimation by agglutination and glomerular filtration, opsonization and macrophage phagocytosis or most effectively by complement-mediated cell lysis (Engstler et al., 2007). However, trypanosomes have a large repertoire of VSG genes (~800), which serve in immune system evasion by antigenic variation (Berriman et al., 2005). Consequently, a small subset of cells in the population will spontaneously express a different VSG, making them invisible to the antibody response directed against the VSG types in previous parasitemic waves (Berriman et al., 2005). Afterward, the surviving cells will then grow into a new parasitemic wave and continue the cycle (Berriman et al., 2005; Eyford, 2013). On the other hand, as parasite quantity increases, BSFs are replaced by non-proliferative stumpy forms (Matthews K.R. et al., 2004). The accumulation of these stumpy forms limits trypanosome multiplication, thereby maintaining the number of circulating parasites, which prolongs host survival and subsequently increases the probability of disease transmission (Roditi & Liniger, 2002; Matthews et al., 2004).

Short stumpy bloodstream forms are picked up when *tsetse* flies ingest a trypanosomes-infected blood meal from a mammalian host (CDC, 2020). In the fly midgut, the parasites transform into procyclic trypomastigotes leading to morphological changes (elongation and loss of the VSG coat) and biochemical switch from glucose-dependent to proline-dependent energy metabolism (Vickerman, 1985). This switch is necessitated by the fact that glucose is unavailable in *tsetse* flies, which, instead of glucose, depend on proline for energy metabolism. Furthermore, procyclics adapt to cytochrome-mediated terminal respiration by activating their mitochondria (Vickerman, 1985). After multiplication by binary fission (6), procyclic forms leave the midgut and migrate to the salivary gland, where they proliferate and attach to the gland wall by the flagellar membrane as epimastigote forms (7). Eventually, epimastigotes arrest multiplication originating nonproliferative metacyclic forms, in which a VSG coat is re-expressed and is kept into the salivary gland lumen awaiting a new mammalian infection (8) (CDC, 2020; Oliveira, 2012).

## African Trypanosomiasis

*Trypanosoma brucei gambiense* & *Trypanosoma brucei rhodesiense*

**Figure 2:** A simplified sketch of the life cycle of African trypanosomes (CDC 2020).

### 1.1.2.2. Disease transmission and Vector

#### i. Cyclical transmission by tsetse flies

African trypanosomiasis is transmitted by dipterous and brachycera insects belonging to the order Diptera, the Glossinidae family and the genus *Glossina*, commonly known as the "tsetse" fly (Figure 3) (Krinsky, 2002; Rogers & Robinson, 2004). This cyclical transmission mode (Figure 2) in which trypanosomes undergo active multiplication within vectors (tsetse flies) is common for *T. congolense*, *T. simiae*, *T. vivax*, *T. brucei*, and human infective trypanosome species (*T. rhodesiense* and *T. gambiense*) (Finelle, 1983).

*Tsetse* flies include 31 species of the genus *Glossina*, which are further subdivided into three subgenera such as the *Nemorhina* or *palpalis* groups, common in flora near water in western and central Africa, the *Glossina* or *morsitans* group (found in fauna-rich woodland,

‘savannah’ where animals are common), and *Austenina* or *fusca* group (endemic in forest belts and tend to disappear with human activity) (Krinsky, 2002; Rogers & Robinson, 2004).

In Cameroon, HAT is transmitted by the *Glossina* spp. from the *Nemorhina* subgenus (*G. palpalis palpalis*, *G. fuscipes fuscipes*, *G. tachinoïdes*), whereas the species responsible for the transmission of AAT belongs to the subgenera *Nemorhina* (*G. palpalis palpalis*, *G. fuscipes fuscipes*, *G. tachinoïdes*, *G. pallicera pallicera*, *G. caliginea*), *Glossina* subgenus (*G. morsitans submorsitans*, *G. longipalpis*) and *Austenina* subgenus (*G. fusca congolensis*, *G. microfusca*, *G. tabaniformis*, *G. haningtoni*, *G. nashi*) (PRONETRY Cameroon, 2010).



**Figure 3:** *Glossina fuscipes* fly (Robert, 2000).

Trypanosomiasis is mostly transmitted by the bite of an infected tsetse fly, but there are other ways by which hosts are infected.

### ii. Mechanical transmission and other modes of transmission

Trypanosomes are also transmitted mechanically through tsetse and alternative vectors from the blood of an infected host to another in their original form without undergoing development in the insect (Hall & Wall, 2004). Such vectors include *T. evansi* and *T. vivax*, which are transmitted by biting flies, such as *Tabanus*, *Hematopota*, *Chrysops* and *Stomoxys* spp. This has enabled them to spread widely beyond Africa from Asia to Latin America (Desquesnes & Dia, 2003, 2004; Desquesnes et al., 2013; Wilkowsky, 2018).

*T. equiperdum* can also transmit the disease during copulation or acquired congenitally if the mother is infected during pregnancy (WHO, 2022).

### ***1.1.3. Geographical distribution, epidemiology, and socioeconomic impact of African trypanosomiasis***

#### ***1.1.3.1. Geographical distribution***

African trypanosomiasis is found in intertropical Africa between the latitudes 14° North and 29° South, an area of 8 million km<sup>2</sup> corresponding to the distribution of the vector the *tsetse* fly (Molyneux et al., 1996). Trypanosomiasis caused by *T. b. gambiense* is found in 24 countries in western and central Africa, such as the Democratic Republic of Congo, Central African Republic, Cameroon, Angola, Gabon, Chad, Congo, Ivory Coast, Soudan, Gambia, Burkina Faso, Equatorial Guinea, Nigeria, Ghana, and Niger among others. The foci of trypanosomiasis caused by *T. b. rhodesiense* are located in 13 countries in Eastern and Southern Africa: Malawi, Zambia, and Tanzania are the most affected and Uganda is the only country harboring both diseases ( Paquet et al., 1995; Molyneux et al., 1996; WHO, 2022b) (Figure 4).

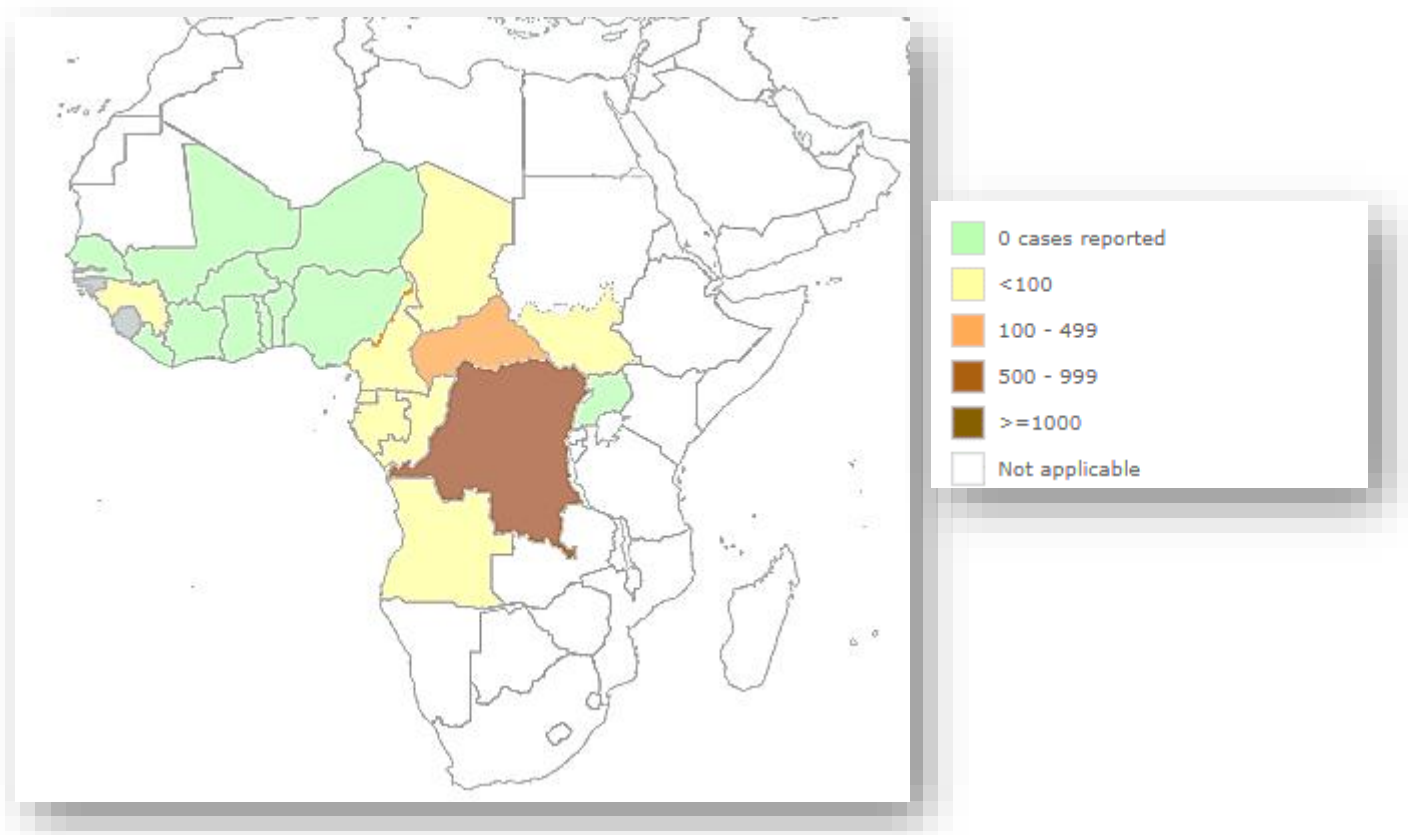


**Figure 4:** Number of sleeping sickness cases reported by country (WHO, 2023a)

### 1.1.3.2. Epidemiology and socioeconomic impact

#### *i. Human African trypanosomiasis*

HAT is endemic in 36 sub-Saharan African countries where more than 55 million people are at risk of infection with trypanosomes, with only 3 million at moderate-high risk for the period 2016–2020 (**Figure 4**). In 1998, 40 000 cases were reported, but estimates were that 300 000 cases were undiagnosed and therefore untreated. Global efforts to eradicate this debilitating disease has reduced the number of new cases to 9878 and 3796 cases (with < 15,000 estimated new cases) in 2009 and 2014 respectively as reported by the World Health Organization (WHO) (**Büscher et al., 2017; Kennedy, 2019**). In 2015, the number of cases diagnosed in both endemic and non-endemic countries was reduced to 2804 cases, of which 2733 were gambiense HAT and 71 were rhodesiense HAT (**Büscher et al., 2017**). Later, estimates of 1446, 992 and 663, new cases were registered in 2017, (**Lindner et al., 2019**), 2019 and 2020 respectively (**WHO, 2023b**).

Certainly, the burden of this disease differs from one country to another, with variations in different localities within the same country. At the beginning of the 20<sup>th</sup> century, there were several active HAT foci, such as Western (Fontem, Mamfe, and Mbo's Plain), Coastal (Douala and Campo), Eastern (Bafia and the villages of the Nyong basin, Doume, Abong-Mbang, Lomie), Northern (Logone and Chari) and Bipindi foci (**Penchenier, 1996; Wang, 2001**). During the 2000s, approximately 235 patients were diagnosed in five Cameroonian HAT historical active foci: Mamfé, Fontem, Campo, Bipindi, and Doumé. Later, 11 new cases were diagnosed, and this reduction in the number of cases continued until 2018, with 7 new cases reported. However, in 2019, an unusual resurgence was observed (**Figure 5B**), with 21 identified cases, (three times the number of cases notified in 2018) in Campo (16), Bipindi (03), Doumé (01) focus and Yokadouma foci (01) (**WHO, 2019**).

In 2021 and 2022, 11 and 07 new cases were identified respectively (**WHO, 2023b**). The majority of these cases were concentrated in the southern region, particularly in Campo near the border with Equatorial Guinea, as well as in the Bipindi area, whereas few cases were reported in the eastern region (**Figure 5A**). Vector control (pyramid traps) efforts against gHAT in Cameroon are coordinated and supported by the Ministry of Health (NSSCP), primarily executed by research institutions such as the Centre for Research in Infectious Diseases (CRID) in partnership with the Liverpool School of Tropical Medicine (LSTM), as well as IRD and the University of Dschang (**FAO and WHO, 2022**).

Furthermore, it has been emphasized that given the impact of African trypanosomiasis on humans, livestock, and wildlife, efforts to address HAT should be firmly grounded in the "One Health" approach, particularly concerning the management of Animal African Trypanosomiasis (AAT) (FAO and WHO, 2022).



Figure 5A

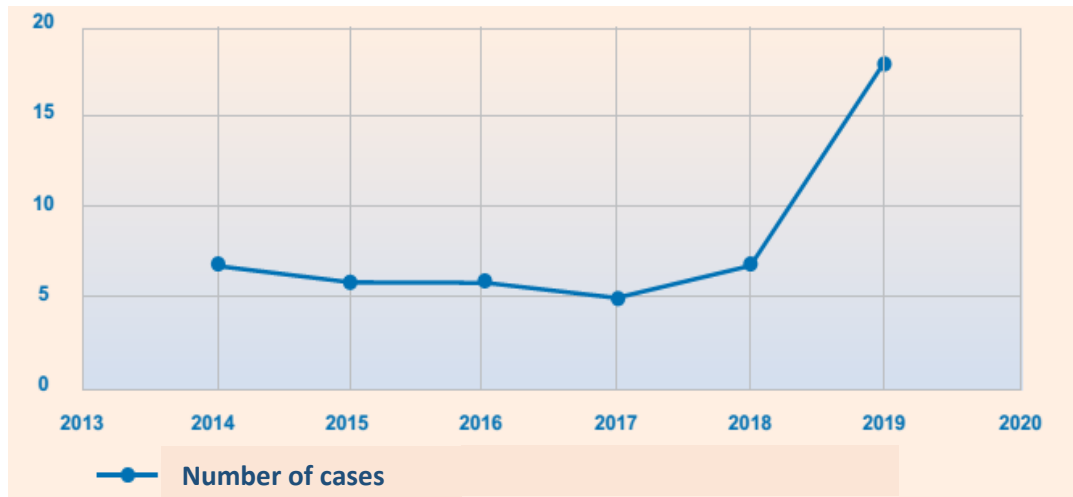


**Figure 5B**

**Figure 5:** 5A. Human African trypanosomiasis (*T. b. gambiense*) in Cameroon. Period: 2011–2020 ; 5B. Cameroon HAT notification cases from 2014 to 2019 (WHO, 2019 ; FAO and WHO, 2022)

Unfortunately, due to the outbreak of the COVID-19 pandemic, the World Health Organization (WHO) recommended a postponement of active case-finding activities and mass treatment campaigns for neglected tropical disease (NTDs) until further notice in April 2020 (Alieea et al., 2021; Toor et al., 2021). Prediction of the impact of COVID-19 interruptions on NTDs has shown that disruptions of control programs might likely induce a slow or fast resurgence of these infections depending on the extent to which the disease was sustained before the disruption. Indeed, the lack of an active diagnosis campaign will likely lead to a late of these diseases, thereby exacerbating the burden of HAT (Alieea et al., 2021; Toor et al., 2021). Consequently, the longer the delay of interventions, the greater the rate of new infections (Toor et al., 2021). For instance, in the 1960s, decolonization and multiple wars has resulted in increasing number of new cases. The threat of resurgence due to a loss of focus on eradication or emerging resistance in the parasite should not be underestimated (Shrimpton, 2017). The risk of new infections could negatively impact the WHO 2030’sgoal toward global elimination of NTDs (Alieea et al., 2021), supporting the idea of pursuing effort for the global view of eradication rather than slackening disease surveillance.

While human African trypanosomiasis (HAT) has reached the point where eradication is being discussed by the WHO, African animal trypanosomiasis (AAT) remains one of the first vector-borne diseases of livestock in Africa to date.

## ii. Animal African Trypanosomiasis

Livestock play a pivotal role in supporting the livelihood of communities in Africa. It is a source of livelihood, income, nutrition, agricultural traction, soil productivity, transport and pride (**Herrero et al., 2013**). Thus, any factor that can affect the health and productivity of livestock will also constrain the development and wellbeing of several families. Therefore, trypanosomiasis, which is known to be a major obstacle to the development of livestock farming in sub-Saharan Africa, represents a major socioeconomic importance (**Baral, 2010; Giordani et al., 2016**). Indeed, the infection is responsible for the death of approximately 3 million cattle each year, with approximately 50 million cattle at risk of infection (**FAO, 2022**). In addition, the production losses in cattle due to trypanosome infections have been estimated to be 20-50% across a range of parameters, including mortality, calving rate, draft power, meat and milk production ( **Swallow, 2000; Holt et al., 2016**). Therefore, AAT constitutes a threat to food security in sub-Saharan African countries and particularly in Cameroon (**PATTEC, 2000**), where 90% of the population of the estimated six million cattle are at risk of trypanosome infection (**Meyer et al., 2016**).

In Cameroon, a survey conducted among cattle breeders in some departments revealed that trypanosomiasis is the most common disease affecting cattle and has the heaviest economic weight (**Figure 6**) (**PRONETRY Cameroon, 2010**). In North Cameroon, the Adamawa plateau is the main area for rearing cattle to supply animal products to the sub region and neighboring countries (**Meyer et al., 2016; Paguem et al., 2019**). In the Faro and Deo, and Vina departments of the North region, the prevalence of this disease was estimated to 61.1, 21.4 and 24.7%, respectively, in non-sanitized areas (areas not treated against vectors), transition areas and sanitized areas (areas treated against vectors) (**Tanenbe et al., 2010**). In 2015, the overall prevalence of trypanosome infection was estimated to be 29.4% in the Faro and Deo division and 55.2% in the Mayo Rey division (**Abdoulmoumini et al., 2016; Abdoulmoumini et al., 2015; Abdoulmoumini et al., 2015b**).

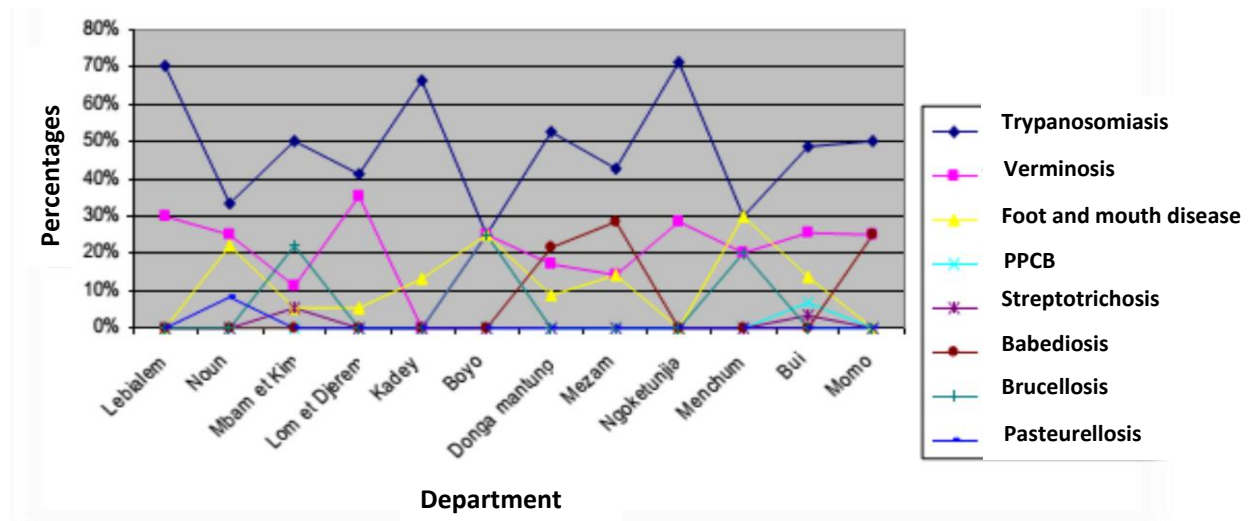


**Figure 6:** The main animal diseases and prevalence (PRONETRY Cameroon, 2010).

### iii. Disease impact and significance

Trypanosomiasis, both in humans and livestock, is one of the most important parasitic infections that constrain economic development in endemic regions (S. Wilson et al., 1963). Indeed, socioeconomic impacts of human African trypanosomiasis include disruption of daily activities, neglect of homesteads, poor academic performance/school drop-outs and death (Bukachi et al., 2017). On the other hand, animal trypanosomiasis has a direct impact on livestock productivity in Africa. The economic losses in cattle production alone are in the range of US\$ 1.0-1.2 billion, and the continent spends at least \$30 million every year to control bovine trypanosomiasis in terms of curative and prophylactic treatments (Angara et al., 2012; FAO, 2022). Thus, AAT constitutes one of the major causes of famine and poverty in several sub-Saharan countries (Feldmann et al., 2005).

#### 1.1.4. Clinical manifestations

##### 1.1.4.1. HAT symptoms

The clinical manifestations of HAT depend on the parasite subspecies infecting the patient and the disease stage. Rhodesiense HAT and Gambiense HAT cause clinically similar diseases, but the main difference between them is at the level of virulence. Indeed, the progression to disease is usually acute in *T. b. rhodesiense* with an incubation period of approximately 2-3 weeks (Odiit et al., 1997), whereas *T. b. gambiense* infection is usually a

slower and chronic infection with an incubation period of several weeks to months (**Checchi et al., 2008**). There are two recognized stages in the clinical presentation of HAT: the early hemolympathic stage and the late encephalitic stage.

✓ **The early hemolympathic phase (stage 1)**

In hemolympathic phase 1, the first symptoms start at the site of the tsetse fly's bite within the first five days, leading to a localized skin reaction known as a trypanosomal chancre due to parasite proliferation and inflammatory responses (**Barry & Emery, 1984; Stich et al., 2002**). Then, the parasites dwell in the intracellular fluids of the body (lymphatic system and bloodstream, etc.) except for cerebrospinal fluid (**Brun et al., 2010**). This colonization causes variable and aspecific symptoms, such as fever, malaise, pruritus, and an enlargement of lymph nodes (also called lymphadenopathy, or Winterbottom's sign) of the neck region, which is commonly observed in *T. b. gambiense* infection. Other clinical signs that may be observed during the 1st stage of HAT include pale mucous membranes indicative of anemia, headache, pruritus, edema, splenomegaly, hepatomegaly, and weight loss (**Barrett et al., 2003; Kennedy, 2004**) (**Figure 7**).



**Figure 7:** Clinical manifestations of HAT in the first stage. A) Winterbottom's sign (Barret et al., 2003); B) Trypanosomal chancre following tsetse fly bite (**Zeinab, 2013**).

✓ **Late meningo-encephalitic phase (Stage 2)**

After years of the early stage in gambiense HAT and months in rhodesiense HAT, a second stage (late stage) begins when the blood–brain barrier is traversed by the trypanosome and the central nervous system is invaded; this is referred to as the meningo-encephalitic stage associated with neurological damage and mental changes (**Barrett et al., 2003; Franco et al., 2014**).

Pathologically, this phase is characterized by meningoencephalitis, with extensive cerebral white matter infiltration by lymphocytes, macrophages, and plasma cells (Atouguia & Kennedy, 2000). A multitude of symptoms result from this encephalitic degeneration of the central nervous system, and not all features are observed in a single patient. In brief, clinically manifestation include motor disturbances, with motor weakness reported in 35% of cases; gait disturbance (22%); tremor (21%); abnormal movements (11%); and speech disturbances 14%) (Brun et al., 2010); myelitis, myelopathy, muscle fasciculation, and peripheral motor neuropathy; (Kennedy, 2008) psychiatric disorders. In addition we have 25% of patients displaying behavioral disturbances, lassitude, hallucinations, delirium, anxiety, irritability, excessive sexual impulses; (Brun et al., 2010) headache, which occurs in 79% of patients in one study (Brun et al., 2010); sensory disturbances (deep hyperaesthesia, pruritus, anesthesia and paraesthesia); and finally visual problems such as optic neuritis, double vision, and optic atrophy (Atouguia & Kennedy, 2000; Kennedy, 2008).

Typically, patients experience severe lethargy, insomnia, and disruption to their diurnal cycle as the disease progresses. According to an extensive study on 2,541 patients with late-stage HAT, sleep disturbances occur in 74% of patients, (Brun et al., 2010) to whom the disease progresses to coma and death if left untreated. The typical sleep disturbances give rise to the appellation ‘sleeping sickness’. Sleep abnormalities encompass a reversal of the normal sleep/wake cycle, nocturnal insomnia (inability to initiate or maintain sleep), narcolepsy (excessive daytime sleepiness), sleep apnea, restless legs syndrome among others (Buguet et al., 2005).



**Figure 8:** Patients with stage 2 HAT (ANOFEL, 2014; Barrett et al., 2003; Oliveira, 2012).

### 1.1.4.2. AAT symptoms

The clinical signs of infection vary considerably according to the species of trypanosome involved and a number of host factors (Wilkowsky, 2018). Depending on the affected species and the genetic background of the animal, the outcome of the disease will fluctuate in either susceptibility or relative resistance to infection, which has been termed “trypanotolerance” (Uilenberg, 1998; Wilkowsky, 2018). General clinical signs of AAT include intermittent fever, anemia, oedema, enlargement of the superficial lymph nodes, abortion, decreased fertility, reduced productivity, emaciation and often mortality (Urquhart et al., 1996; Wilkowsky, 2018). In ruminants, advanced heart failure often leads to death (Wilkowsky, 2018). Other symptoms include enlargement of the liver and spleen, sleeping disorders, emaciation, pica, paralysis, and neuroendocrine dysfunctions (Courtin et al., 2008; Steverding, 2008).



**Figure 9:** Cattle trypanosomiasis (<https://www.dairyknowledge.in/article/trypanosomiasis-surra>)

Because of the wide range of clinical manifestations, the diagnosis of trypanosomiasis cannot be based on clinical signs alone; hence, laboratory confirmation is an absolute necessity.

### 1.1.5. Diagnosis

African trypanosomes are extracellular parasites that live in blood and lymph and can also cross the blood–brain barrier to reach the cerebrospinal fluid. Therefore, for the diagnosis of trypanosomal infections, it is often essential to identify trypanosomes in lymph node aspirate, blood, or cerebrospinal fluid. In this respect, HAT diagnosis follows a three-step procedure that involves screening, diagnostic confirmation and staging of the disease (Chappuis et al., 2005).

**Screening:** In endemic areas, the Card Agglutination Test for Trypanosomiasis (CATT) is mostly used to diagnose trypanosomiasis during mass population screening campaigns. This rapid serological test is an agglutination assay consisting of a lyophilized bloodstream form of

*T. b. gambiense* expressing a particular variable antigen type that detects specific antibodies in the blood, plasma or serum of patients (Magnus et al., 1978). Unfortunately, CATT test does not react with *T.b. rhodesiense*; thus, populations from the Eastern Africa rely solely on clinical manifestations for the diagnosis of trypanosomiasis. Advanced methods such as immunofluorescence and ELISA techniques, are used by trained professionals to diagnose patients at the clinical treatment centers (Bouteille & Buguet, 2012).

**Diagnosis confirmation:** For all HAT patients, there is a need for parasitological confirmation to demonstrate the presence of trypanosomes in the body fluid or tissue. This is often carried out by microscopic examination of chancre aspirate, lymph node aspirate, wet and thick blood films, and/or cerebrospinal fluid (Henry et al., 1981; Van Meirvenne, 1999). The low sensitivity of the microscopic examination, advent of a number of modern techniques for concentration determination such as amplification of *T. brucei* DNA using PCR (Levine et al., 1989), the microhematocrit centrifugation (Woo, 1970), quantitative buffy coat (Ancelle et al., 1997) and fluorescence microscopy with acridine orange (Biéler et al., 2012). Despite the fact that these procedures are time consuming and use sophisticated equipment they are routinely used in field diagnosis.

**Stage determination:** Due to the absence of sufficiently specific clinical signs and blood tests indicating the progress from first- to second-stage HAT, staging of patients still relies on examination of cerebrospinal fluid (CSF) obtained by lumbar puncture (Kennedy, 2008). According to the WHO, the second-stage HAT is defined by the presence of trypanosomes and/or >5 white blood cells/ $\mu$ L in the CSF or increased protein content (>370 mg/L). In addition, a high IgM concentration in CSF is considered a reliable marker of neurological involvement ( Lejon & Büscher, 2005; Bouteille & Buguet, 2012). This observation helps to distinguish the hemolymphatic stage from the encephalitic stage and is therefore the basis for the selection of an appropriate treatment as few trypanocides can cross the blood–brain barrier (Rodgers, 2009).

### ***1.1.6 Control measures***

Generally, vaccination, chemotherapy, and vector management are key strategies that are mostly employed to fight vector-borne diseases, including trypanosomiasis.

### ***1.1.6.1. Vector control and prospects for vaccine development***

Vector control is one of the most reliable methods of disease control as it interrupts trypanosomiasis transmission from one vertebrate host to the other. Many vector control methods have been developed such as the ecological control of *tsetse* flies (Aksoy et al., 2003), the use of stationary attractants such as traps and screens impregnated with synthetic pyrethroid insecticides (Hargrove et al., 2003), the use of insecticides (Hargrove, 2003), and the use of sterile insect techniques (Vreysen, 2006).

As previously stated, trypanosomes have the capacity for antigenic variation due to the presence of their variant surface glycoproteins (VSGs), which are the basis of their ability to escape from the host immune response. Because of the high antigenic variation, a prospect for the development of a vaccine against trypanosomiasis is a challenge (Debela, 2016). With the limitations of the other forms of intervention (vector control and vaccine), chemotherapy offers the most effective and sustainable solution for controlling trypanosomiasis.

### ***1.1.6.2. Chemotherapy for African Trypanosomiasis***

#### ***i. Human trypanosomiasis treatments and limitations***

##### ***i.1. Chemotherapeutic agents and mode of action***

Due to the existence of two disease phases, chemotherapeutic treatments were separated into two categories. The first aims to treat the hemolymphatic phase and involves intravenous or intramuscular injections of one or two drugs. The second is used at the neurological phase and therefore must overcome the challenge of BBB penetrance (Bouteille & Buguet, 2012). Thus, the earlier the disease is identified, the better the prospect for appropriate treatments. New treatment guidelines for the management HAT were recently published by the WHO in 2019, and a total of six antitrypanosomal drugs were selected to be used either alone or in combination (WHO, 2022b). A detailed description of these drugs is provided in the section below (1).

#### **✓ First-stage treatment**

Drugs used for the first stage of HAT include pentamidine isethionate (Figure 10.1) and suramin (10.2). Pentamidine isethionate is a water-soluble aromatic diamidine (Figure 10.1) molecule used for the treatment of early-stage *T. b. gambiense* HAT. It has many reported side effects, but the most important are liver, kidney and pancreatic injuries; the latter results in hypoglycemia due to the massive release of insulin that causes diabetes (Fairlamb, 2003).

Similar to other diamidines, pentamidine has a predilection for DNA-containing organelles, including the kinetoplast and nucleus, where it binds to the minor groove of DNA at A-T rich sites (W. Wilson et al., 2008).

Early-stage *T. b. rhodesiense* HAT is treated with suramin, a colorless polyanionic sulfonated naphthylamine (Figure 10.2) that is chemically related to trypan red and to other dyes with *in vivo* trypanocidal activity. Because of its ionic nature, suramin does not cross the BBB and is not used for the last stage of the disease (Fairlamb, 2003). The mode of action of suramin is related to the fact that suramin has six negative charges, which it uses for binding via an electrostatic interaction with positively charged areas of several protein targets. Therefore, suramin might inhibit a wide spectrum of enzymes, such as dihydrofolate reductase, fumarase, glycerol-3-phosphate dehydrogenase, hexokinase, 1-glycerophosphate oxidase, reverse transcriptase, receptor-mediated uptake of low density lipoprotein, RNA polymerase and kinases, thymidine kinase, and trypsin (Delespaux & de Koning, 2007).

#### ✓ Second-stage treatment

Several drugs have been approved for the management of the encephalitic stage, including melarsoprol, eflornithine and nifurtimox-eflornithine combination therapy (NECT). Melarsoprol is an organic arsenical derivative (Figure 10.3) that is effective against both human subspecies of trypanosomes: *T.b. gambiense* and *T. b. rhodesiense* (WHO, 2022b). Once administered to patients, this prodrug is rapidly converted into melarsen oxide. Once in parasites, melarsen oxide forms a toxic molecule with trypanothione, which is a competitive inhibitor of trypanothione reductase, an essential enzyme that maintain the correct intracellular thiol-redox balance. This toxic molecule kills the parasites ( Fairlamb, 2003; Delespaux & de Koning, 2007). However, toxicity remains a key issue with the use of this drug. Indeed, treatment with melarsoprol produces post treatment reactive encephalopathy in 5-10% of patients, half of whom die, leading to an overall mortality from treatment of approximately 5% (Kennedy, 2008).

Eflornithine, also called  $\alpha$ -difluoromethylornithine (DFMO) (Figure 10.4), is the treatment of choice for the second-stage *T. b. gambiense* HAT (WHO, 2022b), is a repurposed drug the treatment of cancer. DFMO was particularly administered to patients who were not responding to treatment with melarsoprol (Steverding, 2010). DFMO is an irreversible inhibitor of ornithine decarboxylase, an enzyme involved in polyamine (spermidine and

putrescine) metabolism, leading to the loss trypanothione, an important antioxidant metabolite (Delespaux & de Koning, 2007; Fairlamb, 2003). Trypanothione is thought to have two important roles in trypanosomatid metabolism: the maintenance of intracellular thiols in the correct redox state and in the removal of hydrogen peroxide and other hydroperoxides (Fairlamb et al., 1987). In these conditions, the growth of the parasite is interrupted. The major disadvantage of the use of eflornithine is the difficulty to administer this drug. Because of the short half-life of eflornithine in plasma, it is necessary to administer four i.v. infusions per day for two weeks (56 infusions in total) (Fairlamb, 2003).

Nifurtimox-eflornithine combination therapy (NECT) was approved for use in treating late-stage HAT caused by *T. b. gambiense*. Basically, NECT consists of a coadministration of intravenous ornithine and oral nifurtimox (Yun et al., 2010). Indeed, nifurtimox is a nitroheterocycle (Figure 10.5) prodrug clinically used for the treatment of American trypanosomiasis (Chagas disease). This drug is reduced by parasites to generate cytotoxic nitrile metabolites, which in turn will interact with cellular parasite constituents to cause cell death (B. S. Hall et al., 2011). Despite the lower activity of nifurtimox against parasites, NECT was validated for HAT treatment because of its lower toxicity to human as compared to melarsoprol, its ease of administration, and it is cheaper (than eflornithine): just four injections a day (Yun et al. 2010). The short term administration of NECT has overcome the problem of long term monotherapy by eflornithine (WHO, 2022b)

#### ✓ Drugs used for the treatment of both stages

Most of the drugs highlighted above were developed and used for over 50 years. This is because in the past, private organizations and pharmaceutical companies did not find the development of drugs targeting NTDs profitable. However, over the last decade, NTDs have attracted the attention of several organizations, such as the Drugs for Neglected Diseases initiative (DNDi) (Pollastri & Avenue, 2019).

As a result, fexinidazole was validated by the WHO in 2019 as an oral treatment for gambiense HAT (WHO, 2022b). This nitroheterocyclic molecule (Figure 10.6) was identified as a broad-spectrum anti-infective agent (Raether & Seidenath, 1983), with activity against trypanosomes as well (Jennings & Urquhart, 1983), and was found to be safe and effective in late preclinical experimentation. However, the development of this drug was discontinued by Hoechst AG (now Sanofi Aventis) the company that discovered this drug. Thirty years later, the DNDi evaluated a collection of approximately 700 nitroaromatic compounds for their potential

as antiparasitic agents, and fexinidazole resurfaced (**Torreale et al., 2010**). Studies have shown that fexinidazole is a prodrug that is reduced by nitroreductase into two reactive metabolites that can damage the trypanosome genome and its proteins. Later on, Fexinidazole was reported to cure *T. b. rhodesiense*- and *T. b. gambiense*-infected mice at acute and chronic stages (**Kaiser et al., 2011**). It was well tolerated in humans during phase I clinical trials (**Torreale et al., 2010**), and following a positive phase 2/3 trial, it was validated as a new oral drug for the treatment of first-stage and non-severe second-stage gambiense HAT. However, the drug has not yet been validated for rhodesiense HAT.

#### ✓ Potential new drugs for HAT treatment

Other potential drug candidates are being developed for the management of HAT. These includes SCYX-7158 or acoziborole (Figure 10.7), a benzoxaborole derivative, which is efficient against both strains and stages of HAT. The compound was identified after screening of a library of boron-based compounds by Anacor Pharmaceuticals (**Ding et al., 2010**). Although acoziborole exhibits moderate potency against *T. brucei in vitro* ( $IC_{50} \approx 0.25 \mu M$ ), its favorable pharmacokinetic profile enables significant efficacy, resulting in a 100% cure rate in a mouse model of stage 2 disease (**Jacobs et al., 2011**). Moreover, the drug was found to be 55% orally bioavailable, CNS penetrant, metabolically stable, and less toxic, and it is currently awaiting Phase II/III completion. However, *in vitro* experiments have demonstrated that this compound readily induce the development of a resistant *T. brucei* cell line. (**Steketee et al., 2021**).

#### *i-2. Limitations of current antitrypanosomal drugs*

The current antitrypanosomal drugs are associated with one or more limitations, including the following:

#### ✓ Complexity of treatments

Except nifurtimox and fexinidazole, almost all antitrypanosomal treatments are administered either intravenously or intramuscularly by a trained professional, and required multiple doses over the course of days. For example melarsoprol, requires daily administration for ten days, while eflornithine administration requires a very intensive regimen of 56 i.v doses over 14 days (**Fairlamb, 2003**). The affected individuals who live in remote or poor countries, and in most cases are not able to afford travel transportation fees to reach specialized health centers for the days or weeks requested to receive appropriate treatments (**WHO, 2022b**).

✓ Acute toxicities:

Most phase 2 drugs are highly toxic. Melarsoprol is extremely painful to administer, and its administration is associated with severe reactive encephalopathies in 10% of cases and kills 5% of patients (**Delespaux & de Koning, 2007**). Moreover, eflornithine monotherapy has an approximate 2.1% mortality (**Priotto et al., 2009**).

✓ Limited therapeutic spectrum

None of the current drugs have a broad spectrum of action (stages and parasite strains). For instance, eflornithine and pentamidine are only active against *T. b. gambiense*, while suramin acts only on *T. b. rhodesiense*.

✓ Poor pharmacokinetics profile

✓ The protracted and intricate treatment regimen associated with most contemporary trypanocidal compounds arises from their suboptimal pharmacokinetic profiles. Consequently, administering high doses becomes imperative to sustain serum concentrations sufficiently potent to diminish the relapse rates observed with lower doses. Parasite drug resistance

Partial treatment of humans with antitrypanosomal agents, due to incomplete application resulting in partial clearance of the parasite, has allowed the parasite to coexist in a host with nonlethal drug concentrations. These noncurative concentrations have provided selective pressure in response to which antitrypanocidal drug resistance has evolved for both melarsoprol and pentamidine. *In vitro* studies have shown that eflornithine and nifurtimox are also susceptible to the development of resistance (**Wilkinson et al., 2008; Vincent et al., 2010**).

### *ii. Animal trypanosomiasis treatments and limitations*

Chemotherapy and chemoprophylaxis represent the mainstay of animal trypanosomiasis control in endemic countries. These strategies rely on the use of both curative and prophylactic drugs independent of the infecting species. Curative drugs include diminazene aceturate and homidium salts, and isometamidium is the only prophylactic drug used (**Giordani et al., 2016**).

Diminazene aceturate ( an aromatic diamidine) (Figure 10-10)is the most commonly used trypanocide in cattle, sheep, and goats because of its activity against both *T. congolense* and *T. vivax* (**Giordani et al., 2016**). It is mainly associated with kinetoplast DNA (kDNA), where it binds specifically and interacts with sites that are rich in adenine-thymine (A-T) base

pairs (**Peregrine & Mamman, 1993**). However, this class of drugs tends to accumulate in tissues; to cause a very long half-life followed by residual problems in food-producing animals ( **Peregrine & Mamman, 1993; Giordani et al., 2016**).

Homidium, commonly called ethidium bromide (Figure 10-9), is known to be active against *T. evansi*, *T. vivax* and *T. congolense* infections in cattle (**Delespaux & de Koning, 2007**). This molecule is basically used as a curative drug, but its prophylactic effect has also been reported. However, it was found to be highly mutagenic, and consequently, its use has been significantly reduced ( **Uilenberg, 1998; Sutcliffe et al., 2014**). This drug intercalates with DNA, thereby inhibiting kinetoplast and nuclear DNA replication (**Chowdhury et al., 2010**).

Isometamidium is a phenanthridinium salt (Figure 10-8) that is chemically a hybrid molecule from ethidium and diminazene (**Delespaux & de Koning, 2007**). Isometamidium is used as a prophylactic drug with up to six months of protection in cattle against *T. vivax* and *T. congolense* (**Delespaux et al., 2010**). The main mode of action of isometamidium chloride is thought to be the cleavage of kDNA-topoisomerase complexes, causing the desegregation of the minicircle network within the kinetoplast (**Shapiro & Englund, 1990**).

It has been reported that 35 million doses of trypanocides are used annually in sub-Saharan Africa (**Holmes, 2013**), and this is the result of ineffective treatments and resistance (**Delespaux & de Koning, 2007**). Regarding inefficiency, most of the drugs used to treat animal trypanosomiasis (diminazene and isometamidium) are ineffective as they do not cross the blood–brain barrier. Thus, parasites from inaccessible body sites, such as the CNS, will eventually re-establish infection in the bloodstream to cause relapse following treatment with these drugs (**Myburgh et al., 2013**). Consequently, the presence of parasites in sites other than the bloodstream might represent a potentially important issue for the treatment of *T. brucei* infection. On the other hand, drug resistance has already been reported in 17 countries. More importantly, strains of *T. congolense* resistant to both isometamidium and diminazene have been detected in several countries, including Cameroon (**Mamoudou et al., 2008**). In fact, the development of drug resistance occurs with time under some conditions, such as the insufficient dose due to dilution or underestimation of the weight of the animal and reduced volume of drug to be administered and huge gaps in between prophylactic treatments, even beyond the manufacturer’s specifications (**Geerts et al., 2001**). Current drugs are also associated with one or more side effects and toxicity toward animals. As most of the available antitrypanosomal

drugs are structurally related, their common potential mechanism of action might cause a cross-resistance as they might share the same uptake mechanism in trypanosomes (**Delespaux & de Koning, 2007**).

Considering limitations experienced with the current treatments, it is anticipated that an ideal drug that can be used to successfully manage AAT and HAT should be active against both parasite subspecies, and the two stages of the disease. Moreover, the treatment should be nontoxic, orally available, and should be chemically different to a certain extent from existing drugs.. . Irrespective of the number of promising drugs under clinical trials, the continuous search for alternative treatments should not be neglected. In fact, the existence of cross-resistance between nifurtimox and fexinidazole (**Shrimpton, 2017**) or homidium and isometamidium (**Delespaux & de Koning, 2007**) raises the high risk of relying on a limited number of treatment options for HAT and AAT, especially when the causative parasite tends to develop resistance and rapidly adapt to new conditions. Consequently, it is important to search for untargeted and new pharmacological chemical scaffolds to develop alternative therapies to manage African trypanosomiasis. Based on the foregoing, we examined some potential chemotherapeutic targets that can be used to design new drugs against HAT and AAT.

**Table I:** Drugs approved for the treatment of human and animal African trypanosomiasis

Drug name (Year of Discovery)	Drug class	Molecular targets	Disease form and Stage	Drug form	Dosage	Major limitations and side effects
<b>Human African Trypanosomiasis treatment ( Kasozi et al., 2022; Büscher et al., 2017; Rodgers, 2009; WHO, 2022b)</b>						
Pentamidine (1940)	Diamidine	Binding to parasite DNA, Inhibition of type II topoisomerase, Disruption of mitochondrial DNA	<i>T. b. gambiense</i> (First stage)	Colorless powder	4 mg/kg/day IM or IV (diluted in saline in 2-h infusions) × 7 d	Hypoglycemia, hypotension, drug resistance, reasonably tolerable, do not permeate through the BBB highly polar
Suramin (1920)	Polysulfonated naphthyl amine	Nonspecifically binds to L- $\alpha$ -glycerophosphate oxidase	<i>T. b. rhodesiense</i> (first stage)	Powder and ready-to-use solution	IM or IM route. Test dose of 4–5 mg/kg (day 0), then 20 mg/kg IV weekly x 5 weeks (max 13 g/injection). For children, 10–20 mg/kg	Nephrotoxicity, allergic reaction, although reasonably tolerable, do not cross BBB, highly polar, short half-life.

Melarsoprol (1949)	Melaminophenyl arsenical (MPA)	Inhibition of trypanothione reductase	Both <i>T. b. gambiense</i> and <i>T.b.rhodesiense</i> infections (second stage)	Ready-to-use solution in propylene glycol	IV route 2.2 mg/kg per day (max 180–200 mg/day) IV × 10 d	Narrow therapeutic index, highly toxic, reactive encephalopathy, has a long half-life of 35 hours, therefore is widely used during treatment of late stages of the disease, but the associated encephalopathy and drug resistance limit its use
Eflornithine (1990)	Ornithine analog	Inhibits ornithine decarboxylase	<i>T. b. gambiense</i> (Second Stage)	IV infusion	IV route	Large doses (400 mg/kg), complex regimen cumbersome to apply, short half-life
Nifurtimox-eflornithine combination therapy (2009)		Synergistic effect of individual drugs	<i>T. b. gambiense</i> (second stage 2)	Nifurtimox tablets and eflornithine IV infusion	Nifurtimox 15 mg/kg/day orally in three doses x 10 days eflornithine 400 mg/kg/day i.v. in two 2- h infusions (each dose diluted in 250 ml water for injection) a x 7 days	Less effective against <i>T. b. rhodesiense</i>

Fexinidazole (2019)	Nitroimidazole	Metabolic activation by a bacteria-like nitroreductase to form reactive intermediates, which are capable of damaging DNA and proteins	<i>T. b. gambiense</i> (Both stages)	Oral tablets	Oral route	There is decreased efficacy in patients with severe stage 2 HAT), therefore it should be used in case of no other available treatment options
<b>Animal African Trypanosomiasis treatment (Delespaux &amp; de Koning, 2007; Giordani et al., 2016)</b>						
Diminazene aceturate (1955)	Diamidine	Inhibition of the kinetoplasmatic DNA biosynthesis	<i>T. congolense</i> , <i>T. vivax</i> (less active on <i>T. b. brucei</i> , <i>T. b. evansi</i> )/Cattle, sheep, goats, and dogs	Powder for reconstitution	IM or IV route	Highly polar, poor permeation, toxicity, poor brain permeation due to its cationic polar nature, although it is well tolerated, it requires repeated administration, leading to poor patient compliance.
Homidium Bromide (1952)	Phenanthridine	Inhibits topoisomerase-II during DNA biosynthesis	Prophylaxis and treatment of <i>T. evansi</i> , <i>T. vivax</i> , <i>T. congolense</i> , <i>T. b. brucei</i> /in cattle, sheep, goats, pigs.	Powder for reconstitution	IM route	Highly toxic, Potentially carcinogenic, drug resistance, highly polar,

Isometamidium chloride (1960)	Phenanthridine	Inhibits topoisomerase-II during DNA biosynthesis	<i>T. congolense</i> , <i>T. vivax</i> (less active on <i>T. b. brucei</i> , <i>T. b. evansi</i> )/Cattle, sheep, goats, horses, and camels	Powder for reconstitution	IM (deep)	Toxicity, highly irritant, Possible local reactions in cattle
-------------------------------	----------------	---	---	---------------------------	-----------	---

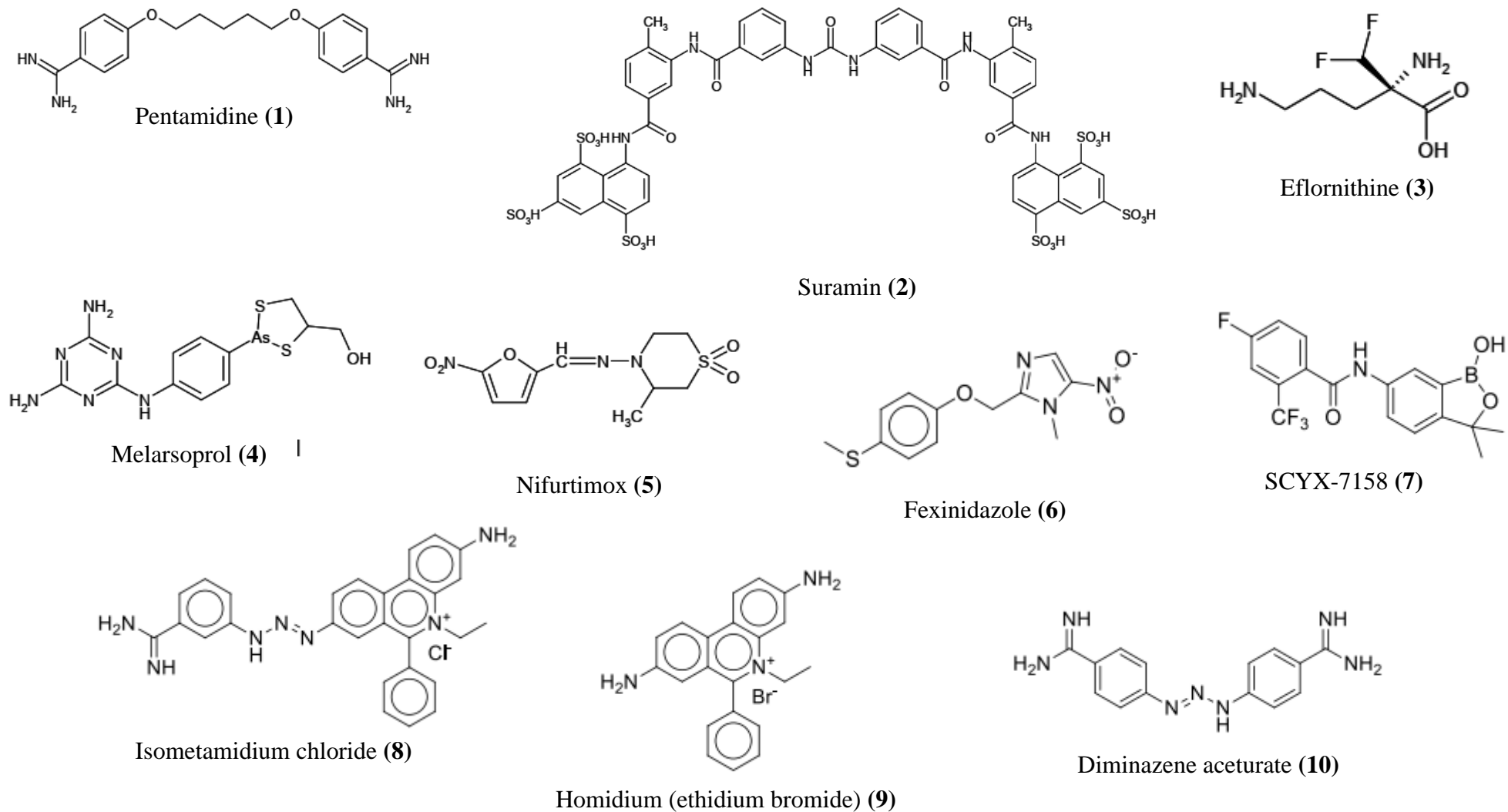


**Figure 10:** Chemical structure of drugs used for the treatment human and animal African Trypanosomiasis.

### ***1.1.7 Dihydrofolate reductase and trypanothione reductase as drug targets in *Trypanosoma brucei****

Inhibition of metabolic enzymes has been established as an attractive strategy for anti-infectious drug development. In this regard, many enzymes, which are essential for the metabolic pathways of *T. brucei* were found to be putative targets for the development of new antitrypanosomal drugs. These includes dihydrofolate reductase and trypanothione reductase (Spinks et al., 2009; Sharma & Chauhan, 2012).

#### ✓ **dihydrofolate reductase**

Dihydrofolate reductase (DHFR; tetrahydrofolate dehydrogenase; 5,6,7,8-tetrahydrofolate-NADP<sup>+</sup> oxidoreductase; EC 1.5.1.3) is a ubiquitous enzyme for several human diseases, such as bacterial and fungal infections, autoimmune diseases, psoriasis, neoplastic diseases, and protozoal diseases, such as trypanosomiasis (Sharma & Chauhan, 2012). It is an enzyme of pivotal importance that acts as a catalyst for the synthesis of nucleic acid precursors via the reduction of dihydrofolate to tetrahydrofolate for DNA synthesis (Schweitzer et al., 1990). Folate and its derivatives are essential cofactors in one-carbon metabolism that are required for the biosynthesis of purines, thymidylate, serine, and methionine in a wide variety of organisms (Sienkiewicz et al., 2008b). It is a water-soluble B vitamin that consists of pteridine with a side-chain incorporating both benzamide and glutamic acid (Sirichaiwat et al., 2004; Sharma & Chauhan, 2012) (Appendix 1). Most bacteria, fungi, protozoa (e.g., *Plasmodium falciparum*), and plants synthesize folates de novo from pterins by a multiple step pathway, whereas trypanosomatids (*Trypanosoma brucei* and *Leishmania donovani*) and their mammalian hosts lack this pathway and thus require exogenous folate for this biosynthetic function.

Trypanosomatids do not have the ability to synthesize purines and therefore salvage them from their environment, yet they have retained the complete biosynthetic pathway to pyrimidines necessary for nucleic acid synthesis (Sienkiewicz et al., 2008). Their DHFR (EC 1.5.1.3) enzyme facilitates the conversion of dihydrofolate (DHFR) to tetrahydrofolate (THF) through reduction using NADPH. Subsequently, THF can be converted to N<sup>5</sup>, N<sup>10</sup>-methylenetetrahydrofolate (CH<sub>2</sub>THF) either through the glycine cleavage system or via serine hydroxymethyltransferase (the latter being absent in *T. brucei*). CH<sub>2</sub>THF serves as a carbon donor for the reductive methylation of deoxyuridine monophosphate (dUMP) to form

thymidylate (dTMP) catalyzed by thymidylate synthase (TS; EC 2.1.1.45) (Carreras & Santi, 1995). dTMP is ultimately phosphorylated to thymidine triphosphate (dTTP) and used for DNA synthesis and DNA repair (Figure 11). In *T. brucei*, DHFR and TS are expressed from a single gene as a homodimer comprising an N-terminal DHFR domain fused via a linker peptide to a TS domain at the C-terminus. In contrast, DHFR and TS are expressed separately from independent genes in many other organisms, including humans (Sienkiewicz et al., 2008; Gibson et al., 2016).

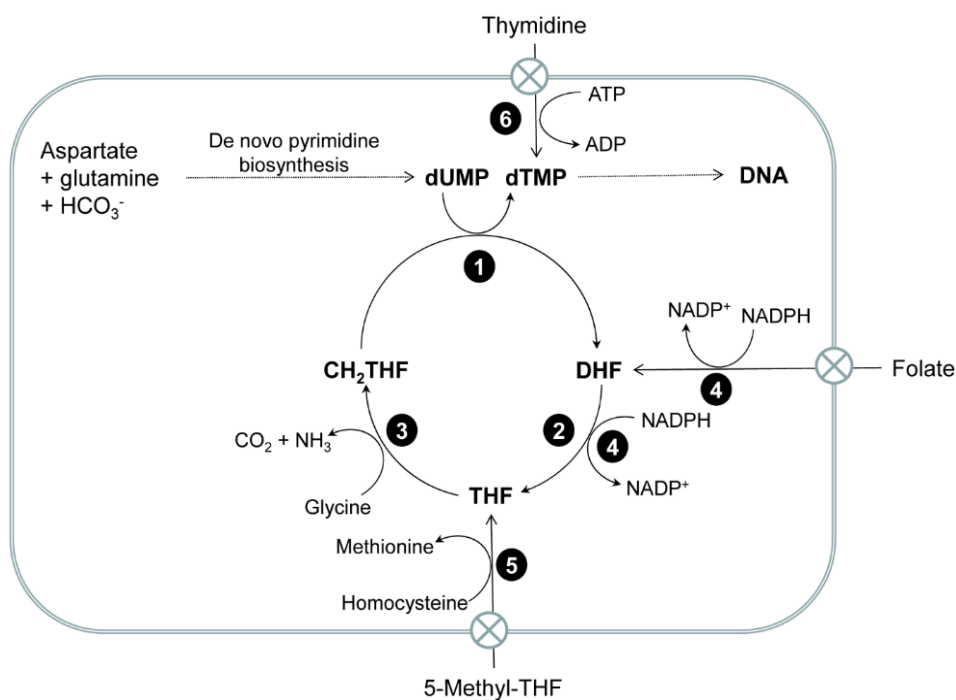


**Figure 11:** Folate metabolism and the thymidylate cycle in *T. brucei*. Enzymes catalyzing key metabolic steps are 1, thymidylate synthase (EC 2.1.1.45); 2, dihydrofolate reductase (EC 1.5.1.3); 3, glycine cleavage system (EC 1.4.4.2, 1.8.1.4 and 2.1.2.10); 4 pteridine reductase (EC 1.5.1.33); 5, methionine synthase (EC 2.1.1.13); and 6, thymidine kinase (EC 2.7.1.21) (Gibson et al., 2016).

On the other hand, selective inhibition of DHFR or TS in prokaryotic and eukaryotic cells results in ‘thymine-less death’ by necrosis or apoptosis because of thymidine starvation (Van Triest et al., 2000). In addition, the bifunctional folate and pyrimidine-metabolizing enzyme DHFR-TS has been validated both genetically and chemically as being essential for *T. brucei* survival (Sienkiewicz et al., 2008). Moreover, *T. brucei* DHFR was found to be different from its human homolog, with only 28% identity (Gibson et al., 2016). The involvement of DHFR in the survival and virulence of the *Trypanosoma* parasites make this enzyme a promising target for the development of new drugs against African trypanosomiasis. To date, no antitrypanosomal drug has been developed using DHFR-based approach. Although some

researchers have pointed out the selective inhibitory effect of folates against *T. brucei* DHFR (Vanichtanankul et al., 2011), there is a lack of reports on their effectiveness on the whole parasite. Thus, research on target-based and whole-cell phenotypic screens should be considered for the search of antitrypanosomal drugs.

### ✓ Trypanothione reductase

Trypanothione reductase (TR, E.C. 1.6.4.8) is an NADPH-dependent flavoprotein disulfide oxidoreductase, which is unique to trypanosomatid parasites whose function is to convert trypanothione disulfide (N1, N8-bis(glutathionyl)spermidine disulfide, T[S]<sub>2</sub>; **Figure 12**) into the physiologically relevant reduced dithiol called trypanothione (T[SH]<sub>2</sub>) (**Krieger et al., 2000**). Trypanothione is the main thiol molecule responsible for maintaining the intracellular reducing environment in parasites (**Cavalli et al., 2010**). Indeed, trypanosomatid parasites lack catalase following oxidative stress resulting from host immune defense; they therefore base their defense on trypanothione (**Battista et al., 2020**). The trypanothione/trypanothione reductase coupling replace many of the antioxidant and metabolic functions of the glutathione/glutathione reductase (GSH/GR) system found in mammals (**Battista et al., 2020**).

Both GR and TR reduce a disulfide bridge that is intermolecular for GR and intramolecular for TR. Trypanothione is an analog of glutathione, as it is derived from the conjugation of 2 glutathione and one spermidine molecule (**Figure 12**). The most significant differences between the two proteins reflect the differences between their respective cognate substrates. TS<sub>2</sub> is bulkier than glutathione disulfide (GSSG) and is positively charged due to the spermidine moiety, while GSH is negatively charged at physiological pH. As a consequence, the TS<sub>2</sub> binding site in TR is wider and negatively charged with respect to the GSSG binding site in GR (**Figure 12**) (**Battista et al., 2020**). Therefore, for the search of novel compounds, it was hypothesized that a scaffold protonated at a physiological pH might be fundamental in conferring TR inhibition (**Cavalli et al., 2010**).

Regarding the enzymes, glutathione reductase (GR) is the closest human homolog of TR with 38% sequence identity, yet there are some significant differences in their active site architecture. The disparity between TR and its mammalian homolog GR renders TryR an appealing target for selective drug design (**Spinks et al., 2009**). Moreover, the structure of TR is almost identical for all characterized species, in accordance with the high degree of sequence

similarity. TRs from all Trypanosomatidae share a minimum of 67% of their primary sequence, with over 82% identity among *Leishmania* spp. and more than 80% among *Trypanosoma* spp. This finding implies that findings regarding new inhibitors in one TR can potentially be extrapolated to others, offering the prospect of discovering a universal inhibitor effective against all TRs. Such a discovery could pave the way for the development of a broad-spectrum trypanocidal drug. (Battista et al., 2020). Finally, TR was validated by different genetic approaches to be essential for the proliferation of *Leishmania* and *Trypanosoma*, and parasites with reduced TR levels were found to be highly sensitive to oxidative stress ( Tovar et al., 1998; Krieger et al., 2000). Taken together, the facts, suggest that TR is another promising target for the development of selective antitrypanosomal inhibitors.

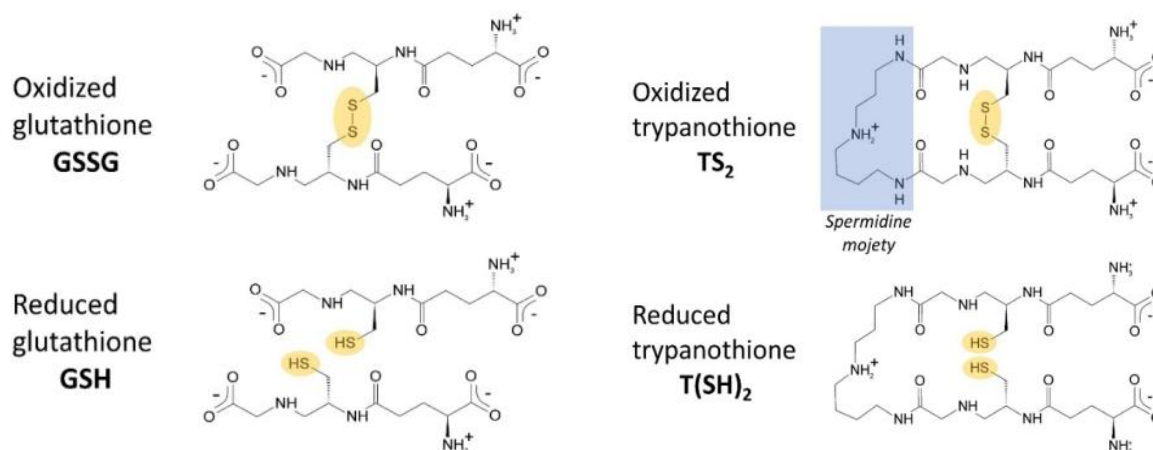


**Figure 12:** Substrates of glutathione reductase (GR) and trypanothione reductase (TR)

Following the identification of a molecule effective against both targeted enzymes and whole parasites, the compound of interest should be integrated in the antiparasitic drug discovery pipeline, which includes several distinct phases and employs various strategies.

## 1.2. Drug discovery and development of new candidates for management of trypanosomiasis

### 1.2.1. Steps in drug discovery phases

Drug research is a unique multidisciplinary process heading toward the development of therapeutic agents in case of currently unmet medical needs (Panchagnula & Thomas, 2000). There are two major drug discovery processes: target-based drug discovery (modern) and phenotype-based drug discovery (empiric). The primary difference between them is whether

the molecular target is identified at the beginning or end. The empirical drug research process can be functionally divided into two stages: **1)** the drug discovery stage which is a long and arduous process broadly grouped into high-throughput identification of hits and leads, target deconvolution, and lead optimization, and **2)** the drug development stage which focuses on evaluating the safety/toxicity and efficacy of new drug molecules through preclinical and clinical evaluations. The key objective of drug development is the generation of a scientific database that supports the effectiveness and safety profile of a drug and its dosage regimen intended for marketing (**Panchagnula & Thomas, 2000**).

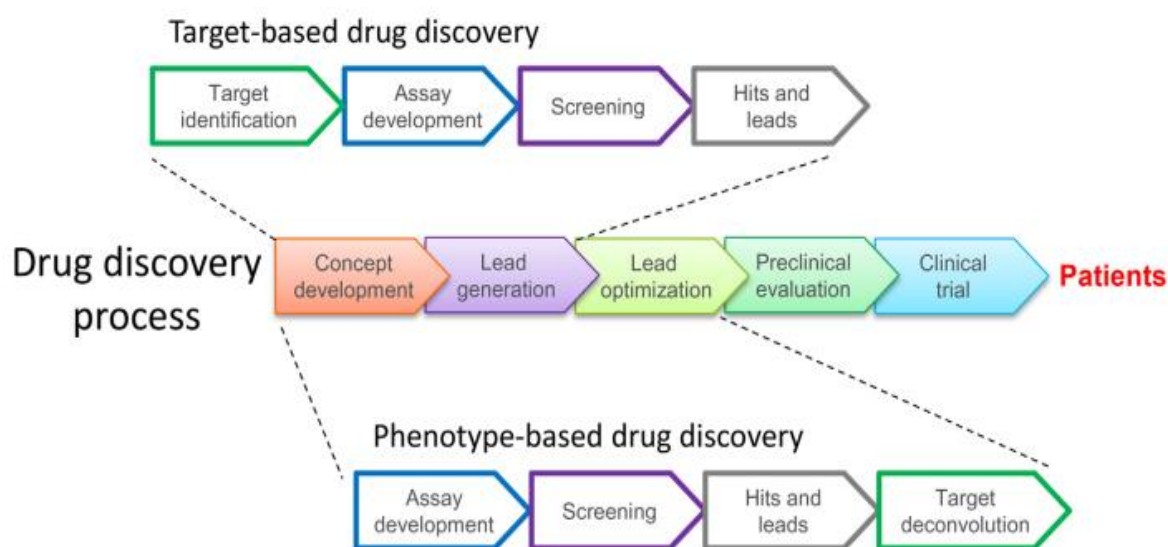


**Figure 13:** Overview of the drug discovery and development process (**Kubota et al., 2019**).

### ***1.2.1.1. Hit identification and hit to lead phase***

Hits can be defined as compounds having the desired activity that can be confirmed upon retesting using *in vitro* screening assays (**Hughes et al., 2011**). The aim of this process is to refine the hit of interest to produce more potent and selective compounds that possess adequate PK properties using intensive structure-activity-relationship (SAR) around the core compound structure (**Hughes et al., 2011**). In general, the lead identification phase involves the identification and characterization of drug targets in the case of phenotypic approaches, synthesis of new molecules, screening of their *in vitro* potency and *in vivo* efficacy in suitable animal models, and further characterization of the pharmacokinetic parameters of promising candidates (**Panchagnula & Thomas, 2000; Prakash & Devangi, 2010**).

### ***1.2.1.2. Lead optimization phase***

The aim of this final drug discovery stage is to improve deficiencies in the lead structure while maintaining its favorable properties in view of identifying the best analog that might become a drug (Prakash & Devangi, 2010; Hugues et al., 2011).

### ***1.2.1.3. Target identification***

A drug target is a biological molecule that is known or hypothesized from basic research to be involved in a physiopathological process of a particular disease (Davis, 2020). It is a molecule through which a drug exerts its action to induce a biological response (Andrade et al., 2016). Target identification is the first key stage in the drug discovery pipeline consisting of the identification of these attractive drug targets, such as metabolic enzymes, RNA molecules, genes and receptors, using experimental models or bioinformatic approaches (Hughes et al., 2011).

### ***1.2.1.4. Target validation***

Once identified, the target needs to be in-depth studied and validation methods range from *in vitro* tools to the use to *in vivo* models (Hughes et al., 2011). Validation of a new target might be of great help, not only to new drug research and development but also to provide more insight into the pathogenesis of the related diseases (Wang et al., 2004). To be classified as a validated drug target, the enzymatic target should meet three main criteria. The first is that the enzyme must be essential for the viability of the parasite (Smirlis & Pereira Soares, 2014; Vasaikar et al., 2016). The second criterion reveals that the selected target should be different from the host protein, so as to exert its inhibitory effect without affecting the human host (Smirlis & Pereira Soares, 2014; Vasaikar et al., 2016). The third criterion specifies that the target should be expressed in the infectious form of the parasites.

### ***1.2.1.5. Preclinical and clinical evaluation***

#### ***i. Preclinical development***

Preclinical development includes large-scale synthesis and drug formulation experiments, *in vivo* screening of drug candidates in suitable animal models (rodent, monkey, etc.), pharmacokinetic and toxicokinetic tests (carcinogenicity, genotoxicity, etc.) (Prakash & Devangi, 2010). Once the candidate drug reaches this phase, a document called Investigational new drug (IND) is filed with the drug regulating authorities. The IND contains animal toxicity data, protocols for early clinical phase trials, and an outline of specific details and plans for

evaluation. With this document, the pharmaceutical company obtains permission to start human clinical trials (**Mishra, 2013**).

### *ii. Clinical development*

After IND application approval, the clinical phase starts with testing in human subjects and is divided into 4 phases that aim at efficacy, metabolism, and toxicity studies.

✓ **Phase 1:** safety and tolerability in healthy volunteers

A small group of healthy volunteers (20-80) were selected to assess the safety, pharmacokinetics, and pharmacodynamics of the therapy. This phase normally includes dose-ranging studies so that doses for clinical use can be adjusted (**Prakash &Devangi, 2010**).

✓ **Phase 2:** efficacy and dose-effect relationship

This phase is performed on small groups (20-300 volunteers) to assess the efficacy of the drug, and double-blinded studies are normally adopted to ensure objectivity (**Prakash &Devangi, 2010**).

✓ **Phase 3:** efficacy studies using a large number of patients

Randomized controlled trials on large patient groups (hundreds to thousands) are used to definitively assess the efficacy of the new therapy in comparison with standard therapy. Side effects are also monitored. Once a drug is proven acceptable, the trial results, formulation details, and shelf life are reported in the document that is later submitted to authorities for review (**Prakash &Devangi, 2010**).

✓ **Phase 4:** postmarketing surveillance

The pharmaceutical company is obliged to report any subsequent drug-induced long-term side effects or adverse reactions over a large patient population (**Prakash &Devangi, 2010**).

Overall, drug discovery is a time-consuming and expensive process, which most often starts from basic research focusing on the identification of potential hit compounds that can be further optimized into leads and then developed into approved drugs. To increase the likelihood of identifying active compounds or ‘hits’, several approaches have been developed and are described in the next section.

## 1.2.2. Drug discovery strategies

### 1.2.2.1. De novo drug discovery strategy

De novo drug design (DNDD) refers to the design of novel chemical entities based only on information regarding a biological target (receptor) or its known active binders (ligands found to possess good binding affinity or inhibitory activity against the receptor) using computational algorithms (Mouchlis et al., 2021). The word “de novo” means “from the beginning”, indicating that with this method, novel molecular entities can be generated without a starting template (Devi et al., 2015). Chemical entities should fit a set of constraints, for instance, toxicity below a threshold and predefined solubility range. Here, the design strategy includes a description of the receptor active site or ligand pharmacophore modeling, followed by construction of the molecules (sampling) and then evaluation of the generated molecules. The advantages of de novo drug design include the development of drug candidates in a cost- and time-efficient manner, the design of compounds that constitute novel intellectual property, the exploration of a broader chemical space and the potential for novel and improved therapies. However, the major challenge faced in de novo drug design is the difficulty find in synthesizing the generated molecular structures (Schneider & Fechner, 2005).

### 1.2.2.2. Target-based approach

The target-based approach, also known as reverse pharmacology or reverse chemical biology, aims to develop or identify compounds that interact with a specific and known target of interest (Andrade et al., 2016). Here, the strategy used to identify new lead compounds involves *in vitro* screening of the target followed by testing of antiparasitic activity on the whole parasite. This approach is called structure-based approach if a particular inhibitor is designed based on the structure (X-ray crystallography) of the biological target of interest using computational chemistry (Field et al., 2017). The advantages of target-based models include direct structure-activity relationship (SAR) investigation, information concerning the mechanism of action and high screening capacity through HTS (Andrade et al., 2016). However, despite all the identified targets thus far, there has been very limited success from target-based approaches. This is often due to a lack of correlation between inhibition of the target in a cell-free environment and inhibition of proliferation of the parasite or subsequent activity in an animal disease model (Field et al., 2017).

### 1.2.2.3. Phenotypic drug screening

Phenotypic screening is an empirical approach that aims to evaluate the biological effects of potential drugs on an organism or cell culture lines (*in vitro*), isolated tissues/organs (*ex vivo*), or whole animals (*in vivo*) (Moffat et al., 2017). This approach is referred to as phenotypic high-throughput screening (HTS) if a large number of compounds are tested (An & Tolliday, 2010). For the screening approach to work efficiently, the developed assay should be pharmacologically relevant, reproducible, not too expensive, and of high quality (Hughes et al., 2011). The latter is determined according to the Z' factor (Zhang et al., 1999) or through the inclusion of pharmacological controls within the assay (Hughes et al., 2011). Like any method, the phenotypic approach has many advantages and disadvantages. The primary advantage is that it directly provides information about the impact of compounds on the parasite. Unfortunately, phenotypic screening rarely provides information on the molecular targets of active compounds (Reguera et al., 2014; Elisabet, 2019) since direct interaction with a single target is not always responsible for phenotypic observations (Andrade et al., 2016). Another inconvenient of phenotypic assays is the low screening capacity when whole animals are used and the difficulty of developing appropriate disease models, such as for Alzheimer's disease (Khachaturian, 2002). Despite all these observations, phenotypic approaches have been successful in discovering new compounds or series. For instance, in the case of HAT, the recently validated Fexinidazole and the candidate oxaborole SCYX-7158 were both obtained from phenotypic approaches (Field et al., 2017). Therefore, phenotypic screening could represent a valuable alternative for hit identification.

Both phenotypic and target-based approaches represent tools of interest for the successful exploitation of another widely used hit identification strategy called drug repositioning.

### 1.2.1.4. Drug repositioning approach

#### *i. Description of the method*

Drug development is an expensive and lengthy process of at least 10 years with the possibility of failure at the end. To overcome this problem, researchers have developed a strategy that consists of screening drugs already approved for other indications (Ferreira & Andricopulo, 2016). This approach, also known as drug repurposing, repositioning, drug reprofiling or drug redirecting, reduces the overall costs and the timeframe required for drug

development by bypassing certain steps of the process as well as shortening the “bench to market” period ( **Padhy & Gupta, 2011; Ferreira & Andricopulo, 2016**). Indeed, a repositioned drug does not necessarily need the initial six to nine years period, which is typically required for the development of new drugs (hit identification, hit-to-lead optimization and lead optimization) but instead goes directly to preclinical testing and clinical trials, thus reducing risk of failure and costs (**Ashburn & Thor, 2004**). Most importantly, repositioned drugs generally include drugs that have been discontinued, those in clinical development whose mechanism of action is relevant to multiple diseases, drugs that have failed to demonstrate efficacy for a particular indication during phase II or III trials but have no major safety concerns, marketed drugs for which patents are close to expiry, and drug candidates from academic institutions and public sector laboratories not yet fully pursued (**Padhy & Gupta, 2011**). In the case of NTDs specifically, drug repositioning has been explored as a strategy to overcome decades of the paucity of newly designed compounds (**Ferreira & Andricopulo, 2016**), and successful results were obtained.

For instance, most of the leishmaniasis drug arsenal was repurposed from other indications. This is the case for marketed amphotericin B, which was originally used in fungal infections and later redirected for the treatment of leishmaniasis ( **Wong-Beringer et al., 1998; Ferreira & Andricopulo, 2016**). On the other hand, paromomycin, a natural aminoglycoside isolated from *Streptomyces krestomuceticus*, was previously prescribed as a broad-spectrum antibiotic as well as for the management of intestinal infections such as amebiasis (**Stanley, 2003**). Moreover, miltefosine, the most recent antileishmanial introduced into the clinic, was initially developed for cutaneous metastases of breast cancer and solid tumors (**Sindermann et al., 2004**). Other examples are summarized in the table **II**.

**Table II:** Examples of successfully repurposed drugs

Drugs	Original Indication	Repurposed for	References
Eflornithine	Anticancer	HAT	(Abeloff et al., 1986)
Nifurtimox	Chagas disease	HAT	(Alirol et al., 2013)
Astemizole	Antihistamine	Malaria	(Chong et al., 2006)
Avermectin	River blind and elephantiasis	Tuberculosis	(Lim et al., 2013)
Tamoxifen	Anticancer	Leishmaniasis	(Silva et al., 2021)
Miltefosine	Antineoplastic	Leishmaniasis	(Sindermann et al., 2004)
Amphotericin B	Antifungal	Leishmaniasis	(Wong-Beringer et al., 1998)
Paromomycin	Antibiotic/antiamoebiasis	Leishmaniasis	(Ferreira & Andricopulo, 2016)

Globally, drug repositioning is an interesting approach to rapidly provide new alternatives against communicable or noncommunicable diseases. This approach owes its success to public–private partnerships (PPPs), which consist of the establishment of collaborations to connect fundamental knowledge coming from academic groups with the expertise and infrastructure provided by pharmaceutical companies. One such successful example include the partnership between Sanofi and DNDi, which results in the codevelopment of fexinidazole for HAT (Ferreira & Andricopulo, 2016).

Interestingly, the source of repositionable compounds for use in laboratories which are committed to drug discovery has been eagerly facilitated and recently encouraged by the efforts of some organizations, such as the Medicines for Malaria Venture (MMV), through an open access drug discovery (Samby et al., 2021).

### *ii. The open access MMV Pathogen Box as a potential source of drug candidates*

Medicines for Malaria Venture (MMV) is a nonprofit organization established in Switzerland in 1999 whose mission is to reduce the burden of malaria by discovering, developing, and facilitating new and affordable antimalarial drugs in endemic countries. MMV's vision is that these innovative medicines will cure and protect vulnerable and underserved populations at risk of malaria and help to ultimately eradicate this terrible disease (MMV, 2022). MMV views drug repositioning as an attractive option for providing cost-effective and timely access to drugs to patients in the developing world (Samby et al., 2021). To facilitate research in the area of infectious diseases (malaria and other NTDs), they provided researchers several cost-free open access compounds, including the Pathogen Box (2016-2020):

a set of 400 diverse drug-like molecules previously shown to be active against pathogens causing tropical and neglected diseases. The box includes a collection of approved drugs used for the treatment of such diseases. They are distributed as follows (**Figure 14**): 33% of the collection comprises compounds with activity against *Plasmodium*, 30% active against tuberculosis, 18% against kinetoplastid species and 19% for other pathogens indications (**Duffy et al., 2017; Preston et al., 2016**).

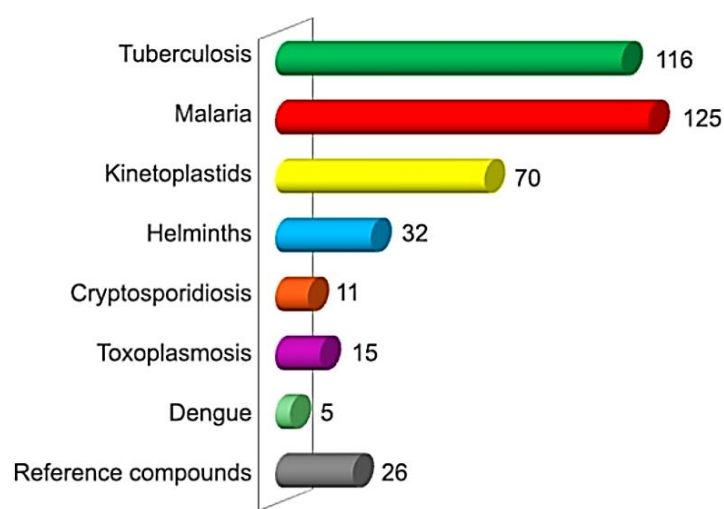


**Figure 14:** Distribution of the disease targeted by the MMV pathogen box compounds and references (<https://www.mmv.org/mmv-open/pathogen-box/about-pathogen-box>)

All compounds are categorized into subsets according to the type of parasite on which they have been tested (disease set) by partners of the MMV group. The compounds have also been tested for cytotoxicity in the human HepG2 cell line, and those considered acceptable (5-fold less toxic against the human cell line than the pathogen) were included in the library. MMV has also provided the plate layout and compound details (structures, trivial names, salt forms, and cLogP). These data are provided as an Excel spreadsheet called the Pathogen Box supporting information (<https://www.mmv.org/mmv-open/pathogen-box/pathogen-box-supporting-information>). The library also contains a set of 26 reference compounds with biological activity associated with at least one pathogen (**Spalenka et al., 2018**).

The pathogen Box has been previously investigated, leading to the discovery of newly identified activity against various pathogens; for instance, MMV010576, MMV028694 and MMV676501 showed an inhibitory activity at micromolar levels with dual efficacy toward *Giardia lamblia* and *Cryptosporidium parvum* (**Hennessey et al., 2018**). On the other hand,

MMV688934 (tolfenpyrad) showed good activity against the helminth and barber's pole worm (Preston et al., 2016). The anti-*Toxoplasma gondii* activity of the PBox library was investigated by Spalenka et al., (2018), leading to the identification of eight hit and selective compounds. Duffy et al., (2017) also identified chemical starting points for malaria, human African trypanosomiasis, Chagas disease and leishmaniasis drug discovery through *in vitro* antiprotozoal screening using the same open access box. Interestingly, the old drug buparvaquone (MMV689480) was repurposed from an *in vitro* screening of 400 compounds against *Echinococcus multilocularis* (Rufener et al., 2018). Consequently, the supply of PBox by the Medicines for Malaria Venture represents a promising and unique opportunity to provide new chemical starting points for several tropical and neglected diseases, including trypanosomiasis, through repurposing. Based on this observation, our research focuses on the identification of promising starting points for drug discovery against trypanosomiasis.

### 1.3. Molecular docking tools in the drug discovery and development process

#### 1.3.1. Overview

Molecular docking is the process of using computational methods to simulate and demonstrate how two molecules, the receptor and ligand, bind together to form a stable complex (Figure 15) without performing any laboratory experiment (Gaba et al., 2015). Molecular docking tools try to find and select the complex with the lowest binding energy, the energy required to drive a chemical reaction. A low amount of energy indicates a more stable system and therefore a potential binding interaction. Molecular docking provides useful information since many drugs work by fitting into a particular target or protein with the consequence of inhibiting another molecule from binding (Matthews, 2019).

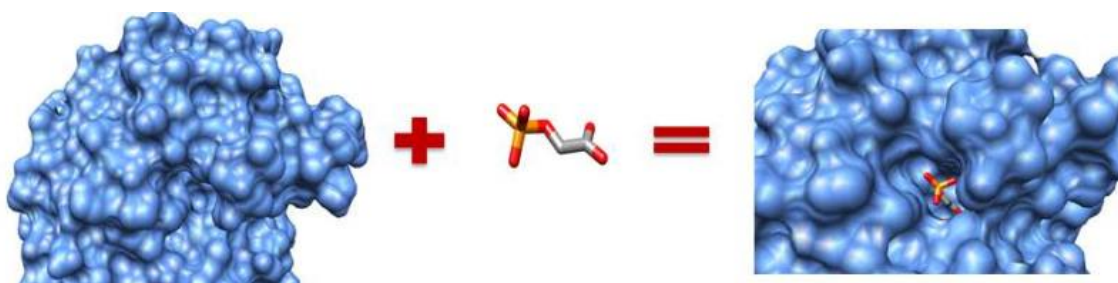


**Figure 15:** Example of a drug candidate (gray–red colors) binding to a target (blue color) (Hernández-Santoyo et al., 2013).

Several computer programs have been developed and used in research leading to the discovery of drug candidates that were successfully validated experimentally. These include AutoDock, Dock, FlexX, FRED, GOLD, Glide, Schrodinger, etc. (Adelusi et al., 2022). Basically, the docking process usually involves two main phases:

✓ Sampling steps or pose prediction

The sampling method aims to predict the molecular orientation of a ligand as well as the molecular orientation of a ligand as well as its position and conformation within a receptor (usually referred to as pose) (Meng et al., 2012). This is done through search algorithms that produce an optimum number of ligand geometries (Adelusi et al., 2022). Docking algorithms generally use 3 models: (a) Rigid body docking, where both the receptor and small molecule are treated as rigid; it does not consider the flexibility of the agents. Therefore, it is fast but not accurate; (b) Flexible ligand docking, whereby the receptor is held rigid, but the ligand is treated as flexible; (c) Flexible docking, whereby both the receptor and ligand flexibility are considered. This causes a larger search space with many possible combinations. Therefore, flexible docking is more computationally intense but more accurate (Gaba et al., 2015; Oztas, 2021). Most docking tools assume that the ligand is flexible and that the receptor is rigid (Gaba et al., 2015). For that purpose, they use two categories of algorithms, namely, systemic (exhaustive search algorithms and fragment-based search algorithms) and stochastic algorithms (genetic algorithms and Monte Carlo algorithms) (Sliwoski et al., 2014).

✓ Scoring function

Docking is not only used to find the lowest energy poses of a ligand. It is also used to measure how strongly a ligand will interact with a particular protein using a scoring function (Oztas, 2021; Priya, 2015). The purpose of the scoring function is to compare the performance of different ligands in terms of binding affinities to rank, two or more ligand or various poses of a protein–ligand complex (Kitchen et al., 2004). This function help to sieve the correct poses from the incorrect poses or binders from inactive compounds (Kitchen et al., 2004). Scoring functions are mathematical approximation methods for free energy calculations. There are several scoring functions that are used in different docking tools: such as force-field, empirical, and knowledge-based scoring functions (Adelusi et al., 2022).

### ***1.3.4. Application and limits of docking studies***

Although first developed to understand how compounds interact with their molecular targets, molecular modelling is widely used to assist different tasks of drug discovery programmes. For this reason, it is currently considered a viable tool that could accelerate the discovery of novel chemical entities for the management of diverse diseases (**Pinzi & Rastelli, 2019**). Molecular docking can be applied for hit identification, as databases of potential drugs can be screened *in silico* to identify molecules that are likely to bind to protein targets of interest (**Gaba et al., 2015**). Docking has also been used to study or predict the molecular mechanism of action of a molecule of interest by predicting its biological targets (**Xu et al., 2018**). This is usually applicable for drugs discovered through laboratory experiments, and docking studies might provide molecular details of binding, interactions, and inhibition modes. Conversely, experimental findings can be used to validate the computationally discovered drugs (**Adelusi et al., 2022**). Moreover, screening drugs on proteins known to be linked with adverse reactions enables the early prediction of potential side effects of compounds during both clinical and preclinical development phases. (**Ji et al., 2006**). Moreover, molecular docking is among the most popular computational approaches used to repurpose compounds for the discovery of novel therapeutic targets (**Kharkar et al., 2014; Xu et al., 2018**).

Although molecular docking presents many advantages and applications, several limitations to this technique can be noted. In fact, reports point out a lack of correlation between experimentally determined activity and the predicted binding affinity obtained using scoring functions. There are several reasons for this observation, including underestimation of the water molecules in the binding pocket during the docking process (**Adelusi et al., 2022**). Indeed, proteins and ligands are usually surrounded by the solvent; typically, water molecules act as bridging molecules between the ligand and the receptor (**Spyrakis & Civasotto, 2015; Sethi et al., 2019**). The lack of information regarding the exact position of hydrogen could lead to inaccuracies in identifying water molecules. The worst and main challenge faced with docking studies resides on the protein flexibility. A protein can adopt various conformations depending upon the ligand to which it binds. As a result, docking performed using a rigid receptor will correspond to a single receptor conformation, which might lead to false negatives (**Shoichet et al., 1999**). This happens because the ligand and the receptor may exist in a different conformations when in free solution, which might be different from the conformation when the ligand is bound to a protein (**Koh, 2003**).

Overall, molecular docking software algorithms have not been written to incorporate or consider active site water molecules and protein flexibilities, which could contribute significantly to the binding energy of a protein–ligand complex. Contrarily to docking simulation, molecular dynamics considers all these parameters, which could account for the conformational dynamics of the protein (**Adelusi et al., 2022**).

### ***1.3.5. Molecular dynamics***

Molecular dynamics simulation is a computational technique useful in understanding protein folding, refining docked conformations and calculating free energies (**Kasam, 2009**). In contrast to docking, molecular dynamics methods have strengths, including protein flexibility and inclusion of solvent parameters, and weaknesses, including longer simulation times and the need for significant computational resources (**Alonso et al., 2006**). Hence, using molecular docking to initially screen a database of compounds and then subject the best docked complexes to molecular dynamics is a valid approach to find new lead compounds (**Adelusi et al., 2022**).

The common analyses computed after molecular dynamic simulation include the root mean square deviations (RMSD), root mean square fluctuations (RMSF), radius of gyration (ROG), and H-bond. These analyses are used to evaluate the stability of the protein–ligand complex during the simulation period and are relevant to evaluate their functional reliability in a living system (**Adelusi et al., 2022**). RMSD measures stability, RMSF evaluates the flexibility of the amino acid residues of the active site of the protein, which are of interest in drug discovery. ROG addresses the compactness of the complex, and H-bond analysis examines the degree of interaction between the ligand and the protein. The ability of the complex to maintain the H-bond interaction seen in docking throughout the MD simulation indicates stability (**Adelusi et al., 2022**).

The drug discovery pathway comprises many critical points that can lead to the discontinuance of this process. In fact, it has been estimated that 30% of compounds fail due to poor efficacy, while 50% of active compounds fail to become successful drugs because of poor pharmacokinetics or toxicity (**Jianling Wang; Laszlo Urban, 2004**). Thus, early evaluation of the pharmacokinetic (ADME) properties of drug candidates becomes a priority to successfully perform their clinical studies.

## ***1.4. Pharmacokinetic evaluation in the drug discovery and development process***

### ***1.4.1. Overview***

Pharmacokinetics (PK) is the study of the time course of absorption, distribution, metabolism, and elimination (ADME) of the drug in a given biological system. PK helps to understand the relationship between pharmacological effects and toxicological effects and the concentration of a drug and its metabolites in the body. Many drugs fail to reach or complete clinical trials due to lack of efficacy or toxicity, and pharmacokinetics (PK) govern them to a large extent ( **Robert, 2003; Ruiz-Garcia et al., 2008**). It is therefore becoming apparent that in addition to pharmacological properties, ADME properties are crucial determinates of the ultimate clinical success of a drug.

Fundamentally, ADME/PK information is critical in all phases of the drug development program, starting from drug discovery and lead optimization, safety evaluation continuing into clinical development and finally helping to position the new chemical entity as a drug (**Balani et al., 2005**) (**Table III**). Once a lead compound is identified, it is subjected to preclinical ADME studies through *in vivo* and *in vitro* testing. Furthermore, preclinical studies in laboratory animals help in selecting the first dose in clinical studies and the appropriate dosing regimen (**Smith, 1992; Heykants & Meuldermans, 1993; Mishra, 2013**). Moreover, it provides information on clearance routes (renal, biliary, or metabolic), which is helpful in guiding the selection of compounds that exhibit a balance between elimination pathways and thus would not be unduly dependent on a single organ for excretion (**Mishra, 2013**). Altogether, the selection of drug candidates with best ADME properties should enhance the probability of clinical success (**Mishra, 2013**).

**Table III:** Role of pharmacokinetics in the development of new drugs (Mishra, 2013)

Phase	Stage	Purpose
Preclinical	Discovery	To choose the optimum candidate
	Development	To understand the pharmacology in experimental
Phase I	Dose ranging	To assess the tolerability over range of
	Kinetics for single or multiple dose	To measure parameters such as the half-life, clearance, and maximum
Phase II	Sex differences and Food interaction	Assessment of the influence of gender and food on the PK profile
	Bioavailability	Quantitative determination of the distribution of a compound in body
Phase III	Effect of disease	Determination of the PK profile in the target population
	Final dosage form PK	Determination of the PK profile of the final formulation of the drug candidate
Phase IV	Dosage form improvements	Determination of the PK profile of new formulations
	Drug interactions	Determination of the possible influence of other

#### ***1.4.2. Key pharmacokinetic parameters***

The drug-like properties of a given drug can be determined by examining its fate after oral administration. When a drug is orally administered, a number of events occur, including: Dissolution: dissociation of the active ingredients of a drug from its matrix. (a) Absorption: passage of the drug through the intestinal epithelium into the systemic circulation. (b) Distribution: entrance of the drug into the circulatory system and distribution to various organs and tissues. (c) Metabolism: biotransformation of drug by the drug-metabolizing enzymes. (d) Biological interaction: interaction of the drug and its metabolites with intended and unintended targets. (e1) Drug–drug interactions: interaction of the drug with co-administered drugs. (e2) Elimination: removal of the drug from the body (Li, 2005). Consequently, the corresponding desirable properties of a drug of interest are (a) high solubility and absorption, (b) good distribution to targeted tissues, (c) appropriate metabolic stability and minimal formation of toxic metabolites, (d) extensive interactions with intended targets and minimal interactions

with unintended targets, and (e) minimal interaction with co-administered drugs, minimal toxicity, and an appropriate rate of elimination. A drug candidate with these desirable properties will probably be successful in clinical trials (Li, 2005).

### ***1.4.2.1. Absorption***

#### **Factors that influence absorption**

- ❖ Physical and chemical properties as key determinants of drug-like properties

The physical and chemical properties of a compound can be used as the first determination of drug-like properties. Based on a review of the physicochemical properties of drug-like and nondrug-like compounds, Lipinski developed the concept stating that better solubility and permeability are closely related to specific physicochemical properties. Lipinski's rule of five (RO5) states that poor absorption or permeation is more probable for a chemical when there are ( Lipinski, 2000; Li, 2005):

- ✓ More than five hydrogen bond donors (expressed as the sum of OHs and NHs): Hydrogen bonds increase solubility in water and must be broken for the compound permeation through the lipid bilayer membrane. Thus, a high number of hydrogen bonds reduces partitioning from the aqueous phase into the lipid bilayer membrane for permeation by passive diffusion (Kerns & Di, 2008).
- ✓ The molecular weight is over 500: The molecular weight (MW) is related to the size of the molecule. As the molecular size increases, a larger cavity is formed in water to solubilize the compound, and solubility decreases. Increasing MW also reduces the compound concentration at the surface of the intestinal epithelium, thus reducing absorption (Kerns & Di, 2008).
- ✓ The hydrophilicity parameter  $C \log P$  (the logarithm of its partition coefficient between n-octanol and water  $\log (C_{\text{octanol}}/C_{\text{water}})$ , is over 5. Hydrophobicity is required for drug permeation through various biological membranes and affects drug absorption, bioavailability, hydrophobic drug-receptor interactions, metabolism and toxicity of the molecules. Consequently, increasing  $\log P$  will decrease aqueous solubility and therefore reduce absorption (Kerns & Di, 2008).
- ✓ More than five hydrogen bond acceptors are expressed as the sum of Ns, and Os is over 10.

Compounds that violate more than one of these rules are considered to have poor absorption (Li, 2005).

- ❖ Lipophilicity is the tendency of a compound to partition into a nonpolar lipid surface and an aqueous surface (**Kerns & Di, 2008**). It is typically expressed as the partition coefficient, log P, and the distribution coefficient, log D.
- ❖ Solubility is the maximum dissolved concentration under given solution conditions. It is a determinant of intestinal absorption and oral bioavailability (**Kerns & Di, 2008**).

#### ***1.4.2.2. Distribution***

Distribution is influenced by several physicochemical properties of the drug and biological factors of the body. One of the most important mechanisms is phospholipid and (plasma) protein binding, which reduces the free drug concentration within the body and can prevent migration to the receptor site/site of action, therefore causing drug–drug interactions (**Trainor, 2007; Valkó, 2016**). Interestingly, binding to plasma proteins can also prolong drug action by releasing the drug over a longer period. The volume of distribution is the amount of drug that is freely available in the blood and is not bound to plasma proteins or other components (**Krüger et al., 2020**).

#### ***1.4.2.3. Metabolism***

Drug metabolism is the biotransformation of a parent drug by drug-metabolizing enzymes. This process can influence adverse drug effects, as it may lead to the detoxification of a toxic parent drug or the activation of a nontoxic parent drug into toxic metabolites through biotransformation. (**Li, 2005**). Drug metabolism is a multi-step process, including: a) phase 1 oxidation, where nonpolar molecules are oxidized via the addition of oxygen atoms, usually in the form of a hydroxyl moiety (–OH group) (Li, 2005) This phase is carried out mainly by P450 mixed-function oxygenases, including CYP1A2, CYP2A6, CYP2C9, CYP2C19, CYP2D6, CYP2E1 and CYP3A4, which are responsible for the majority of the metabolism of xenobiotic (50% of known pharmaceuticals) (**Li, 2001**); and b) phase 2 conjugation, whereby very water-soluble molecules, such as glucose (glucuronidation) or sulfate (sulfation), is added to a chemical group, especially at the –OH site. The key phase 2 enzymes include UDP-dependent glucuronosyl transferase (UGT), phenol sulfotransferase (PST), estrogen sulfotransferase (EST), and glutathione-S-transferase (GST) (**Li, 2005**).

#### ***1.4.2.4. Excretion***

The kidneys and liver are the two main drug elimination organs for xenobiotics and their metabolites. Polar compounds are excreted more efficiently than lipophilic compounds. Thus, lipid-soluble compounds are first metabolized into more polar molecules. Of the existing

ADMET properties, excretion is the least studied. Renal and fecal excretion are generally studied using whole animals, with no appropriate *in vitro* surrogates (Li, 2005).

### ***1.4.3. In silico approach for the prediction of PK parameter***

*In silico* methods using various molecular modeling techniques are currently considered one of the fastest techniques in ADME evaluation, drug discovery and toxicity (Yamashita & Hashida, 2004; Van De Waterbeemd, 2005). To this end, many *in silico* approaches for predicting the ADME properties of compounds have been developed. These range from data-based approaches (quantitative structure-activity relationships and similarity searches) to structure-based methods such as ligand–protein docking and pharmacophore modeling (Yamashita & Hashida, 2004). However, the great challenge for *in silico* methods is the generation of models that correlate more closely with *in vivo* systems, and software producers that require an effort to improve the confidence of the method (Darvas et al., 2002).

## **Aim and objectives**

The main aim of this thesis was to contribute to drug discovery against trypanosomiasis, by repositioning the MMV pathogen Box library. The first part of the project focused on the identification of valuable hits from primary screening and to further perform a rudimentary structure-activity relationship study. In the second part of the project, the focus shifted toward *in silico* and then *in vitro* studies of the most promising hit compounds obtained from SAR studies toward two crucial enzymes (DHFR/TR) of *Trypanosoma brucei*. In the third part of this dissertation, in-depth studies on the antotrypanosomal mode of action of selected bioactives were carried out to predict the drug likeness attributes and pharmacokinetic/ADME properties of the selected analogs.

# *Chapter-II*

## *Materials and Methods*



## II. MATERIALS AND METHODS

### II.1. Materials

#### II.1.1. MMV Pathogen Box acquisition and storage

The MMV Pathogen Box manufactured by Evotec (USA) was obtained free of charge from the Medicines for Malaria Venture (MMV) (Geneva, Switzerland) and contained 400 drug-like compounds. The box was shipped on dry ice and supplied as five 96-well microtiter plates containing 10  $\mu$ L of a 10 mM stock solution of compounds in 100% dimethyl sulfoxide (DMSO). Plates were stored at -20°C until further use. Supporting information for each compound was found at (<https://www.mmv.org/mmv-open/pathogen-box/about-pathogen-box>) and included the plate layout, chemical structures and formula, molecular weights, data on *in vitro* and *in vivo* DMPK (Drug Metabolism and Pharmacokinetics), confirmed biological activities against some neglected disease pathogens and cytotoxicity data.

#### II.1.2. Parasites and mammalian cells

##### II.1.2.1. Strains of *Trypanosoma brucei*

The trypanosome strain used in this study includes the nonhuman infective *T. b. brucei* bloodstream form (BSF) called Lister 427, also known as MiTat 1.2/VSG 221, kindly donated by BEI resources (<https://www.beiresources.org/>).

##### II.1.2.2. Mammalian cell lines

The normal African green monkey kidney Vero ATCC CRL-1586 cell line which was supplied by the Centre Pasteur du Cameroon was used to evaluate the cytotoxic activity of compounds.

#### II.1.3. Material and reagent sources

Unless otherwise specified, all plastic/consumable and chemicals were provided by either Sigma Aldrich (Merck) or Thermo Fisher Scientific (Gibco).

## II.2. Methods

### II.2.1. In vitro antitrypanosomal activity of MMV compounds

As stated in the subsection '1.2.2.3', it is critical to ensure that the phenotypic screening strategy used is robust, relevant, and reliable before starting the hit and lead identification process. In preparation for screening our MMV compound library, we performed a number of activities, including parasite growth confirmation, correlation between cell density and dye fluorescence, and determination of the Z' factor.

#### II.2.1.1 Antitrypanosomal assay development

##### i. Evaluation of trypanosoma growth

##### i.1. Parasite maintenance and growth conditions

The *Trypanosoma brucei* were axenically cultivated in 25 cm<sup>2</sup> sterile vented flasks containing complete Hirumi's modified Iscove's medium 9 (HMI-9) prepared using Iscove's modified Dulbecco's medium (IMDM) supplemented with 10% (v/v) heat inactivated fetal bovine serum (HIFBS), 10% (v/v) serum plus 1% (v/v) penicillin–streptomycin and HMI-9 supplements (1 mM hypoxanthine, 0.16 mM thymidine, 50 µM bathocuproine disulfonic acid, 1.5 mM cysteine, 1.25 Mm pyruvic acid, and 0.2 mM 2-mercaptoethanol) (**Appendix 2**). Cultures were incubated at 37°C in a humidified 5% CO<sub>2</sub> atmosphere. They were routinely monitored every 72 h using a Lumascope LS520 inverted fluorescence microscope (Etaluma, Inc., USA) to assess parasite density and subsequently subcultured in fresh complete medium (**Hirumi & Hirumi, 1989**). To maintain the culture as stable as possible, parasites were subcultured a maximum of 30 times and then substituted with a new, previously preserved aliquot. In addition, the cryopreserved cultures were maintained in freezing medium (**Appendix 2**) at - 80°C.

##### i.2. Confirmation of *T. brucei* growth

Before starting the antitrypanosomal drug screening, it was important to have evidence of parasite growth under our laboratory conditions and then determine the minimum and maximum parasite density necessary for an optimum growth. To this end, parasites at an initial density of 2x10<sup>5</sup> parasites/mL were counted in a Neubauer chamber after an incubation period of 24 h, 48 h, 72 h and 96 h at 37°C and 5% CO<sub>2</sub>. From the obtained values, the doubling time was calculated in the log phase of growth as follows:

$$td = \frac{(t_2 - t_1) \log 2}{\log\left(\frac{q_2}{q_1}\right)}$$

where  $td$  is the doubling time,  $q_1$  is the initial density at time 0 ( $t_1$ ), and  $q_2$  is the density 24 hours after the initial density but at time 1 ( $t_2$ ). In addition, parasites were collected by centrifugation at 2500 rpm for 7 min, colored using acridine orange (1 mg/mL in D-PBS) and subsequently photographed.

### ***ii- Linearity of the resazurin-based cell viability assay***

The aim of this experiment was to establish the linearity between cell density and fluorescence readings in the resazurin-based assay. The method is based on the reduction of resazurin (blue color) to resorufin (pink color) by mitochondrial dehydrogenases in metabolically active parasites. The resulting complex absorbs between 570 nm and 590 nm and is directly proportional to the quantity of viable parasites (**Brien et al., 2000; Bowling et al., 2012**). Briefly, *T. b. brucei* parasites were incubated at 37°C and 5% CO<sub>2</sub> for 72 h at densities ranging from 0.0625x10<sup>5</sup> to 8x10<sup>5</sup> trypanosomes/mL in a total volume of 100 µL. Thereafter, 10 µL of resazurin was added immediately at a 0.15 mg/mL concentration, and the fluorescence intensity was measured at wavelengths of 530 nm for excitation and 590 nm for emission using a Tecan Infinite M200 fluorescence multiwell plate reader.

### ***iii- Determination of 50% inhibitory concentration (IC<sub>50</sub>) of dimethyl sulfoxide (DMSO) and reference compound pentamidine***

The trypanotoxicity of DMSO and pentamidine was determined as follows. Basically, in a 96-well flat-bottomed plate, 10 µL of various concentrations of DMSO (100% à 0.00128%) and pentamidine isothionate (100 µM-0.00128 µM) were distinctly added to 90 µL of parasite inoculum previously adjusted to 2 x 10<sup>5</sup> trypanosomes/mL. Wells containing complete HMI-9 medium with parasites were used as a negative control. After 68 hours at 37°C and 5% CO<sub>2</sub>, 10 µL of resazurin (0.15 mg/ml, DPBS) was added to each well, and the plate was incubated for an additional 4 hours. Next, fluorescence readings were performed using the Tecan Infinite M200 fluorescence multiwell plate reader at wavelengths of 530 nm for excitation and 590 nm for emission. For each sample, the growth inhibition percentages were calculated with Microsoft Excel Software and the obtained data were used to construct concentration–response curves by plotting inhibitory percentages versus the logarithm of concentrations. From these curves, the 50% inhibitory concentration (IC<sub>50</sub>) was deduced using GraphPad Prism 8.0

software with data fitted by nonlinear regression to the variable slope sigmoidal concentration–response formula  $y = 100/[1 + 10^{(\log IC_{50}/99-x)H}]$ , where H is the Hill coefficient or slope factor (Singh and Rosenthal, 2001).

The performed experiments were also validated by calculating the Z' factor using the formula:

$$Selectivity\ Index = 1 - \frac{3\sigma_p + 3\sigma_n}{\mu_p - \mu_n}$$

where  $\mu_p$ ,  $\sigma_p$ ,  $\mu_n$  and  $\sigma_n$  are the means ( $\mu$ ) and standard deviations ( $\sigma$ ) of both the positive (p) and negative (n) controls. A Z-factor between 0.5 and 1.0 indicates an excellent assay and statistically reliable separation between the positive and negative controls (Zhang et al., 1999).

### II.2.1.2 Antitrypanosomal screening of the 400 MMV compounds

#### i. Preparation of compounds and the reference

Compounds were diluted to five subsets for a final intermediate concentration of 100  $\mu$ M in 96-well storage plates using incomplete IMDM culture medium (2  $\mu$ L of stock solution were added to 198  $\mu$ L of sterile incomplete medium). Next, plates were stored at -20°C until biological assays. Pentamidine isethionate was weighed and dissolved in 100% DMSO to a final concentration of 10 mM and used as a positive control for the antitrypanosomal assays. From the prepared stocks solution, dilutions were performed to obtain the required concentrations for each test.

#### ii. In vitro single point antitrypanosomal screening of compounds

The *in vitro* inhibitory potency of the 400 MMVPB compounds against bloodstream forms of *Trypanosoma brucei brucei* was evaluated using the resazurin-based inhibition assay as previously described by Bowling et al., (2012). Briefly, parasites at their mid-logarithmic growth phase were counted, and the cell density was adjusted with fresh complete HMI-9 medium to  $2 \times 10^5$  trypanosomes per mL. Ninety microliters of parasite suspension were then distributed in a sterile flat bottom 96-well plate containing 10  $\mu$ L of compounds for a final test concentration of 10  $\mu$ M. In each plate, the first and last columns served as negative (cells with 0.1% DMSO) and positive (cells with 10  $\mu$ M pentamidine isethionate) controls, respectively. After 68 hours of incubation at 37°C and 5% CO<sub>2</sub>, parasite viability was checked after fluorescence measurement using a Tecan Infinite M200 fluorescence multiwell plate reader (Austria) at wavelengths of 530 nm for excitation and 590 nm for emission following a 4-hour incubation period with resazurin (0.15 mg/mL in DPBS) in darkness. Each assay plate was set

up in duplicate and repeated two times. The percent parasite inhibition was determined for each compound based on fluorescence readouts relative to the mean fluorescence of negative control wells.

Compounds that exhibited mean inhibition percentages greater than or equal to 90% at 10  $\mu\text{M}$  were selected for the concentration–response assay.

### *iii. Concentration–response growth inhibition assay of the selected compounds*

The median inhibitory concentrations ( $\text{IC}_{50}$ ) of the selected compounds were determined as described above, with slight modifications. Briefly, 7-point fivefold serial dilutions of compounds with tested concentrations ranging from 10 - 0.00064  $\mu\text{M}$  for each drug and pentamidine isethionate were used. Experiments were performed in duplicate and repeated twice. Mean fluorescence counts were normalized to percent control activity using Microsoft Excel, and the 50% inhibitory concentrations ( $\text{IC}_{50}$ ) were calculated using Prism 8.0 software (GraphPad) with data fitted by nonlinear regression to the variable slope sigmoidal concentration–response formula  $y = 100/[1 + 10^{(\log\text{IC}_{50}/99-x)H}]$ , where  $H$  is the Hill coefficient or slope factor (Singh & Rosenthal, 2001).

Prioritized compounds ( $\text{IC}_{50} < 4 \mu\text{M}$ ) were further tested for their cytotoxic effect against a mammalian cell line as described below.

### **II.2.1.3. Cytotoxicity study of selected compounds**

Active and nontoxic compounds are increasingly claimed in the early drug discovery stage, especially for HAT, since one of the main challenges faced is toxicity. Therefore, to determine the possible deleterious effects of our compounds on mammalian cells, we evaluated their cytotoxic activity. In this study, the Vero cells were used to sieve nonselective inhibitors determined by the resazurin viability assay, which was previously implemented in our research group.

#### *i. Maintenance of mammalian cells*

Vero cells were first grown (from a -80 aliquot) in T-25 vented cap culture flasks using complete Dulbecco's modified Eagle's medium (DMEM) supplemented with 10% FBS, 1% nonessential amino acids and 1% (v/v) penicillin–streptomycin and incubated at 37°C in an atmosphere containing 5%  $\text{CO}_2$  (Appendix 2). The medium was renewed every 72 h, and the cell density was monitored using an inverted microscope (Lumascop LS520). Subculturing was performed when the cells reached ~80-90% confluence by detachment with 0.25% trypsin-

EDTA followed by centrifugation at 1800 rpm for 5 min. The resulting pellet was resuspended in 1mL complete medium and counted in a Neubauer chamber in the presence of trypan blue to exclude nonviable, blue-colored cells. Once the cell load was estimated, they were either used for the next passage in a new flask or processed for the cytotoxicity assay. As recommended by the manufacturers, cells were subcultured for a maximum of 32 times and then substituted with a new aliquot. In addition, the cryopreserved cells were maintained in freezing medium at -80°C (**Appendix 2**).

### *ii. Assessment of the cytotoxic effect of compounds*

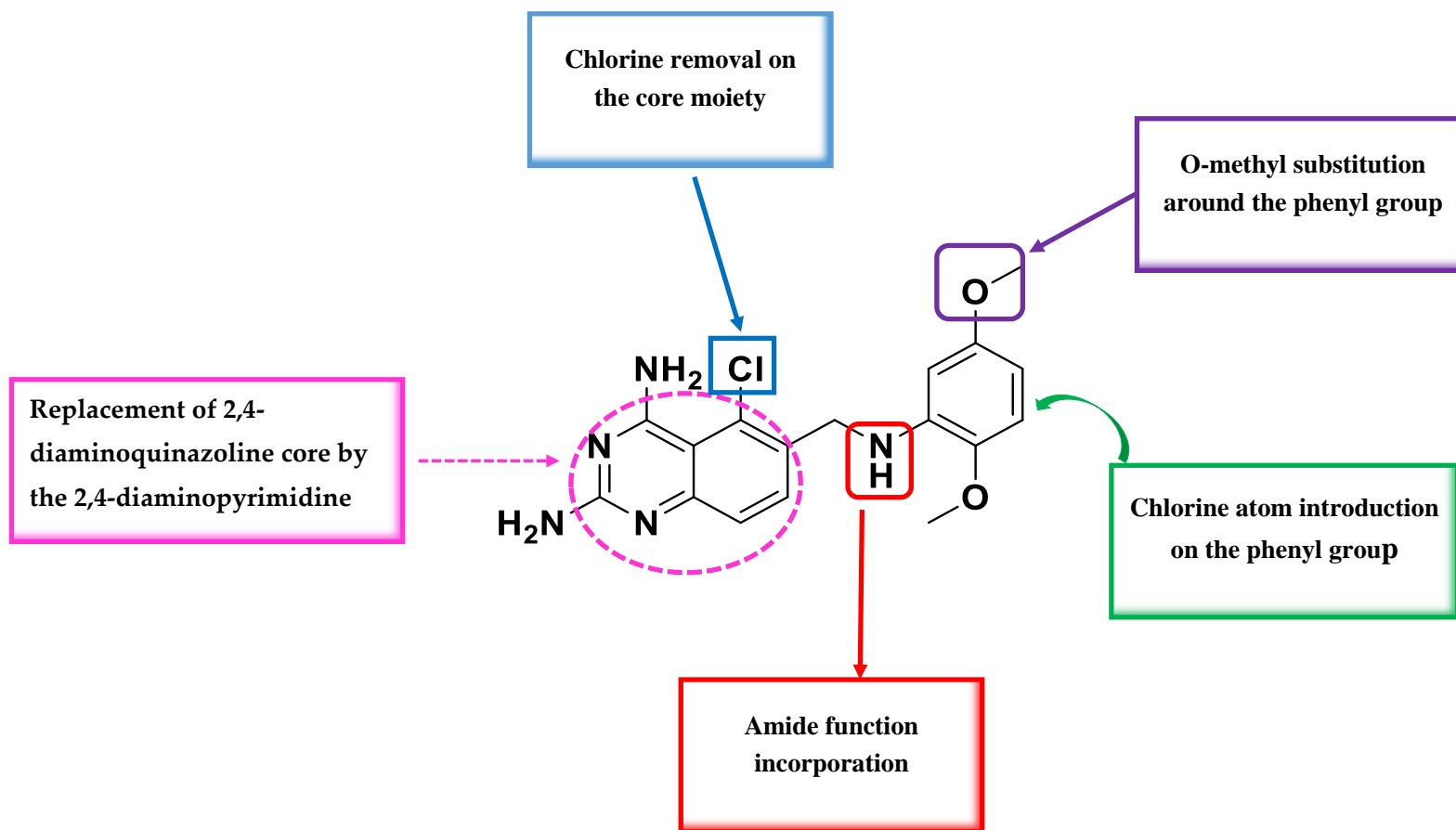
The cytotoxicity of promising compounds was assessed as previously described by **Bowling et al. (2012)** in a 96-well tissue culture-treated plate. Briefly, Vero cells at a density of  $10^4$  cells per well were plated in 100  $\mu$ L of complete DMEM and incubated overnight to allow cell attachment. Plates were then controlled under an inverted fluorescence microscope (Lumascop LS520) to assure adherence, sterility, and cell integrity. Thereafter, the culture medium from each well was carefully emptied, and the plates were filled with 90  $\mu$ L of fresh complete medium followed by the addition of 10  $\mu$ L of serial 5-fold dilutions of compound solutions. Podophyllotoxin (100  $\mu$ M-0.16  $\mu$ M) and 0.5% DMSO (100% cell viability) were also included in assay plates as positive and negative controls, respectively. After an incubation period of 48 h at 37°C in a humidified atmosphere and 5% CO<sub>2</sub>, 10  $\mu$ L of a stock solution of resazurin (0.15 mg/mL in DPBS) was added to each well and incubated for an additional 4 h. Fluorescence was then read using a Magelan Infinite M200 fluorescence multiwell plate reader (Tecan) with excitation and emission wavelengths of 530 and 590 nm, respectively. The percentage of cell viability was calculated from readouts, and the median cytotoxic concentration (CC<sub>50</sub>) for each compound was deduced from concentration–response curves using GraphPad Prism 8.0 software. Selectivity indexes were then determined for each test substance as follows:

$$\text{Selectivity Index} = \frac{CC_{50} (\text{Vero})}{IC_{50} (\text{T. b. brucei})}$$

where the numerator and the denominator represent the concentration of a compound required for 50% *in vitro* inhibition of Vero cells and the concentration of the same compound needed for 50% *in vitro* inhibition of *Trypanosoma brucei* parasites, respectively.

### ***II.2.2. Structure-activity and selectivity relationship study***

Several derivatives from the selected hits were designed and provided by the MMV organization. The synthesized analogs were submitted to antitrypanosomal screening and cytotoxicity on Vero cells as described above. Based on the different substituted and unsubstituted groups or chemical modifications that have been performed on the initial compound, a structure-activity relationship (SAR) was established for these biological properties (antitrypanosomal and cytotoxicity). These modifications are summarized in **Figure 16**. Compounds with good pharmacological profiles were selected for the study of the mode of action studies.



+-

**Figure 16:** Simplified scheme of the structural modifications performed on the initial compound

### ***II.2.3. In silico and in vitro activities of compounds on their likely molecular target***

#### ***II.2.3.1. In silico exploration of the DHFR and TR binding properties of selected analogs***

##### ***i. Compound preparation***

Compound structures were drawn and converted to SMILES format using the SMILES generator window of the Cheminfo webserver (<http://www.cheminfo.org/>). Accessible protonation states of the compounds at physiological pH were assessed using the dimorphite-DL program (Ropp et al., 2019). Dimorphite-DL uses a straightforward empirical algorithm that leverages substructure searching and makes use of a database of experimentally characterized ionizable molecules to enumerate small-molecule ionization states (Ropp et al., 2019). Herein, the SMILES format of the compounds was used as input, generating a list of SMILES of all the possible protonation states at the default physiological pH (6.4 – 8.4). The output from dimorphite-DL was streamlined by measuring the pKa values using MolGpka (Pan et al., 2021). The MolGpka webserver predicts pKa through a graph-convolutional neural network model that works by learning pKa-related chemical patterns automatically and building reliable predictors with the learned features (Pan et al., 2021). Matching the pKa values of the different ionizable sites with the physiological pH resulted in the retention of only the physiologically feasible compounds. The retained SMILES were then converted to the vina compatible pdbqt format using the format converter window of the Cheminfo webserver in preparation for docking.

##### ***ii. Protein structure preparation***

The protein structures used in this study were obtained from the Research Collaboratory for Structural Bioinformatics, Protein Data Bank (RCSB PDB) (Berman et al., 2000). For *Trypanosoma brucei brucei* trypanothione reductase, the crystal structure (PDB ID: 2 WP6) is freely available and was downloaded online. However, the *T. brucei brucei* DHFR crystal structure was not deposited in the RCSB PDB. On the other hand, it shares 100% sequence identity with *T. brucei rhodesiense* DHFR; hence, the latter's crystal structure (PDB ID: 3RG9) was downloaded and prepared for use. The protein structures were preprocessed using Discovery Studio Visualizer version 4.1 (Discovery Studio Predictive Science Application | Dassault Systèmes BIOVIA, 2016). Initially, the structure of DHFR was examined for the presence of the recently identified DHFR crystal structural error reported in *P. falciparum* (Tata

et al., 2022). The implicated loops were identified to be shorter and capable of no entanglements, hence ruling out the possibility of a crystallographic error. The cofactors NADPH and FAD were maintained in both the DHFR and TR structures, respectively. Partial charges and AutoDock atom types (pdbqt format) were incorporated into the protein and cofactor structures, respectively, using the prepare\_receptor4.py and the prepare\_ligand4.py python scripts from AutoDock4 tools (Morris et al., 2009).

### *iii. Molecular Docking*

A blind docking protocol was implemented using the molecular docking and virtual screening tool AutoDock Vina (Trott & Olson, 2010). Docking validation was accomplished through redocking of the cocrystallized ligands of the DHFR and TR structures into their respective active sites. The docking parameters adopted following the validation were as follows: DHFR - box size (in Å)  $x = 42.75$ ,  $y = 42.75$ ,  $z = 41.62$ ; box center  $x = 64.64$ ,  $y = 32.86$ ,  $z = 36.54$ ; and an exhaustiveness of 290. TR - box size (in Å)  $x = 83.62$ ,  $y = 65.62$ ,  $z = 84.00$ ; center  $x = 43.17$ ,  $y = 5.75$ ,  $z = -0.05$ ; and an exhaustiveness of 290. After docking a split of the top nine predicted poses from AutoDock vina were performed using the vina\_split script and the pose with the lowest docking score was retained for further evaluations. Protein-ligand complexes were then prepared for the top scoring ligands using an inhouse Python script and visualization was performed in Discovery Studio Visualizer version 4.1 and PyMOL (Discovery Studio Predictive Science Application | Dassault Systèmes BIOVIA, 2016; Schrödinger and DeLano, 2020).

### *iv. Molecular dynamics simulations*

Molecular dynamics (MD) simulations were performed within the Amber forcefield a99SB-disp (Robustelli et al., 2018), using the GROMACS v.2018 software package (Kutzner et al., 2019). The GROMACS-compatible version of the a99SB-disp forcefield was obtained from Paulrobustelli, (2021) and used to perform all-atom MD simulations. Ligand parameters were determined by the ACPYPE tool (Sousa Da Silva & Vranken, 2012). TIP4P (a99SBdisp\_water) water molecules were used to embed each system within a cubic simulation box, leaving a clearance space of 1.0 Å from the edges of the protein. Appropriate amounts of Na<sup>+</sup> and Cl<sup>-</sup> ions were added to neutralize the total system charges. This was followed by system relaxation through energy minimization using the steepest descent algorithm with a force threshold of 1000 kJ/mol/nm and a maximum of 50,000 steps. The temperature and pressure were equilibrated using the modified Berendsen thermostat (at 300 K for 100 ps),

according to the NVT ensemble, and the Parrinello–Rahman barostat (Parrinello & Rahman, 1981), to maintain the pressure at 1 bar. During the equilibration steps, the protein was position restrained, and constraints were applied to all the bonds using the LINCS algorithm (Hess et al., 1997). Finally, unrestrained production runs were performed for 100 ns each under periodic boundary conditions (PBCs) and the equilibration step thermostat and barostat were both maintained for temperature and pressure coupling. The leap-frog integrator was used with an integrator time step of 2 fs, while the Verlet cutoff scheme was implemented using default settings, and coordinates were written at 10.0 ps intervals. Long-range electrostatic interactions were treated using the Particle–Mesh Ewald (PME) algorithm (Essmann et al., 1995), while short-range nonbonded contacts (Coulomb and van der Waals interactions) were defined at a 1.4 nm cutoff. All analyses were accomplished using GROMACS tools. The trajectories were first corrected for periodic boundary conditions using the gmx trjconv tool, starting with the system centering within the simulation box, fitting the structures to the reference frame, and putting back atoms within the box. Furthermore, gmx rms, gmx rmsf, and gmx gyrate were utilized for the calculation of the root mean square deviation (RMSD), root mean square fluctuation (RMSF), and radius of gyration (Rg), respectively. The gmx\_cluster tool was used for ligand clustering, and the gromos method was used with an RMSD cutoff value of 0.12 nm.

### ***II.2.3.2. In vitro screening against T.b.b. crude protein extract***

#### ***i. Preparation of crude Trypanosoma brucei brucei lysates and protein quantification***

At their logarithmic phase, *T. brucei brucei* bloodstream parasites were collected by centrifugation at 3500rpm for 30 min at 4°C (Allegra X-15R, Beckman Coulter, Brea, CA, USA) and washed twice in sterile DPBS 1X pH 7.4. The resulting cell pellets (from  $5 \times 10^9$  cell/mL inoculum) were lysed by adding 300  $\mu$ L of RIPA (Radioimmunoprecipitation) lysis buffer consisting of 50 mM Tris HCl, pH 7.5, 150 mM NaCl, 1% Triton X-100 v/v, and 1% protease inhibitor cocktail. The homogenate was stirred for 30 min at 25°C followed by 10 freeze (–80°C)/thaw (42°C) cycles to maximize lysis and extraction. The protein extract was centrifuged at 14,000rpm (Eppendorf 5418-RG, Eppendorf AG, Hamburg, Germany) for 15 min at 4°C, and the supernatant was collected and stored at –80°C until further use.

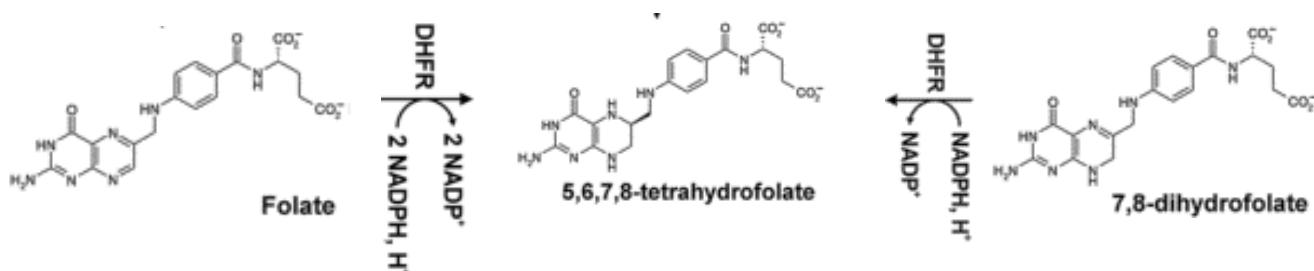
The protein concentration of the crude extract was determined by the Bradford method (Bradford protein assay kit 23200) using a bovine serum albumin standard curve obtained by plotting the optical density measurement at 595 nm of the BSA (standard) vs. quantity of protein in  $\mu$ g (Appendix 3) (Bradford, 1976). Briefly, 5  $\mu$ L of the crude protein extract was

introduced three times into the wells of a 96-well microplate containing 195  $\mu\text{L}$  of Coomassie reagent. The plate was incubated for 10 minutes at room temperature (RT), and the absorbance was measured at 595 nm with a Magellan Infinite M200 fluorescence plate reader. The average 595 nm measurement for the blank replicates was subtracted from the 595 nm measurements of the test samples, and then the amount of protein in the crude *T.b.b.* protein extract was deduced based on the linear regression equation (**Appendix 3**).

Protein extraction was confirmed using sodium dodecyl sulfate–polyacrylamide gel electrophoresis (SDS–PAGE) (Owl Dual-Gel Vertical Electrophoresis systems, Thermo Scientific, Waltham, MA, USA) (**Garfin, 1990**). To this end, acrylamide separating and stacking gels (**Appendix 4**) were run at approximately 100 to 120 V for 1 h. At the end of the electrophoresis, the gels were stained with Coomassie brilliant blue G-250 and destained with distilled water for visualization.

#### ii. *T. b. brucei* protein activity assay and primary screening of inhibitors

In an attempt to estimate folate reduction (dihydrofolate reductase activity), we monitored the overall decrease in absorbance at 340 nm due to the oxidation of NADPH and the reduction in folic acid into tetrahydrofolate (Reaction 1) as previously described by Bailey and Ayling (**Bailey & Ayling, 2009**) with slight modifications.



#### Reaction 1: Enzymatic reduction of folic acid to tetrahydrofolic acid.

Briefly, in a 96-well quartz microplate, 0.3 mg/mL total protein from *Trypanosoma brucei brucei* lysate was preincubated for 1 min at 25°C with 120  $\mu\text{M}$  NADPH in an assay buffer containing 50 mM Tris HCl, pH 7.5, 150 mM NaCl, and 2 mM DTT. The assay was initiated by the addition of 50  $\mu\text{M}$  folic acid (Sigma–Aldrich, Darmstadt, Germany) to yield a total reaction volume of 200  $\mu\text{L}$ , and the absorbance was measured at 340 nm (A<sub>340</sub>) in kinetic mode every 15 s for 20 min at room temperature. Methotrexate (Sigma–Aldrich, Darmstadt, Germany), which binds to and inhibits the enzyme dihydrofolate reductase, was used as a positive control at 20  $\mu\text{M}$  and was introduced before the addition of NADPH. Similarly,

predicted DHFR inhibitors were screened at 20  $\mu\text{M}$  such that the DMSO concentration did not exceed 0.5%. Inhibitor control wells containing test compounds in the reaction buffer (as an inhibitor background control to test the absorbance of the compounds alone) and solvent control wells containing protein extract and DMSO (0.2%) (to test the effect of DMSO on enzyme activity) were included in the assay. The background control wells consisting of NADPH and folic acid, and prepared in the same reaction buffer were also included. Next, the enzymatic folate reduction activity was then measured as changes in A340 per min using the combined molar extinction coefficient for NADPH oxidation and folic acid reduction in  $\epsilon_{[\text{NADPH/THF}]} = 12.3 \text{ mM}^{-1} \text{ cm}^{-1}$ . In the presence or absence of the inhibitors, the enzyme-specific activity was calculated using the formula:

$$\text{Specific activity (Units/mg P)} = \frac{[(\Delta\text{OD}/\text{min}_{\text{sample}} - \Delta\text{OD}/\text{min}_{\text{blank}}) \times \text{df}]}{12300 \times V \times \text{mg protein/mL}} \quad (1)$$

where  $\Delta\text{OD}/\text{min}_{\text{blank}}$  represents the activity rate for the blank,  $\Delta\text{OD}/\text{min}_{\text{sample}}$  is the activity rate for the sample (enzymatic reaction),  $V$  is the protein volume in mL (the volume of protein extract used in the assay),  $\text{df}$  is the dilution factor of the protein extract,  $\text{mg protein/mL}$  is the protein concentration of the original sample before dilution, and  $\text{Units/mg P}$  is the specific activity expressed in  $\mu\text{mole}/\text{min}/\text{mg protein}$ .

### iii. Determination of the $\text{IC}_{50}$ values of test compounds

The  $\text{IC}_{50}$  values of each test compound were determined by measuring the reaction rate ( $\Delta\text{OD}/\text{min}$ ) at several inhibitor concentrations (20–0.00128  $\mu\text{M}$ ) as described above. The test was performed in duplicate, and the results were normalized to those of the *T. b. b.* protein control containing no inhibitor (100% activity). The relative activity percentages were then deduced for each of the tested concentrations using the following formula.

$$\% \text{ Relative activity} = \frac{\text{Specific activity of } T. b. b. \text{ Protein with inhibitors}}{\text{Specific activity of } T. b. b. \text{ Protein without inhibitors}} \quad (2)$$

The 50% inhibitory concentrations ( $\text{IC}_{50}$ ) were deduced from a concentration–response curve using GraphPad Prism 8.0 software with data fitted by nonlinear regression to the variable sigmoidal concentration–response slope formula  $y = 100/[1 + 10^{(\log\text{IC}_{50}/99-x)H}]$ , where  $H$  is the Hill coefficient or slope factor.

#### ***II.2.4. Attempts to elucidate other antitrypanosomal modes of action of the promising analogs and prediction of pharmacokinetic properties***

First, the effects of treatments on *T.b.brucei* growth after short or continuous exposure to selected derivatives were evaluated and they were also screened for their ability to weaken the plasma membrane, produce ROS, induce DNA fragmentation and reduce ferric iron.

##### ***II.2.4.1. In vitro determination of parasite-killing kinetics of selected derivatives***

The effect of various concentrations of compounds on the proliferation rate of BSF *Trypanosoma brucei brucei* was assessed using microscopic cell counts. Briefly, parasites at their exponential growth phase were seeded into a 24-well flat-bottomed plate and incubated for 72 h at a cell density of  $2 \times 10^5$  trypanosomes per mL with compounds at their IC<sub>99</sub>, IC<sub>90</sub>, IC<sub>50</sub>, and IC<sub>10</sub> values (**Appendix 5**). After cell exposure for 0, 4, 8, 12, 24, 30, 36, 48, 60, and 72 h, the content of each well was harvested and counted on a Neubauer hemocytometer to determine the number of mobile parasites (**Nnadi et al., 2019**). The obtained values were used to plot the growth curves as parasite density (cells/mL) versus incubation time using GraphPad Prism 8.0 software. All experiments were performed in duplicate and included positive (pentamidine) and negative (parasites without inhibitor) controls.

##### ***II.2.4.2. Assessment of the cidal or static effect of the inhibitors***

To establish whether the potent compounds cause persistent and irreversible effects, *T. b. brucei* parasites were assessed for their ability to recover from the conditions following exposure to test compounds. Briefly, parasites at  $2 \times 10^5$  trypanosomes/mL were incubated at 37°C and 5% CO<sub>2</sub> with compounds at their respective IC<sub>99</sub> and IC<sub>90</sub> concentrations for a given incubation period (4 hours or 24 hours depending on compound efficiency). Next, the cells were washed three times with fresh complete medium by centrifugation at 2500 rpm for 7 minutes. Cell pellets were thereafter resuspended in fresh complete culture medium in a 24-well plate and subcultured under the same conditions to achieve a complete parasite cycle. Thereafter, the cells were enumerated using a Neubauer cell counter at each time point. The assay was performed in duplicate, and the mean cell counts were plotted against time using GraphPad Prism 8.0 to assess the cidal or static effect of inhibitors.

##### ***II.2.4.3. Effect of compounds on trypanosome plasma membrane integrity***

The plasma membrane is the first barrier protecting the cell from the external environment and therefore might represent an important challenge for compounds to exert their

inhibitory action. Thus, compounds were assessed for their ability to induce alterations in cell integrity as previously described (O' Nnadi et al., 2019) with a modification consisting of using a SYBR green assay (Faria et al., 2015) instead of propidium iodide. The principle of states that upon treatment with membrane disruptors, trypanosomes with compromised plasma become fluorescent as a result of SYBR green entry and fixation to the exposed DNA. Briefly, in a 96-well microtiter plate, 90  $\mu\text{L}$  of trypanosome suspension ( $2 \times 10^6$  cells/mL/well) was preincubated with SYBR Green (2X) for 15 min at  $37^\circ\text{C}$  and 5%  $\text{CO}_2$  in darkness. Next, the reaction was allowed to start following the addition of 10  $\mu\text{L}$  of compounds at their  $\text{IC}_{99}$ ,  $\text{IC}_{90}$ ,  $\text{IC}_{50}$ , and  $\text{IC}_{10}$  (Appendix 5). Afterward, the plate was incubated at  $37^\circ\text{C}$  on a Magelan Infinite M200 multiwell plate reader (Tecan), and fluorescence was further recorded every 5 min for up to 120 min at excitation and emission wavelengths of 485 and 538 nm, respectively. Wells containing saponin at 0.075 g/mL were used as a positive control for maximal permeabilization, whereas untreated trypanosomes and HMI-9 medium were used as negative control and background signal, respectively. The results are expressed as the mean  $\pm$  SD of two experiments carried out in duplicate after deducting the background signal (wells containing HMI-9 medium) and then used to plot the graph of fluorescence intensity versus time (min).

#### ***II.2.4.4. Induction of intracellular reactive oxygen species (ROS) production by trypanosomes upon treatment with inhibitors***

The production of ROS was detected using a 2',7'-dichlorofluorescein diacetate (DCFDA) probe as described by Rea et al., (2013). Briefly, parasites ( $2 \times 10^6$  cells/mL/well) were washed in incomplete IMDM medium and incubated with compounds at their respective  $\text{IC}_{99}$ ,  $\text{IC}_{90}$ ,  $\text{IC}_{50}$ , and  $\text{IC}_{10}$  values (Appendix 5) for 2 hours at  $37^\circ\text{C}$ . DCFDA (100  $\mu\text{L}$ , 5  $\mu\text{M}$ ) was then added to the parasites, and incubation was continued for 15 min at  $37^\circ\text{C}$ . Hydrogen peroxide ( $\text{H}_2\text{O}_2$  0.1% v/v) was used as a positive control for maximal ROS production, and wells with untreated parasites were included as a negative control. Of note, DCFDA is cleaved by ROS to produce fluorescent 2',7'-dichlorofluorescein (DCF). The fluorescence intensity was measured at excitation and emission wavelengths of 485 and 520 nm, respectively. Data obtained from duplicate readouts were used to determine the percentage of ROS relative to the positive control (100% production).

$$\% \text{ ROS production} = \frac{\text{OD Test}}{\text{OD control (H}_2\text{O}_2)}$$

#### ***II.2.4.5. Induction of cellular DNA fragmentation upon trypanosome treatment with inhibitors***

In an attempt to understand the tentative mechanism (apoptosis-like or cytolysis) by which trypanosomes are eliminated following exposure to compounds, DNA fragmentation analysis was performed using a cellular DNA fragmentation ELISA kit as per to the manufacturer's recommendations (ROCHE Cat No. 11585045 001). To this end, 5'-bromo-2'-deoxy-uridine (BrdU) was used as a metabolic labeling agent by the nuclear DNA of target cells. In this experiment, apoptotic cell death was quantified by detection of fluorescent dye-labeled DNA fragments in the cytoplasm of affected cells or to measure cell-mediated cytotoxicity through detection of dye-labelled DNA fragments released from damaged cells into the culture supernatant.

Briefly, parasites ( $4 \times 10^5$  parasites/mL/well) were incubated at 37°C for 24 hours with BrdU, a nonradioactive thymidine analog that is incorporated into the genomic DNA. BrdU-labeled parasites were harvested (by spinning at 2500 rpm for 7 min) followed by a centrifugal washing using BrdU-free HMI-9 medium. One hundred microliters of the labeled and washed parasites at a final density of  $4 \times 10^5$  parasites/mL/well were treated in duplicate wells on a 96-well round-bottom plate with 100  $\mu$ L of analogs at IC<sub>99</sub>, IC<sub>90</sub>, IC<sub>50</sub>, and IC<sub>10</sub> (**Appendix 5**) for 4 hours. Next, the plate was centrifuged at 2500 rpm for 7 min, and the pellets were collected and kept at 4°C until further use. For cytolysis measurement, the supernatants were added to a microplate coated with anti-DNA antibody (**Appendix 6**) to allow DNA capture from the test samples. The captured DNA fragments were subsequently denatured using microwave irradiation (LG NeoChef Charcoal Healthy Ovens) at 500 W for 5 minutes to separate the DNA strands and display the BrdU. Thereafter, an anti-BrdU-antibody-POD (peroxidase) conjugate was added to detect the BrdU contained in the captured DNA fragments. One hundred microliters of the POD substrate solution were added to each well, and the absorbance was read at 370 nm every 30 s until development of a color, which was green in the case of this study.

For apoptosis-like measurement, the cell pellets from each well were resuspended in 200  $\mu$ L of the kit's incubation buffer (**Appendix 6**) and incubated for 30 min. The lysed cells were centrifuged at 1700 rpm for 10 min, and the supernatants were added to a microplate coated with anti-DNA antibody to capture DNA fragments and detect the BrdU in these DNA fragments. Triton X-100 (1%) was used as a positive control for both apoptosis and cell-mediated cytotoxicity. The absorbance values were proportionally correlated to the amount of

DNA fragments in the treated cultures. Data are expressed as the mean $\pm$ SD of two independent experiments performed in duplicate and compared to the negative control (untreated parasites) at a significance level of  $p < 0.05$ .

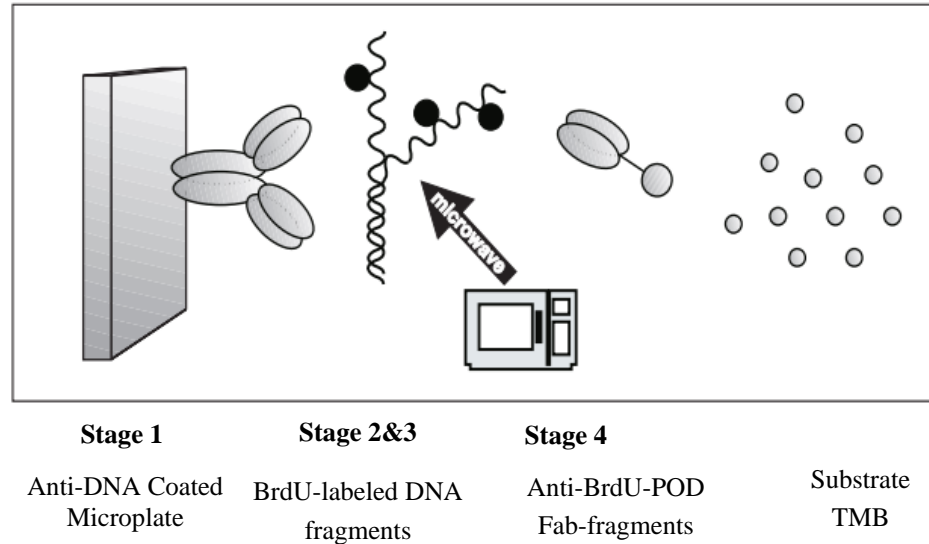


**Figure 17:** Principle of the cellular DNA fragmentation assay

#### ***II.2.4.6. Determination of the Ferric Ion Reducing Antioxidant Power (FRAP) of inhibitors***

Iron is one of the vital elements for all parasites, including trypanosomes, as it plays a key role in pathogenesis and the host immune response. Therefore, iron bioavailability reducing agents to the parasite could be potential candidates for drug development against trypanosomiasis. To this end, we determined the capacity of the test compounds to reduce iron from ferric to ferrous status using the method described by **Benzie et al. (1996)**. Briefly, 25  $\mu$ L of each compound were added to 25  $\mu$ L of a solution of  $\text{Fe}^{3+}$  prepared at 1.2 mg/mL in distilled water in a 96-well microplate. The plate was incubated for 15 min at room temperature in darkness, then 50  $\mu$ L of ortho-phenanthroline (0.2% in methanol) were added to achieve final compound concentrations ranging from 400  $\mu$ M to 0.19  $\mu$ M. The plates were reincubated for 15 min, and the absorbance was measured at 510 nm. Ascorbic acid was used as a positive control and tested at concentrations ranging from 100 to 0.048  $\mu$ g/mL. The median reducing concentration ( $\text{RC}_{50}$ ) of compounds were determined through sigmoidal concentration–response curves using GraphPad Prism version 8.0 software.

### II.2.4.7. Prediction of ADME parameters of selected analogs

The structures of the test compounds (MMV675968, MMV1578467 and MMV1578445) were drawn using ChemBio2D Draw, and their SMILES codes were generated. These codes were used as the main materials for running the online SwissADME (<http://www.swissadme.ch/>- accessed on 12<sup>th</sup> September 2022) and Protox ([https://tox-new.charite.de/protox\\_II/](https://tox-new.charite.de/protox_II/), [https://tox-new.charite.de/protox\\_II/](https://tox-new.charite.de/protox_II/)- accessed on 12 September 2022) tools to predict ADME and toxicity properties, respectively.

### II.3. Statistical analysis

Data collected from at least two independent experiments performed in duplicate are expressed as the mean  $\pm$  SD (standard deviation). They were analyzed using Tukey's multiple comparison test using GraphPad 8.0 software. Differences were considered statistically significant at  $P < 0,05$  (\*),  $P < 0.001$  (\*\*), and  $P < 0.0001$  (\*\*\*)).

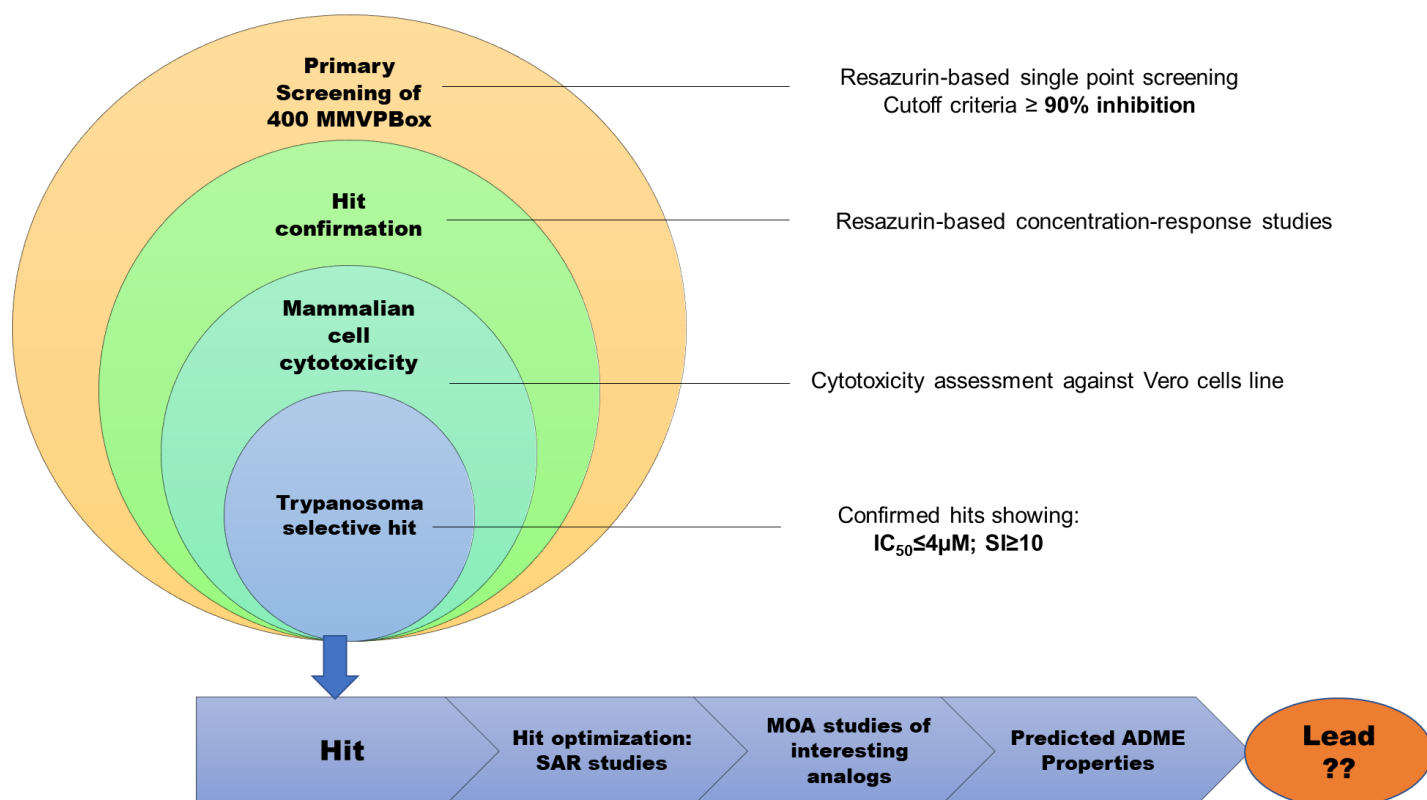


**Figure 18:** Summary of the screening funnel used for the hit optimization process. **Filter 1:** Primary single point screening using a resazurin-based viability assay. **Filter 2:** Assessing differential toxicity against mammalian cells eliminates drugs exhibiting general toxicity. **Filter 3:** Compounds showing good trypanotoxic activity and selectivity to Vero cells were considered hit compounds. Hit optimization was performed using related analogs available in the MMV library. The mode of action of the optimized hits was later studied and their ADME properties were predicted to confirm lead-like compounds.

# *Chapter-III*

## *Results and Discussion*



### III. RESULTS AND DISCUSSION

#### III.1. Identification of pathogen box compounds as inhibitors of bloodstream forms of *Trypanosoma brucei brucei*

##### III.1.1. Assay development of the antitrypanosomal test

##### III.1.1.1. *Trypanosoma brucei brucei* growth profile

Trypanosome multiplication was determined after 24, 48, 72 and 96 h of incubation at 37°C and 5% CO<sub>2</sub> to define the conditions necessary to obtain parasites at their exponential growth phase. The results are presented in **Figure 19**. On this curve, we can observe that the lag phase lasts from 0 to 16 hours, the exponential growth phase from 16 to 72 hours, and the decline phase begins after 72 hours.

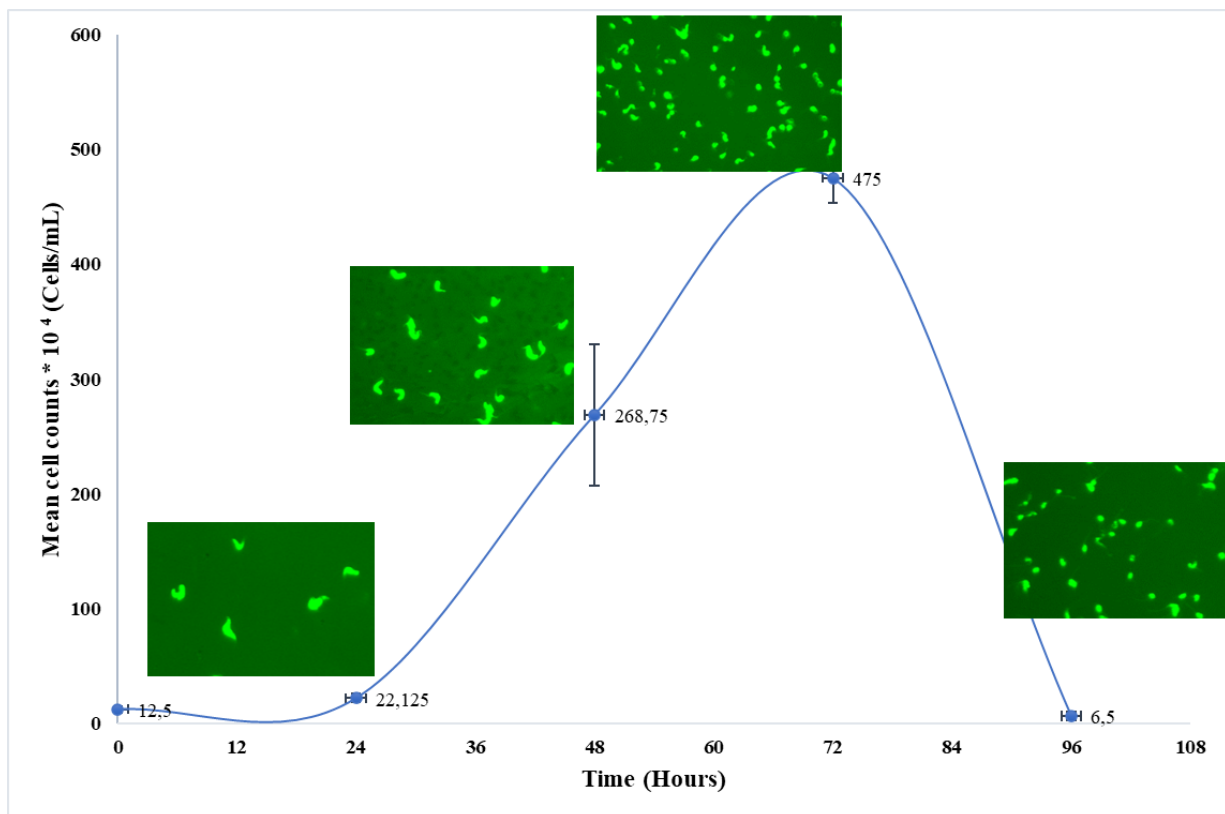


**Figure 19:** Illustration of bloodstream counts of *Trypanosoma brucei brucei* using a Lumascope LS520 inverted fluorescence (Etaluma, magnification x 40, scale bar 10 µm) following treatment with acridine orange after 24, 48, 72, 96 h incubation.

The obtained results indicate that the parasite density increases over time by approximately 1.77-fold, 21.5-fold, and 38-fold after a 24, 48 and 72 h incubation times respectively. The estimated 38-fold increase in growth per trypanosome corresponds to a doubling time of 13.72 hours as graphically illustrated in Figure 19. Additionally, in our context, the maximum number of cells that could be grown in a 25-cm<sup>2</sup> flask was estimated to be  $48 \times 10^6$  parasites/mL (**Figure 19**). Concurrently, a reduction of approximately 1.92-fold of the initial cell population ( $t_0$ ) was observed after 96 h (**Figure 19**). This observation attests that the cell death phase of the *Trypanosoma brucei brucei* strain Lister 427 occurs after 72 h.

### III.1.1.2. Linearity of resazurin cell viability assays

Resazurin is a commonly used reagent to determine cell viability *in vitro*. In the present study, resazurin was used to implement the antitrypanosomal assays in our research group. Resazurin when added into wells is metabolically reduced by viable cells into resorufin, a product which emits fluorescence that can be measured using an appropriate plate reader. These data generated allowed us to establish the relationship between the parasite density and the fluorescent signal, as presented in **Figure 20**.

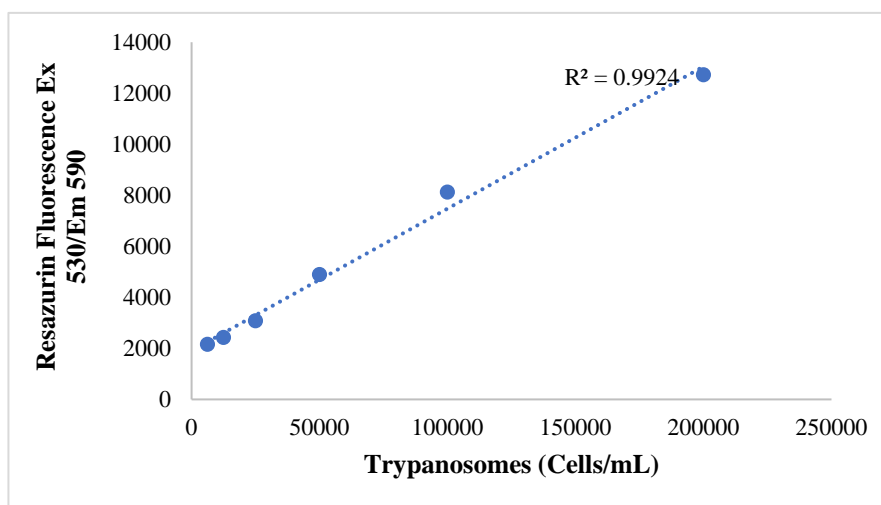


**Figure 20:** Linearity between the detected numbers of *T. b. brucei* parasites and the resazurin reduction signal after 72 h of incubation

According to this figure, the fluorescence increases proportionally with the cell density at initial densities between  $6.25 \times 10^3$  and  $2 \times 10^5$  parasites/mL. This is confirmed by a high linearity coefficient  $r^2 = 0.99$ . On the other hand, a reduction in the number of cells after three days was observed at initial densities of  $4 \times 10^5$  and  $8 \times 10^5$  parasites/mL and confirmed by the

reduction of the fluorescence values (data not shown). This result suggests that the ideal parasite density for the development of an antitrypanosomal assay should be lower than or equal to  $2 \times 10^5$  parasites/mL. Therefore,  $2 \times 10^5$  parasites/mL was used throughout the study.

### III.1.1.3. DMSO tolerance of trypanosomes, median inhibitory concentration ( $IC_{50}$ ) of pentamidine and robustness of the test

The test compounds were prepared at 10 mM in 100% DMSO, a solvent which is reported to be toxic to the parasite. For this reason, it was important to determine the maximum DMSO concentration that would not affect the parasite growth during the assay. The degree of trypanosomes' tolerance was defined by testing DMSO at concentrations ranging from 10% and 0.0064% (**Figure 21**). In addition, pentamidine, a standard antitrypanosomal drug, was used as positive control and tested at concentrations ranging from 0.0016  $\mu$ M to 10  $\mu$ M to validate our resazurin-based cell viability assay. On the other hand, the quality of the test was assessed by calculating the Z-Factor, and the values are presented in Table IV. The test was carried out in duplicate three times.

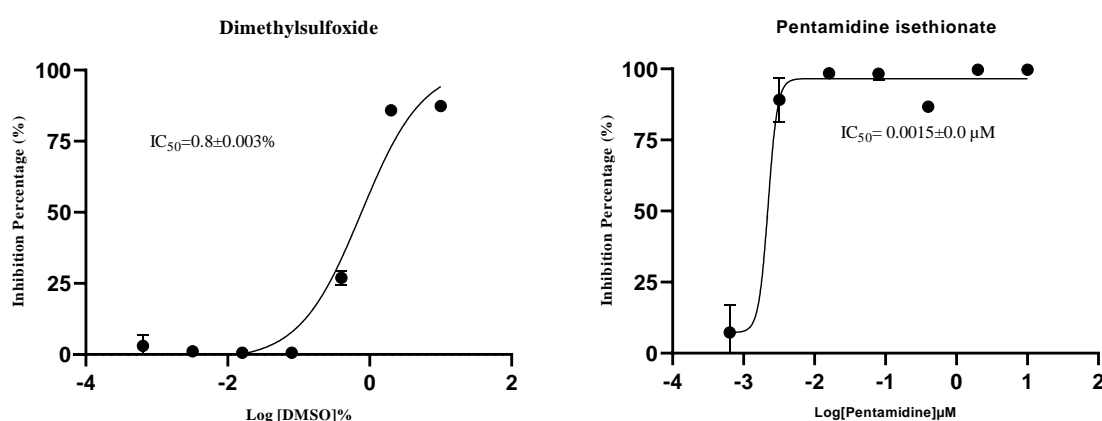


**Figure 21:** DMSO tolerance and pentamidine isethionate 50% inhibitory concentration estimation from *Trypanosoma brucei brucei* resazurin-based viability

The results revealed that the  $IC_{50}$  of DMSO was approximately 0.8% and that the concentration of 0.1% was well tolerated by the parasites, with a viability percentage between 74 and 94% (**Appendix 7**). Similarly, pentamidine gave  $IC_{50}$  values ranging from 0.0015 to 0.0017  $\mu$ M (**Figure 21**), values which are almost similar to reported data (0.0015  $\mu$ M) (**Thomas et al., 2018**). Additionally, the Z'-factor calculated for the three trials ranged 0.70 to 0.79, indicating the robustness of the test. Indeed, the more the Z'-factor is close to 1, the more the

test is robust (Zhang et al., 1999). This experiment allowed to confirm the reliability of the antitrypanosomal assay.

**Table IV:** Z'-Factor and IC<sub>50</sub> of pentamidine

	Assay 1	Assay 2	Assay 3
<b>Z'-factor</b>	0,77	0,70	0,79
<b>IC<sub>50</sub> Pentamidine ± SD (µM)</b>	0,0015 ±0.0	0,0017 ± 0.0006	0,0016 ±0.0002

Having confirmed the accuracy of the antitrypanosomal assay, compounds from the Medicines for Malaria Venture Pathogen Box were screened on bloodstream forms of *Trypanosoma brucei brucei* using the same protocol

### III.1.2. Preliminary screening and median inhibitory concentrations (IC<sub>50</sub>) of selected compounds from the MMV Pathogen Box

The primary screening of the 400 MMVPB compounds at a fixed concentration of 10 µM led to the identification of 70 (17.5%) compounds that inhibited the viability of trypanosomes by at least 90% (Figure 22-A). According to the MMVPB supporting information (Medicines for Malaria Venture, 2022b), 7 of these hits were reference compounds, including 2 antimalarial drugs (mefloquine and primaquine) and 5 antitrypanosomatid drugs, viz. Two anti-HAT drugs (pentamidine and suramin), 2 anti-chagasic drugs (nifurtimox and benznidazole) and 1 antileishmanial drug (sitamiquine), which data validated the antitrypanosomal assay (Table V). The remaining 63 active MMVPB compounds included 25 inhibitors of the causative agents of kinetoplastids (*Trypanosoma* and *Leishmania* spp.), 16 against tuberculosis, 14 against malaria, 3 against schistosomiasis, 2 against toxoplasmosis, 2 against cryptosporidiosis, and one against filariasis (Figure 22-B).

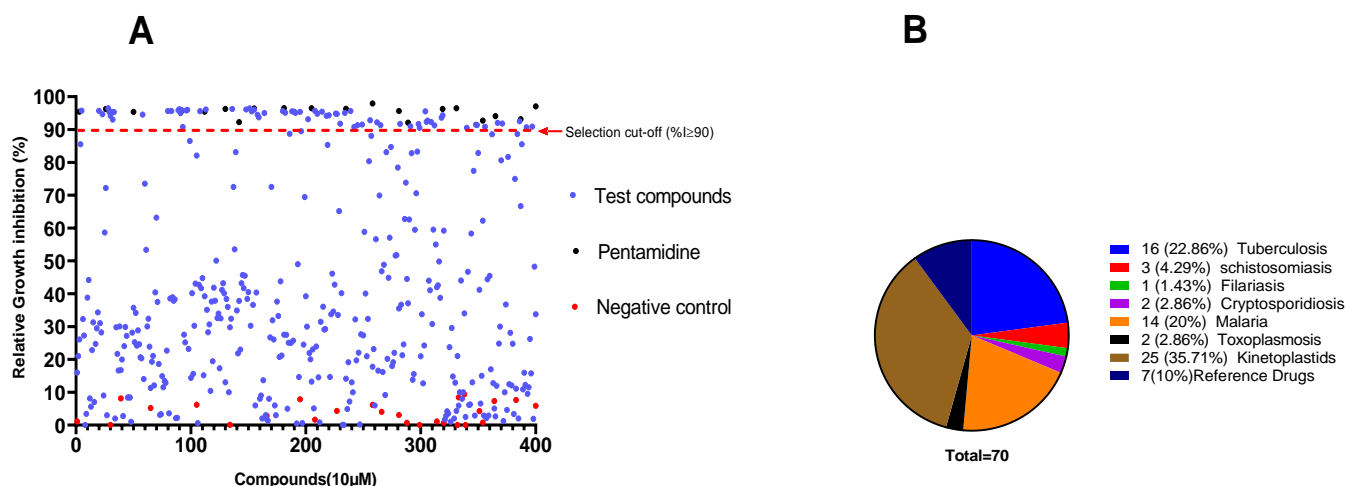


**Figure 22:** Antitrypanosomal activity cutoff of the 400 MMVPB compounds.

(A) Compounds were screened at 10  $\mu\text{M}$  using the resazurin assay, and inhibition percentages were determined with respect to the negative control. The 90% cutoff criterion (red dotted line) was used to select the most promising inhibitors for concentration–response assays. (B) Pie chart showing the distribution of selected inhibitors according to reported disease targets.

The 70 preselected compounds were submitted to concentration–response analysis for the determination of their  $\text{IC}_{50}$  values. All compounds inhibited the growth of *Trypanosoma brucei brucei* with  $\text{IC}_{50}$  values varying from 0.0023  $\mu\text{M}$  (MMV688180) to 9.78  $\mu\text{M}$  (MMV024311). All 7 reference drugs were active (Table V) with antitrypanosomal  $\text{IC}_{50}$  values ranging from 0.002  $\mu\text{M}$  for MMV000062 (pentamidine- reference trypanosomiasis drug) to 8.4  $\mu\text{M}$  for MMV000023 (primaquine- antimalarial drug).

**Table V:** Antitrypanosomal activity of reference drugs included from the MMV Pathogen Box

MMVPB ID	* $\text{IC}_{50} \pm \text{SD } T. b. b.$ ( $\mu\text{M}$ )/ $\text{pIC}_{50}$	** $\text{CC}_{50}$ ( $\mu\text{M}$ )	SI_Vero Cells	Trivial Name	Target Disease
MMV637953	0.08 $\pm$ 0.01/7.09	>100	>1128	Suramine	Trypanosomiasis
MMV000062	0.002 $\pm$ 0.0003/8.7	NT	NT	Pentamidine	
MMV001499	0.20 $\pm$ 0.09/6.7	>100	>539	Nifurtimox	Chagas disease
MMV688773	0.30 $\pm$ 0.01/6.52	>100	>302	Benznidazole	
MMV000063	1.50 $\pm$ 0.03/5.8	>100	>66	Sitamaquine	Leishmaniasis
MMV000016	1.60 $\pm$ 0.008/5.8	11.31	6.89	Mefloquine	
MMV000023	8.40 $\pm$ 0.01/5.07	43.30 $\pm$ 0.40	5	Primaquine	Malaria

\*Reference drugs of the MMVPB were tested in culture against *T. b. brucei* at serially diluted concentrations.  $\text{CC}_{50}$ : 50% Cytotoxicity concentration. Selectivity indexes (SI) were calculated as  $\text{CC}_{50}$  (Vero cells)/ $\text{IC}_{50}$  (*T. b. brucei*).  $\text{pIC}_{50}$  = negative log of  $\text{IC}_{50}$  when converted into the molar form. MMVPB: Medicines for Malaria Venture Pathogen Box; NT: not tested.

Among the 63 remaining compounds, 21 exhibited very high potency ( $IC_{50} \leq 1 \mu M$ ), among which compound MMV688180 ( $IC_{50} = 2.3 \text{ nM}$ ) was by far the most active. Previous data indicate that this compound has high potency against kinetoplastids (*T. brucei brucei* and *T. brucei rhodesiense*) with  $IC_{50} < 0.13 \mu M$  (Pathogen Box supporting information). Additionally, **Duffy et al., (2017)** reported the antitrypanosomal potency of this compound ( $IC_{50} 0.01 \mu M$ ) against *T. b. brucei*. Thirty-one (31) compounds out of 63 displayed  $IC_{50}$  values between 1.0 and 4.0  $\mu M$ , whereas 11 other compounds were moderately active ( $IC_{50} 4.38\text{-}9.78 \mu M$ ) (Tables VI and VII). Overall, 25 bioactives out of the 63 hit compounds have known activity against kinetoplastids and thus were not further considered in this study. Moreover, thirty-eight (38) other compounds have known activity against different disease agents but not kinetoplastids (Table VI). Generally, the identified inhibitors displayed acceptable cytotoxicity profiles against the African green monkey kidney Vero cell line, with selectivity indexes greater than 10. Their chemical structures and classes are provided in Appendices 8 and 9.

**Table VI:** *In vitro* antitrypanosomal and cytotoxic activities of the 25 MMVPB compounds with reported anti-kinetoplastid activity

MMVPB ID	* IC <sub>50</sub> ± SD <i>T. b. b.</i> (μM)/pIC <sub>50</sub>	** CC <sub>50</sub> Vero	SI	† Chemical Classes	# Reported IC <sub>50</sub> (μM)
MMV688180	0.0023 ± 0.001/8.64	>100	>42,826	benzenesulfonamide	<0.13
MMV688796	0.03 ± 0.01/7.52	>100	>3416	2,4 substituted furan	0.1
MMV676604	0.036 ± 0.001/7.44	8.30 ± 1.20	232	2-aminopyrimidine	0.26
MMV688797	0.06 ± 0.02/7.22	>100	>1598	2-aryl oxazole	0.13
MMV652003	0.06 ± 0.04/7.22	>100	>1557.87	Benzamide	0.15
MMV688958	0.087 ± 0.01/7.06	>100	>1154	2-aryl oxazole	0.15
MMV675998	0.34 ± 0.03/6.47	>100	>296	benzenecarboximidamide	0.25
MMV688798	0.30 ± 0.025/6.52	NT	NT	benzamide	0.555
MMV688795	0.35 ± 0.02/6.45	>100	>282	2-aryl oxazole	0.15
MMV688793	0.36 ± 0.04/6.44	>100	>255	2-pyridyl benzamides	2.07
MMV689028	0.40 ± 0.02/6.39	>100	>248	benzyl piperazine	0.14
MMV676600	0.65 ± 0.007/6.18	>100	>154	genzamide	1.02
MMV188296	1.01 ± 0.25/5.99	>100	>98	2-indolinecarboxamide	0.49
MMV688271	1.07 ± 0.16/5.97	>100	>93	Guanidine	0.6

MMV689029	1.30 ± 0.60/5.88	>100	>76	benzyl piperazine	0.5
MMV688371	1.60 ± 0.10/5.79	7.5 ± 0.1	5	benzamide	<0.13
MMV689061	1.90 ± 0.10/5.72	>100	>54	acetamide	32.3
MMV001561	1.90 ± 0.05/5.72	41.5 ± 1.0	22	propanamine (fluoxetine)	3.97
MMV687706	1.90 ± 0.006/5.72	41.0 ± 6.5	21	piperazine	0.99
MMV659004	1.90 ± 0.003/5.72	>100	>50	pyrimidine	6.6
MMV689060	2.40 ± 0.06/5.61	NT	NT	iperazine	31.6
MMV690027	2.80 ± 0.07/5.55	>100	>36	hexahydrophthalazinones	0.02
MMV688467	3.10 ± 0.50/5.50	>100	>32	butyl sulfanilamide	0.3
MMV688514	3.20 ± 0.30/5.49	17 ± 2.5	5	benzenecarboximidamide	4.06
MMV688410	8.50 ± 0.10/5.07	NT	-	acetamide	3.8

\* MMVPB compounds were tested in culture against *T. b. brucei* at serially diluted concentrations. Median inhibitory concentrations (IC<sub>50</sub>) were generated from concentration–response curves using GraphPad Prism 8.0 software. CC<sub>50</sub>: 50% Cytotoxicity Concentration. Selectivity indexes (SI) were calculated as CC<sub>50</sub> (Vero cells)/IC<sub>50</sub> (*T. b. brucei*). pIC<sub>50</sub> = negative log of IC<sub>50</sub> when converted into molar form. MMVPB: Medicines for Malaria Venture Pathogen Box; † The chemical classes of the compounds were obtained from the PubChem NIH database (<https://pubchem.ncbi.nlm.nih.gov>; accessed on August 21 2019). # Data retrieved from the MMV Pathogen Box supporting information; NT: Not tested.

**Table VII:** *In vitro* antitrypanosomal and cytotoxic activities of the 38 MMVPB compounds with known potency against other diseases

MMVPB ID	* IC <sub>50</sub> ± SD <i>T. b. b.</i> (μM)/pIC <sub>50</sub>	** CC <sub>50</sub> Vero	SI	† Chemical Class
MMV687807	0.50 ± 0.04/7.30	11 ± 1.30	23	benzamide
MMV687248	0.50 ± 0.07/7.30	>100	>199	1H-Benzimidazol-2-amine
MMV687138	0.50 ± 0.01/7.30	>100	>199	benzamide
MMV495543	0.70 ± 0.25/7.15	NT	NT	benzamide
MMV675996	0.80 ± 0.02/7.09	NT	NT	cyclohexanecarboxamide
MMV688763	0.80 ± 0.10/7.09	8.14 ± 0.01	10	pyridazinone
MMV085210	0.90 ± 0.10/7.04	>100	>107	benzenesulfonamide
MMV054312	1.29 ± 0.42/5.88	>100	>77	pyrroloquinoline
MMV667494	1.30 ± 0.50/5.88	>100	>75	quinolone 4-carboxamide
MMV024937	1.40 ± 0.50/5.85	14.63 ± 0.60	11	oxazolecarboxamide
MMV010576	1.50 ± 0.30/5.82	>100	>66	2-amino Pyridines
MMV687812	1.70 ± 0.10/5.76	2.66 ± 0.30	1.5	2-Pyrazinecarboxamide
MMV022029	1.70 ± 0.70/5.76	13.10 ± 0.20	8	biaryl sulfonamide
MMV153413	1.70 ± 0.10/5.76	>100	>57	tetrasubstituted thiophene
MMV687703	1.70 ± 0.06/5.76	>100	>56	Benzimidazole
MMV062221	1.70 ± 0.60/5.76	NT	NT	phenylpyrazolamine
MMV022478	1.70 ± 0.01/5.76	11.42 ± 0.07	6	pyrazolo (1.5-a)pyrimidine
MMV028694	1.80 ± 0.10/5.74	10.36 ± 0.10	6	2.4 disubstituted pyrimidine
MMV024035	1.80 ± 0.10/5.74	35.75 ± 0.08	19	thiophene carboxamide
MMV676512	1.90 ± 0.07/5.72	NT	NT	1H-Imidazole-5-carboxamide
MMV661713	1.90 ± 0.02/5.72	>100	>51	4-pyridyl-2-aryl pyrimidine
MMV687251	1.90 ± 0.01/5.72	6.4 ± 2.0	3	pyrimidine
MMV020670	1.90 ± 0.02/5.72	NT	NT	6-naphthyridine-2-carboxamide
MMV687765	2.30 ± 0.30/5.64	>100	>44	Pyrimidine
π MMV675968	2.80 ± 0.07/5.55	>100	>35.6	aminoquinazoline
MMV688124	2.90 ± 0.08/5.53	>100	>34	benzenesulfonamide

MMV688703	3.18 ± 1.30/5.49	NT	NT	pyridines
MMV688417	4.38 ± 0.90/5.36	13.60 ± 2.90	3	pyrazolo [3,4-d]pyrimidinamine
MMV023969	8.09 ± 0.30/5.09	26.26 ± 0.40	3	isoquinoline
MMV688761	8.33 ± 0.09/5.08	>100		benzamide
MMV688768	8.36 ± 0.08/5.07	>100		2,3 disubstituted indole
MMV023233	8.43 ± 0.06/5.07	29.75 ± 0.70	3	quinolineamine
MMV006901	8.45 ± 0.05/5.07	14.60 ± 0.02	1.73	2,4-aminoquinoline
MMV688854	8.50 ± 0.06/5.07	13.41 ± 1.50	1.57	pyrazolo pyrimidineamine
MMV016136	8.61 ± 0.30/5.06	NT	NT	pyrazolo pyridineamine
MMV011511	8.94 ± 0.70/5.05	>100	>11	piperidineamine
MMV676411	9.44 ± 0.09/5.02	NT	NT	propanamide
MMV024311	9.78 ± 0.20/5.00	NT	NT	1H-Indole

\* MMVPB compounds were tested in culture against *T. b. brucei* at serially diluted concentrations. Median inhibitory concentrations (IC<sub>50</sub>) were generated from concentration–response curves using GraphPad Prism 8.0 software; CC<sub>50</sub>: 50% Cytotoxicity concentration. Selectivity indexes (SI) were calculated as CC<sub>50</sub> (Vero cells)/IC<sub>50</sub> (*T. b. brucei*). pIC<sub>50</sub> = negative log of IC<sub>50</sub> when converted into the molar form. MMVPB: Medicines for Malaria Venture Pathogen Box; † The chemical classes of the compounds were obtained from the PubChem NIH database (<https://pubchem.ncbi.nlm.nih.gov>; accessed on August 21 2019); π Hit candidate for structure–activity-relationship study; NT: Not tested.

## Discussion

Sleeping sickness remains a public health emergency, particularly in endemic regions where it causes significant damage to both cattle and humans (Steverding, 2008). As a matter of fact, control measures mainly based on chemotherapy have been established for decades. However, currently available drugs have several drawbacks, such as cumbersome and lengthy treatment, adverse and toxic effects, and the development of resistant trypanosome mutants (Fairlamb, 2003; Delespaux & de Koning, 2007; Giordani et al., 2016). This situation emphasizes the need of more attention to this neglected tropical disease (NTD) for its complete elimination. Consequently, new therapeutic options are urgently needed to supply the antitrypanosomal drug discovery and development pipeline. The present study was designed to identify potential inhibitors of *Trypanosoma brucei subsp. brucei* from the Medicines for Malaria Venture's Open Access Pathogen Box (MMVPBox). To this end, the reliability of the phenotypic screening approach used was ascertained by evaluating parameters such as parasite growth, linearity of the resazurin viability test and the toxicity of DMSO and the reference drug.

The evaluation of *T. b. brucei* growth as a function of time showed that from an initial population of  $2 \times 10^5$  trypanosomes/ml, the exponential growth and mortality phases were reached after 48 h and 72 h of incubation, respectively (Figure 14, picture 2). Indeed, the maximum cell number in culture after 72 h was found to be  $4.75 \times 10^6$  trypanosomes/ml (Figure 19), which is consistent with previous estimations using HMI-9 medium for other bloodstream species. For instance, Sykes & Avery, (2009) obtained a maximum density of  $3 \times 10^6$  trypanosomes/ml in HMI-9 culture medium confirming that HMI-9 is a good choice for optimum growth of bloodstream forms of *T. b. brucei*. Prior to this report, Hirumi & Hirumi, (1989) also used HMI-9 medium for the continuous culture of *T. b. brucei* strain GUTat3.1. Subsequently, a reduction in cell density was noted on the fourth day (96 h) of incubation (Figure 19), and microscopic observation of parasite viability allowed to detect the presence of the nondividing short forms of the parasite. Similarly, (Hirumi et al., 1977) demonstrated that after 72 hours of incubation of *T. brucei brucei* Lister 427 at an initial density of  $5 \times 10^5$  parasites/mL, short forms of the parasite were observed in the medium. Indeed, it has been demonstrated that in the case of high parasite density, the bloodstream forms of *T. b. brucei* secrete a low molecular weight marker called stumpy induction factor (SIF), which induces the cell cycle arrest and differentiation of long slender forms into short forms (Vassella et al., 1997). Moreover, the increase in cell number, which is estimated to be 38-fold (0-72 h)

corresponds to a doubling time of 13.72 h, that is closely similar to the values (10-12 h) reported by **Hirumi et al. (1977)** for the same strain *T. brucei* Lister 427. During the exponential phase (between 24-48 hours), this doubling time (7.49 hours) was close to the 6.8 hours as obtained by **Sykes & Avery, (2009)**. In this experiment, the linearity ( $r^2=0.993$ ) between the number of viable parasites and the resazurin fluorescence (**Figure 20**) was effective when the parasite density was found between  $2 - 0.0625 \times 10^5$  parasites/mL (**Sykes & Avery, (2009)** also obtained a  $r^2$  of 0.99 using the resazurin viability assay.

Despite the number of reports on the toxicity of DMSO, this organic solvent is commonly used to solubilize many natural and synthetic. Thus, in all drug discovery assays that use DMSO as a solvent, it is crucial to define the tolerance of the organism to be studied to ensure the activity is not related to the toxicity by the solvent used (DMSO) in the compounds' preparation. Prior to the phenotypic screening of compounds from the MMVPBox, the effect of pentamidine, a standard antitrypanosomal drug was evaluated against *T. b. brucei* and data obtained were compared to the literature to ensure our working conditions were adequate. As a result, 0.4% (v/v) was the maximum concentration that did not affect the parasite growth (**Appendix 7**). This level of DMSO tolerance in the assay is consistent with previously reported studies ( **Sykes & Avery, 2009; Bowling et al., 2012**). To evaluate the sensitivity of the performed antitrypanosomal test against *T. brucei brucei*, the  $IC_{50}$  values which were obtained for pentamidine (1.5-1.7 nM) were compared with previously reported data by **Thomas et al., (2018)** ( $IC_{50}$  2.5 nM), **Sykes & Avery, (2009)** ( $IC_{50}$  4.4 nM) and **Kaiser et al., (2011)** ( $IC_{50}$  2 nM). As the  $Z'$ -factor was found to be 0.7, a value that occurs within the cutoff values' range ( $0.5 < Z'$ -factor  $< 1$ ), the resazurin-based test used in this study was considered robust, reliable, and reproducible.

Based on the foregoing, the resazurin-based viability assay was used to screen the Medicines for Malaria Venture's Open Access Pathogen Box against the bloodstream form trypomastigotes of *Trypanosoma brucei subsp. brucei*, Lister 427 VSG 221. Out of 400 compounds tested, 70 was found to inhibit the growth of the parasite by at least 90% (**Figure 22**), and their  $IC_{50}$  values stretched from micromolar ( $\sim 9.8 \mu\text{M}$ ) to nanomolar ( $IC_{50} \sim 2 \text{ nM}$ ) range. **Veale & Hoppe, (2018)** obtained almost same results by screening the MMVPB, with 65 hits identified against *T. b. brucei* ( $> 80\%$  growth inhibition at  $20 \mu\text{M}$ ). However, 21 potential hits from this study did not match with some of the 65 hits reported by Veale and Hoppe (2018). In another report, after screening the MMVPB at  $10 \mu\text{M}$  against the *T.b.brucei*,

**Duffy et al., (2017)** selected 95 active antitrypanosomal compounds with a 50% inhibition cutoff. Cross examination of the data generated spotted 46 common hits whereas 49 compounds differed from those found in this study. Additionally, 19 hits were selected in this study that were not reported by these authors. The observed discrepancies in the activity profiles are probably due to differences in the culture and assay conditions used. **Veale and Hoppe, (2018)** evaluated the antitrypanosomal activity of the Pathogen Box library using an initial parasite density of  $2.4 \times 10^4$  parasites/200  $\mu\text{L}$ /well with an incubation period of 48 hours, resulting in an  $\text{IC}_{50}$  of 1.2  $\mu\text{M}$  for compound MMV675968. On the other hand, **Duffy et al. (2017)** used an initial parasite density of 1200 cells/mL and incubated for 50 hours, leading to an  $\text{IC}_{50}$  of 2.07  $\mu\text{M}$  for the same compound (MMV675968). Meanwhile, in our study, the antitrypanosomal activity of the MMVPBox library was assessed using an initial parasite density of  $2 \times 10^5$  cells/mL and an incubation period of 72 hours, resulting in an  $\text{IC}_{50}$  of 2.6  $\mu\text{M}$  for compound **MMV675968**. The cell density used in the current study was greater than that considered in Veale and Hoppe's and Duffy et al.'s assays. Furthermore, **Sykes and Avery (2009)** used an alamar blue assay to screen the antitrypanosomal activity with initial parasite densities of 2,000 cells/mL and 250 cells/mL to afford  $\text{IC}_{50}$  values of 4.4 nM and 1.7 nM, respectively, suggesting that a reduction in cell inoculum size may result in an increase in the sensitivity of the parasites to test compounds (**Sykes & Avery, 2009**).

From the 70 compounds that emerged from our preliminary screening, internal controls (reference compounds) were excluded from further studies, including 5 anti-trypanosomatids (MMV637953 (Suramine)- Trypanosomiasis; MMV001499 (Nifurtimox)- Chagas disease; MMV688773 (Benzimidazole)- Chagas disease; MMV000062 (Pentamidine)- Trypanosomiasis; MMV000063 (Sitamaquine)- Leishmaniasis) and 2 antimalarials (MMV000016-Mefloquine and MMV000023-Primaquine). Another set of 25 other compounds previously reported to inhibit trypanosomatid parasites was also identified (Table 2). One such compound include the benzenesulfonamide **MMV688180** ( $\text{IC}_{50}$  0.0023  $\mu\text{M}$ ) (**Table VI**), which was the most active compound and previously reported to inhibit N-myristoyl transferase, an enzyme that is essential for the survival and virulence of *T. b. brucei* (**Brand et al., 2012; Price et al., 2010**). Additionally, the two benzyl piperazines **MMV689029** and **MMV689028**, and the 2,4-substituted furan **MMV688796** were previously reported by Duffy et al., (2017) as promising starting points for drug discovery against both *T. cruzi* and *T. brucei*. Moreover, the 2-aminopyrimidine MMV676604 is a kinase inhibitor that has been reported to exhibit trypanocidal activity through inhibition of TbERK8 (extracellular signal-regulated kinase 8)

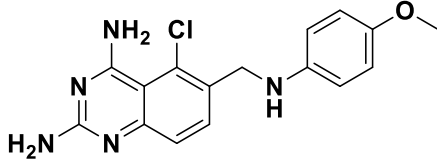
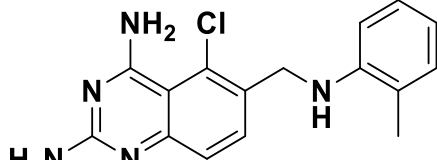
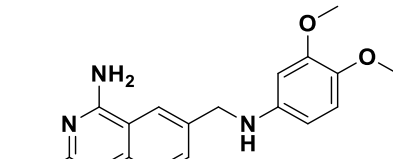
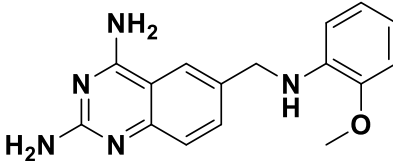
was identified by **Valenciano et al., (2016)**. **MMV652003**, which is a member of the benzamide class of molecules, has also been reported to inhibit one of the trypanosoma target: leucyl-tRNA synthetase (**Rodríguez et al., 2008; Zhao et al., 2012**). The butyl sulfanilamide **MMV688467** was proven to inhibit microtubule formation in trypanosomes (**George et al., 2007**). As predicted for other guanidine derivatives, we can hypothesize that the antiplasmodial **MMV688271 (Patra et al., 2020)** binds to the DNA minor groove at AT-rich regions (**Nagle et al., 2012**). All these compounds were equally excluded from further investigations.

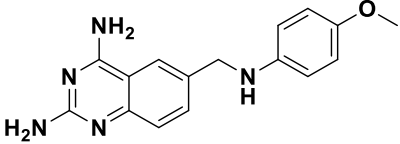
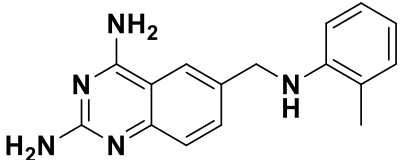
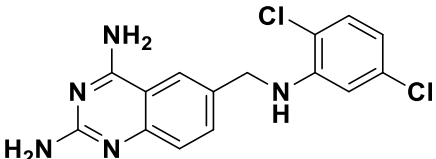
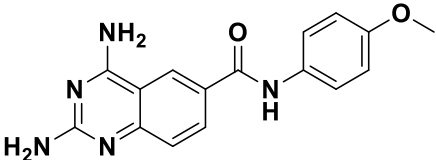
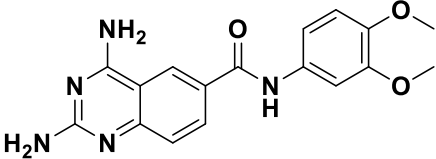
The other set of 38 identified hits were previously reported for their activity against other disease, including malaria (14), tuberculosis (16), toxoplasmosis (2), schistosomiasis (3), cryptosporidiosis (2) and filariasis (1) (**Table VII**). Among these compounds, **MMV675968** (2,4-diaminoquinazoline) was selected for further detailed study. In fact, compound **MMV675968** presented low  $IC_{50}$  value (2.8  $\mu M$ ) with high selectivity index ( $>35$ ). In addition, the generous donation of a small library of 2,4-diaminoquinazoline analogs by the MMV highly supported in-depth study of this very important antitrypanosomal scaffold (**MMV675968**). Interestingly, compound **MMV675968** was previously reported to strongly inhibit the dihydrofolate reductase (DHFR) enzyme in *Cryptosporidium*, (**Nelson, 2001**), *Pneumocystis carinii* and *Toxoplasma gondii* (**Rosowsky et al., 1994**). More recently, **MMV675968** emerged as the most active pathogen box compound from a screening against *Toxoplasma gondii* ( $IC_{50}$  0.02  $\mu M$ ; SI 275) (**Spalenka et al., 2018**). Additionally, this compound was active against other pathogens, such as the planktonic forms of *C. albicans* (**Vila & Jose L, 2017**) and *P. falciparum* ( $IC_{50}$  0.07  $\mu M$ ) (**Duffy et al., 2017**). This strong rationale motivated the SAR study of its analogs.

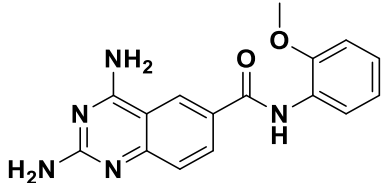
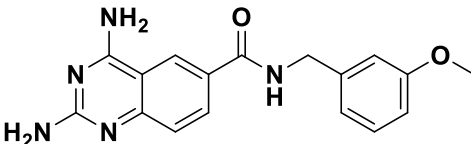
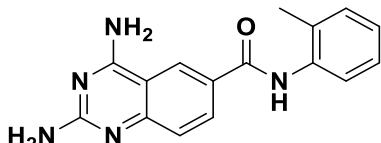
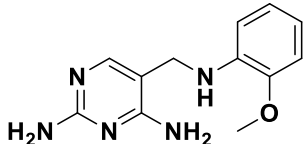
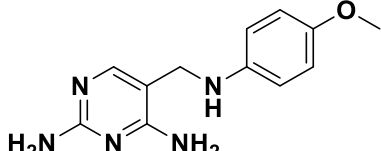
### ***III.2. Rudimentary Structure-Activity-Relationship (SAR) study with 23 analogs of 2,4-diaminoquinazoline (MMV675968)***

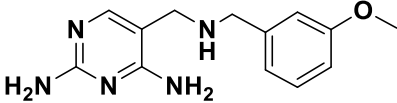
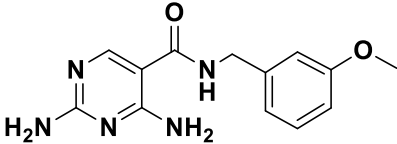
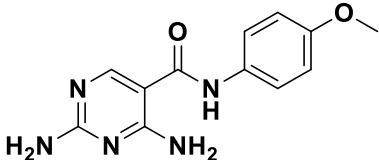
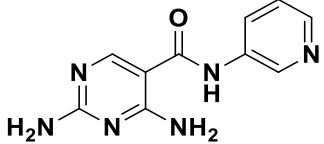
Twenty-three (23) analogs of 2,4-diaminoquinazoline were generously donated by MMV for activity and selectivity testing against *T. b. brucei* and Vero cells respectively. The results achieved, portraying the SAR of the compounds are summarized in **Table VIII**.

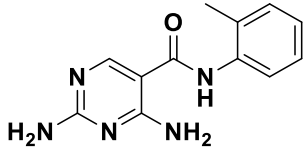
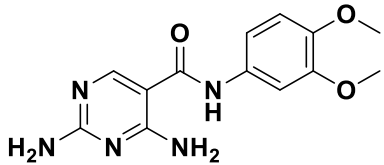
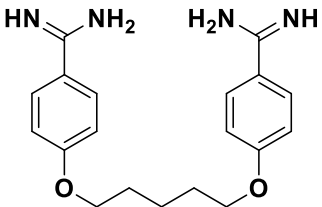
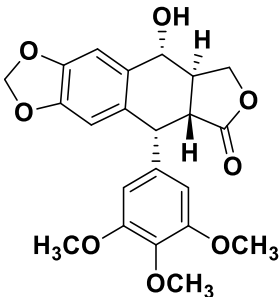


4	MMV1578538		$2.50 \pm 0.15^{ns}/5.60$	$16.93 \pm 0.20$	7.05
5	MMV1578539		$2.30 \pm 0.20^{ns}/5.64$	>100	>43.47
6	MMV1578510		$0.56 \pm 0.07^*/6.25$	>100	>178.98
7	MMV1578467		$0.06 \pm 0.008^{***}/7.22$	$24.80 \pm 0.87$	412.75

8	MMV1578519		$0.25 \pm 0.01$ ***/6.60	$30.86 \pm 2.30$	123.44
9	MMV1578468		$0.19 \pm 0.003$ ***/6.72	$22.03 \pm 1.30$	115.97
10	MMV1578445		$0.045 \pm 0.005$ ***/7.34	$78.20 \pm 0.80$	1737.44
11	MMV1578388		$4.00 \pm 1.30$ **/5.40	$22.86 \pm 0.50$	5.60
12	MMV1578389		>10 ***	>100	NA

13	MMV1578390		$3.20 \pm 0.30$ <sup>ns</sup> /5.49	>100	>31.25
14	MMV1578446		$2.50 \pm 0.13$ <sup>ns</sup> /5.60	>100	>40
15	MMV1578531		>10 <sup>***</sup>	>100	NA
16	MMV1578540		>10 <sup>***</sup>	>100	NA
17	MMV1578523		>10 <sup>***</sup>	>100	NA

18	MMV1578541		>10 ***	>100	NA
19	MMV1578470		>10 ***	>100	NA
20	MMV1578442		>10 ***	>100	NA
21	MMV1578430		>10 ***	>100	NA
22	MMV1578487		>10 ***	>100	NA

23	MMV1578429		>10 ***	>100	NA
24	MMV1578441		>10 ***	>100	NA
Pentamidine			$0.0022 \pm 0.0045/8.65$	>100	>45,450
Podophyllotoxin			NA	$0.43 \pm 0.14$	NA

Analogs were tested in culture against *T. b. brucei* at serially diluted concentrations. Median inhibitory concentrations ( $IC_{50}$ ) were generated from concentration–response curves using GraphPad Prism 8.0 software.  $pIC_{50}$  = negative log of  $IC_{50}$  when converted into the molar form.  $CC_{50}$ : 50% Cytotoxicity concentration. Selectivity indexes (SI) were calculated as  $CC_{50}$  (Vero cells)/ $IC_{50}$  (*T. b. brucei*). † Antitrypanosomal activity and cytotoxicity of the parent hit were confirmed through the screening of solid material provided by MMV; Results are means  $\pm$  standard deviations (SD) from duplicate values obtained from two independent experiments. Mean  $IC_{50}$  within each column superscripted with (\*), (\*\*), (\*\*\*) indicates statistically significant difference with the parent hit compound (1-MMV675968) at  $p < 0,05$ ,  $p < 0,001$  and  $p < 0,0001$ , respectively; ns denotes no difference as referred to the parent hit as given by the Tukey’s multiple comparison test. NA = not applicable.

Out of the 23 analogs, 11 compounds were inactive at  $IC_{50} \leq 10 \mu M$ , and 12 exhibited activities with  $IC_{50} \leq 4 \mu M$ , of which five were more active than the parent compound ( $IC_{50}$  0.56-0.045  $\mu M$ ). From the SAR analysis, analogs 2-5 bearing different substitution patterns around the phenyl moiety of compound 1 while keeping the 5-chloro-2,4-diaminoquinazoline core unchanged displayed an average  $IC_{50}$  value of 2.6  $\mu M$ , similar to that of parent compound **1** ( $IC_{50}$  2.6-2.8  $\mu M$ ). Concurrently, these substitutions on analogs **2-4** led to an increase in cytotoxicity by ~5-fold compared to the parent hit, with SI dropping from > 37 down to 6.4. For analog **5**, the substitutions did not significantly impact the potency and selectivity ( $IC_{50}$  = 2.3  $\mu M$ ; SI > 43.47) compared to the parent hit compound ( $IC_{50}$  = 2.6  $\mu M$ , SI > 37.87). Similarly, following the incorporation of an amide functionality in analogs **2, 3, 4**, and **5**, the resulting analogs **11-15** exhibited  $IC_{50}$  values similar to or higher than that of the parent compound ( $IC_{50}$  2.5 to >10  $\mu M$ ), suggesting that neither the substitution pattern of the phenyl nor the amide group is essential for the antitrypanosomal activity. On the other hand, except for compound **11** (SI 5.60), hits **13** and **14** of this series exhibited selectivity indexes greater than 30. Additionally, removal of the chlorine atom from the core moiety resulted in a 4-fold (compound **6**-  $IC_{50}$  0.56  $\mu M$ ) to 53-fold (compound **7**-  $IC_{50}$  0.06  $\mu M$ ) increase in antitrypanosomal potency (series **6-9**) with respect to their corresponding congeners **3** and **2** (series **1-5**) while concurrently improving their safety profile by 3-10-fold (SI 115-412) compared to parent compound 1. In contrast, the introduction of chlorine atoms not on the 2,4-diaminoquinazoline core moiety but at positions 2 and 5 of the phenyl group afforded the most active and selective compound identified in this study, analog **10** ( $IC_{50}$  0.045  $\mu M$ ; SI 1737). Unfortunately, the replacement of the 2,4-diaminoquinazoline core by the 2,4-diaminopyrimidine core moiety led to a total loss of activity (series **16-24**,  $IC_{50}$ >10  $\mu M$ ).

Overall, SAR studies on parent hit **1** (**MMV675968**) ( $IC_{50}$  2.6-2.8  $\mu M$ ; SI >37) improved the *in vitro* potency and safety of analogs against bloodstream forms of *Trypanosoma brucei brucei*, with up to an ~40-58-fold increase in activity and selectivity with analogs **7** ( $IC_{50}$  0.06 and SI 412) and **10** ( $IC_{50}$  0.045  $\mu M$  and SI 1737) bearing higher promise (**Table VII**, **Figure 15**).

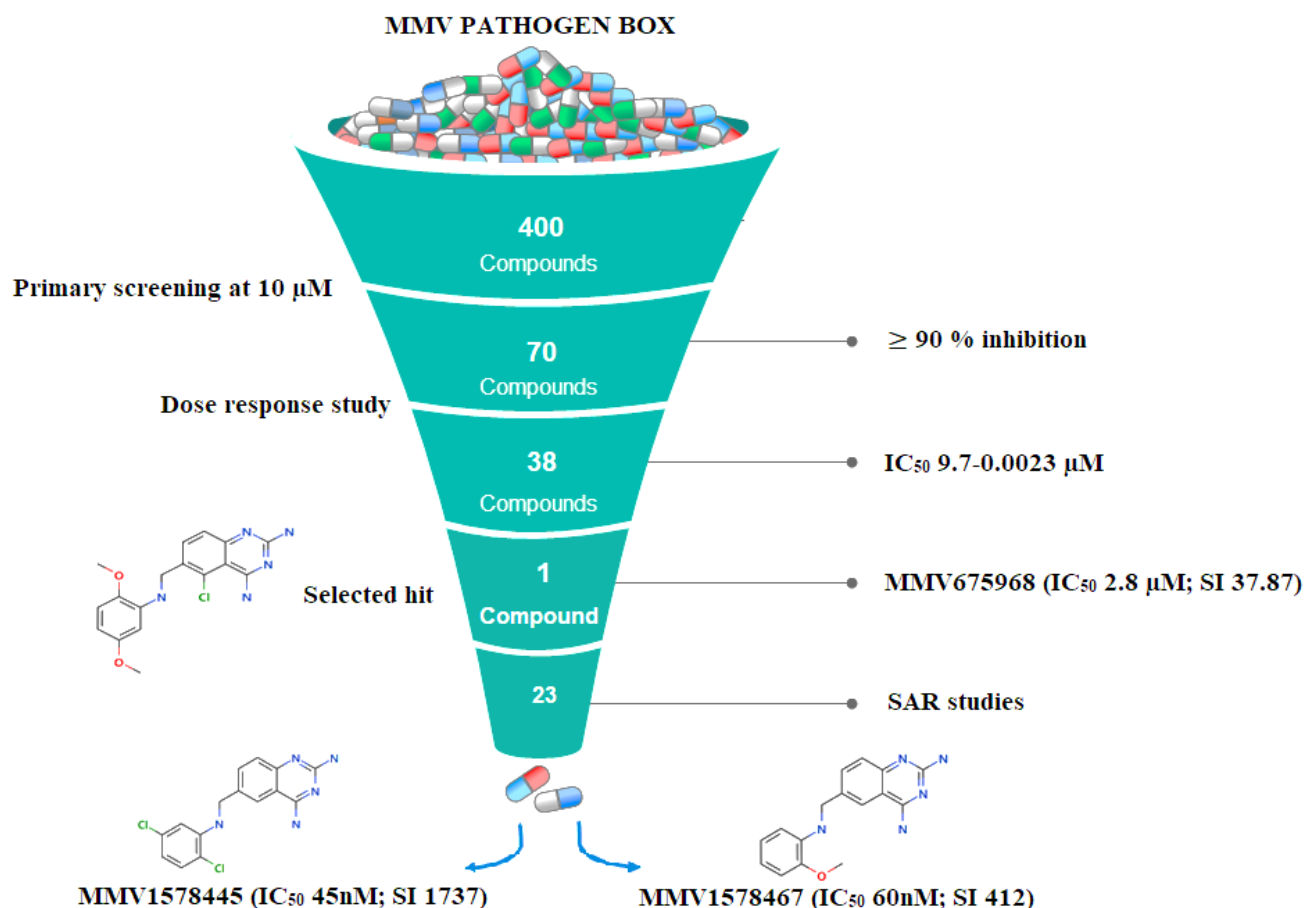


**Figure 23:** Funnel pipeline of the performed antitrypanosomal drug screening process

## Discussion

As previously outlined, the drug discovery phase encompasses many steps, including hit optimization step, whereby chemists use the structure-activity relationship (SAR) to modify the chemical structure of a compound to improve its *in vitro* activity and selectivity. In the current study, among the 38 active compounds with known activity against different disease pathogens, except kinetoplastids, compound **MMV675968** (2,4-diaminoquinazoline) was the only inhibitor ( $\text{IC}_{50}$  2.8  $\mu\text{M}$ ; SI > 35) with a small library of analogs available at MMV and was therefore selected for further investigation.

The antitrypanosomal pharmacomodulation study of **MMV675968** (Table VII) revealed that the activity varied consistently according to the various substituents added to the core 2,4-diaminoquinazoline structure and the adjacent phenyl portion. For instance, a change in the position of the methoxy substituents in analogs **2**, **3**, **4** and **5** did not significantly influence ( $P > 0.05$ ) affect their activity compared to that of the parent hit **1** (**MMV675968**). Chlorine

removal from the core structure appeared to be beneficial for antitrypanosomal activity and selectivity, as the resultant non chlorinated analogs **6**, **7**, **8**, and **9** were more potent and selective than their corresponding chlorinated congeners **2**, **3**, **4**, and **5**. Of note, the withdrawal of the chlorine group from the core structure led to the identification of analog **7** (6-(((2-methoxyphenyl)amino)methyl)quinazoline-2,4-diamine), which was ~43-fold and ~11-fold more active and selective, respectively, than the parent hit **1**. Additionally, analog **7** was ~53-fold more active and ~64-fold more selective than the closest analog **3**. Conversely, chlorination of the phenyl portion of the parent hit (**1**) at positions 2 and 5 led to analog **10** (6-(((2,5-dichlorophenyl)amino)methyl)quinazoline-2,4-diamine), which exhibited outstanding ~58-fold and ~46-fold increases in activity ( $IC_{50}$  45 nM) and selectivity (SI ~1737)  $P < 0.0001$ . Previously, **Iwatsuki et al., (2010)** reported an improved antitrypanosomal activity by up to 54-fold for chlorinated antibiotic derivatives compared to nonchlorinated analogs. However, it is noteworthy that depending on the chlorination point on the core or adjacent portion, the chlorine atoms may confer antitrypanosomal activity to the afforded compound. In this line, compound **7** is the most attractive in terms of lipophilic efficiency. Indeed, swapping one methoxy for 2 chlorine substituents in compound **10** increased lipophilicity and might explain the marginal improvement in potency. On another note, polarizing the bond between the phenyl ring and the quinazoline core resulted in a drastic loss in activity ( $P < 0.0001$ ), as evidenced by increased  $IC_{50}$  and mild selectivity values for analogs **11-15** ( $IC_{50}$  2.5 to  $>10$   $\mu$ M) when compared to the profile of close analogs **2**, **3**, **4** and **5**. The discrepancies observed in the pharmacological properties of the 23 analogs of **MMV675968** indicate that any modification around the quinazoline core may redefine its binding properties to the parasitic target of interest.

Analog **7** (**MMV1578467**) and **10** (**MMV1578445**) identified above have not, to our knowledge, been previously studied for antitrypanosomal activity. However, positional isomers of compound **10** had already been tested on *Leishmania* (**Berman et al., 1989**). Both analogs emerged from the SAR study as the more promising candidates and were therefore prioritized and progressed for additional analyses.

### ***III.3. In silico and in vitro activities of compounds on their likely molecular target***

#### ***III.3.1. In silico exploration of trypanosomal DHFR and TR inhibition by analogs 7 (MMV1578467) and 10 (MMV1578467)***

##### ***III.3.1.1. Accessible protonation states of the compounds and molecular docking***

While molecules containing ionizable groups such as amines and carboxylates are stored in databases as neutral entities, they are mostly ionic under physiological conditions. For instance, amines become protonated to the quaternary form, while carboxyl and other acidic groups, like phosphates and sulfates or hydroxylamines, are deprotonated (**Ten Brink & Exner, 2009; Akhter, 2016**). This observation has implications for *in silico* screening experiments, as the protonation state tends to influence the binding strength and pose of a ligand within a binding pocket (**Akhter, 2016; Ropp et al., 2019**). To account for the protonation states of compounds **7** and **10** at physiological pH, the dimorphite-DL (**Ropp et al., 2019**) program and MolGpka (**Pan et al., 2021**) webserver were utilized as detailed in the methods section. This revealed that positions 2 and 4 of the 2,4-diaminoquinazoline moiety of both compounds were ionizable at physiological pH [compound **7**: position 2 (pKa = 7.1) position 4 (pKa = 6.5); compound **10**: position 2 (pKa = 7.0), position 4 (pKa = 6.5)]. Hence, a total of three states were considered for each of the compounds: unprotonated (cmpd\_7\_unprot, cmpd\_10\_unprot), protonated at position 2 (cmpd\_7\_prot\_2, cmpd\_10\_prot\_2), and protonated at position 4 (cmpd\_7\_prot\_4, cmpd\_10\_prot\_4). Post docking analyses revealed that in DHFR, all the accessible protonation states of both compounds shared similar poses within the same ligand recognition site in the binding pocket. This resulted in hydrogen bond formation between the diaminopyrimidine moiety and key DHFR ligand recognition residues (**Yuvaniyama et al., 2003; Amusengeri et al., 2020; Tassone et al., 2021**), including the highly conserved Val32 (**Figure 24A, B**). Unlike DHFR, the TR enzyme consists of a wide binding site, where substrates and inhibitors have been shown to adopt different conformations with stacking observed for some inhibitor binding poses (**Hunter et al., 1992; Battista et al., 2020**). While both compounds **7** and **10** are bound to similar sites within the binding pocket of DHFR (**Figure 24A, B**), in TR, compound **7** bind farther away from the cofactor FAD than compound **10** (**Figure 24C, D**). Furthermore, the docking scores revealed that both compounds had relatively stronger binding in DHFR than in TR, as follows: cmpd\_7\_unprot -8.8 vs. -8.2; cmpd\_7\_prot\_2 -8.9 vs. -8.4; cmpd\_7\_prot\_4 -9.2 vs. -8.2; cmpd\_10\_unprot -9.1 vs. -8.1; cmpd\_10\_prot\_2 -9.1 vs. -8.3; and cmpd\_10\_prot\_4 -9.2 vs. -8.0 for DHFR and TR, respectively.

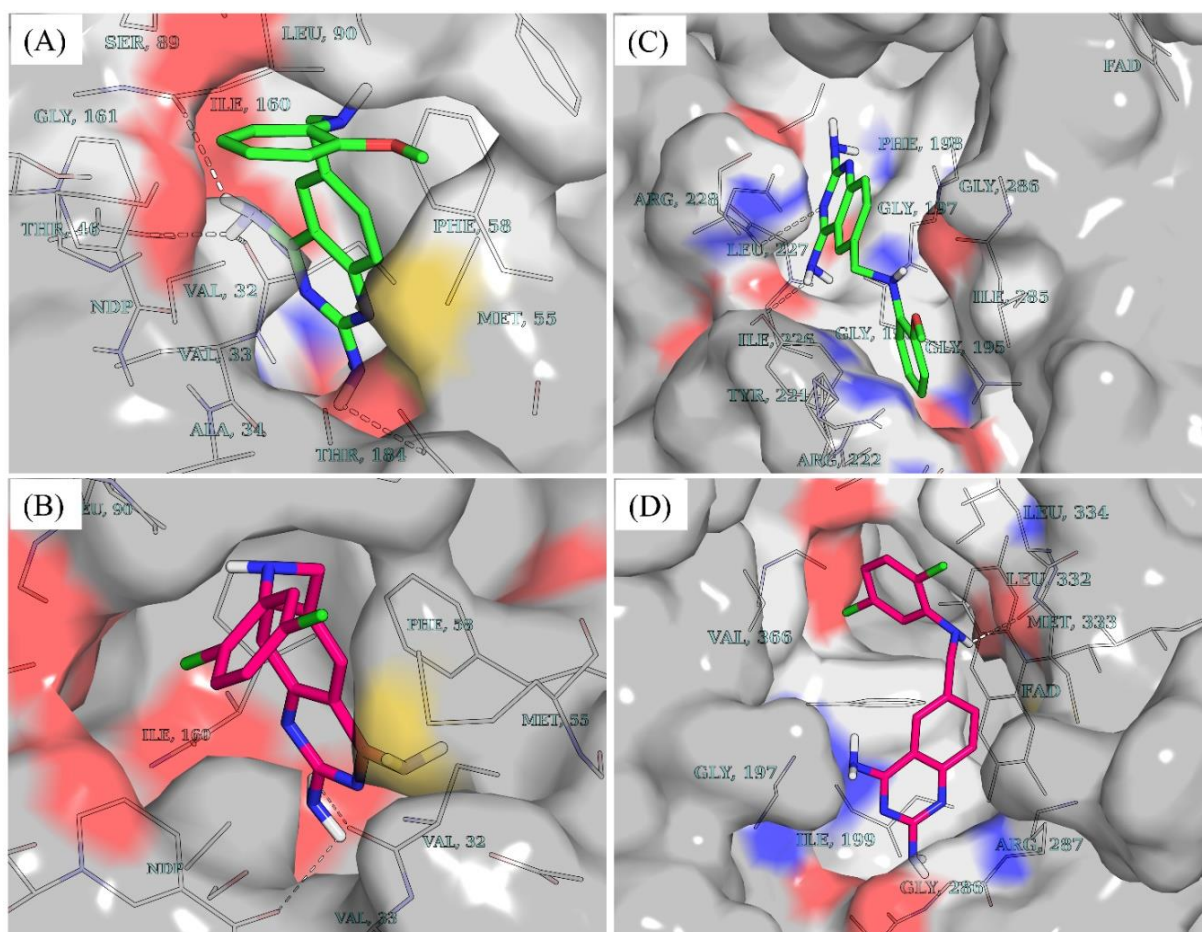


**Figure 24:** Docking poses and Vina docking scores. (A) Docking pose of unprotonated compound 7 (cmpd\_7\_unprot) in DHFR. (B) Docking pose of unprotonated compound 10 (cmpd\_10\_unprot) in DHFR. (C) Docking pose of cmpd\_7\_unprot in TR. (D) Docking pose of cmpd\_10\_unprot in TR. Compound 7 is colored green, while compound 10 is colored dark pink. Cmpd\_7\_prot\_2 and cmpd\_7\_prot\_4 represent protonated compound 7 at positions 2 and 4 of the 2,4-diaminoquinazoline ring, respectively, while cmpd\_7\_unprot refers to the unprotonated form of compound 7. The same notations apply to compound 10.

### III.3.1.2. Ligand conformational refinement and binding stability monitoring through molecular dynamics simulations

The dynamic nature of drug binding and molecular recognition is only partially considered, mainly through ligand flexibility, in docking simulations (Choi et al., 2018). Thus, MD simulation of the protein–ligand complex is required to further refine the predicted pose from docking and to ascertain the stability of binding. Herein, 100 ns of all-atom MD simulations were performed on all eight predicted poses from docking alongside the holoenzymes, making a total of ten systems (i.e., DHFR and TR bound to cmpd\_7\_prot\_2, cmpd\_7\_prot\_4, cmpd\_7\_unprot, cmpd\_10\_prot\_2, cmpd\_10\_prot\_4, cmpd\_10\_unprot,

DHFR\_holo and TR\_holo). Plots of protein RMSD and Rg were used to check for convergence of the different trajectories between the ligand unbound and bound states. While the number of hydrogen bonds formed by a ligand within the binding site of an enzyme is crucial for its stability, monitoring the ligand RMSD across the simulation reveals the post docking dynamics of the bound ligand, which informs the stability and strength of binding of the ligand (Amusengeri et al., 2020). To monitor the stability of binding of the different compounds, ligand RMSD with respect to protein structure and hydrogen bond numbers were computed across the different simulations. This revealed stable binding for all the DHFR-bound compounds, forming between 1 and 7 hydrogen bonds (Figure 25). The total number of hydrogen bonds formed tended to increase with protonation, such that the unprotonated form had the lowest maximum number of hydrogen bonds compared to the protonated form of the compounds (Figure 25A). Unlike the DHFR-bound compounds, TR-bound compounds generally showed reduced stabilities. For instance, compd\_7\_prot\_4 and compd\_10\_prot\_2 lost hydrogen bonds completely during the simulation, with the latter exiting from the binding site (Figure 25B). On the other hand, although compd\_10\_prot\_4 maintained some hydrogen bonding during the simulation, its RMSD values varied considerably, indicating unstable binding. It has been shown that microenvironmental differences within the binding site of an enzyme can influence its preference for binding to certain protonation states of a compound (Abdizadeh et al., 2017). Thus, it is possible that while compounds 7 and 10 are good binders of DHFR in all their accessible protonation states, both compounds may have difficulties binding to and staying within the binding site of the TR enzyme, with only their unprotonated forms, as well as the position 2 protonated compound 7, having the possibility of binding successfully to the enzyme.

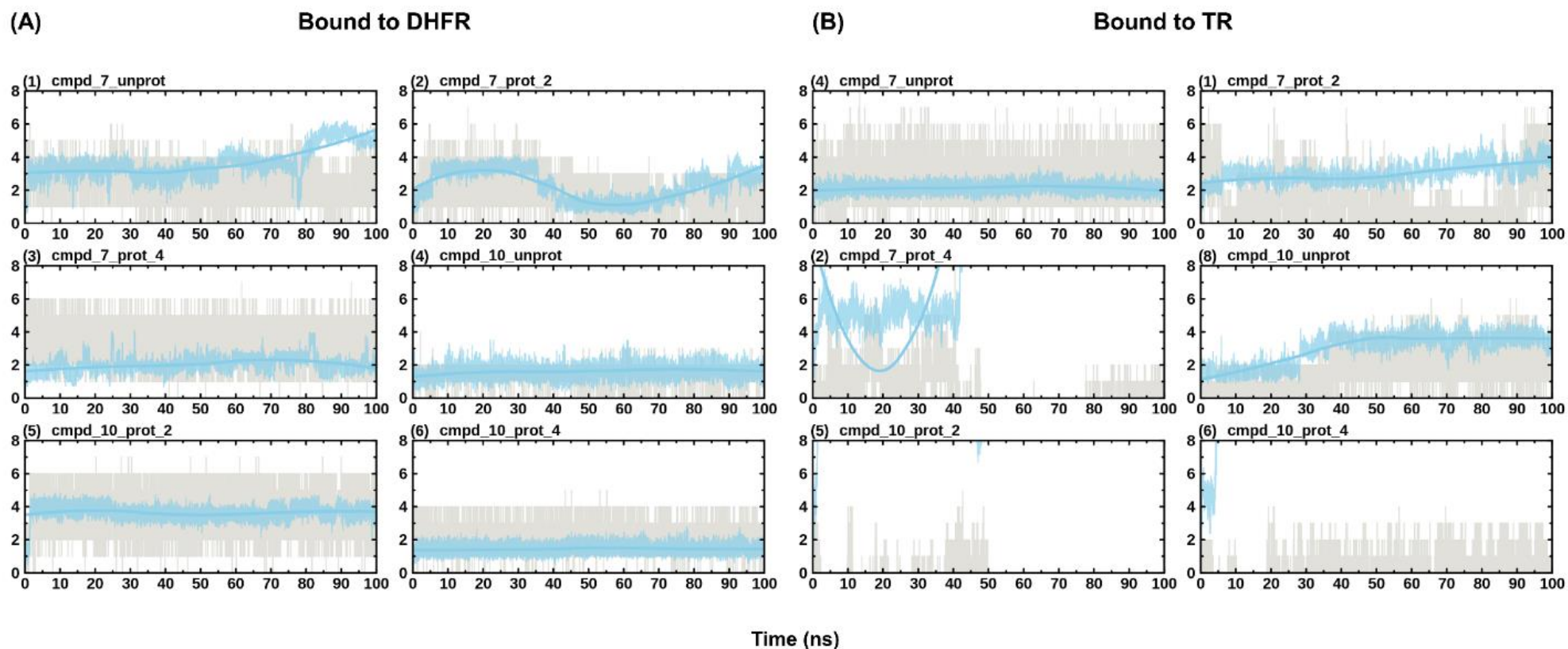


**Figure 25:** Evolution of ligand RMSD with respect to protein and hydrogen bond numbers during simulation. (A) shows the evolution of the different protonation states of the compounds in DHFR. (B) shows the evolution of the different protonation states of the compounds in TR. Hydrogen bond numbers are shown in gray, while the evolution of the ligand RMSD is shown in blue. RMSD values have been scaled up by a factor of 10 to fit into the scale of the hydrogen bonding numbers plot.

To further elucidate the key residues responsible for ligand recognition in both enzymes, ligand clustering of the last 10 ns of the MD trajectories was conducted as outlined in the methods section. In DHFR, all the ligands populated a single cluster, further supporting the stability of binding of both compounds to DHFR in all their protonation states. This, however, was not the case with TR, where multiple clusters were populated, particularly for the protonated forms of compound **10**. Examination of the ligand interaction patterns of the representative structures from the populated single clusters revealed the residues Val32, Asp54, and Ile160 as key interacting residues, forming hydrogen bonds with the diaminoquinazoline (DMQ) moiety of both compounds in DHFR (**Table IX**). The rest of the residues mainly formed stacking and other interactions. In TR, however, no key residues were seen cutting across all the systems in terms of interaction. This may be expected due to the wide nature of the TR binding pocket, as explained above.

**Table IX:** Residues interacting with compounds 7 and 10 within the binding sites of DHFR and TR

DHFR	Ring 1 of DMQ	Ring 2 of DMQ	Tail Ring
cmpd_7_unprot	Val32, Asp54, Ile160	Val33, Ala34, Ile47, NDP	NDP
cmpd_7_prot_2	Val32, Ile160, NDP	Ile47, Phe58	Pro91, Met55
cmpd_7_prot_4	Asp54, Ile160	Phe58	Pro91, Leu90
cmpd_10_unprot	Asp54, Met55, Ile160, NDP	Phe58, NDP	Ile47, Pro90, Phe94
cmpd_10_prot_2	Val33, Asp54	Ile160, Phe58, NDP	Leu90, Pro91
cmpd_10_prot_4	Val32, Asp54, Ile160	Phe58, NDP	Ile47, Pro91, Phe94
TR			
cmpd_7_unprot	Arg228	Gly196	Arg222, Ile285
cmpd_7_prot_2	Tyr221, Asn223, Arg228		Arg222, Ile285
cmpd_10_unprot	Ala284, Ala286, Ala287	Ile199, Phe198, FAD	Leu332, Met333, Leu334

DMQ - diaminoquinazoline

### III.3.2. Preliminary in vitro validation of DHFR as a target for compounds 7 (MMV1578467) and 10 (MMV1578467)

#### III.3.2.1. Protein quantification and confirmation

The total protein content of the prepared *T. b. b.* crude lysate was determined using the Bradford method. From a starting cell density of  $5 \times 10^9$  cells/mL, a protein concentration of 7.7 mg/mL was obtained. To confirm the protein extraction, SDS-PAGE profiling indicated successful extraction of proteins with molecular weights ranging from 3.5 to 240 kDa (**Figure 26**). The SDS-PAGE profile indicated a band resolving at a MW of approximately 25 kDa, which likely corresponds to a complex containing the dihydrofolate reductase (DHFR) enzyme (**Tai et al., 2002**)

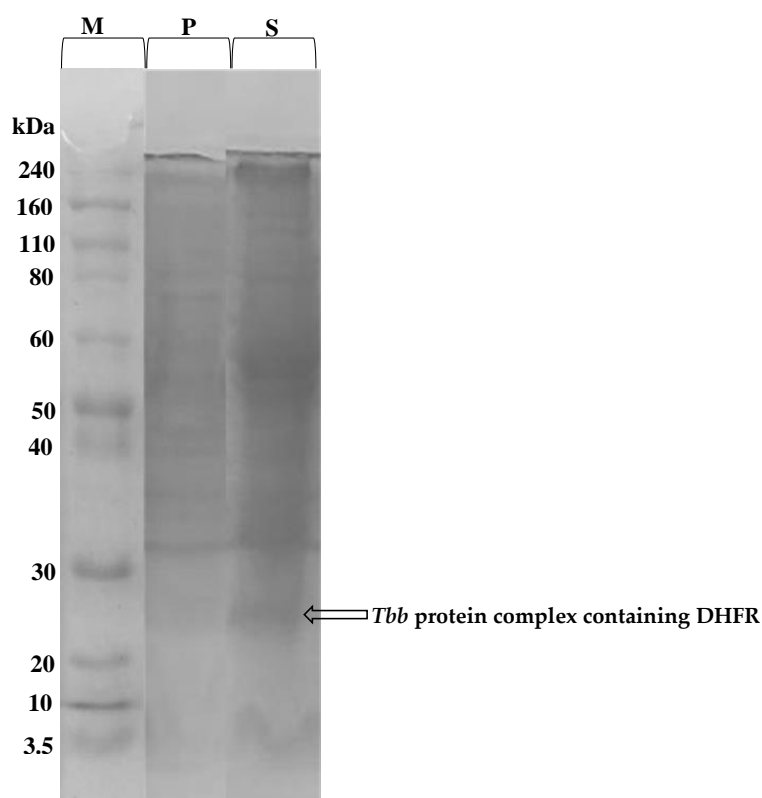


**Figure 26:** Coomassie blue stained SDS-PAGE gel showing the proteins eluted from *T. b. b.* lysates. *T. b. b.* Total protein extract was subjected to SDS-PAGE to confirm the presence of our protein extraction protocol. *T. b. b.* crude extract was run on 12% resolving and 4% stacking gels at 100 to 120 volts for 1 h. M = Molecular weight marker ranging from 3.5 to 240 kDa; P = Cell pellets; S = Protein-containing supernatant.

### III.3.2.2. Enzyme activity and inhibitory effect of 7 (MMV1578467) and 10 (MMV1578467)

Enzyme activity is usually estimated by measuring the consumption rate of the substrate or the rate of product formation over a given time period and is expressed as a specific activity. In this study, the spectrophotometric evaluation of protein activity depended on the decrease in absorbance at 340 nm pertaining to the oxidation of NADPH cofactor in the presence of folic acid and DHFR. Hence, the results from the estimation of the specific activity of the predicted DHFR contained in the *T. b. b.* lysate are shown in **Figure 27**.

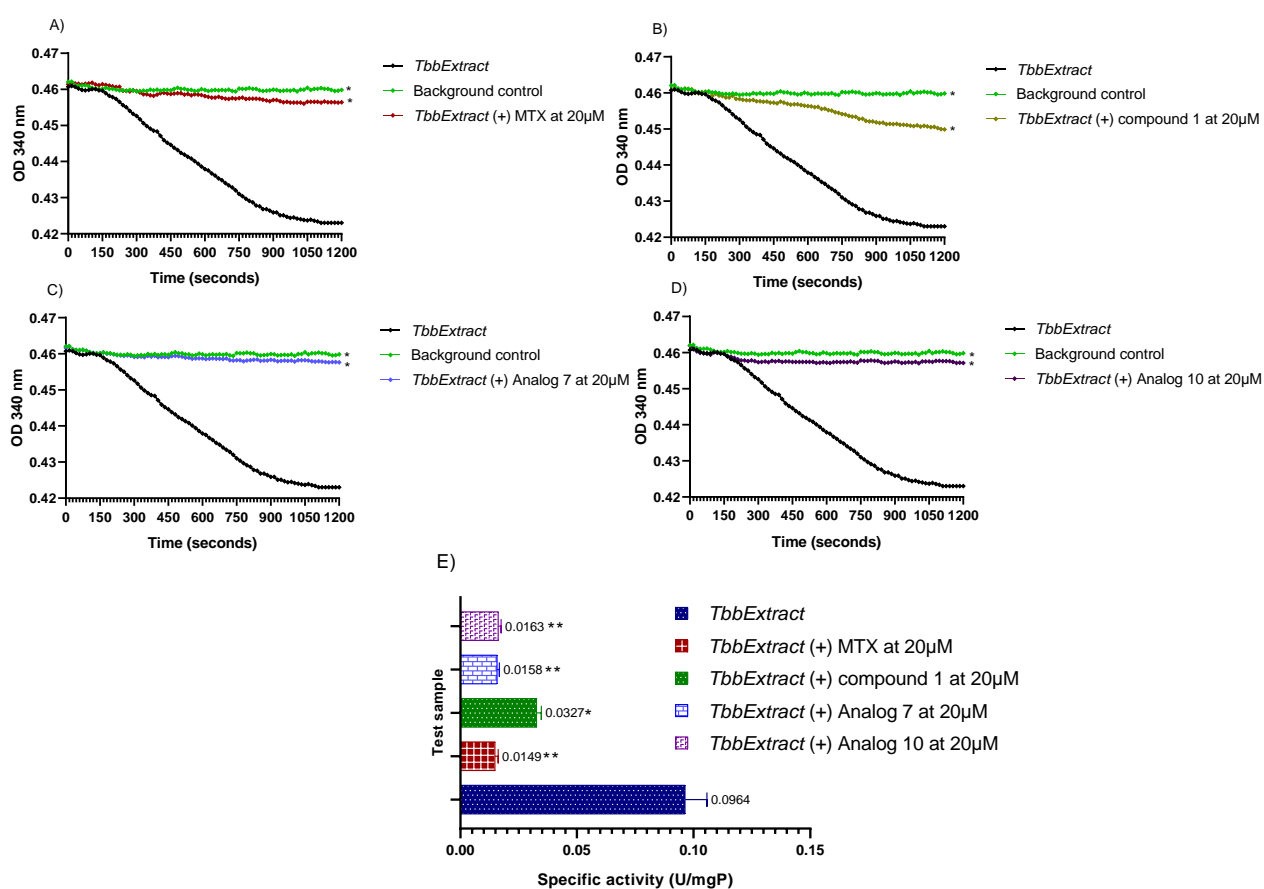


**Figure 27:** Measurement of the *T. b. b.* lysate protein activity in the presence of methotrexate (A), parent compound 1 (B), analog 7 (C) and analog 10 (D). Protein-specific activities were deduced in the presence or absence of the test inhibitors at a single concentration of 20 µM (E). *T. b. b.* Extract: crude protein extract of *Trypanosoma brucei brucei*; MTX: methotrexate; compound 1: parent hit MMV675968; analog 7: MMV1578467; analog 10: MMV1578445. The results are expressed as the mean  $\pm$  standard deviation of two independent experiments performed in duplicate. Mean values superscripted with (\*) indicate statistically significant difference with the *T. b. b.* protein extract control at  $p < 0.05$  and (\*\*) indicate statistically significant difference with the *T. b. b.* protein extract control at  $p < 0.001$  as given by Tukey's multiple comparison test.

The results indicated a constant decrease in optical densities at 340 nm over 20 min, denoting the disappearance of NADPH in the reaction mixture and thereby suggesting the presence of the predicted dihydrofolate reductase enzyme in the *T. b. b.* crude protein extract. This disappearance of NADPH highly correlated with enzymatic folate reduction. However, the achieved specific activity of 0.0964 U/mg (**Figure 27A–E**) was considerably lower than the values reported for purified DHFR enzymes from recombinant *E. coli* (**Burton et al., 2018**) and *Leishmania major* (**Nare et al., 1997**). Obviously, the portrayed activity by the crude protein extract is not 100% attributable to the DHFR enzyme as other enzyme (or multiple enzymes) that uses/use NADPH could be inhibited. Interestingly, the tested compounds (**7&10**) displayed inhibitory activities at 20  $\mu\text{M}$ , as depicted by the linear profile of their graphs, similar to that of the background control (without protein extract) (**Figure 27A–D**). As a consequence of inhibitor action, there was a significant ( $p < 0.05$ ) decrease in the specific activity compared to the enzyme in the absence of inhibitors (**Figure 27E**). The investigated inhibitors were subsequently submitted to concentration–response studies to determine their median inhibitory concentration ( $\text{IC}_{50}$ ). As depicted in Figure 7, compound **1** (MMV675968), analog **7** (MMV1578467), analog **10** (MMV1578445) and methotrexate (reference DHFR inhibitor) inhibited *T. b. b.* crude protein extract in a dose-dependent manner with  $\text{IC}_{50}$  values of 0.4, 0.18, 2.45 and 0.1  $\mu\text{M}$ , respectively.

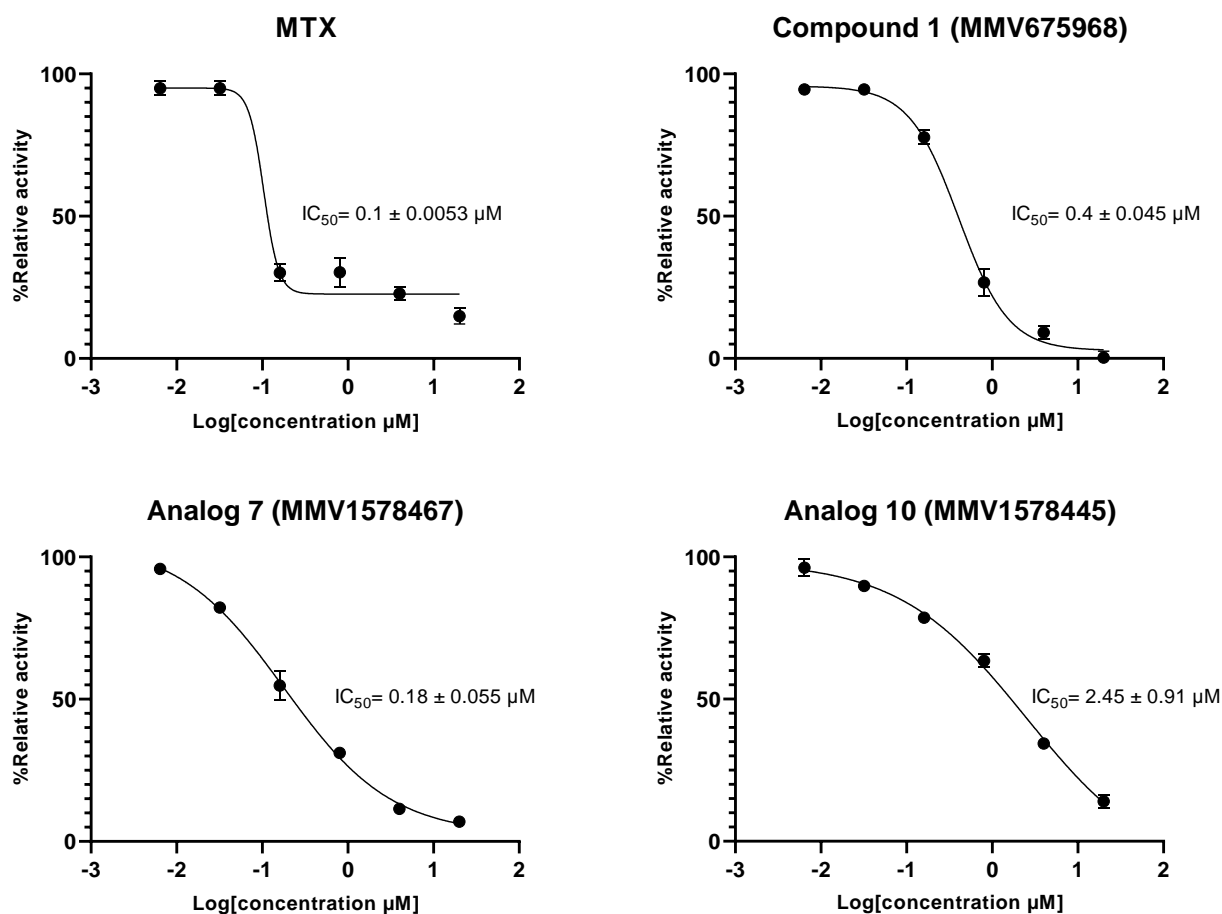


**Figure 28:** *In vitro* concentration-dependent effect of inhibitors on the predicted *T. b. b.* DHFR enzyme activity. Six-point fivefold diluted concentrations of compounds ranging from 20 to 0.00064  $\mu\text{M}$  were tested in the *in vitro* enzymatic assay. Experiments were performed in duplicate and mean absorbance counts were normalized to percent *T. b. b.* protein control activity using Microsoft Excel. Concentration–response curves were generated using GraphPad Prism software.

## Discussion

Literature data indicate that the diaminoquinazoline core is a suitable ligand for protein inhibition, including parasite enzymatic targets. More specifically, the quinazoline core was reported to be a good motif for the inhibition of trypanothione reductase (TR) (Cavalli et al., 2010; Patterson et al., 2011), a validated therapeutic target for antitrypanosomal drug development (Spinks et al., 2009). Moreover, several studies have reported the efficacy of 2,4-diaminoquinazoline analogs against the enzyme DHFR, which is also a validated drug target in trypanosomes (Sienkiewicz et al., 2008a). Specifically, the parent hit compound MMV675968 was previously reported to have antifolate activity. Indeed, Rosowsky et al., (1994) explored the *in vitro* activity of 10 synthesized different analogs of 2,4-diamino-5-chloroquinazoline, including

the hit compound **MMV675968** (referred to as 2,4-diamino-5-chloro-6-[(2,5-dimethoxyanilino)methyl]quinazoline), against DHFR enzymes of both *Pneumocystis carinii* and *Toxoplasma gondii* and determined IC<sub>50</sub> values of 0.051  $\mu$ M and 0.03  $\mu$ M, respectively. More recently, Nelson and Rosowsky identified compound **MMV675968** (IV.18) as a highly potent inhibitor of *Cryptosporidium parvum*-I DHFR *in vitro* with an IC<sub>50</sub> of 0.0065  $\mu$ M. This inhibitory activity was further confirmed (IC<sub>50</sub> of 0.2  $\mu$ M) using phenotypic whole parasite testing (Nelson, 2001). Based on this rationale, the two potent antitrypanosomal analogs of **MMV675968** (MMV1578467 and MMV1578445) identified in this study were submitted to *in silico* confirmation of DHFR and TR as their potential targets using molecular docking and molecular dynamics simulations. However, direct binding interactions through *in silico* studies may not guarantee the activity of a compound in *in vitro* screening. To validate the *in silico* binding affinity of trypanosome DHFR with compound **7** & **10**, the inhibitory activity of these compounds was carried out against DHFR-based *T. b. brucei* crude protein extract. Although lower activity was demonstrated against the *T. b. brucei* crude protein extract, the results nevertheless portrayed a consistent inhibition of the NADPH oxidation cofactor by the parent hit (MMV675968) and the two promising analogs (MMV1578467 and MMV1578445) (**Figure 28**). By contrast to previously reported data (Gibson et al., 2016; Tassone et al., 2021) the low inhibitory activity observed for compound **7** & **10** toward DHFR might be due to the use of DHFR-based protein extract rather than the pure enzyme. Two positional isomers of compound **10** (compounds 6 and 8 in the article) demonstrated an inhibition of 82-88% of DHFR at 7.5  $\mu$ g/mL, but this inhibition did not correlate with the inhibition of *Leishmania mexicana* (Berman et al., 1989). Later, another series of 2,4-diaminoquinazoline analogs were described as selective inhibitors of Leishmania and Trypanosoma DHFR with good activities against *T. rhodesiense* and *T. cruzi* (Khabnadideh et al., 2005). These data justify the activity of the compounds obtained in the present study.

Future *in vitro/in vivo* studies using recombinantly purified DHFR enzyme and appropriate animal models of trypanosomiasis will provide more insights to validate this assertion. Furthermore, time kill kinetics, induction of intracellular ROS production, membrane permeabilization, DNA fragmentation and ferric ion reducing antioxidant power (FRAP) assays of analogs **7** and **10** were performed.

### III.4. Tentative elucidation of other modes of action of analogs 7 and 10 against *T.b. brucei*

#### III.4.1. In vitro kinetics of *T.b. brucei* killing upon treatment with analogs 7 (MMV1578467) and 10 (MMV1578445)

Analog **7** and **10** were assessed at their respective IC<sub>99</sub>, IC<sub>90</sub>, IC<sub>50</sub> and IC<sub>10</sub> for their impact on the growth rate of *Trypanosoma brucei brucei* in culture (**Figure 29**). The results indicated a concentration-dependent reduction in trypanosome growth (**Figure 29A and 29B**) compared to untreated cells when exposed to compounds **7** and **10** at their IC<sub>99</sub>, IC<sub>90</sub>, IC<sub>50</sub> and IC<sub>10</sub>. A similar trend was observed for the positive control (pentamidine- **Figure 29C**). Of particular interest, compound **10** completely suppressed the growth of trypanosomes throughout the 72h incubation period, whereas the effect of compound **7** tended to decrease after 60 h of treatment (**Figure 29B**). Data generated from the time-kill kinetics also indicated that analogs **10** and **7** at their respective IC<sub>99</sub> values completely inhibited the growth of trypanosomes within 4 and 24 hours, respectively. Therefore, the ability of parasites to recover post exposure to inhibitors was further evaluated for 68 hours and 48 hours for analogs **10** and **7**, respectively.

Inhibitor removal at 4 h for analogs **10** and 24 h for analog **7** when tested at their respective IC<sub>90</sub> and IC<sub>99</sub> values followed by subculture in inhibitor-free complete medium indicated a cidal effect for compound **10** (**Figure 29D**). Conversely, the removal of compound **7**, initiated a consistent growth between 24 and 48 h, followed by an exponential growth between 48 and 60 h, denoting a static effect for this compound (**Figure 29E**). Of note, pentamidine (positive control) portrayed a static profile because its effect gradually decreased from 48 h to 72 h (**Figure 29F**). Overall, from the comparison of the individual effects of the 2 inhibitors and pentamidine depicted in **Figure 29G and 29H**, analog **10** appeared to exhibit a more potent (cidal) effect on trypanosomes than analog **7** and pentamidine.

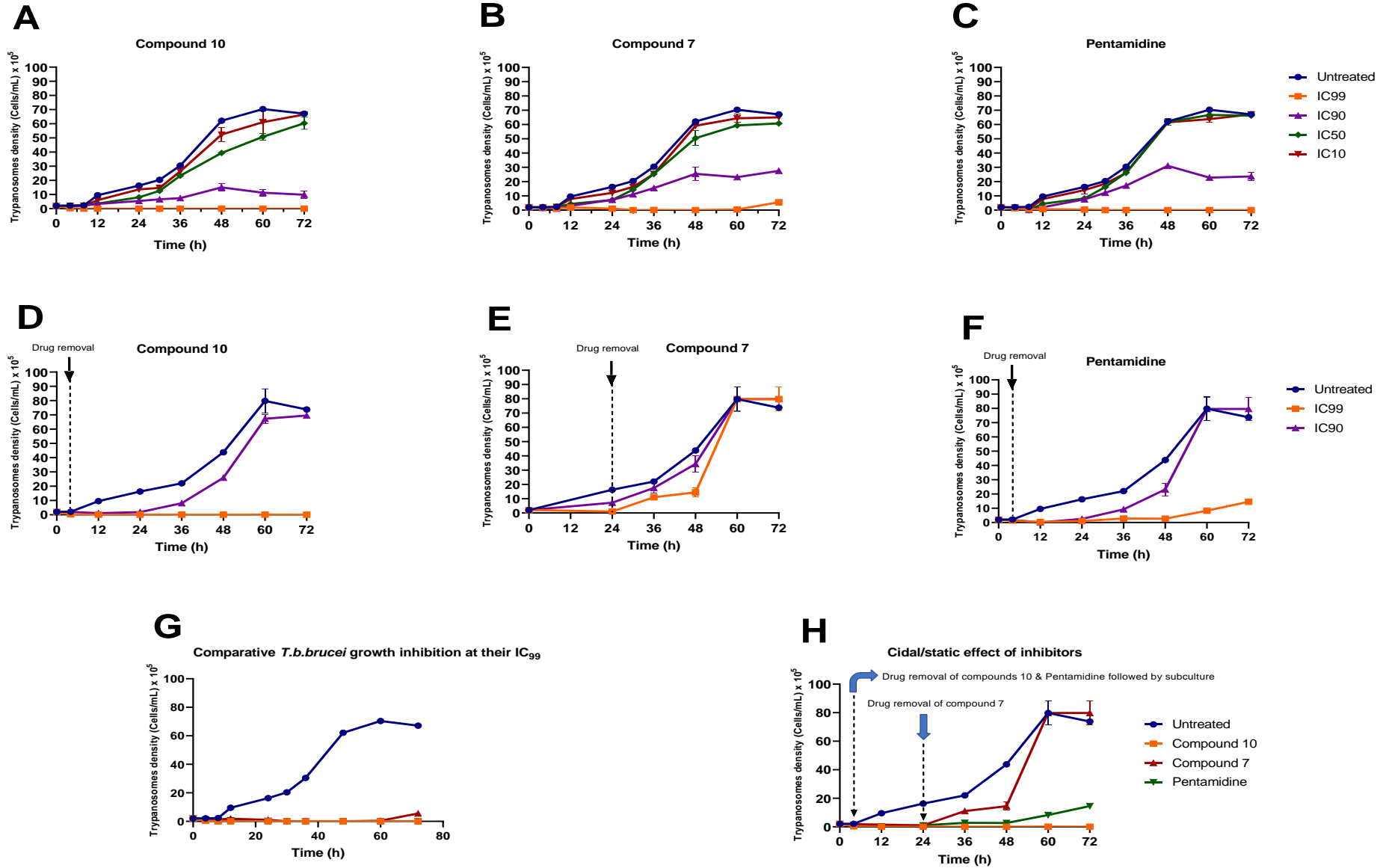


**Figure 29:** Growth curves of *T.b. brucei* in the presence or absence of various concentrations of compounds **7** and **10** and pentamidine.

Parasites were seeded at  $2 \times 10^5$  cells/mL and incubated for 72 h at 37°C and 5% CO<sub>2</sub>. At the indicated time points, trypanosomes were counted microscopically (for IC<sub>10</sub>, IC<sub>50</sub>, IC<sub>90</sub> and IC<sub>99</sub> wells), and the obtained cell counts were averaged and then plotted versus time using GraphPad Prism 8.0. After treatment for 4 h (analog 10) and 24 h (analog 7), drugs were washed out from the cultures, and the parasites were subcultured in drug-free complete medium for an additional 68 h and 48 h for analogues 10 and 7, respectively. Cells were then microscopically counted, and the counts were used to plot the growth curves over time. The activity profiles of compounds 7 and 10 and pentamidine are compared in **Figs 21G and 21H**. The results are expressed as the mean  $\pm$  SD from duplicate experiments.

### III.4.2. Effect of analogs 7 (MMV1578467) and 10 (MMV1578445) on plasma membrane integrity

To evaluate their possible effect on plasma membrane integrity, various concentrations (IC<sub>99</sub>, IC<sub>90</sub>, IC<sub>50</sub>, and IC<sub>10</sub>) of compounds **7** and **10** were incubated with parasites for up to 120 minutes. Plasma membrane disruption was examined using the fluorescent probe SYBR Green, which binds to DNA when the plasma membrane permeability is compromised due to the direct or indirect action of the compounds. The results indicated that the parasite membrane maintained its integrity even after 120 min of incubation with inhibitors. This unchanged status of the plasma membrane was evidenced by a nonsignificant difference in the fluorescence profile of drug-treated versus untreated parasites. Conversely, there was a highly significant difference between the effects of compounds **7** and **10** on the one hand and the positive control (saponin) on the other hand, at  $p < 0.05$  (**Figure 30**), denoting no impairment or a rather mild effect of the test compounds on the plasma membrane permeability of the parasite.

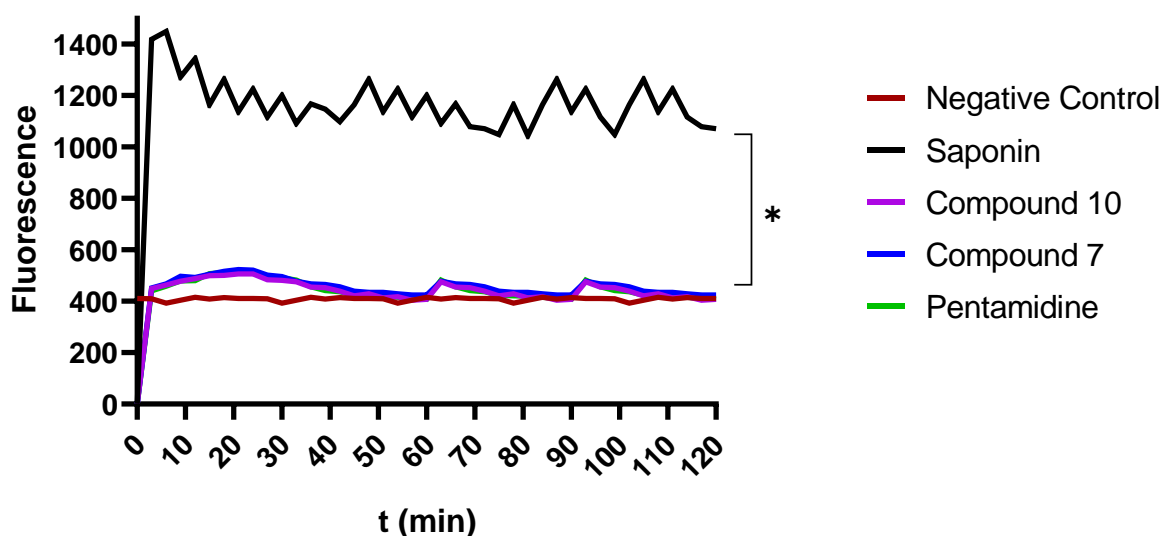


**Figure 30: Effect of compounds 7 and 10 on plasma membrane permeability of *T. b. brucei*.** The fluorescence intensity of the trypanosome DNA-SYBR Green (SG) complex was measured over 120 min. Parasites at  $2 \times 10^6$  cells/mL were preincubated with SG followed by treatment with compounds 7 and 10 at their IC<sub>99</sub>, IC<sub>90</sub>, IC<sub>50</sub>, and IC<sub>10</sub> for 120 min. SG uptake was then fluorometrically monitored, and data were obtained to plot corresponding curves versus time. The results were compared to the negative and the positive controls (\*Significant difference at  $p < 0.05$ ). Negative control (NC): trypanosomes untreated with inhibitors; Saponin: 100% permeability.

### III.4.3. Induction of oxidative stress in trypanosomes by compounds 7 and 10

We assessed the influence of the test compounds on the production of reactive oxygen species (ROS) by trypanosomes as an indication of oxidative stress induction. Trypanosomes

were incubated with compounds **7** and **10** for 120 min, and the intracellular level of ROS was determined using the fluorescent probe H<sub>2</sub>DCF-DA. The results obtained indicated no significant changes ( $P < 0.05$ ) in ROS production in parasites treated with compounds when compared to the untreated parasites (negative control); however, the production of ROS significantly increased in the group treated with the positive control (H<sub>2</sub>O<sub>2</sub>) at 0.1% (v/v) (Figure 31).

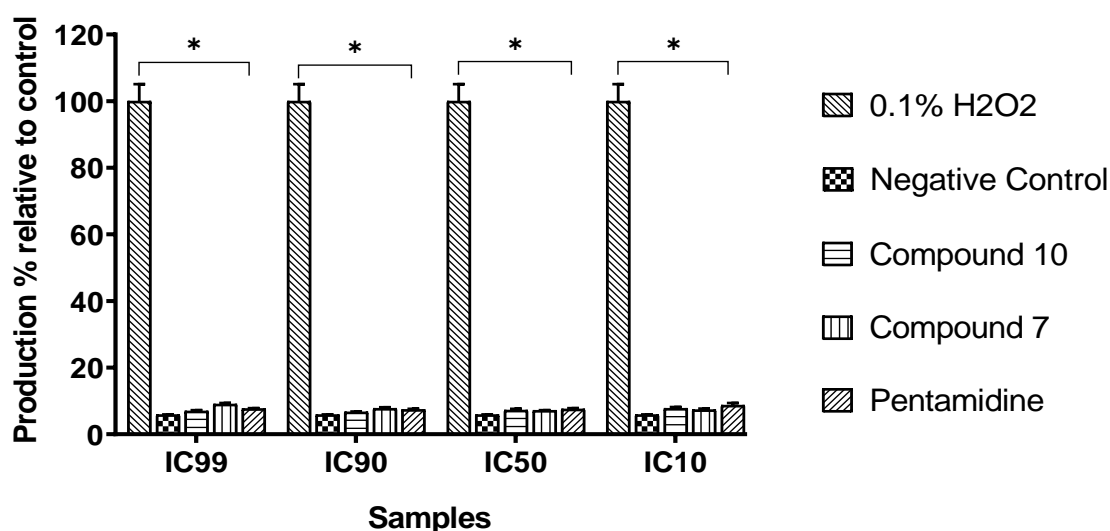


**Figure 31: Effect of compounds 7 and 10 on the production of intracellular reactive oxygen species (ROS).**

Parasites were treated with or without compounds at their respective IC<sub>99</sub>, IC<sub>90</sub>, IC<sub>50</sub> and IC<sub>10</sub> values for 120 min, and ROS production was measured using DCF-DA reagent. H<sub>2</sub>O<sub>2</sub> (0.1%) was included as a positive control and further used to calculate the ROS production percentages. The obtained results are expressed as the mean  $\pm$  standard deviation of two independent experiments performed in duplicate. \* Significant difference at  $p < 0.05$ .

#### ***III.4.4. Analog 10 induces DNA fragmentation in trypanosomes as a marker of cell death***

To shed light on the mode of parasite killing induced by the inhibitors, we further determined the type of cell death elicited by analogs **7** and **10** using a DNA fragmentation kit. The technique used consisted of an immunological detection of BrdU (5'-bromo-2'-deoxyuridine)-labeled DNA fragments in the parasitic cytoplasm for apoptosis and in the culture supernatant for cell-mediated cytotoxicity. The results achieved are summarized in Figure 32.

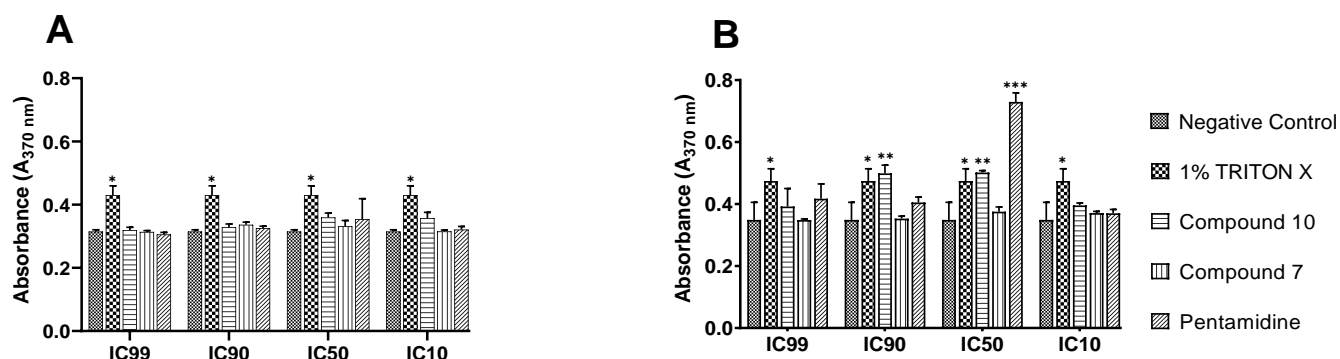


**Figure 32: DNA fragmentation and cytolysis induced by compound 10 in bloodstream forms of *Trypanosoma brucei brucei*.** BrdU-labeled parasites at  $4 \times 10^5$  cells/mL were incubated in the presence or absence of analogs **7** and **10** at their IC<sub>99</sub>, IC<sub>90</sub>, IC<sub>50</sub> and IC<sub>10</sub> for 4 hours in growth conditions, and the culture supernatant (Figure 32A, cytolysis) and lysate (Figure 32B) were further processed using the cellular DNA fragmentation kit. \*\*\*Significant difference at  $p < 0.001$ ; \*\*Significant difference at  $p < 0.01$ , \* Significant difference at  $p < 0.05$ ; ns: No significant difference; Negative control: untreated parasites; 1% Triton-X was used as a positive control.

Mediated cell death was evidenced through the measurement of stronger absorbance emitted by DNA-labeled fragments with a characteristic green color. According to **Figure 32A**, no cell lysis was induced by compounds **7** and **10**, as well as pentamidine, whereas treatment with Triton-X (standard cell disruptor) led to cell lysis. Concerning the apoptotic DNA fragmentation, analog **10** exhibited a significant inducing effect. However, the observed effect was by far lower than that of pentamidine, a standard trypanocidal drug (**Figure 32B**). Of note, mediated apoptosis was not seen for all inhibitors at IC<sub>99</sub>, IC<sub>90</sub> and IC<sub>10</sub>. This observation might be due to the high parasite death rates obtained at IC<sub>99</sub> and IC<sub>90</sub>, which did not allow the development of a measurable green anti-BrdU-DNA complex. On the other hand, parasite killing rate was not significant at IC<sub>10</sub> (due to subinhibitory drug concentration) to enable measurement of the drug effect. It should also be noted that analog **7** did not exert any effect through the two cell-mediated death modes investigated.

### III.4.5. Ferric ion reducing antioxidant power (FRAP) of Inhibitors

To assess the potential of analogs **7** & **10** in reducing ferric ions, these compounds were incubated with a solution of Fe<sup>3+</sup> and ortho-phenanthroline and the median reducing concentration (RC<sub>50</sub>) was calculated. The results showed that analog **7** exhibited weak Fe<sup>3+</sup>-reducing activity with a median reducing concentration (RC<sub>50</sub>) of 96.37  $\mu$ M. In addition, analogue 10 (RC<sub>50</sub> > 400  $\mu$ M) was  $\sim$  4-fold less active than analog **7**. The latter being more potent than standard reducing agent ascorbic acid (RC<sub>50</sub>: 165  $\mu$ M). These results suggest that

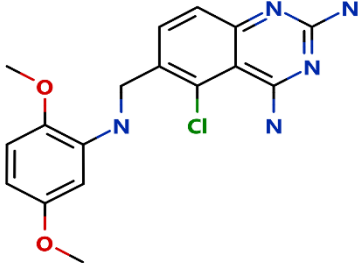
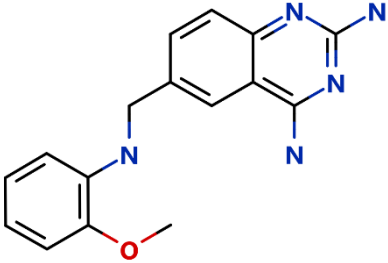
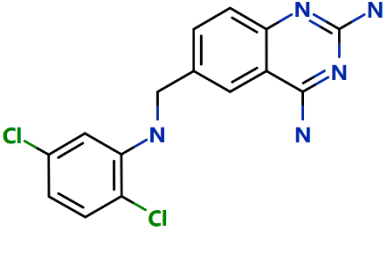
analog **7** might have exerted antitrypanosomal activity through deprivation of ferric iron bioavailability to trypanosomes. However, further studies should be performed to confirm this assertion.

#### ***III.4.6. Predicted pharmacokinetic profile of the compounds of interest***

The pharmacokinetic properties of the compounds were assessed using StarDrop software and the results obtained are presented in Table X.

The prediction revealed that all derivatives presented partition coefficient (cLogP) values in the range of 2.29 to 3.58 (cLogP < 5), the number of hydrogen bond acceptors and donors in the derivatives were in the acceptable range (HBA < 10 and HBD < 5), and the molecular weight of all compounds was less than 500, which indicated that the derivatives met the Lipinski's rule of five (**Lipinski, 2000**). The number of rotatable bonds were less than 10, which was in accordance with Veber's rule (**Veber et al., 2002**). Moreover, the pharmacokinetic results of compounds **7** & **10** have met the rules of druglikeness reported by Ghose, Egan, and Muegge. In fact, water solubility (cLogS) values ranged between -4.51 and -3.39, indicating moderate solubility. The diaminoquinazoline analogs were predicted to have high percent human intestinal absorption, indicating that these derivatives may have good membrane permeability. Furthermore, the molecular interactions between analogs **7** & **10** with P-glycoprotein (P-gp; a transporter protein that plays a number of important roles during drug absorption, especially for expelling molecules out of cells) aid to predict the extent/degree of absorption of these compounds (**Lagorce et al., 2017**). The analogs **7** & **10** were predicted to bind onto P-glycoprotein, inferring that these compounds are substrates of P-gp. Cytochrome P450s are important enzymes for drug metabolism and, inhibition of such enzymes may lead to potential toxicity or side effects caused by drug–drug interactions. The metabolism of targeted compounds was predicted based on a model proposed in the software for the main CYP isoforms involved in drug metabolism. The results showed that these compounds are expected to be CYP2D6 substrates, that mediates the biotransformation of several important classes of drugs (**Bozina et al., 2009**). In addition, cytochromes 2C9, 3A4 and 1A2 were predicted to be involved in the metabolism of compounds **7** & **10**. Unfortunately, the computational data did not indicate that the target compounds are capable of crossing the BBB. Moreover, plausible immunotoxicity of compounds **7** & **10** was also anticipated.

**Table X:** Prediction of ADME/TOX parameters of compound **1** (MMV675968) and structural analogs **7** (MMV1578467) and **10** (MMV1578445).

Compounds			
	MMV675968 (1)	MMV1578467 (7)	MMV1578445 (10)
<b>Physicochemical properties</b>			
MW	359.81	295.34	334.20
Number of rotatable bonds	5	4	3
Number of heavy atoms	16	16	16
Molar refractivity	100.13	88.63	92.16
TPSA	108.31 A	99.08 A	89.85 A
Number of H-bond acceptors	4	3	3
Number of H-bond donors	3	3	3
<b>Druglikeness</b>			
Lipinski	Yes	Yes	Yes
Ghose	Yes	Yes	Yes
Weber	Yes	Yes	Yes
Egan	Yes	Yes	Yes
Muegge	Yes	Yes	Yes

<b>Absorption</b>			
Water solubility (Log S)	-4.04	-3.39	-4.51
CLog P o/w	2.89	2.29	3.58
HIA (%)	High	High	High
P-gp substrate	Yes	Yes	Yes
<b>Distribution</b>			
BBB penetration	No	No	No
<b>Metabolism</b>			
CYP1A2 inhibitor	Yes	Yes	Yes
CYP2C19 inhibitor	No	No	Yes
CYP2C9 inhibitor	Yes	Yes	Yes
CYP2D6 inhibitor	Yes	Yes	Yes
CYP3A4 inhibitor	Yes	Yes	Yes
<b>Toxicity</b>			
Predicted toxicity	380 mg/kg	290 mg/kg	450 mg/kg
Hepatotoxicity	No	No	No
Carcinogenicity	Yes (0.5 probability)	Yes (0.5 probability)	No
Immunotoxicity	Yes (0.9 probability)	Yes (0.9 probability)	Yes (0.82 probability)
Mutagenicity	Yes (0.5 probability)	Yes (0.5 probability)	No

MW: molecular weight of the compounds; log S. aqueous solubility (scale: <-10<poorly<-6<moderately<-4<soluble<-2, very<0<highly); CLogP o/w: lipophilicity, octanol/water partition coefficient (recommended value: LogP <5); TPSA: topological polar surface area; BBB: blood–brain barrier; P-gp: P-glycoprotein; PPB: blood–brain barrier; HIA: human intestinal absorption; Lipinski (criteria: MW ≤500, LogP ≤4, N or O ≤ 10, NH or OH ≤5); Ghose (criteria: 160 ≤MW ≤480, -0.4 ≤LogP ≤5, 40 ≤molar refractivity ≤130, 20 ≤number of heavy atoms ≤70); Weber (criteria: rotatable bonds ≤10, TPSA ≤140); Egan (criteria: ClogP <5, TPSA ≤131.6); Rodrigues (criteria: ≤MW ≤500, -2 ≤cLogP ≤5, TPSA ≤150, number of rings ≤7, number of heteroatoms >1, rotatable bonds ≤15 CYP2D6: cytochrome P450 family 2 subfamily D member 6; CYP1A2: cytochrome P450 family 1 subfamily A member 2; CYP2C19: cytochrome P450 family 2 subfamily C member 19, CYP2C9: cytochrome P450 family 2 subfamily C member 9; CYP3A4: cytochrome P450 family 3 subfamily A member 4.

## Discussion

Understanding the mode of action of a compound is essential for its development as a drug. Following confirmation studies of the likely molecular targets for compounds **7** and **10** additional studies were performed (time kill kinetics, induction of intracellular ROS production, membrane permeabilization, DNA fragmentation and ferric ion reducing antioxidant power). Compound **7** was found to alter the growth of parasites after a period of 24 hours at IC<sub>99</sub> and presented a parasitostatic effect on trypanosomes, which was further confirmed by the reversibility effect of this compound after its removal and subculturing (**Figure 28**). Therefore, it can be argued that this compound is either a slow-acting inhibitor or might be involved in a reversible interaction with the trypanosome metabolic target. Such a compound might rapidly induce resistance to *T.b.brucei* and might require either multiple and high doses for a complete parasite elimination *in vivo* or a very long treatment period. This profile of compound **7** is of limited advantage compared to the current remedies used for the treatment of trypanosomiasis. Lead optimization is expected to improve antitrypanosomal properties of compound **7**. Of particular interest, compound **10** presented a fast-killing effect within 4 h and irreversible cidal activity during the whole monitoring period of 72 h at IC<sub>99</sub> (**Figure 28**). As previously demonstrated, this feature of compound **10** is an additional advantage since fast-acting and trypanocidal compounds can eliminate the parasite in few doses, therefore improving the treatment regimens (**Rycker et al., 2012**). In the time-kill kinetic test, compound **10** emerged as the most promising candidate amenable for drug development. Membrane permeability and oxidative stress might not be cited among the antitrypanosomal mechanisms of action of compounds **7** and **10**. This corroborates with the absence of cell lysis (**Figure 32A**) inferring that these compounds might have exerted cell death through other mechanisms. Subsequent detection of DNA fragments in the cell lysate of parasites exposed to compound **10** confirmed its apoptosis-like-inducing effect through elicitation of DNA fragmentation in treated bloodstream trypanosomes as evidenced by a significant increase in absorbance compared to the negative control (**Figure 31**). Moreover, the positive control (pentamidine) displayed a high DNA fragment signal. Previous reports demonstrated that strong DNA binding properties (particularly to the minor groove of AT-rich regions), DNA fragmentation, and apoptosis cell death are among the antitrypanosomal mechanisms of action of pentamidine. (**W. Wilson et al., 2008, G. Singh & Dey, 2007; Thomas et al., 2018**). This finding further validates the the ELISA DNA fragmentation kit used in our study. However, additional studies are required to better understand the mechanisms of action by which

compound **10** induces a cidal effect in trypanosomes. Finally, the assessment of the ferric iron reducing ability of the inhibitors showed moderate reducing power for compound **7**. Iron is a vital element in most living organisms, including trypanosomes, and is involved in several important biological processes, such as mitochondrial respiration, DNA replication, antioxidant defense, and glycolysis. In fact, three enzymes were described as being iron-dependent and crucial for the survival of trypanosomes. These include superoxide dismutase, which eliminates superoxide radicals released during the production of the tyrosyl radical in the R2 subunit of ribonucleotide reductase (**Le Trant et al., 1983; Fontecave et al., 1987**). Alternative oxidase is an important enzyme for the reoxidation of nicotinamide adenine dinucleotide (NADH) produced during glycolysis (**Fairlamb, 1977; Clarkson et al., 1989**). In addition, **Ajayi et al., (2002)** investigated the iron dependence of oxidase alternative and terminal trypanosomes (AOT) by chelating iron using o-phenanthroline, which resulted in strong inhibition of this enzyme. Ribonucleotide reductase is another iron-dependent enzyme that catalyzes the reduction of ribonucleotides to deoxyribonucleotides needed for DNA synthesis (**Dormeyer et al., 1997; Hofer et al., 1997**). Therefore, iron deprivation in parasites by compound **7** might induce a loss functionality of such enzymes, thereby inducing a rapid decrease in DNA synthesis, increase in oxidative stress and cessation of electron transfer to the AOT enzyme, leading to the death of the parasite.

As already discussed, prior to successful drug development, the identification of potential hit compounds should be accompanied by pharmacokinetic experiments through *in vitro* or *in silico* approaches to evaluate drug-likeness or ADME (absorption, distribution, metabolism, and elimination) properties. To determine whether the selected compounds are likely to be further developed as antitrypanosomal agents, their pharmacokinetic properties (absorption, distribution, metabolism, elimination, and toxicology) were evaluated through *in silico* studies (**Table X**). The results demonstrated that analogs **7** and **10** did not violate the Lipinski rule of five, as well as other drug-likeness rules established by Ghose, Weber, Egan, and Muegge. Despite their good absorption in the human intestine and moderate water solubility, these compounds were not anticipated to potentially cross the BBB. In some circumstances, parasites can be localized in the CNS causing the so-called late meningo-encephalitic phase of HAT. Therefore, the inability of analogs **7** & **10** to cross the BBB might limit their effectiveness in case of drug development against the late meningo-encephalitic phase of HAT. Moreover, analogs **7** and **10** are not substrate of P-gp and may not be expelled from the cells following absorption.

These predictive evaluations provide guidance about the physio-chemical as well as pharmacokinetic parameters of the tested compounds, thus promoting hit optimization for future drug development.

# Conclusion and Perspectives



## CONCLUSION

The following conclusions were drawn at the conclusion of this work, which aimed to investigate the antitrypanosomal activity of compounds from the MMVPBox library and elucidate their possible mode of action:

1. Seventy (70) of the 400 compounds tested positive for antitrypanosomal single-point inhibition of *T. brucei* growth, with an inhibition percentage up to 90%. At a unique concentration of 10  $\mu\text{M}$ . In a dose–response study, they demonstrated moderate-to-high *in vitro* inhibition with  $\text{IC}_{50}$  values ranging from 0.0023 to 9.78  $\mu\text{M}$  and high selectivity toward Vero cells.
2. A structure-activity relationship study centered on the 2,4 diaminoquinazoline compound **MMV675968** ( $\text{IC}_{50} = 2.8 \mu\text{M}$ ;  $\text{SI} = 37.87$ ) yielded two promising analogs, **MMV1578445 (10)** and **MMV1578467 (7)**. They were almost 60-fold (**MMV1578445**  $\text{IC}_{50} = 0.045 \mu\text{M}$ ,  $\text{SI}=1737$ ) and 40-fold (**MMV1578467**  $\text{IC}_{50} = 0.06 \mu\text{M}$ ;  $\text{SI}=412$ ) more active and selective, respectively than their common parent counterpart (**MMV675968**).
3. Both analogs were found to be potent binders of DHFR, eliciting important diaminoquinazoline ring-mediated interactions with key DHFR ligand recognition residues such as Val32, Asp54 and Ile160. This observation was confirmed to have significant *in vitro* activity against the DHFR trypanosome crude protein isolate.
4. Analog **10 (MMV1578445)** displayed a fast and irreversible growth arrest, but a slow-acting and reversible activity on the parasite growth was noticed for analog **MMV1578467 (7)**. Mechanistic studies of the antitrypanosomal analogs **7 & 10** excluded membrane permeabilization and ROS generation as the plausible mechanisms of action of these compounds. Nevertheless, analog **MMV1578445 (10)** was found to induce *Trypanosoma* death through DNA fragmentation thereby revealing its late apoptosis-like activity, while analog **MMV1578467 (7)** showed a moderate ferric iron reducing ability. Prediction of ADME/TOX properties revealed that the selected derivatives possess favorable drug-like characteristics and acceptable pharmacokinetic properties that should be further exploited for lead optimization.

Overall, owing to their favorable pharmacological and physicochemical properties, compounds **7** and **10** qualify as suitable starting points for the development of alternative treatments against trypanosomiasis.

---

## PERSPECTIVES

In view of the results obtained from this study, more research is needed to prospect the most promising antitrypanosomal hit compounds as scaffolds for the development of new drugs against HAT/AAT. As a result, we propose the following as future short-term studies:

- ❖ Performing in-depth structure-activity and structure-property relationship studies and carry out *in vitro* pharmacokinetic and toxicity studies,
- ❖ Delve deeper into the mechanisms of action of the newly synthesized analogs
- ❖ Undertaking *in vivo* safety and efficacy trials on appropriate animal models.

# References



## REFERENCES

- Abdizadeh, H., Tamer, Y. T., Acar, O., Toprak, E., Atilgan, A. R., & Atilgan, C. (2017). Increased substrate affinity in the Escherichia coli L28R dihydrofolate reductase mutant causes trimethoprim resistance. *Physical Chemistry Chemical Physics*, 19(18), 11416–11428. <https://doi.org/10.1039/c7cp01458a>
- Abdoulmoumini, M., Ebene, N. J., Fongho, S. P., & Youssouf, M. M. (2015). Prevalence and impact of bovine trypanosomiasis in Mayo Rey division , a Soudano-Sahelian zone of Cameroon. *Journal of Parasitology and Vector Biology*, 7(5)(2141–2510), 80–88. <https://doi.org/10.5897/JPVB2015.0189>
- Abdoulmoumini, M., Khan, P. V., & Lendzele, S. S. (2015). Current prevalence of cattle trypanosomiasis and of its vector in Alme , the infested zone of Adamawa plateau Cameroon , two decades after the tsetse eradication campaign. *International Journal of Biological and Chemical Sciences*, 9(June), 1588–1598. <https://doi.org/10.4314/ijbcs.v9i3.38>
- Abdoulmoumini, M., Njanloga, A., Hayatou, A., Suh, P. F., & Achukwi, M. D. (2016). Animal trypanosomosis in clinically healthy cattle of north Cameroon: epidemiological implications. *Parasites & Vectors*, 1–8. <https://doi.org/10.1186/s13071-016-1498-1>
- Abeloff, M., Rosen, R., Luk, G., Baylin, S., Zeltzman, M., & Sjoerdsma, A. (1986). Abeloff MD, Rosen ST, Luk GD, et al. Phase II trials of alpha-difluoromethylornithine, an inhibitor of polyamine synthesis, in advanced small cell lung cancer and colon cancer. *Cancer Treatment Reports*, 70(7), 843–845.
- Adelusi, I. T., Oyedele, A. K., Damilare, I., Tunde, A., Oluwabusola, R., Divine, C., Oluwaseun, M., Tosin, O., Olaide, I., Elijah, O., Xiaoxing, Y., & Abdul-hammed, M. (2022). Molecular modeling in drug discovery. *Informatics in Medicine Unlocked*, 29(February), 100880. <https://doi.org/10.1016/j.imu.2022.100880>
- Ahmad, S. I., Kirk, S. H., & Eisenstark, A. (1998). Thymine metabolism and thymineless death in prokaryotes and eukaryotes. *Annual Review of Microbiology*, 52, 591–625. <https://doi.org/10.1146/annurev.micro.52.1.591>
- Ajayi, W. U., Chaudhuri, M., & Hill, G. C. (2002). Site-directed mutagenesis reveals the essentiality of the conserved residues in the putative diiron active site of the trypanosome alternative oxidase. *Journal of Biological Chemistry*, 277(10), 8187–8193. <https://doi.org/10.1074/jbc.M111477200>
- Akhter, M. (2016). Challenges in docking: Mini review. *JSM Chemistry*, 4(2), 1025. <https://www.jscimedcentral.com/Chemistry/chemistry-4-1025.pdf>
- Aksoy, S., Gibson, W. C., & Lehane, M. J. (2003). Interactions between tsetse and trypanosomes with implications for the control of trypanosomiasis. *Advances in Parasitology*, 53, 1–83. [https://doi.org/10.1016/S0065-308X\(03\)53002-0](https://doi.org/10.1016/S0065-308X(03)53002-0)
- Alieea, M., Soledad, C., N, D. C., Patel, S., Mwamba, M. E., Spencer, S. E. F., Keeling, M. J., Chitnis, N., & Rock, K. S. (2021). Predicting the impact of COVID-19 interruptions on transmission of gambiense human African trypanosomiasis in two health zones of the Democratic Republic of Congo. *Transactions of the Royal Society of Tropical Medicine*

- and Hygiene*, 115(February), 245–252. <https://doi.org/10.1093/trstmh/trab019>
- Alirol, E., Schrupf, D., Amici Heradi, J., Riedel, A., De Patoul, C., Quere, M., & Chappuis, F. (2013). Nifurtimox-eflornithine combination therapy for second-stage gambiense human African trypanosomiasis: Médecins Sans Frontières experience in the Democratic Republic of the Congo. *Clinical Infectious Diseases*, 56(2), 195–203. <https://doi.org/10.1093/cid/cis886>
- Alonso, H., Bliznyuk, A. A., & Gready, J. E. (2006). Combining docking and molecular dynamic simulations in drug design. *Medicinal Research Reviews*, 26(5), 531–568. <https://doi.org/10.1002/med.20067>
- Ammar, Z. (2013). *Caractérisation de l'interaction entre les trypanosomes africains et les cellules endothéliales : activation, inflammation et rôle des trans-sialidases*. UNIVERSITÉ DE BORDEAUX 2, Ecole doctorale Sciences de la Vie et de la Santé; Mention : Sciences, Technologies, Santé Option :
- Amusengeri, A., Tata, R. B., & Bishop, Ö. T. (2020). Understanding the pyrimethamine drug resistance mechanism via combined molecular dynamics and dynamic residue network analysis. *Molecules*, 25(4), 1–24. <https://doi.org/10.3390/molecules25040904>
- An, W. F., & Tolliday, N. (2010). Cell-based assays for high-throughput screening. *Molecular Biotechnology*, 45(2), 180–186. <https://doi.org/10.1007/s12033-010-9251-z>
- Ancelle, T., Paugam, A., Bourlioux, F., Merad, A., & Vigier, J. (1997). Detection of trypanosomes in blood by the Quantitative Buffy Coat (QBC) technique: experimental evaluation. *Medicine Tropicale*, 57(3), 245–248.
- Andrade, E. L., Bento, A. F., Cavalli, J., Oliveira, S. K., Freitas, C. S., Marcon, R., Schwanke, R. C., Siqueira, J. M., & Calixto, J. B. (2016). Non-clinical studies required for new drug development – Part I: early in silico and in vitro studies , new target discovery and validation , proof of principles and robustness of animal studies. *Brazilian Journal of Medical and Biological Research*, 49, 1–9. <https://doi.org/10.1590/1414-431X20165644>
- Angara, T.-E. , Ismail, A., & Ibrahim, A. (2012). An Overview on the Economic Impacts of Animal Trypanosomiasis. *Global Journal for Research Analysis*, 3, 275–276.
- ANOFEL. (2014). *Parasitologie médicale. Généralités et définitions*.
- Ashburn, T. T., & Thor, K. B. (2004). Drug repositioning: Identifying and developing new uses for existing drugs. *Nature Reviews Drug Discovery*, 3(8), 673–683. <https://doi.org/10.1038/nrd1468>
- Atouguia, J. L. M., & Kennedy, P. G. E. (2000). Neurological aspects of human African trypanosomiasis. In L. E. David & P. G. E. Kennedy (Eds.), *Infectious Diseases of the Nervous System* (pp. 321–372). Butterworth-Heinemann.
- Auty, H., Torr, S. J., Michoel, T., Jayaraman, S., & Morrison, L. J. (2015). Cattle trypanosomosis : the diversity of trypanosomes and implications for disease epidemiology and control Trypanosome species of relevance to cattle. *Revue Scientifique et Technique-Office International Des Epizooties*, 34(2), 587–598.
- Bailey, S. W., & Ayling, J. E. (2009). The extremely slow and variable activity of dihydrofolate reductase in human liver and its implications for high folic acid intake. *PNAS*, 106(36), 15424–15429. <https://doi.org/10.1073/pnas.0902072106>

- Balani, S., Miwa, G., Gan, L.-S., Wu, J.-T., & Lee, F. (2005). Strategy of Utilizing In Vitro and In Vivo ADME Tools for Lead Optimization and Drug Candidate Selection. *Current Topics in Medicinal Chemistry*, 5(11), 1033–1038. <https://doi.org/10.2174/156802605774297038>
- Baral, T. N. (2010). Immunobiology of African Trypanosomes: Need of Alternative Interventions. *Journal of Biomedicine and Biotechnology*, 2010:38915(389153), 1–24. <https://doi.org/10.1155/2010/389153>
- Barrett, M. P., Burchmore, R. J. S., Stich, A., Lazzari, J. O., Frasc, A. C., Cazzulo, J. J., & Sanjeev, K. (2003). The trypanosomiasis. *The Lancet*, Vol 362.
- Barry, J., & Emery, D. L. (1984). Parasite development and host responses during the establishment of *Trypanosoma brucei* infection transmitted by tsetse fly. *Parasitology*, 88(1), 67–84. <https://doi.org/10.1017/S0031182000054354>
- Battista, T., Colotti, G., Ilari, A., & Fiorillo, A. (2020). Targeting trypanothione reductase, a key enzyme in the redox trypanosomatid metabolism, to develop new drugs against leishmaniasis and trypanosomiasis. *Molecules*, 25(8). <https://doi.org/10.3390/molecules25081924>
- Berman, M. H., Westbrook, J., Zukang, F., Gilliland, G., Bhat, T. N., Weissig, H., Shindyalov, L. N., & Bourne, E. P. (2000). The Protein Data Bank. *Nucleic Acids Research*, 28(1), 1–8. <https://doi.org/10.1093/nar/28.1.235>
- Berman, J. D., King, M., Edwards, N. (1989). Antileishmanial Activities of 2,4-Diaminoquinazoline Putative Dihydrofolate Reductase Inhibitors. *Antimicrobial Agents And Chemotherapy*, 11(33), 1860-1863
- Berriman, M., Ghedin, E., Hertz-Fowler, C., Blandin, G., Renault, H., Bartholomeu, D. C., Lennard, N. J., Caler, E., Hamlin, N. E., Haas, B., Böhme, U., Hannick, L., Aslett, M. A., Shallom, J., Marcello, L., Hou, L., Wickstead, B., Alsmark, U. C. M., Arrowsmith, C., ... El-Sayed, N. M. (2005). The genome of the African trypanosome *Trypanosoma brucei*. *Science*, 309(5733), 416–422. <https://doi.org/10.1126/science.1112642>
- Biéler, S., Matovu, E., Mitashi, P., Ssewanyana, E., Bi Shamamba, S. K., Bessell, P. R., & Ndung'u, J. M. (2012). Improved detection of *Trypanosoma brucei* by lysis of red blood cells, concentration and LED fluorescence microscopy. *Acta Tropica*, 121(2), 135–140. <https://doi.org/10.1016/j.actatropica.2011.10.016>
- Bouteille, B., & Buguet, A. (2012). The detection and treatment of human African trypanosomiasis. *Research and Reports in Tropical Medicine*, 3, 35–45.
- Bowling, T., Mercer, L., Don, R., Jacobs, R., & Nare, B. (2012). Application of a resazurin-based high-throughput screening assay for the identification and progression of new treatments for human african trypanosomiasis. *International Journal for Parasitology: Drugs and Drug Resistance*, 2, 262–270. <https://doi.org/10.1016/j.ijpddr.2012.02.002>
- Bozina, N., Bradamante, V., & Lovric, M. (2009). Genetic polymorphism of metabolic enzymes p450 ( cyp ) as a susceptibility factor for drug response , toxicity ,. *Arh Hig Rada Toksikol*, 60, 217–242. <https://doi.org/10.2478/10004-1254-60-2009-1885>
- Bradford, M. M. (1976). A rapid and sensitive method for the quantitation of microgram quantities of protein utilizing the principle of protein-dye binding. *Analytical Biochemistry*, 72, 248–254. [https://doi.org/10.1016/0003-2697\(76\)90527-3](https://doi.org/10.1016/0003-2697(76)90527-3)

- Brand, S., Cleghorn, L. A. T., McElroy, S. P., Robinson, D. A., Smith, V. C., Hallyburton, I., Harrison, J. R., Norcross, N. R., Spinks, D., Bayliss, T., Norval, S., Stojanovski, L., Torrie, L. S., Frearson, J. A., Brenk, R., Fairlamb, A. H., Ferguson, M. A. J., Read, K. D., Wyatt, P. G., & Gilbert, I. H. (2012). Discovery of a novel class of orally active trypanocidal N-Myristoyltransferase inhibitors. *Journal of Medicinal Chemistry*, *55*(1), 140–152. <https://doi.org/10.1021/jm201091t>
- Brien, J. O., Wilson, I., Orton, T., & Pognan, Ę. (2000). *Investigation of the Alamar Blue (resazurin) fluorescent dye for the assessment of mammalian cell cytotoxicity*. 5426, 5421–5426.
- Brun, R., Blum, J., Chappuis, F., & Burri, C. (2010). Human African trypanosomiasis. *The Lancet*, *375*(9709), 148–159. [https://doi.org/10.1016/S0140-6736\(09\)60829-1](https://doi.org/10.1016/S0140-6736(09)60829-1)
- Buguet, A., Bisser, S., Josenando, T., Chapotot, F., & Cespuglio, R. (2005). Sleep structure: A new diagnostic tool for stage determination in sleeping sickness. *Acta Tropica*, *93*(1), 107–117. <https://doi.org/10.1016/j.actatropica.2004.10.001>
- Bukachi, S. A., Wandibba, S., & Nyamongo, I. K. (2017). The socio-economic burden of human African trypanosomiasis and the coping strategies of households in the South Western Kenya foci. *PLoS Neglected Tropical Diseases*, *11*(10), 1–21. <https://doi.org/10.1371/journal.pntd.0006002>
- Burton, M., Abanobi, C., Wang, K. T., Ma, Y., & Rasche, M. E. (2018). Substrate Specificity Analysis of Dihydrofolate / Dihydromethanopterin Reductase Homologs in Methylotrophic  $\alpha$ -Proteobacteria. *Frontiers in Microbiology*, *9*(October), 1–12. <https://doi.org/10.3389/fmicb.2018.02439>
- Büscher, P., Cecchi, G., Jamonneau, V., & Priotto, G. (2017). Human African trypanosomiasis. *The Lancet*, *390*(10110), 2397–2409. [https://doi.org/10.1016/S0140-6736\(17\)31510-6](https://doi.org/10.1016/S0140-6736(17)31510-6)
- Carreras, C. W., & Santi, D. V. (1995). The catalytic mechanism And structure of Thymidylate synthase. *Annual Review of Biochemistry*, *64*, 721–762.
- Cavalli, A., Lizzi, F., Bongarzone, S., Belluti, F., Piazzini, L., & Bolognesi, M. L. (2010). Complementary medicinal chemistry-driven strategies toward new antitrypanosomal and antileishmanial lead drug candidates. *FEMS Immunology and Medical Microbiology*, *58*(1), 51–60. <https://doi.org/10.1111/j.1574-695X.2009.00615.x>
- Center for Disease Control and prevention. (2020). *Parasites - African Trypanosomiasis (also known as Sleeping Sickness)*. Global Health, Division of Parasitic Diseases and Malaria, March 9, 2020. <https://www.cdc.gov/parasites/sleepingsickness/biology.html>
- Chappuis, F., Loutan, L., Simarro, P., Lejon, V., & Büscher, P. (2005). Options for field diagnosis of human African trypanosomiasis. *Clinical Microbiology Reviews*, *18*(1), 133–146. <https://doi.org/10.1128/CMR.18.1.133-146.2005>
- Checchi, F., Filipe, J. A. N., Haydon, D. T., Chandramohan, D., & Chappuis, F. (2008). Estimates of the duration of the early and late stage of gambiense sleeping sickness. *BMC Infectious Diseases*, *8*, 1–10. <https://doi.org/10.1186/1471-2334-8-16>
- Choi, S. B., Yap, B. K., Choong, Y. S., & Wahab, H. (2018). Molecular dynamics simulations in drug discovery. *Encyclopedia of Bioinformatics and Computational Biology: ABC of Bioinformatics*, *1–3*, 652–665. <https://doi.org/10.1016/B978-0-12-809633-8.20154-4>
- Chong, C. R., Chen, X., Shi, L., Liu, J. O., & Sullivan, D. J. (2006). *A clinical drug library*

- screen identifies astemizole as an antimalarial agent. 2(8). <https://doi.org/10.1038/nchembio806>
- Chowdhury, A. R., Bakshi, R., Wang, J., Yildirim, G., Liu, B., Pappas-Brown, V., Tolun, G., Griffith, J. D., Shapiro, T. A., Jensen, R. E., & Englund, P. T. (2010). The killing of African trypanosomes by ethidium bromide. *PLoS Pathogens*, 6(12). <https://doi.org/10.1371/journal.ppat.1001226>
- Claes, F., Buscher, P., Touratier, L., & Goddeeris, B. M. (2005). Trypanosoma equiperdum: master of disguise or historical mistake? *Trends in Parasitology*, 21(316–321).
- Clarkson, A. B., Bienen, E. J., Pollakis, G., & Grady, R. W. (1989). Respiration of bloodstream forms of the parasite Trypanosoma brucei brucei is dependent on a plant-like alternative oxidase. *Journal of Biological Chemistry*, 264(30), 17770–17776. [https://doi.org/10.1016/s0021-9258\(19\)84639-2](https://doi.org/10.1016/s0021-9258(19)84639-2)
- Courtin, D., Berthier, D., Thevenon, S., Dayo, G. K., Garcia, A., & Bucheton, B. (2008). Host genetics in African trypanosomiasis. *Infection, Genetics and Evolution*, 8(3), 229–238. <https://doi.org/10.1016/j.meegid.2008.02.007>
- Darvas, F., Keseru, G., Papp, A., Dorman, G., Urge, L., & Krajcsi, P. (2002). In Silico and Ex Silico ADME Approaches for Drug Discovery. *Current Topics in Medicinal Chemistry*, 2(12), 1287–1304. <https://doi.org/10.2174/1568026023392841>
- Davis, R. L. (2020). Mechanism of Action and Target Identification: A Matter of Timing in Drug Discovery. *IScience*, 23(9), 101487. <https://doi.org/10.1016/j.isci.2020.101487>
- Debela, A. (2016). *In vitro and in vivo antitrypanosomal effects of hydromethanolic extracts of Solanum anguivi fruits and Echinops kebericho roots*. Addis-Ababa.
- Delespaux, V., & de Koning, H. P. (2007). Drugs and drug resistance in African trypanosomiasis. *Drug Resistance Updates*, 10(1–2), 30–50. <https://doi.org/10.1016/j.drug.2007.02.004>
- Delespaux, V., Vitouley, H. S., Marcotty, T., Speybroeck, N., Berkvens, D., Roy, K., Geerts, S., & van den Bossche, P. (2010). Chemosensitization of Trypanosoma congolense strains resistant to isometamidium chloride by tetracyclines and enrofloxacin. *PLoS Neglected Tropical Diseases*, 4(9). <https://doi.org/10.1371/journal.pntd.0000828>
- Desquesnes, M., Dargantes, A., Lai, D. H., Lun, Z. R., Holzmuller, P., & Jittapalapong, S. (2013). Trypanosoma evansi and surra: a review and perspectives on transmission, epidemiology and control, impact, and zoonotic aspects. *Biomed Research International*, 321237. <https://doi.org/doi:10.1155/2013/321237>.
- Desquesnes, M., & Dia, M. L. (2003). Mechanical transmission of Trypanosoma congolense in cattle by the African tabanid Atylotus agrestis. *Experimental Parasitology*, 105(3–4), 226–231. <https://doi.org/10.1016/j.exppara.2003.12.014>
- Desquesnes, M., & Dia, M. L. (2004). Mechanical transmission of Trypanosoma vivax in cattle by the African tabanid Atylotus fuscipes. *Veterinary Parasitology*, 119(1), 9–19. <https://doi.org/10.1016/j.vetpar.2003.10.015>
- Devi, R. V., Sathya, S. S., & Coumar, M. S. (2015). Evolutionary algorithms for de novo drug design - A survey. *Applied Soft Computing Journal*, 27, 543–552. <https://doi.org/10.1016/j.asoc.2014.09.042>

- Ding, D., Zhao, Y., Meng, Q., Xie, D., Nare, B., Chen, D., Bacchi, C. J., Yarlett, N., Zhang, Y. K., Hernandez, V., Xia, Y., Freund, Y., Abdulla, M., Ang, K. H., Ratnam, J., McKerrow, J. H., Jacobs, R. T., Zhou, H., & Plattner, J. J. (2010). Discovery of novel benzoxaborole-based potent antitrypanosomal agents. *ACS Medicinal Chemistry Letters*, 1(4), 165–169. <https://doi.org/10.1021/ml100013s>
- Dormeyer, M., Schöneck, R., Dittmar, G. A. G., & Krauth-Siegel, R. L. (1997). Cloning, sequencing and expression of ribonucleotide reductase R2 from *Trypanosoma brucei*. *FEBS Letters*, 414(2), 449–453. [https://doi.org/10.1016/S0014-5793\(97\)01036-3](https://doi.org/10.1016/S0014-5793(97)01036-3)
- Duffy, S., Sykes, M. L., Jones, A. J., Shelper, T. B., Simpson, M., Lang, R., Poulsen, S. A., Sleebs, B. E., & Avery, V. M. (2017). Screening the medicines for malaria venture pathogen box across multiple pathogens reclassifies starting points for open-source drug discovery. *Antimicrobial Agents and Chemotherapy*, 61(9), 1–22. <https://doi.org/10.1128/AAC.00379-17>
- Elisabet, V. (2019). *Drug discovery against leishmaniasis: Bio- and chemoinformatic guided strategies for target evaluation and hit identification*. Uppsala.
- Engstler, M., Pfohl, T., Herminghaus, S., Boshart, M., Wiegertjes, G., Heddergott, N., & Overath, P. (2007). Hydrodynamic Flow-Mediated Protein Sorting on the Cell Surface of Trypanosomes. *Cell*, 131(3), 505–515. <https://doi.org/10.1016/j.cell.2007.08.046>
- Essmann, U., Perera, L., Berkowitz, M. L., Darden, T., Lee, H., & Pedersen, L. G. (1995). A smooth particle mesh Ewald method. *The Journal of Chemical Physics*, 103(19), 8577–8593. <https://doi.org/10.1063/1.470117>
- Eyford, B. A. (2013). *Protein Discovery in African Trypanosomes: Studying Differential Protein Expression Throughout the Parasite life Cycle and Identification of Candidate Biomarkers for Diagnosing Trypanosome Infections*. University of Victoria.
- Fairlamb, A. H. (1977). *the Isolation Particulate and Characterisation From*. 8.
- Fairlamb, A. H. (2003). Chemotherapy of human African trypanosomiasis: Current and future prospects. *Trends in Parasitology*, 19(11), 488–494. <https://doi.org/10.1016/j.pt.2003.09.002>
- Faria, J., Moraes, C. B., Song, R., Pascoalino, B. S., Lee, N., Siqueira-Neto, J. L., Cruz, D. J. M., Parkinson, T., Ioset, J. R., Cordeiro-Da-Silva, A., & Freitas-Junior, L. H. (2015). Drug discovery for human African trypanosomiasis: Identification of novel scaffolds by the newly developed HTS SYBR green assay for *trypanosoma brucei*. *Journal of Biomolecular Screening*, 20(1), 70–81. <https://doi.org/10.1177/1087057114556236>
- Feldmann, U., Dyck, V., Mattioli, R., & Jannin, J. (2005). Potential impact of tsetse fly control involving the sterile insect technique. In V. Dyck, J. Hendrichs, & A. Robinson (Eds.), *Sterile insect technique. Principles and practice in area-wide integrated pest management*. (pp. 701-723.). Springer.
- Ferreira, L. G., & Andricopulo, A. D. (2016). Drug repositioning approaches to parasitic diseases: a medicinal chemistry perspective. In *Drug Discovery Today* (Vol. 21, Issue 10). Elsevier Ltd. <https://doi.org/10.1016/j.drudis.2016.06.021>
- Field, M. C., Horn, D., Fairlamb, A. H., Ferguson, M. A. J., Gray, D. W., Read, K. D., Rycker, M. De, Torrie, L. S., Wyatt, P. G., Wyllie, S., & Gilbert, I. H. (2017). Anti-trypanosomatid drug discovery: an ongoing challenge and a continuing need. *Nature Reviews*

- Microbiology*, 15, 217–231. <https://doi.org/10.1038/nrmicro.2016.193>
- Finelle, P. (1983). *African animal trypanosomiasis*. In: *World Animal Review*. Food and Agriculture Organization of the United Nations.
- Fontecave, M., Gräslund, A., & Reichard, P. (1987). The function of superoxide dismutase during the enzymatic formation of the free radical of ribonucleotide reductase. *Journal of Biological Chemistry*, 262(25), 12332–12336. [https://doi.org/10.1016/s0021-9258\(18\)45357-4](https://doi.org/10.1016/s0021-9258(18)45357-4)
- Food and Agriculture Organization. (2022). *Programme Against African Trypanosomiasis (PAAT): The Disease*. <https://www.fao.org/paat/the-programme/the-disease/en/>
- Food and Agriculture Organization and the World health organization. (2022). Vector control and the elimination of gambiense human African trypanosomiasis (HAT) -
- Joint FAO/WHO Virtual Expert Meeting - 5-6 October 2021. PAAT Meeting Report Series. No. 1. Rome.
- <https://doi.org/10.4060/cc0178en>
- Franco, J. R., Simarro, P. P., Diarra, A., & Jannin, J. G. (2014). Epidemiology of human African trypanosomiasis. *Clinical Epidemiology*, 6(1), 257–275. <https://doi.org/10.2147/CLEP.S39728>
- Gaba, M., Punam, G., Sarbjot, S., & Gupta, G. (2015). An overview on Molecular Docking International Journal of Drug Development & Research ISSN 0975-9344 Available online <http://www.ijddr.com> Review Paper. *International Journal of Drug Development & Research*, 2(February 2010), 2.
- Garfin, D. E. (1990). One-dimensional gel electrophoresis. *Methods in Enzymology*, 182, 425–441. [https://doi.org/10.1016/0076-6879\(90\)82035-Z](https://doi.org/10.1016/0076-6879(90)82035-Z)
- Geerts, S., Holmes, P. H., Diall, O., & Eisler, M. C. (2001). African bovine trypanosomiasis: The problem of drug resistance. *Parasitology Today*, 17(1), 25–28. [https://doi.org/10.1016/S0169-4758\(00\)01827-5](https://doi.org/10.1016/S0169-4758(00)01827-5)
- George, T. G., Endeshaw, M. M., Rachel E. Morgan, Mahasenan, K. V., Delfín, D. A., Mukherjee, M. S., Yakovich, A. J., Fotie, J., Li, C., & Werbovetz, A. K. (2007). Synthesis, Biological Evaluation, and Molecular Modeling of 3,5- Substituted-N1-phenyl-N4, N4-di-n-butylsulfanilamides as Antikinetoplastid Antimicrotubule Agents. *Bioorg Med Chem*, 15(18), 1–18.
- Gibson, M. W., Dewar, S., Ong, H. B., Sienkiewicz, N., & Fairlamb, A. H. (2016). Trypanosoma brucei DHFR-TS Revisited: Characterisation of a Bifunctional and Highly Unstable Recombinant Dihydrofolate Reductase-Thymidylate Synthase. *PLoS Neglected Tropical Diseases*, 10(5), 1–20. <https://doi.org/10.1371/journal.pntd.0004714>
- Giordani, F., Morrison, L. J., Rowan, T. G., De Koning, H. P., & Barrett, M. P. (2016). The animal trypanosomiasis and their chemotherapy: A review. *Parasitology*, 143(14), 1862–1889. <https://doi.org/10.1017/S0031182016001268>
- Hall, B. S., Bot, C., & Wilkinson, S. R. (2011). Nifurtimox activation by trypanosomal type I nitroreductases generates cytotoxic nitrile metabolites. *Journal of Biological Chemistry*, 286(15), 13088–13095. <https://doi.org/10.1074/jbc.M111.230847>

- Hall, M., & Wall, R. (2004). Biting flies: their role in the mechanical transmission of trypanosomes to livestock and methods for their control. In I. Maudlin, P. H. Holmes, & M. A. Miles (Eds.), *The Trypanosomiases* (pp. 583–594). CABI Publishing.
- Hameed, N. H. (2019). *An evaluation of the antiparasitic activities of a novel natural product and open-access Pathogen Box libraries*. Keele University.
- Hargrove, J. (2003). Tsetse eradication: sufficiency, necessity and desirability. In: Research report, DFID Animal Health Programme., *Tsetse Eradication: Sufficiency, Necessity and Desirability*.
- Hargrove, J., Torr, S. J., & Kindness, H. M. (2003). Insecticide-treated cattle against tsetse (Diptera: Glossinidae): what governs success? *Bulletin of Entomological Research*, 93(3), 203–217. <https://doi.org/10.1079/ber2003234>
- Hennessey, K. M., Rogiers, I. C., Shih, H. W., Hulverson, M. A., Choi, R., McCloskey, M. C., Whitman, G. R., Barrett, L. K., Merritt, E. A., Paredes, A. R., & Ojo, K. K. (2018). Screening of the Pathogen Box for inhibitors with dual efficacy against *Giardia lamblia* and *Cryptosporidium parvum*. *PLoS Neglected Tropical Diseases*, 12(8), 1–16. <https://doi.org/10.1371/journal.pntd.0006673>
- Henry, M. C., P. K., Ruppel, J., Bruneel, H., & Claes, Y. (1981). Evaluation of field diagnosis of trypanosomiasis caused by *Trypanosoma brucei gambiense*. *Annales de La Société Belge de Médecine Tropicale*, 61:79-92.
- Hernández-Santoyo, A., Tenorio-Barajas, A. Y., Altuzar, V., Vivanco-Cid, H., & Mendoza-Barrera, C. (2013). Protein-Protein and Protein-Ligand Docking. In *Protein Engineering - Technology and Application* (pp. 63–81). Intech Open Science. <https://doi.org/10.5772/56376>
- Herrero, M., Grace, D., Njuki, J., Johnson, N., Enahoro, D., Silvestri, S., & Rufino, M. C. (2013). The roles of livestock in developing countries. *Animal*, 7(SUPPL.1), 3–18. <https://doi.org/10.1017/S1751731112001954>
- Hess, B., Bekker, H., Berendsen, H. J. C., & Fraaije, J. G. E. M. (1997). LINCS: A Linear Constraint Solver for molecular simulations. *Journal of Computational Chemistry*, 18(12), 1463–1472. [https://doi.org/10.1002/\(SICI\)1096-987X\(199709\)18:12<1463::AID-JCC4>3.0.CO;2-H](https://doi.org/10.1002/(SICI)1096-987X(199709)18:12<1463::AID-JCC4>3.0.CO;2-H)
- Heykants, J., & Meuldermans, W. (1993). Nonclinical Kinetics and Metabolism Studies in Support of the Safety Assessment of Drugs. *Therapeutic Innovation & Regulatory Science*, 28(1), 163–172. <https://doi.org/10.1177/009286159402800120>
- Hirumi, H., Doyle, J. J., & Hirumi, K. (1977). Cultivation of bloodstream *Trypanosoma brucei* \*. *Bulletin of the World Health Organization*, 55(2–3), 405–409.
- Hirumi, H., & Hirumi, K. (1989). Continuous cultivation of *Trypanosoma brucei* blood stream forms in a medium containing a low concentration of serum protein without feeder cell layers. *Journal of Parasitology*, 75(6), 985–989. <https://doi.org/10.2307/3282883>
- Hoare, C. (1972). Systematic description of mammalian trypanosomes of Africa. In: *The African Trypanosomiases*. Ed. Mulligan HW. George Allen and Unwin London Ltd., London, pp.222-259.
- Hofer, A., Schmidt, P. P., Gräslund, A., & Thelander, L. (1997). Cloning and characterization of the R1 and R2 subunits of ribonucleotide reductase from *Trypanosoma brucei*.

- Proceedings of the National Academy of Sciences of the United States of America*, 94(13), 6959–6964. <https://doi.org/10.1073/pnas.94.13.6959>
- Holmes, P. (2013). Tsetse-transmitted trypanosomes - Their biology, disease impact and control. *Journal of Invertebrate Pathology*, 112(SUPPL.1), S11–S14. <https://doi.org/10.1016/j.jip.2012.07.014>
- Holt, H. R., Selby, R., Mumba, C., Napier, G. B., & Guitian, J. (2016). Assessment of animal African trypanosomiasis ( AAT ) vulnerability in cattle-owning communities of sub-Saharan Africa. *Parasites & Vectors*, 1–13. <https://doi.org/10.1186/s13071-016-1336-5>
- Hughes, J. P., Rees, S., Kalindjian, S. B., & Philpott, K. L. (2011). Principles of early drug discovery. *British Journal of Pharmacology*, 162, 1239–1249. <https://doi.org/10.1111/j.1476-5381.2010.01127.x>
- Hunter, W. N., Bailey, S., Habash, J., Harrop, S. J., Helliwell, J. R., Aboagye-Kwarteng, T., Smith, K., & Fairlamb, A. H. (1992). Active site of trypanothione reductase. A target for rational drug design. *Journal of Molecular Biology*, 227(1), 322–333. [https://doi.org/10.1016/0022-2836\(92\)90701-K](https://doi.org/10.1016/0022-2836(92)90701-K)
- Iwatsuki, M., Otoguro, K., Ishiyama, A., Namatame, M., Nishihara-Tukashima, A., Hashida, J., Nakashima, T., Masuma, R., Takahashi, Y., Yamada, H., & Ömura, S. (2010). In vitro antitrypanosomal activity of 12 low-molecular-weight antibiotics and observations of structure/activity relationships. *Journal of Antibiotics*, 63(10), 619–622. <https://doi.org/10.1038/ja.2010.99>
- Jackson, A. P., Sanders, M., Berry, A., Mcquillan, J., Aslett, M. A., Quail, M. A., Chukualim, B., Capewell, P., Macleod, A., Melville, S. E., Barry, J. D., Berriman, M., & Hertz-fowler, C. (2010). *The Genome Sequence of Trypanosoma brucei gambiense, Causative Agent of Chronic Human African Trypanosomiasis*. 4(4). <https://doi.org/10.1371/journal.pntd.0000658>
- Jacobs, R. T., Nare, B., Wring, S. A., Orr, M. D., Chen, D., Sligar, J. M., Jenks, M. X., Noe, R. A., Bowling, T. S., Mercer, L. T., Rewerts, C., Gaukel, E., Owens, J., Parham, R., Randolph, R., Beaudet, B., Bacchi, C. J., Yarlett, N., Plattner, J. J., ... Don, R. (2011). Scyx-7158, an orally-active benzoxaborole for the treatment of stage 2 human african trypanosomiasis. *PLoS Neglected Tropical Diseases*, 5(6). <https://doi.org/10.1371/journal.pntd.0001151>
- Jennings, F. W., & Urquhart, G. M. (1983). The use of the 2 substituted 5-nitroimidazole, fexinidazole (Hoe 239) in the treatment of chronic T. brucei infections in mice. *Zeitschrift Für Parasitenkunde Parasitology Research*, 69(5), 577–581. <https://doi.org/10.1007/BF00926669>
- Ji, Z. L., Wang, Y., Yu, L., Han, L. Y., Zheng, C. J., & Chen, Y. Z. (2006). In silico search of putative adverse drug reaction related proteins as a potential tool for facilitating drug adverse effect prediction. *Toxicology Letters*, 164(2), 104–112. <https://doi.org/10.1016/j.toxlet.2005.11.017>
- Jianling Wang; Laszlo Urban. (2004). The impact of early ADME profiling on drug discovery and. *Drug Discovery World Fall*, 73–86.
- Jones, T. W., & Davila, A. M. (2001). Trypanosoma vivax: out of Africa. *Trends in Parasitology*, 17(2), 99–101.

- Kaiser, M., Bray, M. A., Cal, M., Trunz, B. B., Torreele, E., & Brun, R. (2011). Antitrypanosomal activity of fexinidazole, a new oral nitroimidazole drug candidate for treatment of sleeping sickness. *Antimicrobial Agents and Chemotherapy*, *55*(12), 5602–5608. <https://doi.org/10.1128/AAC.00246-11>
- Kasam, K. V. (2009). *In silico drug discovery on computational Grids for finding novel drugs against neglected diseases*. Rheinische Friedrich-Wilhelms-Universität Bonn.
- Kasozi, K. I., MacLeod, E. T., Ntulume, I., & Welburn, S. C. (2022). An Update on African Trypanocide Pharmaceuticals and Resistance. *Frontiers in Veterinary Science*, *9*(March). <https://doi.org/10.3389/fvets.2022.828111>
- Kaufer, A., Ellis, J., Stark, D., & Barratt, J. (2017). The evolution of trypanosomatid taxonomy. *Parasites and Vectors*, *10*(1).
- Kennedy, P. G. E. (2004). Human African trypanosomiasis of the CNS: current issues and challenges. *Journal of Clinical Investigation*, *113*(4), 496–504. <https://doi.org/10.1172/jci21052>
- Kennedy, P. G. E. (2008). The continuing problem of human African trypanosomiasis (sleeping sickness). *Annals of Neurology*, *64*(2), 116–126. <https://doi.org/10.1002/ana.21429>
- Kennedy, P. G. E. (2019). Update on human African trypanosomiasis (sleeping sickness). *Journal of Neurology*, *266*(9), 2334–2337. <https://doi.org/10.1007/s00415-019-09425-7>
- Kerns, E. H., & Di, L. (2008). Drug-like Properties: Concepts, Structure Design and Methods. *Drug-like Properties: Concepts, Structure Design and Methods*.
- Khabnadideh, S., Pez D., Musso, A., Brun, R., Pérez, L. M. R., González-Pacanowskac, D., Ian, G. H. (2005). Design, synthesis and evaluation of 2,4-diaminoquinazolines as inhibitors of trypanosomal and leishmanial dihydrofolate reductase. *Bioorganic and Medicinal Chemistry*, *13*, 2637–2649. doi:10.1016/j.bmc.2005.01.025
- Khachaturian, Z. S. (2002). Models and modeling systems in Alzheimer disease drug discovery. *Alzheimer Disease and Associated Disorders*, *16*(SUPPL. 1). <https://doi.org/10.1097/00002093-200200001-00002>
- Kharkar, P. S., Warriar, S., & Gaud, R. S. (2014). Reverse docking: A powerful tool for drug repositioning and drug rescue. *Future Medicinal Chemistry*, *6*(3), 333–342. <https://doi.org/10.4155/fmc.13.207>
- Kioy, D., Jannin, J., & Mattock, N. (2004). Human African trypanosomiasis. *Nature Reviews Microbiology*, *2*(3), 186–187. <https://doi.org/10.1038/nrmicro848>
- Kitchen, D. B., Decornez, H., Furr, J. R., & Bajorath, J. (2004). Docking and scoring in virtual screening for drug discovery: Methods and applications. *Nature Reviews Drug Discovery*, *3*(11), 935–949. <https://doi.org/10.1038/nrd1549>
- Koh, J. T. (2003). Making virtual screening a reality. *Proceedings of the National Academy of Sciences of the United States of America*, *100*(12), 6902–6903. <https://doi.org/10.1073/pnas.1332743100>
- Krieger, S., Schwarz, W., Arlyanayagam, M. R., Fairlamb, A. H., Krauth-Siegel, R. L., & Clayton, C. (2000). Trypanosomes lacking trypanothione reductase are avirulent and show increased sensitivity to oxidative stress. *Molecular Microbiology*, *35*(3), 542–552. <https://doi.org/10.1046/j.1365-2958.2000.01721.x>

- Krinsky, W. L. (2002). TSETSE FLIES ( Glossinidae ). *Medical and Veterinary Entomology*, 1971, 303–316.
- Kristensson, K., Masocha, W., & Bentivoglio, M. (2013). Mechanisms of CNS invasion and damage by parasites. *Handbook of Clinical Neurology*, 11(22). <https://doi.org/doi:10.1016/b978-0-444-53490-3.00002-9>
- Krüger, A., Gonçalves Maltarollo, V., Wrenger, C., & Kronenberger, T. (2020). ADME Profiling in Drug Discovery and a New Path Paved on Silica. *Drug Discovery and Development - New Advances*. <https://doi.org/10.5772/intechopen.86174>
- Kubota, K., Funabashi, M., & Ogura, Y. (2019). Target deconvolution from phenotype-based drug discovery by using chemical proteomics approaches. *Biochimica et Biophysica Acta - Proteins and Proteomics*, 1867(1), 22–27. <https://doi.org/10.1016/j.bbapap.2018.08.002>
- Kutzner, C., Páll, S., Fechner, M., Esztermann, A., de Groot, B. L., & Grubmüller, H. (2019). More bang for your buck: Improved use of GPU nodes for GROMACS 2018. *Journal of Computational Chemistry*, 40(27), 2418–2431. <https://doi.org/10.1002/jcc.26011>
- Lagorce, D., Douguet, D., Miteva, M. A., & Villoutreix, B. O. (2017). Computational analysis of calculated physicochemical and ADMET properties of protein- protein interaction inhibitors. *Scientific Reports*, 7(March), 1–15. <https://doi.org/10.1038/srep46277>
- Lai, D. H., Hashimi, H., Lun, Z. R., Ayala, F. J., & Lukes, J. (2008). Adaptations of *Trypanosoma brucei* to gradual loss of kinetoplast DNA: *Trypanosoma equiperdum* and *Trypanosoma evansi* are petite mutants of *T. brucei*. *Proceedings of the National Academy of Sciences of the United States of America*, 105(6)(1999–2004).
- Le Trant, N., Meshnick, S. R., Kitchener, K., Eaton, J. W., & Cerami, A. (1983). Iron-containing superoxide dismutase from *Crithidia fasciculata*. Purification, characterization, and similarity to Leishmanial and trypanosomal enzymes. *Journal of Biological Chemistry*, 258(1), 125–130. [https://doi.org/10.1016/s0021-9258\(18\)33229-0](https://doi.org/10.1016/s0021-9258(18)33229-0)
- Lejon, V., & Büscher, P. (2005). Review Article : Cerebrospinal fluid in human African trypanosomiasis : a key to diagnosis , therapeutic decision and post-treatment follow-up. *Tropical Medicine and International Health*, 10(5), 395–403.
- Levine, R. A., Wardlaw, S. C., & Patton, C. L. (1989). Detection of haematoparasites using quantitative buffy coat analysis tubes. *Parasitology Today*, 5(4), 132–134. [https://doi.org/10.1016/0169-4758\(89\)90056-2](https://doi.org/10.1016/0169-4758(89)90056-2)
- Li, A. P. (2001). Screening for human ADME/Tox drug properties in drug discovery. *Drug Discovery Today*, 6(7), 357–366. [https://doi.org/10.1016/S1359-6446\(01\)01712-3](https://doi.org/10.1016/S1359-6446(01)01712-3)
- Li, A. P. (2005). Preclinical in vitro screening assays for drug-like properties. *Drug Discovery Today: Technologies*, 2(2), 179–185. <https://doi.org/10.1016/j.ddtec.2005.05.024>
- Lim, L. E., Vilchèze, C., Ng, C., Jacobs, W. R., Ramón-garcía, S., & Thompson, J. (2013). Anthelmintic Avermectins Kill Mycobacterium tuberculosis, Including Multidrug-Resistant Clinical Strains. *Antimicrobial Agents and Chemotherapy*, 57(2), 1040–1046. <https://doi.org/10.1128/AAC.01696-12>
- Lindner, A. K., Lejon, V., Chappuis, F., Seixas, J., Kazumba, L., Barrett, M. P., Mwamba, E., Erphas, O., & Akl, E. A. (2019). Review New WHO guidelines for treatment of gambiense human African trypanosomiasis including fexinidazole : substantial changes for clinical practice. 3099(19), 1–9. [https://doi.org/10.1016/S1473-3099\(19\)30612-7](https://doi.org/10.1016/S1473-3099(19)30612-7)

- Lipinski, C. A. (2000). Drug-like properties and the causes of poor solubility and poor permeability. *Journal of Pharmacological and Toxicological Methods*, 44(1), 235–249. [https://doi.org/10.1016/S1056-8719\(00\)00107-6](https://doi.org/10.1016/S1056-8719(00)00107-6)
- Magnus, E., Vervoort, T., & Van Meirvenne, N. (1978). A card-agglutination test with stained trypanosomes (C.A.T.T.) for the serological diagnosis of *T. b. gambiense* trypanosomiasis. In *Annales de la Societe Belge de Medecine Tropicale* (Vol. 58, Issue 3, pp. 169–176).
- Mamoudou, A., Delespaux, V., Chepnda, V., Hachimou, Z., Andrikaye, J. P., Zoli, A., & Geerts, S. (2008). Assessment of the occurrence of trypanocidal drug resistance in trypanosomes of naturally infected cattle in the Adamaoua region of Cameroon using the standard mouse test and molecular tools. *Acta Tropica*, 106(2), 115–118. <https://doi.org/10.1016/j.actatropica.2008.02.003>
- Matthews, K. R. (2005). The developmental cell biology of *Trypanosoma brucei*. *Journal of Cell Science*, 118(2), 283–290. <https://doi.org/10.1242/jcs.01649>
- Matthews, K. R., Ellis, J. R., & Paterou, A. (2004). Molecular regulation of the life cycle of African trypanosomes. *Trends in Parasitology*, 20(1), 40–47. <https://doi.org/10.1016/j.pt.2003.10.016>
- Matthews, N. (2019). *Interactive Molecular Docking with Haptics and Advanced Graphics*. University of East Anglia.
- Medicines for Malaria Venture. (2022a). *MMV Open*. <https://www.mmv.org/mmv-open>
- Medicines for Malaria Venture. (2022b). *The Pathogen Box*. <https://www.mmv.org/mmv-open/archived-projects/pathogen-box>
- Mekata, H., Konnai, S., Witola, W. H., Inoue, N., Onuma, M., & Ohashi, K. (2009). Molecular detection of trypanosomes in cattle in South America and genetic diversity of *Trypanosoma evansi* based on expression-site-associated gene 6. *Infection, Genetic and Evolution*, 9 (6)(1301–1305).
- Meng, X.-Y., Zhang, H.-X., Mezei, M., & Cui, M. (2012). Molecular Docking: A Powerful Approach for Structure-Based Drug Discovery. *Current Computer Aided-Drug Design*, 7(2), 146–157. <https://doi.org/10.2174/157340911795677602>
- Meyer, A., Holt, H. R., Selby, R., & Guitian, J. (2016). *Past and Ongoing Tsetse and Animal Trypanosomiasis Control Operations in Five African Countries : A Systematic Review*. 1–29. <https://doi.org/10.1371/journal.pntd.0005247>
- Mishra, G. (2013). *Estimation of new chemical entities in biological fluids for bioavailability and it's pharmacokinetic evaluation To screen the suitable lead candidate*. Hamdard University, Faculty of Pharmacy.
- Moffat, J. G., Vincent, F., Lee, J. A., Eder, J., & Prunotto, M. (2017). Opportunities and challenges in phenotypic drug discovery: An industry perspective. *Nature Reviews Drug Discovery*, 16(8), 531–543. <https://doi.org/10.1038/nrd.2017.111>
- Molyneux, D., Pentreath, V., & Doua, F. (1996). *African trypanosomiasis in man. Manson's Tropical Diseases*. (G. Cook (ed.); In Manson'). WB Saunder company.
- Morris, G. M., Huey, R., Lindstrom, W., Sanner, M. F., Belew, richard K., Goodsell, D. S., & Olson, A. J. (2009). Software News and Updates Gabedit — AutoDock4 and

- AutoDockTools4: Automated Docking with Selective Receptor Flexibility. *Journal of Computational Chemistry*, 30(16), 2785–2791. <https://doi.org/10.1002/jcc.21256>
- Mouchlis, V. D., Afantitis, A., Serra, A., Fratello, M., Papadiamantis, A. G., Aidinis, V., Lynch, I., Greco, D., & Melagraki, G. (2021). Advances in De Novo Drug Design: From Conventional to Machine Learning Methods. *International Journal of Molecular Science*, 22.
- Myburgh, E., Coles, J. A., Ritchie, R., Kennedy, P. G. E., McLatchie, A. P., Rodgers, J., Taylor, M. C., Barrett, M. P., Brewer, J. M., & Mottram, J. C. (2013). In vivo imaging of trypanosome-brain interactions and development of a rapid screening test for drugs against CNS stage trypanosomiasis. *PLoS Neglected Tropical Diseases*, 7(8). <https://doi.org/10.1371/journal.pntd.0002384>
- Nagle, P. S., Rodriguez, F., Nguyen, B., Wilson, W. D., & Rozas, I. (2012). High DNA affinity of a series of peptide linked diaromatic guanidinium-like derivatives. *Journal of Medicinal Chemistry*, 55(9), 4397–4406. <https://doi.org/10.1021/jm300296f>
- Nare, B., Hardy, L. W., & Beverley, S. M. (1997). The Roles of Pteridine Reductase 1 and Dihydrofolate Reductase-Thymidylate Synthase in Pteridine Metabolism in the Protozoan Parasite *Leishmania major* The Roles of Pteridine Reductase 1 and Dihydrofolate Reductase-Thymidylate Synthase in Pteridine Metabolism. *The Journal of Biological Chemistry*, 272(November 2016), 13883–13891. <https://doi.org/10.1074/jbc.272.21.13883>
- Nelson, R. G. (2001). *Dicyclic and Tricyclic Diaminopyrimidine Derivatives as Potent Inhibitors of Cryptosporidium parvum Dihydrofolate Reductase: Structure-Activity and Structure-Selectivity Correlations*. 45(12), 3293–3303. <https://doi.org/10.1128/AAC.45.12.3293>
- Nnadi, C. O., Ebiloma, G. U., Black, J. A., Nwodo, N. J., Lemgruber, L., Schmidt, T. J., & De Koning, H. P. (2019). Potent antitrypanosomal activities of 3-aminosteroids against African trypanosomes: Investigation of cellular effects and of cross-resistance with existing drugs. *Molecules*, 24(2). <https://doi.org/10.3390/molecules24020268>
- Odiit, M., Kansime, F., & Enyaru, J. (1997). Duration of symptoms and case fatality of sleeping sickness caused by *Trypanosoma brucei rhodesiense* in Tororo, Uganda. *East African Medical Journal*, 74(12), 792–795.
- Oliveira, M. P. V. (2012). *Drug screening of Bisnaphthalimidopropyl derivatives on Trypanosoma brucei*. University of Lisbon, faculty of sciences.
- Oztas, D. Y. (2021). *Drug Repurposing for COVID-19 Using Molecular Docking*. Chapman University.
- Padhy, B., & Gupta, Y. (2011). Drug repositioning: re-investigating existing drugs for new therapeutic indications. *Journal of Postgraduate Medicine*, 57(2), 153–160.
- Paguem, A., Abanda, B., Ndjonka, D., Weber, J. S., Claudine, S., Ngomtcho, H., Manchang, K. T., Adoumoumini, M., Eisenbarth, A., Renz, A., Kelm, S., & Achukwi, M. D. (2019). Widespread co-endemicity of *Trypanosoma* species infecting cattle in the Sudano-Sahelian and Guinea Savannah zones of Cameroon. 1–15.
- Pan, X., Wang, H., Li, C., Zhang, J. Z. H., & Ji, C. (2021). MolGpka: A Web Server for Small Molecule pKa Prediction Using a Graph-Convolutional Neural Network. *Journal of*

- Chemical Information and Modeling*, 61(7), 3159–3165.  
<https://doi.org/10.1021/acs.jcim.1c00075>
- Panchagnula, R., & Thomas, N. S. (2000). Biopharmaceutics and pharmacokinetics in drug research. *International Journal of Pharmaceutics*, 201(2), 131–150.  
[https://doi.org/10.1016/S0378-5173\(00\)00344-6](https://doi.org/10.1016/S0378-5173(00)00344-6)
- Paquet, C., Castilla, J., Mbulamberi, D., Beaulieu, M., & Gastellu-Etchegorry, MG Moren, A. (1995). Trypanosomiasis from *Trypanosoma brucei gambiense* in the center of north-west Uganda. Evaluation of 5 years of control (1987-1991). *Bulletin de La Societe de Pathologie Exotique*, 88(28–41).
- Parrinello, M., & Rahman, A. (1981). Polymorphic transitions in single crystals: A new molecular dynamics method. *Journal of Applied Physics*, 52(12), 7182–7190.  
<https://doi.org/10.1063/1.328693>
- Patra, A. T., Hingamire, T., Belekar, M. A., Xiong, A., Subramanian, G., Bozdech, Z., Preiser, P., Shanmugam, D., & Chandramohanadasa, R. (2020). Whole-Cell Phenotypic Screening of Medicines for Malaria Venture Pathogen Box Identifies Specific Inhibitors of *Plasmodium falciparum* Late-Stage Development and Egress. *Antimicrobial Agents and Chemotherapy*, 64(5), 1–15. <https://doi.org/https://doi.org/10.1128/AAC.01802-19>
- PATTEC. (2000). A continental plan of action for the eradication of Tsetse and trypanosomosis. The OAU pathway for the PATTEC. In *Pan African Tsetse and trypanosomosis Global Veterinaria, Eradication campaign*.
- Patterson, S., Alphey, M. S., Jones, D. C., Shanks, E. J., Street, I. P., Frearson, J. A., Wyatt, P. G., Gilbert, I. H., & Fairlamb, A. H. (2011). Dihydroquinazolines as a novel class of *Trypanosoma brucei* trypanothione reductase inhibitors: Discovery, synthesis, and characterization of their binding mode by protein crystallography. *Journal of Medicinal Chemistry*, 54(19), 6514–6530. <https://doi.org/10.1021/jm200312v>
- Paulrobustelli. (2021). *Force-Fields*. <https://github.com/paulrobustelli/Force-Fields>
- Penchenier, L. (1996). Historique et évolution de la maladie du sommeil au Cameroun. *Bulletin de Liaison Documentaire de l'OCEAC*, 29(3), 23–36.
- Peregrine, A. S., & Mamman, M. (1993). Pharmacology of diminazene: a review. *Acta Tropica*, 54(3–4), 185–203. [https://doi.org/10.1016/0001-706X\(93\)90092-P](https://doi.org/10.1016/0001-706X(93)90092-P)
- Pinzi, L., & Rastelli, G. (2019). Molecular Docking : Shifting Paradigms in Drug Discovery. *International Journal of Molecular Science*, 20. <https://doi.org/10.3390/ijms20184331>
- Pollastri, M. P., & Avenue, H. (2019). Fexinidazole: A New Drug for African Sleeping Sickness on the Horizon. *Trends in Parasitology*, 34(3), 178–179.  
<https://doi.org/10.1016/j.pt.2017.12.002.Fexinidazole>
- Prakash, N., & Devangi, P. (2010). Drug Discovery. *Journal of Antivirals and Antiretrovirals*, 2(4), 063–068. <https://doi.org/10.4172/jaa.1000025>
- Preston, S., Jiao, Y., Jabbar, A., McGee, S. L., Laleu, B., Willis, P., Wells, T. N. C., & Gasser, R. B. (2016). Screening of the ‘Pathogen Box’ identifies an approved pesticide with major anthelmintic activity against the barber’s pole worm. *International Journal for Parasitology: Drugs and Drug Resistance*, 6(3), 329–334.  
<https://doi.org/10.1016/j.ijpddr.2016.07.004>

- Price, H. P., Güther, M. L. S., Ferguson, M. A. J., & Smith, D. F. (2010). Myristoyl-CoA:protein N-myristoyltransferase depletion in trypanosomes causes avirulence and endocytic defects. *Molecular and Biochemical Parasitology*, *169*(1), 55–58. <https://doi.org/10.1016/j.molbiopara.2009.09.006>
- Priotto, G., Kasparian, S., Mutombo, W., Ngouama, D., Ghorashian, S., Arnold, U., Ghabri, S., Baudin, E., Buard, V., Kazadi-Kyanza, S., Ilunga, M., Mutangala, W., Pohlig, G., Schmid, C., Karunakara, U., Torreele, E., & Kande, V. (2009). Nifurtimox-eflornithine combination therapy for second-stage African *Trypanosoma brucei gambiense* trypanosomiasis: a multicentre, randomised, phase III, non-inferiority trial. *The Lancet*, *374*(9683), 56–64. [https://doi.org/10.1016/S0140-6736\(09\)61117-X](https://doi.org/10.1016/S0140-6736(09)61117-X)
- Priya, S. (2015). Design, synthesis, characterization, molecular docking Studies and biological evaluation of benzimidazole Containing 4h-chromen-4-one derivatives [TAMIL NADU DR. M.G.R. MEDICAL University]. In *Syria Studies*. [https://www.researchgate.net/publication/269107473\\_What\\_is\\_governance/link/548173090cf22525dcb61443/download%0Ahttp://www.econ.upf.edu/~reynal/Civilwars\\_12December2010.pdf%0Ahttps://think-asia.org/handle/11540/8282%0Ahttps://www.jstor.org/stable/41857625](https://www.researchgate.net/publication/269107473_What_is_governance/link/548173090cf22525dcb61443/download%0Ahttp://www.econ.upf.edu/~reynal/Civilwars_12December2010.pdf%0Ahttps://think-asia.org/handle/11540/8282%0Ahttps://www.jstor.org/stable/41857625)
- PRONETRY Cameroon. (2010). *Programme National D ' Eradication Des Trypanosomoses Au Cameroun*.
- Raether, W., & Seidenath, H. (1983). The activity of fexinidazole (HOE 239) against experimental infections with *trypanosoma cruzi*, trichomonads and *Entamoeba histolytica*. *Annals of Tropical Medicine and Parasitology*, *77*(1), 13–26. <https://doi.org/10.1080/00034983.1983.11811668>
- Rea, A., Tempone, A. G., Pinto, E. G., Mesquita, J. T., Rodrigues, E., Silva, L. G. M., Sartorelli, P., & Lago, J. H. G. (2013). Soullamarin Isolated from *Calophyllum brasiliense* (Clusiaceae) Induces Plasma Membrane Permeabilization of *Trypanosoma cruzi* and Mitochondrial Dysfunction. *PLoS Neglected Tropical Diseases*, *7*(12), 1–8. <https://doi.org/10.1371/journal.pntd.0002556>
- Reguera, R. M., Calvo-Álvarez, E., Álvarez-Velilla, R., & Balaña-Fouce, R. (2014). Target-based vs. phenotypic screenings in *Leishmania* drug discovery: A marriage of convenience or a dialogue of the deaf? *International Journal for Parasitology: Drugs and Drug Resistance*, *4*(3), 355–357. <https://doi.org/10.1016/j.ijpddr.2014.05.001>
- Reid, S. A. (2002). *Trypanosoma evansi* control and containment in Australasia. *Trends in Parasitology*, *18*(5), 219–224.
- Robert, P. (2000). *Sleeping sickness is back*. <https://www.gettyimages.fr/detail/photo-d'actualité/glossina-morsitans-morsitans-one-of-31-species-or-photo-d'actualité/542335176?adppopup=true>
- Robert, S. A. (2003). Drug metabolism and pharmacokinetics in drug discovery. *Current Opinion in Drug Discovery and Development*, *6*(1), 66–80.
- Robustelli, P., Piana, S., & Shaw, D. E. (2018). Developing a molecular dynamics force field for both folded and disordered protein states. *Proceedings of the National Academy of Sciences of the United States of America*, *115*(21), E4758–E4766. <https://doi.org/10.1073/pnas.1800690115>
- Rodgers, J. (2009). Human African trypanosomiasis , chemotherapy and CNS disease. *Journal*

- of Neuroimmunology*, 211(1–2), 16–22. <https://doi.org/10.1016/j.jneuroim.2009.02.007>
- Roditi, I., & Liniger, M. (2002). Dressed for success: The surface coats of insect-borne protozoan parasites. *Trends in Microbiology*, 10(3), 128–134. [https://doi.org/10.1016/S0966-842X\(02\)02309-0](https://doi.org/10.1016/S0966-842X(02)02309-0)
- Rodríguez, F., Rozas, I., Kaiser, M., Brun, R., Nguyen, B., Wilson, W. D., García, R. N., & Dardonville, C. (2008). New bis(2-aminoimidazoline) and bisguanidine DNA minor groove binders with potent in vivo antitrypanosomal and antiplasmodial activity. *Journal of Medicinal Chemistry*, 51(4), 909–923. <https://doi.org/10.1021/jm7013088>
- Rogers, D. J., & Robinson, T. . (2004). *Tsetse distribution* (D. J. Rogers & T. . Robinson (eds.)). CAB International.
- Ropp, P. J., Kaminsky, J. C., Yablonski, S., & Durrant, J. D. (2019). Dimorphite-DL: An open-source program for enumerating the ionization states of drug-like small molecules. *Journal of Cheminformatics*, 11(1), 1–8. <https://doi.org/10.1186/s13321-019-0336-9>
- Rosowsky, A., Mota, C. E., Wright, J. E., & Queener, S. F. (1994). 2,4-Diamino-5-chloroquinazoline Analogs of Trimetrexate and Piritrexim: Synthesis and Antifolate Activity. *Journal of Medicinal Chemistry*, 37(26), 4522–4528. <https://doi.org/10.1021/jm00052a011>
- Rufener, R., Dick, L., D’Ascoli, L., Ritler, D., Hizem, A., Wells, T. N. C., Hemphill, A., & Lundström-Stadelmann, B. (2018). Repurposing of an old drug: In vitro and in vivo efficacies of buparvaquone against *Echinococcus multilocularis*. *International Journal for Parasitology: Drugs and Drug Resistance*, 8(3), 440–450. <https://doi.org/10.1016/j.ijpddr.2018.10.011>
- Ruiz-Garcia, A., Bermejo, M., Moss, A., & Vicente, C. G. (2008). Pharmacokinetics in Drug Discovery. *Journal of Pharmaceutical Sciences*, 97(2), 654–690. <https://doi.org/10.1002/jps.21009jps>
- Rycker, M. De, Neill, S. O., Joshi, D., Campbell, L., Gray, D. W., & Fairlamb, A. H. (2012). A Static-Cidal Assay for *Trypanosoma brucei* to Aid Hit Prioritisation for Progression into Drug Discovery Programmes. *PLoS Neglected Tropical Diseases*, 6(11). <https://doi.org/10.1371/journal.pntd.0001932>
- Samby, K., Willis, P. A. ., Burrows, N. J., Laleu, B., Peter, J., & Webborn, H. (2021). Actives from MMV Open Access Boxes ? A suggested way forward. *PLoS Pathogens*, 17(4), 1–11. <https://doi.org/10.1371/journal.ppat.1009384>
- Schneider, G., & Fechner, U. (2005). Computer-based de novo design of drug-like molecules. *Nature Reviews Drug Discovery*, 4(8), 649–663. <https://doi.org/10.1038/nrd1799>
- Schrödinger, L. & DeLano, W. (2020). *PyMOL*. <http://www.pymol.org/pymol>
- Schweitzer, B. I., Dicker, A. P., & Bertino, J. R. (1990). Dihydrofolate reductase as a therapeutic target. *The FASEB Journal*, 4(8), 2441–2452. <https://doi.org/10.1096/fasebj.4.8.2185970>
- Sethi, A., Joshi, K., Alvala, K. S., & Alvala, M. (2019). Molecular Docking in Modern Drug Discovery: Principles and Recent Applications. In *Drug Discovery and Development - New Advances* (Issue August). Intech Open Science. <https://doi.org/10.5772/intechopen.85991>

- Shapiro, T. A., & Englund, P. T. (1990). Selective cleavage of kinetoplast DNA minicircles promoted by antitrypanosomal drugs. *Proceedings of the National Academy of Sciences of the United States of America*, 87(3), 950–954. <https://doi.org/10.1073/pnas.87.3.950>
- Sharma, M., & Chauhan, M. (2012). Dihydrofolate reductase as a therapeutic target for infectious diseases: opportunities and challenges. *Future Medicinal Chemistry*, 4(10), 1335–1365.
- Shoichet, B. K., Leach, A. R., & Kuntz, I. D. (1999). Ligand solvation in molecular docking. *Proteins: Structure, Function and Genetics*, 34(1), 4–16. [https://doi.org/10.1002/\(SICI\)1097-0134\(19990101\)34:1<4::AID-PROT2>3.0.CO;2-6](https://doi.org/10.1002/(SICI)1097-0134(19990101)34:1<4::AID-PROT2>3.0.CO;2-6)
- Shrimpton, J. W. (2017). *African Trypanosome Genes Specifically Required for Fitness in vivo*. University of Dundee.
- Sienkiewicz, N., Jarosławski, S., Wyllie, S., & Fairlamb, A. H. (2008a). Chemical and genetic validation of dihydrofolate reductase-thymidylate synthase as a drug target in African trypanosomes. *Molecular Microbiology*, 69(2), 520–533. <https://doi.org/10.1111/j.1365-2958.2008.06305.x>
- Sienkiewicz, N., Jarosławski, S., Wyllie, S., & Fairlamb, A. H. (2008b). *Chemical and genetic validation of dihydrofolate reductase – thymidylate synthase as a drug target in African trypanosomes*. 69(June), 520–533. <https://doi.org/10.1111/j.1365-2958.2008.06305.x>
- Silva, F., Eduardo, L., Reis, S., Guimar, M., Machado, C., Dophine, D. D., Andrade, V. R. De, Lima, W. G. De, Andrade, M. S., Vilela, C., Reis, A. B., Pound-lana, G., Rezende, S. A., Carla, V., & Mosqueira, F. (2021). Repositioning of Tamoxifen in Surface-Modified Nanocapsules as a Promising Oral Treatment for Visceral Leishmaniasis. *Pharmaceuticals*, 13, 1–25. <https://doi.org/10.3390/pharmaceutics13071061>
- Simarro, P., Louis, F., & Jannin, J. (2003). Sleeping sickness, forgotten illness: what are the consequences in the field? *Medecine Tropicale*, 63(3), 231–236.
- Sindermann, H., Croft, S. L., Engel, K. R., Bommer, W., Eibl, H. J., Unger, C., & Engel, J. (2004). Miltefosine (Impavido): The first oral treatment against leishmaniasis. *Medical Microbiology and Immunology*, 193(4), 173–180. <https://doi.org/10.1007/s00430-003-0201-2>
- Singh, A., & Rosenthal, P. J. (2001). Comparison of efficacies of cysteine protease inhibitors against five strains of *Plasmodium falciparum*. *Antimicrobial Agents and Chemotherapy*, 45(3), 949–951. <https://doi.org/10.1128/AAC.45.3.949-951.2001>
- Singh, G., & Dey, C. S. (2007). Induction of apoptosis-like cell death by pentamidine and doxorubicin through differential inhibition of topoisomerase II in arsenite-resistant *L. donovani*. *Acta Tropica*, 103(3), 172–185. <https://doi.org/10.1016/j.actatropica.2007.06.004>
- Sirichaiwat, C., Intaraudom, C., Kamchonwongpaisan, S., Vanichtanankul, J., Thebtaranonth, Y., & Yuthavong, Y. (2004). Target Guided Synthesis of 5-Benzyl-2,4-diamonopyrimidines: Their Antimalarial Activities and Binding Affinities to Wild Type and Mutant Dihydrofolate Reductases from *Plasmodium falciparum*. *Journal of Medicinal Chemistry*, 47(2), 345–354. <https://doi.org/10.1021/jm0303352>
- Sliwoski, G., Kothiwale, S., Meiler, J., & Lowe, E. W. (2014). Computational methods in drug discovery. *Pharmacological Reviews*, 66(1), 334–395.

- <https://doi.org/10.1124/pr.112.007336>
- Smirlis, D., & Pereira Soares, M. B. (2014). Proteins and Proteomics of Leishmania and Trypanosoma. In Als. et al. Santos (Ed.), *Subcellular Biochemistry* (Vol. 74, pp. 1–381). Springer science. <https://doi.org/10.1007/978-94-007-7305-9>
- Smith, G. C. (1992). *The Process of New Drug Discovery and Development*. CRC press.
- Sousa Da Silva, A. W., & Vranken, W. F. (2012). ACPYPE - AnteChamber PYthon Parser interfacE. *BMC Research Notes*, 5, 1–8. <https://doi.org/10.1186/1756-0500-5-367>
- Spalenka, J., Escotte-Binet, S., Bakiri, A., Hubert, J., Renault, J.-H., Velard, F., Duchateau, S., Aubert, D., Huguenin, A., & Villenaa, I. (2018). Discovery of New Inhibitors of Toxoplasma gondii via the Pathogen Box. *Antimicrobial Agents and Chemotherapy*, 62(2), 1–10. <https://doi.org/https://doi.org/10.1128/AAC.01640-17>
- Spinks, D., Shanks, E. J., Cleghorn, L. A. T., McElroy, S., Jones, D., James, D., Fairlamb, A. H., Frearson, J. A., Wyatt, P. G., & Gilbert, I. H. (2009). Investigation of trypanothione reductase as a drug target in Trypanosoma brucei. *ChemMedChem*, 4(12), 2060–2069. <https://doi.org/10.1002/cmdc.200900262>
- Spyrakis, F., & Cavasotto, C. N. (2015). Open challenges in structure-based virtual screening: Receptor modeling, target flexibility consideration and active site water molecules description. *Archives of Biochemistry and Biophysics*, 583, 105–119. <https://doi.org/10.1016/j.abb.2015.08.002>
- Stanley, S. L. (2003). Amoebiasis. *Lancet*, 361(9362), 1025–1034. [https://doi.org/10.1016/S0140-6736\(03\)12830-9](https://doi.org/10.1016/S0140-6736(03)12830-9)
- Steketee, P. C., Giordani, F., Vincent, I. M., Crouch, K., Achcar, F., Dickens, N. J., Morrison, L. J., Macleod, A., & Barrett, M. P. (2021). Transcriptional differentiation of Trypanosoma brucei during in vitro acquisition of resistance to acoziborole. *PLoS Neglected Tropical Diseases*, 15(11), 1–22. <https://doi.org/10.1371/journal.pntd.0009939>
- Stevenson, P., Sones, K. R., Gicheru, M. M., & Mwangi, E. K. (1995). Comparison of isometamidium chloride and homidium bromide as prophylactic drugs for trypanosomiasis in cattle at Nguruman, Kenya. *Acta Tropica*, 59(2), 77–84. [https://doi.org/10.1016/0001-706X\(94\)00080-K](https://doi.org/10.1016/0001-706X(94)00080-K)
- Steverding, D. (2008). The history of African trypanosomiasis. *Parasites and Vectors*, 1(1), 1–8. <https://doi.org/10.1186/1756-3305-1-3>
- Steverding, D. (2010). The development of drugs for treatment of sleeping sickness: A historical review. *Parasites and Vectors*, 3(1), 1–9. <https://doi.org/10.1186/1756-3305-3-15>
- Stich, A., PM, A., & Krishna, S. (2002). August Stich, Paulo M Abel, Sanjeev Krishna. *Clinical Review*, 325, 203–206.
- Sutcliffe, O. B., Skellern, G. G., Araya, F., Cannavan, A., Sasanya, J. J., Dungu, B., Van Gool, F., Münstermann, S., & Mattioli, R. C. (2014). Animal trypanosomosis: Making quality control of trypanocidal drugs possible. *OIE Revue Scientifique et Technique*, 33(3), 813–820. <https://doi.org/10.20506/rst.33.3.2320>
- Swallow, B. (2000). *Impacts of trypanosomiasis on African agriculture*.

- Sykes, M. L., & Avery, V. M. (2009). Development of an Alamar Blue™ Viability Assay in 384-Well Format for High Throughput Whole Cell Screening of *Trypanosoma brucei* bloodstream form strain 427. *The American Society of Tropical Medicine and Hygiene*, 81(4), 665–674. <https://doi.org/10.4269/ajtmh.2009.09-0015>
- Tai, N., Ding, Y., Schmitz, J. C., & Chu, E. (2002). Identification of critical amino acid residues on human dihydrofolate reductase protein that mediate RNA recognition. *Nucleic Acids Research*, 30(20), 4481–4488.
- Tanenbe, C., Gambo, H., Musongong, A., Boris, O., & Achukwi. (2010). Prévalence de la trypanosomose bovine dans les départements du Faro et Déo , et de la Vina au Cameroun : bilan de vingt années de lutte contre les glossines. *Pathologie Parasitaire*, 63(3-4)(19), 63–69.
- Tassone, G., Landi, G., Linciano, P., Francesconi, V., Tonelli, M., Tagliazucchi, L., Costi, M. P., Mangani, S., & Pozzi, C. (2021). Evidence of pyrimethamine and cycloguanil analogues as dual inhibitors of trypanosoma brucei pteridine reductase and dihydrofolate reductase. *Pharmaceuticals*, 14(7). <https://doi.org/10.3390/ph14070636>
- Tata, R. B., Alsulami, A. F., Amamuddy, O. S., Blundell, T. L., & Bishop, Ö. T. (2022). Slipknot or Crystallographic Error: A Computational Analysis of the Plasmodium falciparum DHFR Structural Folds. *International Journal of Molecular Sciences*, 23(3). <https://doi.org/10.3390/ijms23031514>
- ten Brink, T., & Exner, T. E. (2009). Influence of Protonation, Tautomeric, and Stereoisomeric States on Protein–Ligand Docking Results - Journal of Chemical Information and Modeling. *Journal of Chemical Information and Modeling*, 49(6), 1535–1546. <https://doi.org/10.1021/ci800420z%0Ahttp://pubs.acs.org/doi/abs/10.1021/ci800420z>
- Thomas, J., Baker, N., Hutchinson, S., Dominicus, C., Trenaman, A., Glover, L., Alford, S., & Horn, D. (2018). Insights into antitrypanosomal drug mode-of-action from cytology-based profiling. *PLoS Neglected Tropical Diseases*, 12(11), 1–19. <https://doi.org/10.1371/journal.pntd.0006980>
- Toor, J., Adams, E. R., Aliee, M., Amoah, B., Anderson, R. M., Ayabina, D., Bailey, R., Basáñez, M., Das, A., Davis, C. N., Davis, E. L., Deiner, M. S., Diggle, P. J., Fronterre, C., Giardina, F., Malizia, V., Medley, G. F., Meeyai, A., Michael, E., ... Rock, K. S. (2021). Predicted Impact of COVID-19 on Neglected Tropical Disease Programs and the Opportunity for Innovation. 72, 1463–1466. <https://doi.org/10.1093/cid/ciaa933>
- Torrelee, E., Trunz, B. B., Tweats, D., Kaiser, M., Brun, R., Mazué, G., Bray, M. A., & Pécoul, B. (2010). Fexinidazole - a new oral nitroimidazole drug candidate entering clinical development for the treatment of sleeping sickness. *PLoS Neglected Tropical Diseases*, 4(12), 1–15. <https://doi.org/10.1371/journal.pntd.0000923>
- Tovar, J., & Fairlamb, A. H. (1996). Extrachromosomal, homologous expression of trypanothione reductase and its complementary mRNA in *Trypanosoma cruzi*. *Nucleic Acids Research*, 24(15), 2942–2949. <https://doi.org/10.1093/nar/24.15.2942>
- Tovar, J., Wilkinson, S., Mottram, J. C., & Fairlamb, A. H. (1998). Evidence that trypanothione reductase is an essential enzyme in *Leishmania* by targeted replacement of the tryA gene locus. *Molecular Microbiology*, 29(2), 653–660. <https://doi.org/10.1046/j.1365-2958.1998.00968.x>
- Trainor, G. L. (2007). The importance of plasma protein binding in drug discovery. *Expert*

- Opinion on Drug Discovery*, 2(1), 51–64. <https://doi.org/10.1517/17460441.2.1.51>
- Trott, O., & Olson, A. (2010). Software News and Updates Gabedit — AutoDock Vina: Improving the Speed and Accuracy of Docking with a New Scoring Function, Efficient Optimization, and Multithreading. *Journal of Computational Chemistry*, 31(2), 455–461. <https://doi.org/10.1002/jcc.21334>
- Uilenberg, G. (1998). A Field Guide for the Diagnosis, Treatment, and Prevention of African Animal Trypanosomiasis. *Food and Agriculture Organisation of the United Nations (FAO), Rome, Italy*.
- Urquhart, G. M., Armour, J., Duncan, J. L., Dunn, A. M., & Jennings, F. W. (1996). *Veterinary Parasitology* (Second Edi). B- Blackwell Science.
- Valenciano, A. L., Ramsey, A. C., Santos, W. L., & Mackey, Z. B. (2016). Discovery and antiparasitic activity of AZ960 as a Trypanosoma brucei ERK8 inhibitor. *Bioorganic and Medicinal Chemistry*, 24(19), 4647–4651. <https://doi.org/10.1016/j.bmc.2016.07.069>
- Valkó, K. L. (2016). Lipophilicity and biomimetic properties measured by HPLC to support drug discovery. *Journal of Pharmaceutical and Biomedical Analysis*, 130, 35–54. <https://doi.org/10.1016/j.jpba.2016.04.009>
- Van De Waterbeemd, H. (2005). From in vivo to in vitro/in silico ADME: Progress and challenges. *Expert Opinion on Drug Metabolism and Toxicology*, 1(1), 1–4. <https://doi.org/10.1517/17425255.1.1.1>
- Van Meirvenne, N. (1999). Biological diagnosis of human African trypanosomiasis. In Progress in Human African Trypanosomiasis, Sleeping Sickness. In M. Dumas, B. Bouteille, & A. Buguet (Eds.), *editors. Berlin*. 273-292. (Springer-V).
- Van Triest, B., Pinedo, H. M., Giaccone, G., & Peters, G. J. (2000). Downstream molecular determinants of response to 5-fluorouracil and antifolate thymidylate synthase inhibitors. *Annals of Oncology*, 11(4), 385–391. <https://doi.org/10.1023/A:1008351221345>
- Vanichtanankul, J., Taweechai, S., Yuvaniyama, J., Vilaivan, T., Chitnumsub, P., Kamchonwongpaisan, S., & Yuthavong, Y. (2011). *Trypanosomal Dihydrofolate Reductase Reveals Natural Antifolate Resistance*. 905–911.
- Vasaikar, S., Bhatia, P., Bhatia, P. G., & Yaiw, K. C. (2016). Complementary approaches to existing target based drug discovery for identifying novel drug targets. *Biomedicines*, 4(4), 1–17. <https://doi.org/10.3390/biomedicines4040027>
- Vassella, E., Reuner, B., Yutzy, B., Boshart, M., Biochemie, M., Klopferspitz, A., & Martinsried, D.-. (1997). Differentiation of African trypanosomes is controlled by a density sensing mechanism which signals cell cycle arrest via the cAMP pathway. *Journal of Cell Science*, 110, 2661–2671.
- Veale, C. G. L., & Hoppe, H. C. (2018). Screening of the Pathogen Box reveals new starting points for anti-trypanosomal drug discovery. *MedChemComm*, 9(12), 2037–2044. <https://doi.org/10.1039/c8md00319j>
- Veber, D. F., Johnson, S. R., Cheng, H., Smith, B. R., Ward, K. W., & Kopple, K. D. (2002). Molecular Properties That Influence the Oral Bioavailability of Drug Candidates. *Journal of Med*, 45(12), 2615–2623. <https://doi.org/10.1021/jm020017>
- Vickerman, K. (1985). Developmental cycles and biology of pathogenic trypanosomes. *British*

- Medical Bulletin*, 41, 105–114. <https://doi.org/10.1093/oxfordjournals.bmb.a072036>
- Vila, T., & Jose L, L.-R. (2017). Screening the Pathogen Box for Identification of *Candida albicans* Biofilm Inhibitors. . . *Antimicrobial Agents Chemotherapy*, 61(1), 1–9. <https://doi.org/https://doi.org/10.1128/AAC.02006-16>
- Vincent, I. M., Creek, D., Watson, D. G., Kamleh, M. A., Woods, D. J., Wong, P. E., Burchmore, R. J. S., & Barrett, M. P. (2010). A molecular mechanism for eflornithine resistance in African trypanosomes. *PLoS Pathogens*, 6(11), 1–9. <https://doi.org/10.1371/journal.ppat.1001204>
- Vreysen, M. J. B. (2006). Prospects for area-wide integrated control of tsetse flies (Diptera: Glossinidae) and trypanosomiasis in sub-Saharan Africa. *Soc. Entomol. Argent*, 65(12), 1–21.
- Wang, S. (2001). Historique de l'installation et de la propagation de la maladie du sommeil à Bipindi (sud-Cameroun), de 1896 à nos jours. *Médecine Tropicale*, 61, 384–389.
- Wang, S., Sim, T. B., Kim, Y. S., & Chang, Y. T. (2004). Tools for target identification and validation. *Current Opinion in Chemical Biology*, 8(4), 371–377. <https://doi.org/10.1016/j.cbpa.2004.06.001>
- Wheeler, R., Gluenz, E., & Gull, K. (2013). The Limits on Trypanosomatid Morphological Diversity. *PLoS ONE*, 8(11)(e79581).
- Wilkinson, S. R., Taylor, M. C., Horn, D., Kelly, J. M., & Cheeseman, I. (2008). A mechanism for cross-resistance to nifurtimox and benznidazole in trypanosomes. *Proceedings of the National Academy of Sciences of the United States of America*, 105(13), 5022–5027. <https://doi.org/10.1073/pnas.0711014105>
- Wilkowsky, S. E. (2018). Trypanosoma. In Florin-Christensen & L. M., Schnittger (Eds.), *Parasitic Protozoa of Farm Animals and Pets* (Springer, C).
- Wilson, S., Morris, K., Lewis, I., & Krog, E. (1963). The effects of trypanosomiasis on rural economy with special reference to the Sudan, Bechuanaland and West Africa. *Bulletin of the World Health Organization*, 28(5-6), 595–613.
- Wilson, W., Tanious, F. A., Mathis, A., Tevis, D., Hall, J. E., & Boykin, D. W. (2008). Antiparasitic compounds that target DNA. *Biochimie*, 90(7), 999–1014. <https://doi.org/10.1016/j.biochi.2008.02.017>
- Wiser, M. F. (1999). *Kinetoplastid Biology and Human Disease*. <http://www.tulane.edu/~wiser/protozoology/notes/kinet.html>
- Wong-Beringer, A., Richard, A. J., & Guglielmo, B. J. (1998). Lipid Formulations of Amphotericin B: Clinical Efficacy and Toxicities. *Cleveland Clinic Journal of Medicine*, 65(8), 423–427. <https://doi.org/10.3949/ccjm.65.8.423>
- Woo, P. (1970). The haematocrit centrifuge technique for the diagnosis of African trypanosomiasis. *Acta Tropica*, 27(4), 384–386.
- World health organization. (2023a). *Human African trypanosomiasis (sleeping sickness)*. <https://www.who.int/data/gho/data/themes/topics/human-african-trypanosomiasis>
- World health organization. (2023b). *Trypanosomiasis, human African (sleeping sickness)*. Fact Sheets/Detail. <https://www.who.int/news-room/fact-sheets/detail/trypanosomiasis>

human-african-(sleeping-sickness)

World Health Organization. (2019). *Rapport Biennal 2018/2019*. 1–86.

Xu, X., Huang, M., & Zou, X. (2018). Docking-based inverse virtual screening: methods, applications, and challenges. *Biophysics Reports*, 4(1), 1–16. <https://doi.org/10.1007/s41048-017-0045-8>

Yamashita, F., & Hashida, M. (2004). In silico approaches for predicting ADME properties of drugs. *Drug Metabolism and Pharmacokinetics*, 19(5), 327–338. <https://doi.org/10.2133/dmpk.19.327>

Yun, O., Priotto, G., Tong, J., Flevaud, L., & Chappuis, F. (2010). NECT is next: Implementing the new drug combination therapy for trypanosoma brucei gambiense sleeping sickness. *PLoS Neglected Tropical Diseases*, 4(5). <https://doi.org/10.1371/journal.pntd.0000720>

Yuvaniyama, J., Chitnumsub, P., Kamchonwongpaisan, S., Vanichtanankul, J., Sirawaraporn, W., Taylor, P., Walkinshaw, M. D., & Yuthavong, Y. (2003). Insights into antifolate resistance from malarial DHFR-TS structures. *Nature Structural Biology*, 10(5), 357–365. <https://doi.org/10.1038/nsb921>

Zhang, J.-H., Chung, D., & Oldenburg, K. (1999). Zhang et al PRB.pdf. *Journal of Biomolecular Screening*, 4(2), 67–73.

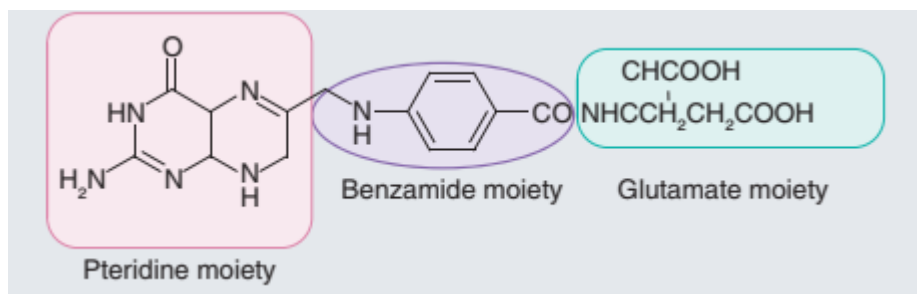
Zhao, Y., Wang, Q., Meng, Q., Ding, D., Yang, H., Gao, G., Li, D., Zhu, W., & Zhou, H. (2012). Identification of Trypanosoma brucei leucyl-tRNA synthetase inhibitors by pharmacophore- and docking-based virtual screening and synthesis. *Bioorganic and Medicinal Chemistry*, 20(3), 1240–1250. <https://doi.org/10.1016/j.bmc.2011.12.035>

# Appendices and Publication



## APPENDICES AND PUBLICATION

### Appendix 1: DHFR substrate structure



### Appendix 2: Preparation of culture media and preservation solutions

#### Preparation of complete HMI-9 culture medium

The first step was to weigh and dissolve the different supplements. To prepare 500 ml of HMI-9, we weighed the following: 0.014 g of bathocuproine; 0.091 g cysteine (added after bathocuproine); 0.055 g of pyruvic acid; 0.0195 g of thymidine; and 0.068 g of hypoxanthine (prepared using 0.1 M NaOH). The weighed supplements were dissolved in 10 ml of sterile distilled water, 7  $\mu\text{l}$  of  $\beta$ -mercaptoethanol was added, and the whole mixture was filtered using a 0.22  $\mu\text{m}$  syringe filter. Thereafter, 50 ml of heat-inactivated fetal bovine serum, 50 ml of serum plus and 10 ml of previously prepared supplements were added to 390 ml of IMDM. The mixture was homogenized, sterilized and then aliquoted into 50 mL sterile tubes. Next, the tubes were sealed and stored at 4°C.

#### Short-term storage of bloodstream forms of trypanosomes and defrosting procedure

**Cryopreservation:** Parasites were collected by centrifugation at 2500 rpm for 7 minutes. After the supernatant was discarded, 500  $\mu\text{L}$  of the pellet was resuspended in fresh medium and mixed with 500  $\mu\text{l}$  of 20 glycerol % solution in sterile freezing vials. The vials were stored at -20°C overnight before storage at -80°C. **Thawing of frozen cells:** a vial of frozen trypanosomes was thawed at 37°C in a water bath. Next, the cells were transferred to a 15 mL Falcon tube containing 9 mL of complete medium. The cells were then centrifuged for 7 minutes at 2500 rpm to remove glycerol. The cell pellet was resuspended in 5 mL of complete HMI-9 medium and incubated at 37°C.

### Preparation of DMEM

Complete DMEM was obtained by mixing one liter 820 ml of DMEM, 10 ml of penicillin/streptomycin antibiotic (100X), 100 ml of heat-inactivated FBS, and 10 mL of nonessential amino acids. The mixture was well homogenized, filtered and stored at 4°C.

### Short-term storage of Vero cells and defrosting procedure

**Cryopreservation:** Cells were collected by centrifugation at 1800 rpm for 5 minutes. After the supernatant was discarded, 500 µL of the pellet was resuspended in fresh medium and mixed with 500 µl of DMSO 10% solution in sterile freezing vials. The vials were stored at -20°C overnight before storage at -80°C.

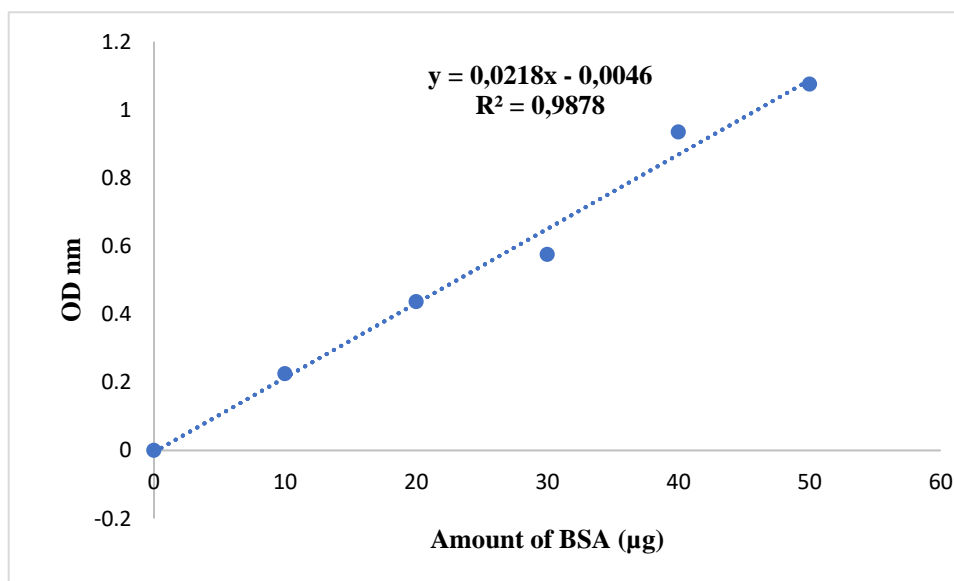
**Thawing of frozen cells,** a vial of frozen cells was thawed at 37°C in a water bath. Next, the cells were transferred to a 15 mL Falcon tube containing 9 mL of complete medium. The cells were then centrifuged for 5 minutes at 1800 rpm to remove the DMSO. The cell pellet was resuspended in 5 mL of complete DMEM and incubated at 37°C.

### Appendix 3: Procedure for BSA standard curve generation

**Measuring BSA Protein Standard:** Six different volumes [0 µl (0 µg), 10 µl (5 µg), 20 µl (10 µg), 30 µl (15 µg), 40 µl (20 µg), 50 µl (25 µg)] of 0.5 mg/ml BSA were pipetted into separate tubes and completed with phosphate buffer saline for a total volume of 1 mL. Five microliters of these intermediate solutions were added to 195 µL of Bradford reagent, and the optical densities were read at 595 nm. The obtained values were used to generate the standard curve from which the linear regression equation was used to deduce the amount of protein in the test sample using the following formula.

$$\mu\text{g of protein} = \frac{(\text{Absorbance} - y \text{ intercept})}{\text{Slope}}$$

$$\text{Concentration assayed} = \frac{\mu\text{g of protein}}{\mu\text{L assayed}}$$



#### Appendix 4: Supplementary information for the SDS–PAGE procedure

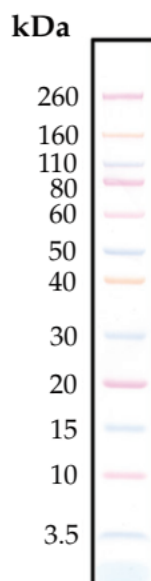
##### Preparation of Gels

Stacking gel 4% acrylamide for sample concentrations: 3.35 mL of acrylamide/bisacrylamide 30, 2.5 mL of 1.5 mM Tris HCl pH 8.8, 100 µL of 10% SDS (sodium dodecyl sulfate), 50 µL of ammonium persulfate (APD), 5 µL of TEMED, and 3.935 mL of sterilized distilled water.

Resolving gel 12% acrylamide for sample separation: 0.66 mL of acrylamide/bisacrylamide 30%, 1.25 mL of 0.5 M Tris-HCl pH 6.8, 50 µL of 10% SDS, 25 µL of 10% APS, 5 µL TEMED, and 3.01 mL of sterilized distilled water.

##### Prestained standard characteristics

The standard used consisted of 12 prestained protein bands ranging in molecular weight from 3.5–260 kDa. This molecular weight standard was used according to the manufacturer's instructions. Briefly, the standard was thawed at room temperature and gently vortexed, and 10 µL was loaded onto a 4–12% Bis-Tris Gel.



### SDS-PAGE procedure

In summary, 16  $\mu\text{L}$  of the crude protein extract was mixed with 4  $\mu\text{L}$  of glycerol loading buffer containing 5%  $\beta$ -mercaptoethanol. The mixture was then heated at 95°C to allow protein denaturation and migration. Fifteen microliters of this mixture were introduced into the wells of the gel, and the gel was run for at least 1 hour. To reveal bands, Coomassie blue reagent was used for staining.

### Appendix 5: IC<sub>99</sub>, IC<sub>90</sub> and IC<sub>10</sub> ( $\mu\text{M}$ ) of the prioritized compounds

The IC<sub>99</sub>, IC<sub>90</sub> and IC<sub>10</sub> of the selected compounds were estimated using their respective Hill slopes with GraphPad Prism 8.0 and used for all experiments.

Compounds	IC <sub>99</sub>	IC <sub>90</sub>	IC <sub>50</sub>	IC <sub>10</sub>
<b>7</b>	6.5	1.3	0.06	0.007
<b>10</b>	10	3	0.045	0.04
<b>Pentamidine</b>	0.12	0.011	0.002	0.0001

### Appendix 6: details of the DNA fragmentation procedure

#### a- Procedure for coating the microplate with the anti-DNA-antibody

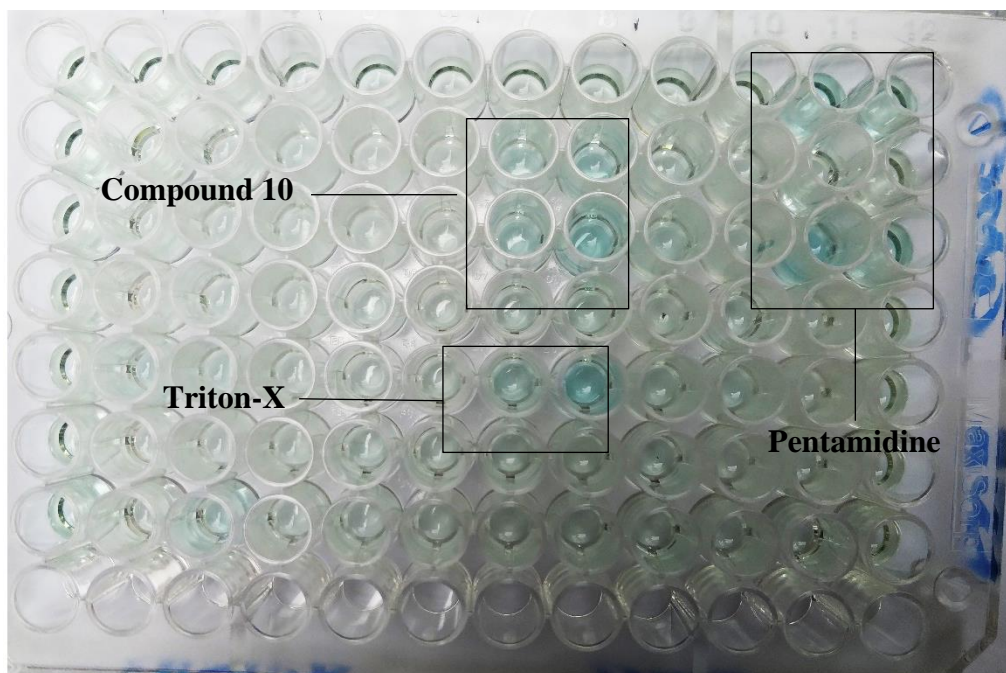
For coating, 100  $\mu\text{L}$  of anti-DNA coating solution (monoclonal antibody solution from mouse) was pipetted into each well of a 96-well, flat-bottom microplate. The plate was covered with an adhesive cover foil and incubated overnight at +2°C to +8°C. Thereafter, the coating solution was removed by aspirating away the buffer. Nonspecific binding sites were then blocked by adding 200  $\mu\text{L}$  of the incubation solution (BSA-EDTA-Tween 20 solution)

followed by incubation for 30 min at 25°C. Next, the solution was removed by aspiration, and the wells were washed three times with 250 µL of washing solution (EDTA-Tween 20 solution) for 2 min each. The washing solution was removed, and the plate was further processed for ELISA and photometric measurements.

#### **b- Procedure for ELISA and photometric measurement**

One hundred microliters of the samples (supernatant from cell-mediated cytotoxicity or apoptosis procedures) were transferred into the well of the precoated 96-well flat-bottom microplate. The plate was covered and incubated for 90 min at 25°C. Following incubation, the solution was aspirated, and the plate was washed three times with 250 µL of washing solution (EDTA-Tween 20 solution). At the last wash-step, the washing solution was not discarded. The uncovered plate was placed in a microwave oven, and irradiation was run for 5 min at medium power (500 W) to fix and denature the DNA. After removing the washing solution in the cooled plate, 100 µL/well of anti-BrdU-POD conjugate solution (monoclonal antibody solution from mouse (clone BMG 6H8, Fab-fragment) conjugated with peroxidase) was added. The plate was incubated for 90 minutes at 25°C. After washing steps, 100 µL of the substrate solution was added to each well used, and the absorbance was directly measured at 370 nm every 30 s until development of a color.

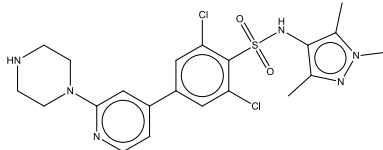
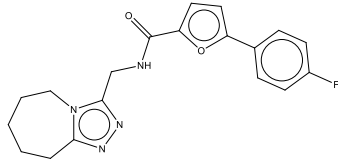
#### **c- Appearance of the microplate at the end of the experiment**

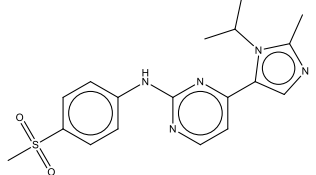
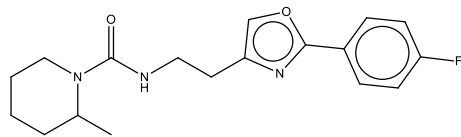
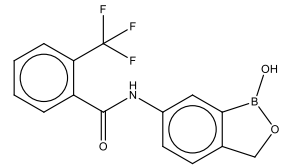


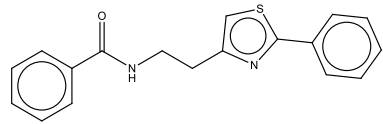
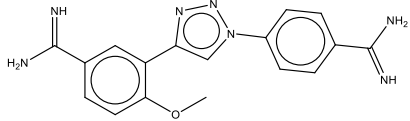
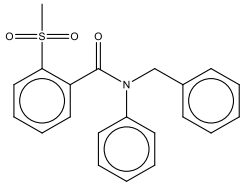
**Appendix 7:** Trypanosome viability percentages following treatment with DMSO and pentamidine at various concentrations

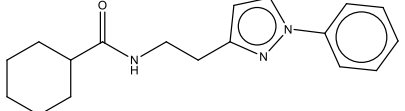
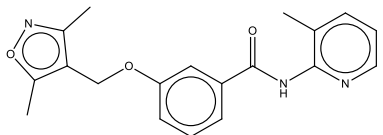
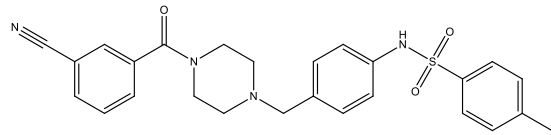
Concentrations	DMSO ( $\mu\text{M}$ )		Pentamidine ( $\mu\text{M}$ )	
<b>10</b>	13.0106309	12.3103605	13.0106309	12.3103605
<b>2</b>	14.0708533	14.1166654	14.0708533	14.1166654
<b>0,4</b>	74.8307612	74.8307612	74.8307612	74.8307612
<b>0,08</b>	98.73157802	100	98.73157802	100
<b>0,016</b>	98.79047927	100	98.79047927	100
<b>0,0032</b>	98.86901426	98.86901426	98.86901426	98.86901426
<b>0,00064</b>	94.37288579	94.37288579	94.37288579	94.37288579

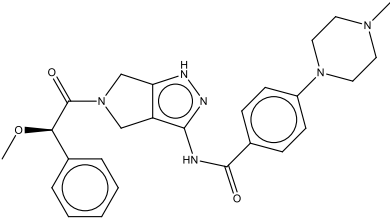
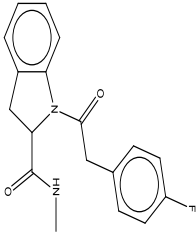
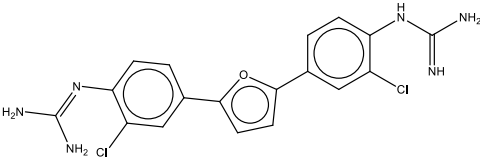
**Appendix 8:** Chemical structures of the 25 antitrypanosomal MMVPB hit compounds with known anti-kinetoplastid activity.

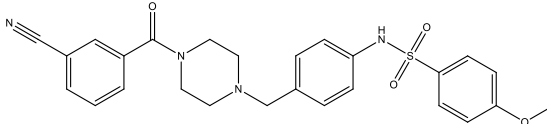
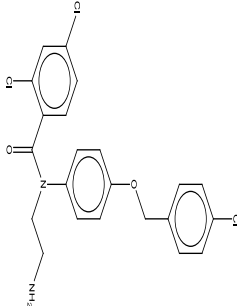
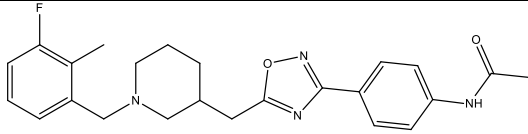
Compound No	MMVPB ID	IC <sub>50</sub> <i>T.b. brucei</i> (μM)	*Known target parasites	Chemical class	Chemical structure
1	MMV688180	0.002±001	<i>Trypanosoma brucei</i> <i>brucei</i> <i>Trypanosoma brucei</i> <i>rhodesiense</i> <i>Trypanosoma cruzi</i>	Benzenesulfonamide	
2	MMV688796	0.03±0.01	<i>Trypanosoma brucei</i> <i>brucei</i> <i>Trypanosoma brucei</i> <i>rhodesiense</i> <i>Trypanosoma cruzi</i> <i>Leishmania infantum</i>	2,4 substituted furan	

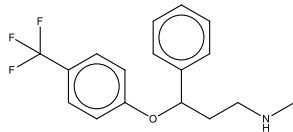
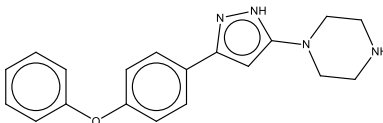
3	MMV676604	0.036±0.001	<p><i>Trypanosoma brucei</i> <i>brucei</i></p> <p><i>Trypanosoma brucei</i> <i>rhodesiense</i></p> <p><i>Trypanosoma cruzi</i></p> <p><i>Leishmania infantum</i></p> <p><i>Leishmania major</i></p>	2-aminopyrimidine	 <p>The structure shows a pyrimidine ring with an amino group at position 2, a methyl group at position 4, and a 4-sulfamoylphenyl group at position 6.</p>
4	MMV688797	0.06±0.02	<p><i>Trypanosoma brucei</i> <i>brucei</i></p> <p><i>Trypanosoma brucei</i> <i>rhodesiense</i></p> <p><i>Trypanosoma cruzi</i></p>	2-aryl oxazole	 <p>The structure shows a 2-oxazole ring substituted with a 4-fluorophenyl group at position 5 and a 2-(2-methylpiperidin-1-yl)acetamide group at position 2.</p>
5	MMV652003	0.06±0.04	<p><i>Trypanosoma brucei</i> <i>brucei</i></p> <p><i>Trypanosoma brucei</i> <i>rhodesiense</i></p>	Benzamide	 <p>The structure shows a benzamide core with a trifluoromethyl group on the benzene ring and a 2-(1,2,4-triazol-5-yl)ethyl group on the amide nitrogen.</p>

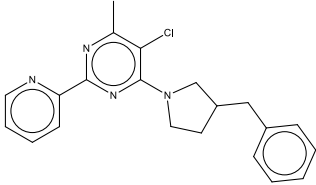
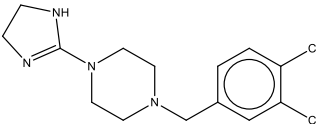
			<i>Trypanosoma cruzi</i> <i>Leishmania infantum</i>		
6	MMV688958	0.087±0.01	<i>Trypanosoma brucei</i> <i>brucei</i> <i>Trypanosoma brucei</i> <i>rhodesiense</i> <i>Trypanosoma cruzi</i>	2-aryl oxazole	
7	MMV675998	0.34±0.03	<i>Trypanosoma brucei</i> <i>brucei</i> <i>Trypanosoma brucei</i> <i>rhodesiense</i> <i>Trypanosoma cruzi</i>	Benzenecarboximidamide	
8	MMV688798	0.30±0.025	<i>Trypanosoma brucei</i> <i>brucei</i> <i>Trypanosoma brucei</i> <i>rhodesiense</i>	Benzamide	

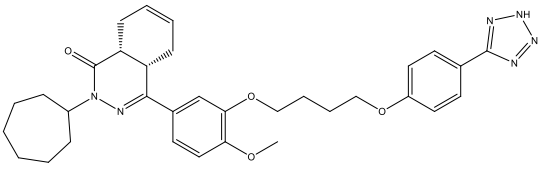
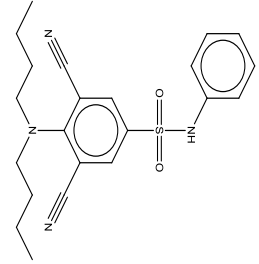
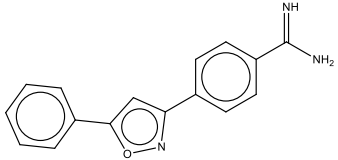
			<i>Trypanosoma cruzi</i>		
9	MMV688795	0.35±0.02	<i>Trypanosoma brucei</i> <i>brucei</i> <i>Trypanosoma brucei</i> <i>rhodesiense</i> <i>Trypanosoma cruzi</i>	2-aryl oxazole	
10	MMV688793	0.36±0.04	<i>Trypanosoma brucei</i> <i>brucei</i> <i>Trypanosoma brucei</i> <i>rhodesiense</i>	2-pyridyl benzamides	
11	MMV689028	0.40±0.02	<i>Trypanosoma brucei</i> <i>brucei</i> <i>Trypanosoma brucei</i> <i>rhodesiense</i> <i>Trypanosoma cruzi</i> <i>Leishmania infantum</i>	benzyl piperazine	

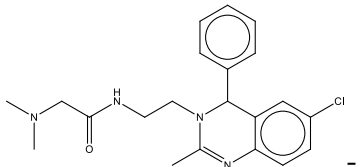
12	MMV676600	0.65±0.007	<i>Trypanosoma brucei</i> <i>brucei</i> <i>Trypanosoma brucei</i> <i>rhodesiense</i> <i>Trypanosoma cruzi</i> <i>Leishmania infantum</i>	Benzamide	
13	MMV188296	1.01±0.25	<i>Trypanosoma brucei</i> <i>brucei</i> <i>Trypanosoma brucei</i> <i>rhodesiense</i>	2-indolinecarboxamide	
14	MMV688271	1.07±0.16	<i>Trypanosoma brucei</i> <i>brucei</i> <i>Trypanosoma brucei</i> <i>rhodesiense</i> <i>Trypanosoma cruzi</i>	Guanidine	

			<i>Leishmania infantum</i>		
15	MMV689029	1.30±0.60	<i>Trypanosoma brucei</i> <i>brucei</i> <i>Trypanosoma brucei</i> <i>rhodesiense</i> <i>Trypanosoma cruzi</i> <i>Leishmania infantum</i>	benzyl piperazine	
16	MMV688371	1.60±0.10	<i>Trypanosoma brucei</i> <i>brucei</i> <i>Trypanosoma brucei</i> <i>rhodesiense</i> <i>Trypanosoma cruzi</i> <i>Leishmania infantum</i>	Benzamide	
17	MMV689061	1.90±0.10	<i>Trypanosoma brucei</i> <i>brucei</i>	Acetamide	

			<i>Trypanosoma brucei</i> <i>rhodesiense</i> <i>Trypanosoma cruzi</i> <i>Leishmania infantum</i>		
18	MMV001561	1.90±0.05	<i>Trypanosoma brucei</i> <i>brucei</i> <i>Trypanosoma brucei</i> <i>rhodesiense</i> <i>Trypanosoma cruzi</i> <i>Leishmania infantum</i>	Propanamine	
19	MMV687706	1.90±0.006	<i>Trypanosoma brucei</i> <i>brucei</i> <i>Trypanosoma brucei</i> <i>rhodesiense</i> <i>Trypanosoma cruzi</i> <i>Leishmania infantum</i>	Piperazine	

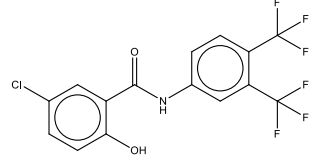
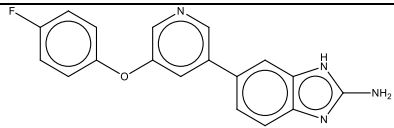
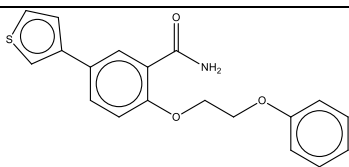
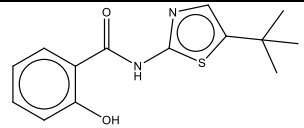
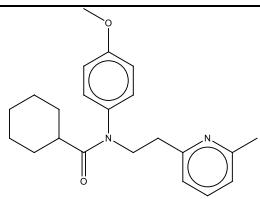
20	MMV659004	1.90±0.003	<p><i>Trypanosoma brucei</i> <i>brucei</i></p> <p><i>Trypanosoma brucei</i> <i>rhodesiense</i></p> <p><i>Trypanosoma cruzi</i></p> <p><i>Leishmania infantum</i></p> <p><i>Leishmania donovani</i></p> <p><i>Leishmania major</i></p>	Pyrimidine	
21	MMV689060	2.40±0.06	<p><i>Trypanosoma brucei</i> <i>brucei</i></p> <p><i>Trypanosoma brucei</i> <i>rhodesiense</i></p> <p><i>Trypanosoma cruzi</i></p> <p><i>Leishmania infantum</i></p>	Piperazine	

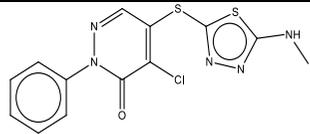
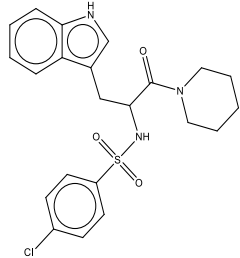
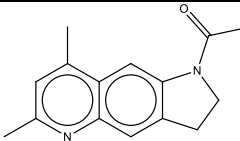
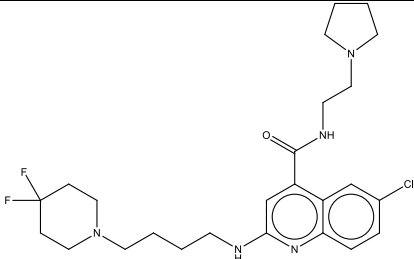
22	MMV690027	2.80±0.07	<i>Trypanosoma brucei</i> <i>brucei</i>	hexahydrophthalazinones	
23	MMV688467	3.10±0.50	<i>Trypanosoma brucei</i> <i>brucei</i> <i>Trypanosoma brucei</i> <i>rhodesiense</i> <i>Trypanosoma cruzi</i> <i>Leishmania infantum</i>	butyl sulfanilamide	
24	MMV688514	3.20±0.30	<i>Trypanosoma brucei</i> <i>brucei</i> <i>Trypanosoma brucei</i> <i>rhodesiense</i> <i>Trypanosoma cruzi</i> <i>Leishmania infantum</i>	Benzenecarboximidamide	

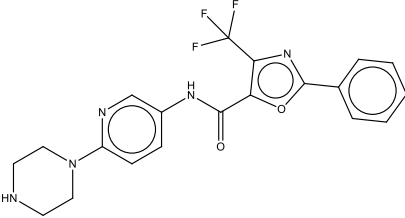
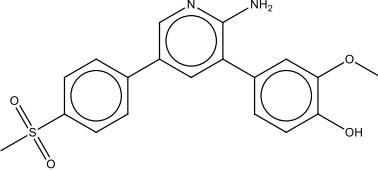
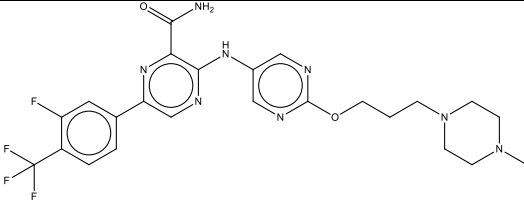
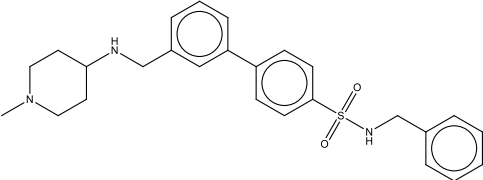
25	MMV688410	8.50±0.10	<i>Trypanosoma brucei</i> <i>brucei</i> <i>Trypanosoma brucei</i> <i>rhodesiense</i> <i>Trypanosoma cruzi</i> <i>Leishmania infantum</i>	Acetamide	
----	-----------	-----------	---	-----------	---

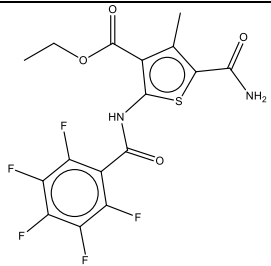
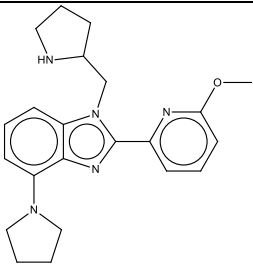
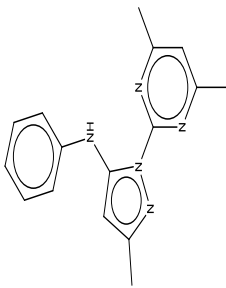
MMV Pathogen Box (MMVPB) compounds were tested in culture against *T. b. brucei* at serially diluted concentrations. Median inhibitory concentrations (IC<sub>50</sub>) were generated from concentration–response curves using GraphPad Prism 8.0 software; MMVPB: Medicines for Malaria Venture Pathogen Box; The chemical classes of the compounds were obtained from PubChem NIH database (<https://pubchem.ncbi.nlm.nih.gov>); \*The parasite targets for compounds were retrieved from the MMV Pathogen Box supporting information.

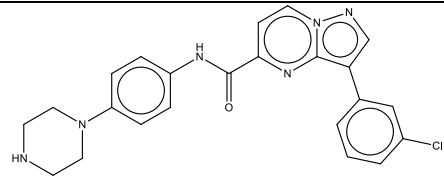
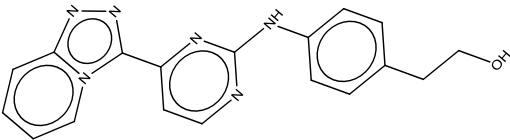
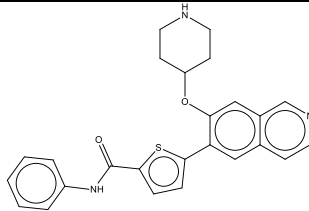
#### Appendix 9: Chemical structures of the 38 antitrypanosomal MMVPB hit compounds with known potency against other diseases.

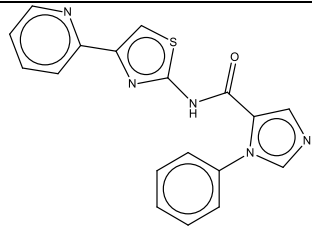
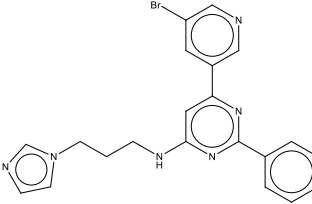
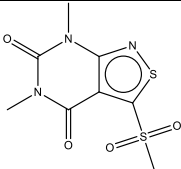
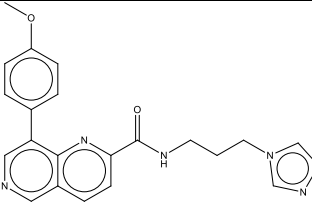
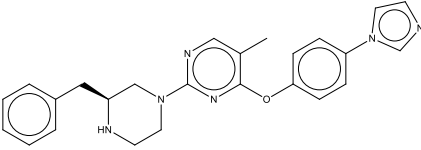
Compound No	MMVPB ID	IC <sub>50</sub> ±SD <i>T.b. brucei</i> (μM)	*Known target disease pathogen	Chemical class	Chemical structure
1	MMV687807	0.50±0.04	<i>Mycobacterium tuberculosis</i>	Benzamide	
2	MMV687248	0.50±0.07	<i>Mycobacterium tuberculosis</i>	1H-Benzimidazol-2-amine	
3	MMV687138	0.50±0.01	<i>Mycobacterium tuberculosis</i>	Benzamide	
4	MMV495543	0.70±0.25	<i>Mycobacterium tuberculosis</i>	Benzamide	
5	MMV675996	0.80±0.02	<i>Onchocerca</i>	Cyclohexancarboxamide	

6	MMV688763	0.80±0.10	<i>Schistosoma mansoni</i>	Pyridazinone	
7	MMV085210	0.90±0.10	<i>Plasmodium falciparum</i>	Benzenesulfonamide	
8	MMV054312	1.29±0.42	<i>Mycobacterium tuberculosis</i>	Pyrroloquinoline	
9	MMV667494	1.30±0.50	<i>Plasmodium falciparum</i>	Quinolone 4-carboxamide	

10	MMV024937	1.40±0.50	<i>Plasmodium falciparum</i>	Oxazolecarboxamide	
11	MMV010576	1.50±0.30	<i>Plasmodium falciparum</i>	2-amino pyridines	
12	MMV687812	1.70±0.10	<i>Mycobacterium tuberculosis</i>	2-Pyrazinecarboxamide	
13	MMV022029	1.70±0.70	<i>Plasmodium falciparum</i>	Biaryl sulfonamide	

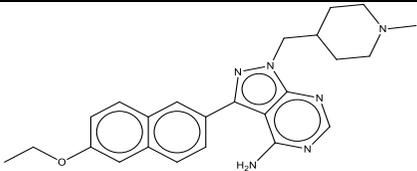
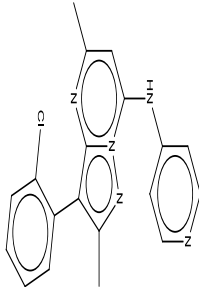
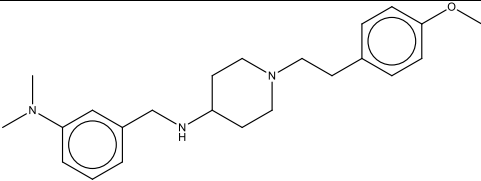
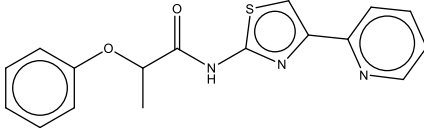
14	MMV153413	1.70±0.10	<i>Mycobacterium tuberculosis</i>	Tetrasubstituted thiophene	
15	MMV687703	1.70±0.06	<i>Mycobacterium tuberculosis</i>	Benzimidazole	
16	MMV062221	1.70±0.60	<i>Plasmodium falciparum</i>	Phenylpyrazolamine	

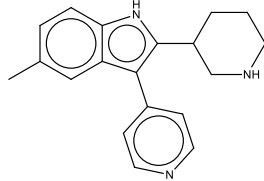
17	MMV022478	1.70±0.01	<i>Plasmodium falciparum</i>	Pyrazolo (1.5-a)pyrimidine	
18	MMV028694	1.80±0.10	<i>Plasmodium falciparum</i>	2,4 disubstituted pyrimidine	
19	MMV024035	1.80±0.10	<i>Plasmodium falciparum</i>	Thiophene carboxamide	

20	MMV676512	1.90±0.07	<i>Mycobacterium tuberculosis</i>	1H-Imidazole-5-carboxamide	
21	MMV661713	1.90±0.02	<i>Mycobacterium tuberculosis</i>	4-pyridyl-2-aryl pyrimidine	
22	MMV687251	1.90±0.01	<i>Mycobacterium tuberculosis</i>	Pyrimidine	
23	MMV020670	1.90±0.02	<i>Plasmodium falciparum</i>	6-naphthyridine-2-carboxamide	
24	MMV687765	2.30±0.30	<i>Mycobacterium tuberculosis</i>	Pyrimidine	

25	MMV675968	2.80±0.07	<i>Cryptosporidium parvum</i>	Aminoquinazoline	
26	MMV688124	2.90±0.08	<i>Mycobacterium tuberculosis</i>	Benzenesulfonamide	
27	MMV688703	3.18±1.30	<i>Toxoplasma gondii</i>	Pyridines	
28	MMV688417	4.38±0.90	<i>Toxoplasma gondii</i>	Pyrazolo [3,4-d]pyrimidinamine	

29	MMV023969	8.09±0.30	<i>Mycobacterium tuberculosis</i>	Isoquinoline	
30	MMV688761	8.33±0.09	<i>Schistosoma mansoni</i>	Benzamide	
31	MMV688768	8.36±0.08	<i>Schistosoma mansoni</i>	2,3 disubstituted indole	
32	MMV023233	8.43±0.06	<i>Plasmodium falciparum</i>	Quinolineamine	
33	MMV006901	8.45±0.05	<i>Plasmodium falciparum</i>	2,4-aminoquinoline	

34	MMV688854	8.50±0.06	<i>Cryptosporidium parvum</i>	Pyrazolo pyrimidineamine	
35	MMV016136	8.61±0.30	<i>Plasmodium falciparum</i>	Pyrazolo pyridineamine	
36	MMV011511	8.94±0.70	<i>Plasmodium falciparum</i>	Piperidineamine	
37	MMV676411	9.44±0.09	<i>Mycobacterium tuberculosis</i>	Propanamide	

38	MMV024311	9.78±0.20	<i>Mycobacterium tuberculosis</i>	1H-Indole	
----	-----------	-----------	-----------------------------------	-----------	---

MMV Pathogen Box (MMVPB) compounds were tested in culture against *T. b. brucei* at serially diluted concentrations. Median inhibitory concentrations (IC<sub>50</sub>) were generated from concentration–response curves using GraphPad Prism 8.0 software; MMVPB: Medicines for Malaria Venture Pathogen Box; The chemical classes of the compounds were obtained from the PubChem NIH database (<https://pubchem.ncbi.nlm.nih.gov>);

\*The disease targets for compounds were retrieved from the MMV Pathogen Box supporting information.

# PUBLICATION